Studies on the Response of Plants to Copper Nanoparticles

CIAN RYNNE

Studies on the Response of Plants to Copper Nanoparticles

Cian Rynne

Submitted for the qualification of Doctor of Philosophy

Department of Biosciences, Durham University

March 31st 2023

Contents

List of Abbreviations

The standard scientific conventions for protein and gene naming have been followed: wild type genes and proteins are in capitals and mutants are denoted by lowercase, gene names are italicized whereas protein names are not.

Standard scientific abbreviations have been used for units of weight, length, amount, molarity, temperature and time.

½ MS10	Half strength Murashige & Skoog media
ABA	Abscisic acid
Cu^{2+}	Copper ions
Col-0	Columbia-0
CSLM	Confocal scanning laser microscopy
DAG	Days after germination
DEGs	Differentially expressed genes
DMSO	Dimethyl sulfoxide
DNA	Deoxyribonucleic acid
Fe	Iron
Cu	Copper
GA	Gibberellic acid

GFP	Green fluorescent protein
GO	Gene ontology
GUS	β-glucuronidase
IAA	Indole-3-acetic acid
JA	Jasmonic acid
ICP-MS	Intercoupled plasma mass spectrometry
LR	Lateral root
NGS	next generation sequencing
PCR	Polymerase chain reaction
PR	Primary root
QC	Quiescent centre
qRT-PCR	Quantitative real time PCR
RNA	Ribonucleic acid
RNA-Seq	RNA Sequencing
ROS	Reactive oxygen species
RSA	Root system architecture
sdH2O	Sterile distilled water
TF	Transcription factor
WT	Wild type

Statement of authorship

I certify that all of the work described in this thesis is my own original research unless otherwise acknowledged in the text or by references, and has not been previously submitted for a degree in this or any other university.

Statement of copyright

Acknowledgements

I've run a fair few marathons at this point but A PhD is a true test of academic endurance. No one individual can lay claim to completing one entirely on their own. So I want to acknowledge all of my friends, colleagues and mentors that have helped me over the last 4 years, years which have included unprecedented historical events that have presented challenges I could have never foreseen.

My academic inspiration has always been Kary Mullis who is the truest kind of scientist. My definition is someone who asks 'why?'. That may sound simplistic until you appreciate how few people actually ask this question in life.

To my family, who have always loved and supported me no matter what bizarre interest or hobby I have taken on, In particular my mother Ethna who has always worked so hard to support and help all of her children. We didn't turn out so bad in the end. To my father, I wish you could see how far I've come but I know you'd be proud. My siblings, Orlagh, Conor and Emer, thank you. My aunt and uncle Dave and Fiona have always been a wealth of help and support to me, in particular, Dave is the main reason I know half the things I know. I also am really appreciative of my auntie Siobhan who shares my passion for science and endurance athletics. I am lucky to have you guys.

My running group need a mention, the first covid lockdown was a difficult time for me and athletics was my salvation. I am more proud of my sub 3 hour marathon completed during the last 3 years over the PhD thesis you are about to read. You learn grit and determination, to suffer and succeed through struggle and pain, sounds familiar in this line of work. The lockdown crew, boomer Stephen Hamil, Dad Matt Gwilym, Spoons Attley, Ash, Paul, Big Pete and Kim Grimoldby. I am so fortunate we became a group during the first lockdown, if it wasn't for you weirdos I would never have accomplished my goals. I also love coaching and chairing the local athletics club, Durham City Harriers. I never would have had the confidence to take on this leadership role prior to this project and its work and leading them to a division trophy in the harrier league will forever be one of my most proud achievements! Shoutout also to the guys in the sub 3 marathon forum, the running fraternity is the friendliest one I've ever joined.

My academic and industrial mentors. Keith and Jen have been so patient and good to me as a PhD student in their lab, you could not ask for better lab heads. This is best exemplified by the respect and high sentiment the entire biosciences department holds for them. PIs that support their students and care about their career progression are hard to come by and it's clear from how many students have come through your lab and succeeded, how well they have been supported. Jen has an amazing knack for showing you how everything you might have been trying to do in a technique or assignment was in fact incorrect but still make you feel positive about it. A true compliment to the field of pedagogy in academia. Matt Wilson has always been a supportive and positive influence in the industrial side of the project, it's been a wild ride.

Lab 1004 and sometimes lab 1003. So many amazing moments shut the whole world down with a new virus (I told you guys not to pour that virus growth plate down the sink), nearly crashed the stock market with George, cling film wrapping Rodrigos entire desk, annoying Flora and May on the daily, beseeching Amy for help with techniques since we did such similar projects. Swapping the tea with Helen. The craic with Xiao yan, Fahad, Mokhles and many others who have come through our lab over the years. My own apprentice Alice, we shall be science influencers yet. Various hijinks with Joey. Of course my son: colleague, captain, king Julien, a wealth of knowledge, experience, calm and hilarity in the chaos of the 4 years. To all members of the lab past and future.

The greater biosciences community, Bekkie Morrell, Ollie Philip (not a bioscience guy but loves a good pint), Chazz Mcleod, Craig and Rebecca Manning, fellow Irishman and fellow gobshite Matthew Quinn, The OG day 1 squad: Abbi Mornement, Sam Firth, Will Micheals, we did it guys.

I also wanted to thank all of the technical and facility staff that have assisted me in this project – Joanne, Tim, Christine, Johan, Deenah, Andrew. The administrative staff including all the PGR admins that have helped oversee the PG program over the years I've been here thanks Emma and Veronica, purchasing staff for always being so helpful for sorting orders and travel and all the money stuff that allows us researchers to do our research; Lucy, Gail, Caroline are always very helpful and accommodating.

To my other good luck charms Ivona, Eric and Luna thanks for all your support, we did it.

Just have a leaf through my plant thesis now. It's immense!

"What greater glory attends a man, while he's alive, than what he wins with his racing feet and striving hands"

(170 book 8 the Odyssey)

Abstract

The use of copper nanoparticles (CuNPs) shows promise in enhancing plant growth, but their effects depend on concentration, size, and surface chemistry. High copper levels can be toxic, causing oxidative stress and cell damage, though plants have developed mechanisms to tolerate metal stress. Proposed pathways activated by CuNPs include hormonal response, phenylpropanoid biosynthesis, and interaction with the cytoskeleton. Nanoparticle size and morphology affect interactions with plants and microbes, and their bioavailability depends on various factors. The aim of the work described in this thesis was to characterise the biological responses of plants to CuNPs at the phenotypic and molecular levels. Proteomic and transcriptomic analysis in Arabidopsis reveals differential expression of stress response genes and cellular signalling pathways, providing new information on plant responses. Willow trees show potential for copper uptake, suggesting phytoremediation possibilities. Understanding CuNP environmental impacts is crucial for safe use, and investigating protein interactions, post-translational modifications, and different nanoparticle types can offer insights. This research can aid in developing sustainable remediation methods and safe industrial applications of CuNPs.

Chapter 1 Introduction

1.1 Tree roots in the built environment

A key application of the work described in this thesis is that of developing new solutions to prevent root ingress into built structures such as pipes, based on our understanding of root development. There has been a long history of civil infrastructure and the natural world struggling to co-exist, An illustration of this problem dates to post-war England. A surveyor assigned to assess bombing damage and associated compensation was baffled by increasing claims from rural areas that were not bombed, however assessing the foundations of buildings found damage and structural issues that were not dissimilar from the bombing. This turned out to be a result of root networks from trees shifting the soil and causing damage in dry weather (Ward, 1948).

There is limited space underneath the soil for everything a built civil society is interested in placing there as well as substantial plant and microbial life.

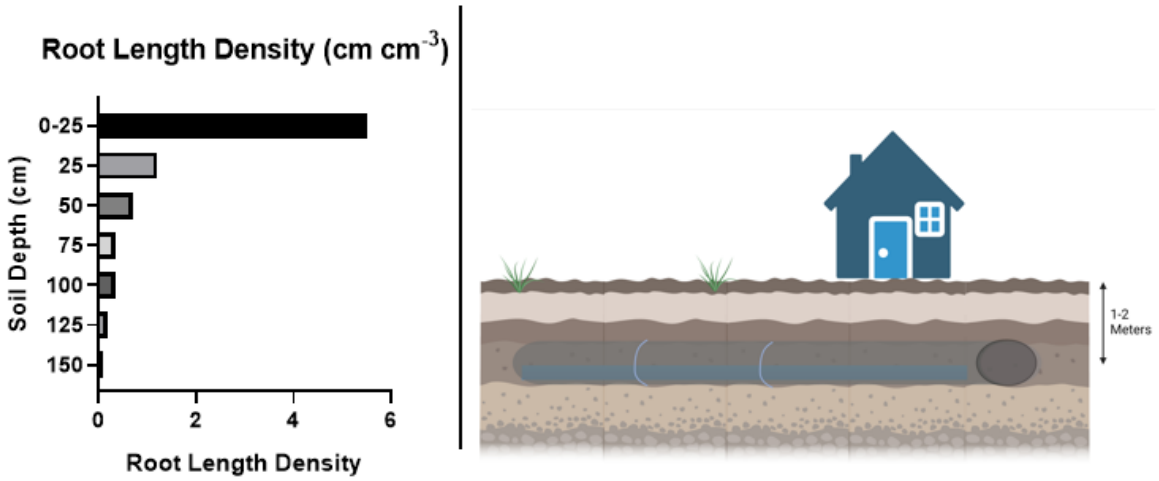

Figure 1.1 : Bar chart indicating the large density of plant life and biomass that shares the exact same region of soil most civil infrastructure including pipe networks are placed, data from (Roberts et al. 2006)

Sewerage systems drain and transport sewage or sanitary water (Bartlett, 1979), ground drainage and stormwater or runoff are usually in separate systems, seldom combined, the general approach is to separate surface water from foul water.

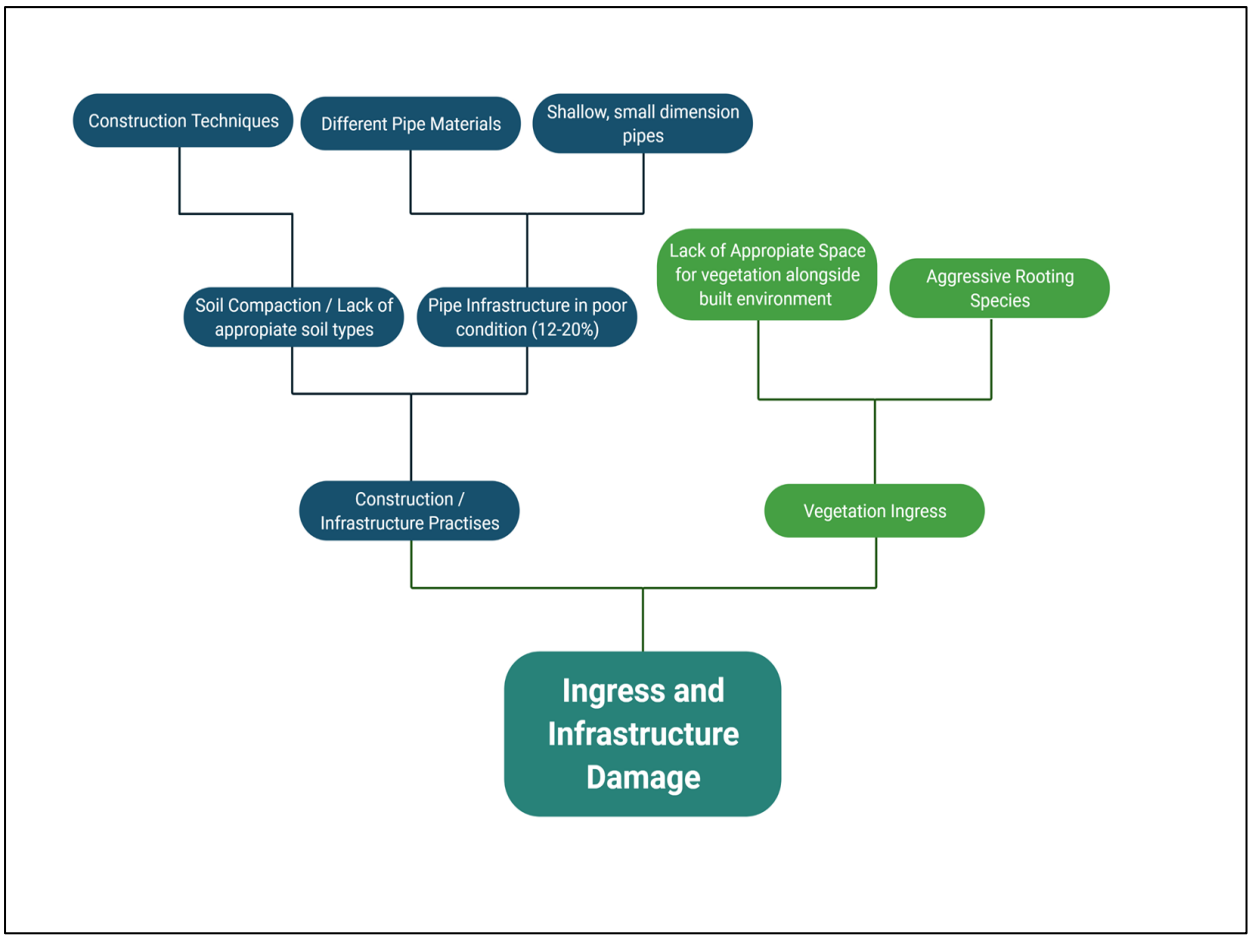

Figure 1.2 : Contributing factors to root ingress and overall infrastructure damage incorporating both biotic and abiotic factors.

The problem of tree roots proliferating within sewer systems has been reported by several publications and authors across many years in different regions. Root invasion is likely to occur in old systems and in cracked pipes. Factors that contribute to damage include old pipes with joints, shallow pipes, small-dimension pipes, and fast-growing tree species. Because roots are reported to cause >50% of all sewer blockages, costs associated with root removal from sewers are substantial. In smaller-dimension pipes, root removal every year or every other year is common. Major resources are put into the replacement and renewal of existing pipes, which is sometimes accelerated because of root intrusion. Collapse repair costs are greater than new construction, but costs associated with root removal may be one-sixth the cost of pipe replacement/renewal due to roots ((Randrup, McPherson and Costello et al., 2001).

Regions reporting problems include the USA (Baxter, 1958); (Geyer & Lentz, 1966), and Scandinavian countries (Rolf & Stål, 1994) which states water authorities had blockages caused on average 54% to 93% of the time by tree roots. Within the United Kingdom root intrusion is potentially causative of up to 5% of sewer blockages and can be held responsible for a significant number of recurring drainage problems (Davidson, 1999). However, it is overall rare for a pipe to break as a result of root intrusion (Brennan et al., 1997). There are a number of different construction styles for underground water pipes utilised over several centuries. Cast iron piping from the 19th century, asbestos cement from the 1960s, ductile iron and PVC utilised since the 1970s. MDPE (medium density polythene) from the 1980s. If all of these pipe networks are in good condition there is no major reason for roots to intrude into them as strong positive water pressure in the pipes would present a barrier (Brennan et al., 1997).

Unfortunately, the general state of repair of a lot of the water pipe infrastructure within the UK is poor. Statisticujs from 1998 categorise up to 7% of mains water pipes as grade 4 (considerable corrosion affecting service performance; nearing end of useful life; frequent bursts) and up to 5% is condition 5 (substantially derelict and source of service problems. N6 residual life) which means up to 12% of pipe infrastructure is in a poor state of repair (Leakage and Water Efficiency Office of Water Services, 2001).

Even with internal pressure reducing root intrusion, any leakage at all will encourage some form of root growth in the locality and may result in future damage to infrastructure, it is both unrealistic and uneconomical to expect to totally reduce leakage of pipes to negligible levels so a different strategy must be undertaken to reduce this impact. (Leakage and Water Efficiency Office of Water Services, 2001).

In 1993 the UK had over 300,000 km of both surface and foul water sewers (Wrc, 2013). This has expanded significantly since then and is known to be in poor condition. The water distribution system in the Uk UK has substantial leaks with total leakage estimated to be 21% of water put into supply between 1999 and 2000 On a European wide basis there is significant loss due to leakage (Leakage and Water Efficiency Office of Water Services, 2001).

Unlike water mains, the flow within sewers and drains relies upon gravity which Is often insufficient to prevent root intrusion.

Gasson & Cutler (1998) report that as pipes are well protected in normal circumstances, it's nearly impossible for roots to detect their presence in any other situation other than a leak. In the absence of any obvious leak, roots must enter at joints between pipe sections.

Once a root has accessed a sewer the conditions inside are optimal to induce growth and proliferation until it blocks the sewer completely (Harris et al., 2004). There is little information about the rate of root growth within pipes compared to how it grows in soil nearby. Which would be a useful comparison to understand the attraction of sewer pipes to roots better.

The most common species that invaded sewer pipes were recorded in a survey carried out in 1989 (Cutler & Richardson, 1989). The biggest offender was the Populus spp family of trees, followed by willow and horse chestnut Acer spp, Castanea, Aesculus and specifically Salix as being particularly invasive.

A

Species	Percentage (%)
Populus spp.	24
Willow	18.5
Horse Chestnut	11
Acer spp.	9.6
Plane	7.5
Birch	5.5
Prunus spp	4.5
Ash	4.5
Oak	3.5
Cypresses	2.5
Apple/pear	2
Hawthorn	1.6
Lime	1
Beech, elm, Sorbus, Robinia	each <1

B

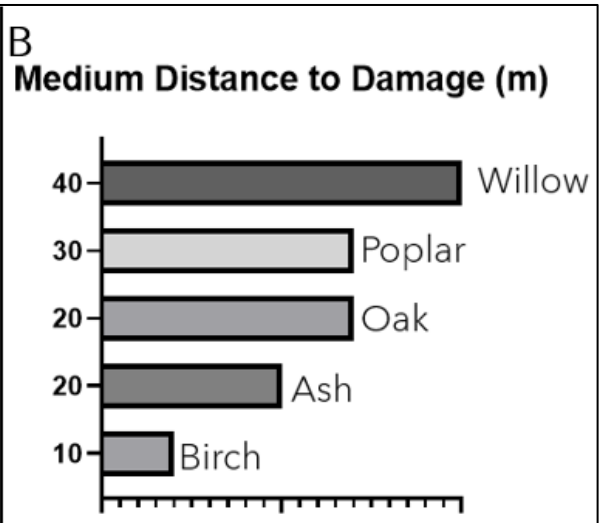

Figure 1.3 – (A) Chart depicting most common species to cause pipe blockage. Adapted from Roberts et al. (2006) *(B) Graph of average distances found between tree root ingress and damage and the tree species responsible, adapted from* Cutler & Richardson (1989).

Poplar and willow as riparian species are more likely to cause problems given their adaptions to waterlogged conditions found within sewers and pipes. It might be expected for other riparian species such as Fraxinus (ash) and Alnus (alder) however alder is not extensively

planted within the urban environment, except for reclamation sites (Cutler & Richardson, 1989).

1.1.1 Methods for controlling root intrusion

1.1.1.1 Mechanical removal:

Rodding: This process uses either a mechanical or manually operated ratchet drive connected to hardened steel rods fitted with a specific head. This type of work is typically undertaken on a reactive basis and is at least a two-stage process, i.e. Stage 1 is with a point type head to "break" the block then Stage 2 is with a cutter type head to clear the pipe.

Jetting: This uses high-pressure water (103 bar to 690 bar) to drive specific heads fitted to the end of a hose. The water used is usually from the reticulation water system, i.e. fireplug. Recent developments have seen the use of recycled water and/or equipment being modified to suit to use "water" from the sewer main itself. The heads fitted are typically for a specific purpose, e.g. removal of rubble, root cutting etc. This process usually removes material from pipe, e.g. rubble. Some authorities refer to this method as "flooding".

Root Cutting: Similar to jetting using high-pressure water but specific heads are used that enables the equipment to cut the tree roots. Basically, two types of heads are used. One where nozzles in the head does the cutting and the other where a hydraulic motor "drives" a cutting head similar to a "hole saw" fitted to an electric drill.

1.1.1.2 Chemical methods:

Chemical: In this process a root inhibitor chemical is applied to the reticulation sewer pipes considered to have tree roots present. The chemical historically has been applied via a "foaming" process but other processes have been trialled, e.g. spot spraying in conjunction with close circuit television (CCTV) equipment. Chemicals often used include copper sulphate which has been shown to control root growth in sewers in the USA (Sprague and Edwards, 2004) the use of copper based chemicals is particularly promising given it is not absorbed too deeply into the plant, likely as a result of killing the root before it can be transported further into the plant. Resulting in localised root death with no overall loss to tree or shrubs (Mitchell, P.J,and Schnele, 1999). However there are environmental concerns for utilising copper

sulphate in the sewer system and increasingly regulations are attempting to cut down on heavy metal pollution of water systems, additionally there have been reports of toxicity interfering with sewerage treatment (DD. Drury and JM. Montgomery, 2006) which makes this strategy questionable as a long term solution.

A significant number of herbicides have been trialled with dichlobenil and metam-sodium having good results (John W. Groninger, 1997) metam sodium is known to have toxic effects on nitrifiers that are used in sewage treatment.

Within Europe there are some stringent laws regarding what which chemicals can be used through wastewater systems. So chemical control of root growth may not be the best solution. An environmentally friendly and sustainable solution would be best.

Dig/Repair: This method is generally restricted to isolated cases and site-specific conditions that require a unique approach to clear a blockage and/or defect. Repairs normally undertaken as part of planned program there are situations where a reactive excavation and repair is required e.g. collapsed pipe, equipment trapped within the sewer pipe. (Thomson, 2006)

The report concluded there is no easy or all-inclusive fix for the issue of tree root intrusion on water pipe systems.

1.2 Root System Architecture:

Roots are an essential biological system through which water and nutrients are uptaken into the plant. Additionally, they have important anchoring and different mechanical support functions. It is an important signalling centre for different biotic and abiotic influences within the soil that affect plant growth. The root system architecture is not as well understood as cotyledon and leaf development given the logistical problems in attempting to dynamically analyse root growth in soil (de Dorlodot et al., 2007). However, a good understanding opens up the possibility of manipulating and exploiting its growth to gain advantages in the production of crops and better optimise land usage (Smith & de Smet, 2012).

Plants display significant variability in their underground networks, specifically in their root systems. Root system architecture differs not only between species but also within the same species due to various genetic and environmental factors.

In biology, the term 'architecture' refers to the spatial arrangement of a complex assembly of subunits, with the understanding that the overall macro configuration has a functional purpose. Root architecture applies this concept to the organization of plant roots. This architecture can be classified into the following categories for plant roots:

The spatial configuration of the root system, Normally studies of root architecture do not consider more specific features such as root hairs, they are more concerned with the overall macro scale of the root network. Architecture is a useful indicator of topology and distribution, neither of these two factors on their own can be used to derive information about the others in comparison to architecture.

It is easier to measure and quantify topology and distribution which can elucidate the overall architecture of the root than it is to directly measure root architecture.

Root architecture, on the whole, can be quite complex, Root systems display significant variations between different species, even within different genotypes of the same species there is significant variation, and within different regions of roots of the same plant there is considerable variation.

So with this complexity, quantifying root architecture is, therefore, both a difficult methodical undertaking as well as potentially providing great insight into the functional morphology of plants (Lynch, 1995).

1.2.1 How does root Architecture affect plant productivity?

Root architecture will have serious implications on how a plant obtains nutrients, given the availability of resources a plant needs in the soil, such as potassium (Leigh RA, 1984) (Shin, 2014) and nitrogen (Kiba & Krapp, 2016), are variable and not always present in sufficient quantities. How the plant responds to scarcity of resources is likely to be reflected in the architectural layout of the root system, which is under both genetic and environmental control (Kochian, 2016).

There can be significant variation in the availability of different resources within very short distances in the soil, and this presents conflicting nutrient gradients competing for plants' attention responses (Lynch, 2022).

Plants can respond to deficiencies by stimulating lateral root growth, as is the case with nitrogen (Kiba & Krapp, 2016) (Postma et al., 2014) when in mild nitrogen-deficient conditions.

Changes in root architecture represent a response to environmental factors, and barriers present within the soil. Plants can modulate root growth patterns in response to different nutrient signals (Giehl et al., 2014). For example, plants can respond to deficiencies by stimulating lateral root growth, as is the case with nitrogen (Kiba & Krapp, 2016; Postma et al., 2014) when in mild nitrogen-deficient conditions. Some of these other environmental factors include temperature, moisture, the presence of beneficial or detrimental microbiota, and mechanical barriers (Waadt et al., 2022a). Plants can modulate root growth patterns in response to different nutrient signals (Giehl et al., 2014).

1.3 Arabidopsis as a model organism

1.3.1 Arabidopsis as a model for root development

Arabidopsis thaliana is a plant that has no inherent agricultural value but has been utilised as a model plant within the research community for over a century, however, and it has come into mainstream popularity amongst plant biologists since the early 1980s. Its useful benefits include its relatively short life cycle of approximately 6 weeks, the small surface size of the plant which allowed it to be grown in limited space, its ability to self-fertilise, and its ability for one plant to produce upwards of 5000 seeds. and its simple diploid genome with approximately 27’000 29,000 protein-coding genes across 5 pairs of chromosomes (making it one of the simplest known plant genomes) were - all useful characteristics that led to its adaptation as a model species throughout the research community (Meinke et al., 1998). The plant was also the first higher plant genome that was sequenced and published (Kaul et al., 2000)which solidified its status for developmental and molecular biology work. Arabidopsis also presents a useful model for root analysis and quantification as it expresses a typically dicotyledonous hierarchical tree root system architecture (Kellermeier et al., 2014).

1.3.2 Structure and growth

The root system of Arabidopsis is quite highly regulated and organised in its development. (Dolan et al., 1993). A figure of the transverse section of a root demonstrates an organised radial symmetry with concentric ring cell files this tissue, consists consisting of (from outer to inner) the outer epidermis, cortex and endodermis which surrounds essential the vascular tissue which consists of the pericycle, phloem, xylem and procambium (Scheres, 2013). This is illustrated in (Fig 1.4). All the differentiated cells indicated originate from a pool of stem cells located at the root tip. The stem cells are undifferentiated due to their proximity and contact with cells of the quiescent centre (QC), the main function of which is to maintain an undifferentiated state (Dolan & Roberts, 1995; Petricka et al., 2012). The stem cells alongside together with the QC form the stem cell niche (SCN).

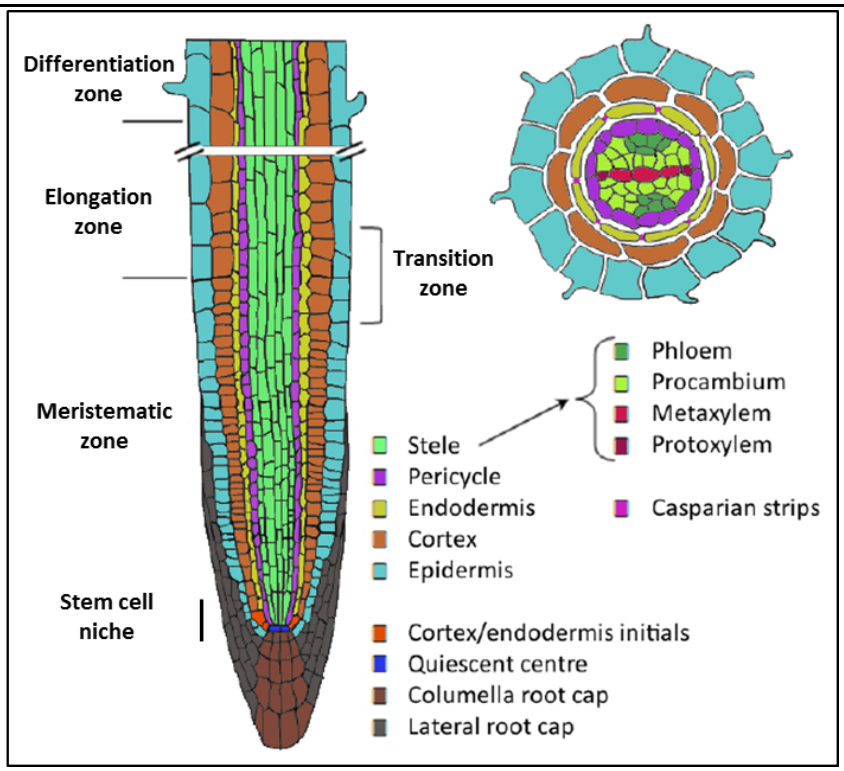

Figure 1.5: Structure of the Arabidopsis root. Longitudinal section through the root (left), and transverse section of the root taken from the zone of differentiation (right). Different cell types marked in different colours and developmental zones are indicated. Image adapted from De Smet et al. (2015).

The longitudinal organisational structure of an Arabidopsis root (Left) demonstrating apical-basal polarity. There are different cell types (separate colours) arranged into cell files which form concentric single-cell layers that surround vascular tissue. There is a distinct

differentiation between different developmental zones in the root tip and this differentiation is highly regulated. Transverse section of the root (Right), radial polarity on the differentiation root zone demonstrating root hair formation and the Casparian strips. Adapted from De Smet et al. (2015); Péret et al. (2009); Petricka et al. (2012).

1.3.3 Primary Root Length:

Primary root length is mainly influenced and determined by an interaction of three different cell biological processes, namely the rate of cellular division, the rate of differentiation of those cells and the extent of expansion and elongation of cells (Scheres et al. 2002). In dicot plants, root development systems initiates with the embryonic root meristem, in which the positioning and pattern of the stem cell niche (SCN), formed by the quiescent centre (QC and the surrounding stem cells, are established (Scheres et al., 1994). This is followed by post-embryonic events that produce a transition amplifying cell population in the proximal meristem. Root The root apical meristem is therefore the main store of all cells that the primary root will consist of during its life. Any disruptions or rearrangements in the spatial arrangement and functional maintenance of the root apical meristem will have implications for the growth of the primary root.

Mitotic activity in the root apical meristem and elongation in the zone proximal to the meristem will be the main determinants of the extent and direction of PR root growth. Cell division will decrease as cells move further away from the SCN (Petricka et al., 2012). The cells will eventually stop dividing and enter into a process of elongation and, subsequently, differentiation and elongation. The location of where cells stop dividing in relation to the SCN will be a determinant of the size of the meristem, which subsequently is directly related to the rate of root growth (Rong et al., 2022).

1.3.4 Lateral Root development

Lateral Roots (LR) in Arabidopsis develop from xylem pole pericycle cells, the development of which occurs initiates in the primary root meristem. These primed cells then gain founder cell identity and go on to develop into lateral roots (Benková et al., 2003; De Smet et al., 2008; Dubrovsky et al., 2000; Laskowski et al., 1995).

These originating founder cells will undergo a succession of periclinal and anticlinal divisions which will form the primordium of the lateral root. This development is further divided into eight more distinct steps of development before a recognisable lateral root bud tip begins to grow from the primary root (Malamy & Benfey, 1997; Fig. 1.6).

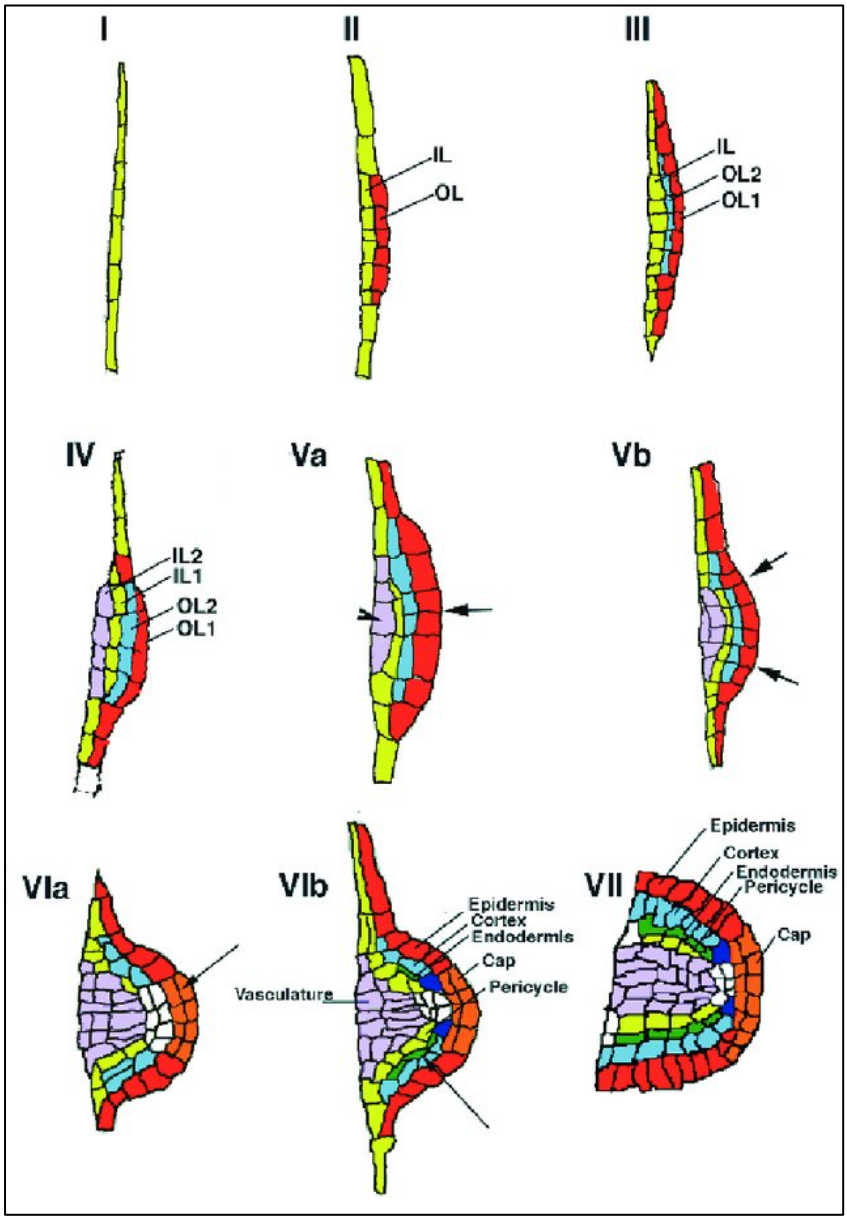

Figure 1.6 adapted from (Malamy & Benfey, 1997) *depicting a putative eight-stage lateral root development pattern based on histological staining studies. Different colours correspond to different cell types. Adapted from* Malamy & Benfey (1997).

1.3.5 Root Hair Development

Root hairs are small, single-celled extensions of the root epidermal tissue (Fig. 1.7). They facilitate the functions of the root (anchorage, nutrient uptake, interaction with soil living micro-organisms) by substantially increasing the surface area of the root (Schiefelbein et al., 1990). The development of the root hair is in a state of constant modulation due to the roots surroundings, which allows for their growth to be optimised to best suit the nutritional needs of the plant. The overall mechanism of regulation relies on position position-dependent signalling and feedback loops. This is mediated by phytohormone and other (e.g. reactive oxygen species, ROS) signalling in response to biotic or abiotic changes in the soil environment which enables flexible, phytohormone-driven alterations in the rate of growth, density, length or morphology of the root and root hairs (Vissenberg et al., 2020).

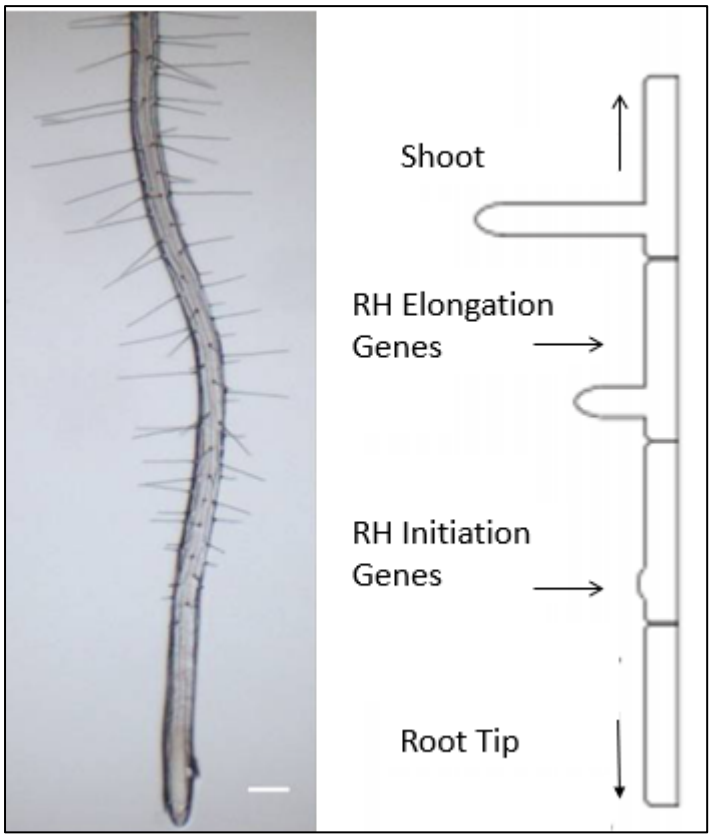

Figure 1.7 Root hair initiation depicted in the proximal region of the root tip. Adapted from Vissenberg et al. (2020). *Scale bar = 200µm.*

1.4 Plant hormones - roles and functions:

A hormone has been described as a signalling molecule with the main function of causing a specific functional effect on another cell or tissue (Huxley, 1935). They are highly prevalent in

the animal and plant kingdoms, coordinating physiology and development. Plant hormones have developed and evolved as a mechanism for plants to respond to external stimuli, be it light availability, nutrition, presence of pathogens or temperature cues. Early botanical research investigated how plants sensed and responded to their environments (Darwin, 1966) and described the hormone, later identified as auxin, as one of the essential hormones in mediating the movement of plants. In more recent times, other hormones have been discovered that regulate and coordinate growth, such as ethylene, gibberellin, cytokinin and abscisic acid (ABA), together these hormones are known as the five classic plant hormones. Others include jasmonic acid, salicylic acid, brassinosteroids and strigolactones (Raza et al., 2022). Their transport around the plant and interactions with each other (synergistically or antagonistically) is crucial to coordinating key developmental processes such as primary root growth, lateral root development and root hair development (Vissenberg et al., 2020; Malamy & Benfey, 1997; Petricka et al., 2012).

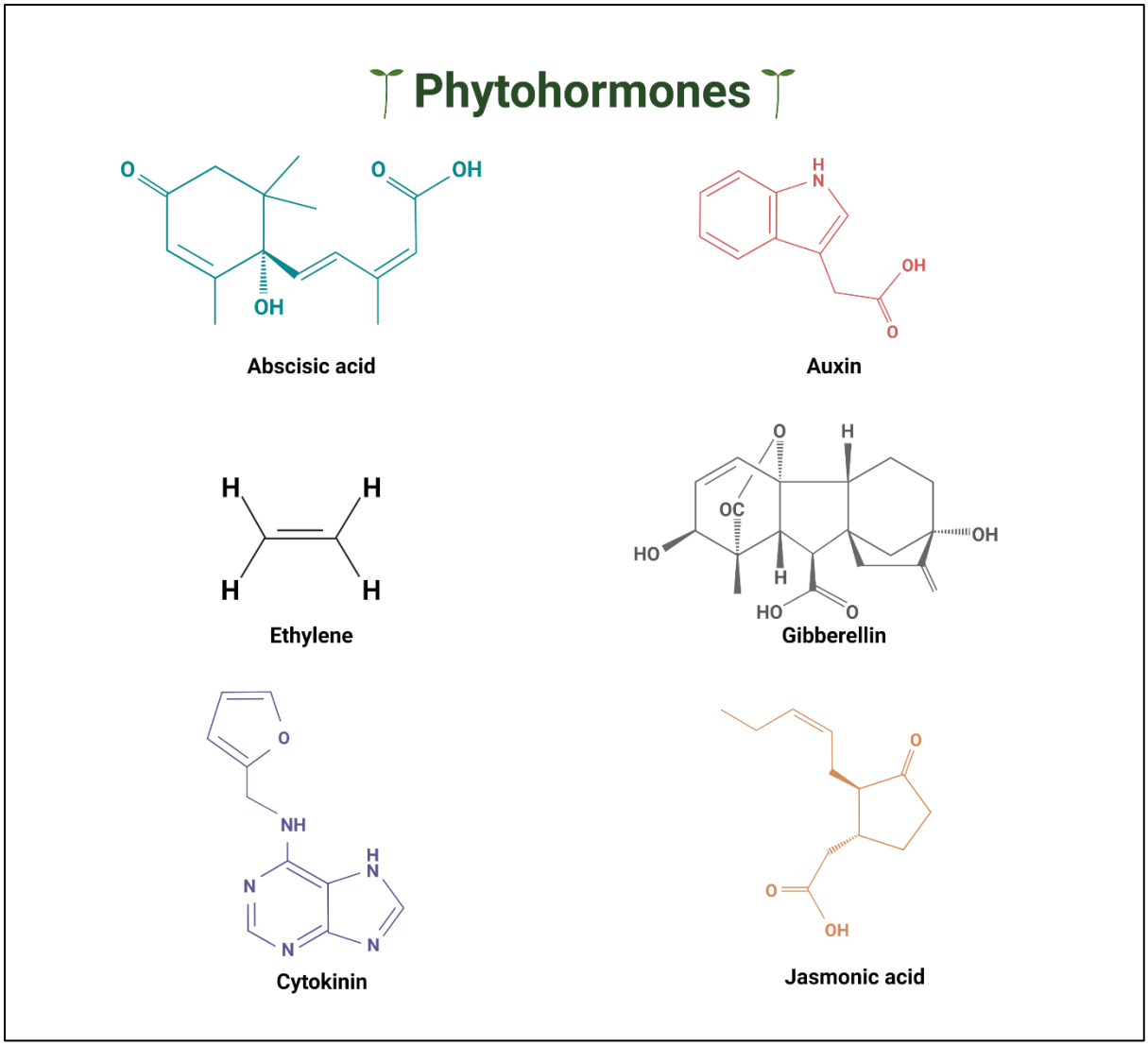

Figure 1.8: A non-exhaustive list of some of the key phytohormones involved in plant growth and development(Vissenberg et al., 2020), (Waadt et al., 2022)

1.4.1 Auxin

Auxin is the most studied phytohormone and is also one of the most prevalent in plants. Its exact function is however dependent upon its concentration and the different precise cell types that perceive it (Leyser, 2018; Vissenberg et al., 2020). Due to the complex demands of regulating root and shoot growth with available nutrients, there is a strong necessity to coordinate growth alongside regulation which requires a dedicated signalling system that functions at both a local and systemic level throughout the plant. Auxin qualifies as one of these growth coordinators having involvement in where, when, the quantity and the type of growth that will occur in the plant. The argument has been made that auxin does not have intrinsic value but is rather utilised, metaphorically, as a currency to facilitate biological

transactions in the plant, - like money, auxin is exchanged and circulated to obtain multiple different results depending on the spender and recipient within the plant (Stewart & Nemhauser, 2010). The manner by which this phytohormone regulates is principally via effecting transcriptional changes through a short signal transduction pathway (Paponov et al., 2008). but may also influence cell wall loosening and cell elongation by non-transcriptional changes (Leyser, 2018).

In plant roots, auxin forms a concentration gradient with the maximum concentration close to the quiescent centre of the root tip (Sabatini et al., 1999). How the auxin is distributed in the root tip is via a polar transport system accommodated by membrane proteins, many of which are localised asymmetrically in order to provide directionality of auxin transport in tissues. There are 3 main families. PIN-formed (PIN), ATP binding cassette subfamily B/P glycoproteins (ABCP/PGP) and Aux/Lax. ABCP and PGP proteins are not currently associated with polar transport within the plant (Barbez et al., 2012). PIN proteins however are essential for the directional movement of auxin in the root tip (Petrášek et al., 2006). *pin* mutants will exhibit disrupted transport and altered auxin localisation, which results in phenotypic changes in growth and development (Křeček et al., 2009).

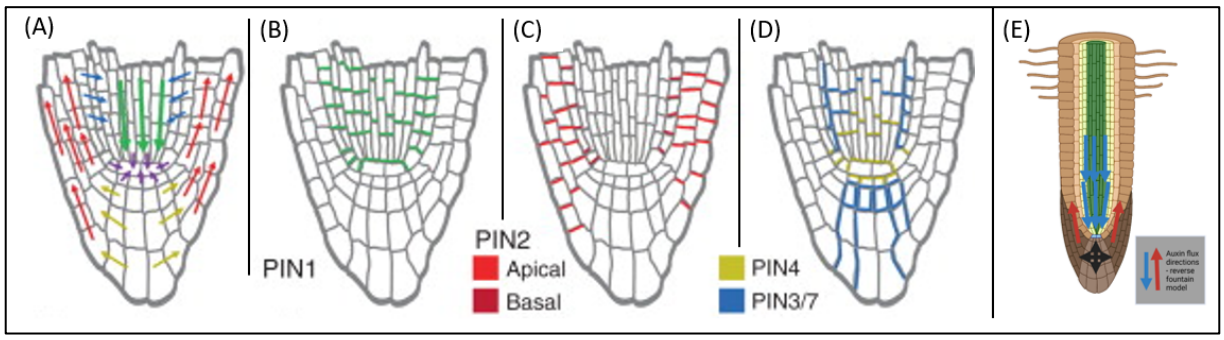

Figure 1.9: (A) Simplified model of auxin flux within the Arabidopsis root meristem. Basal auxin transport (green arrows) from the shoot enters the root meristem and is concentrated in the QC area (purple arrows). In the columella, auxin is transported laterally (gold arrows) and then transported apically in the epidermis and lateral root cap (red arrows). Finally, apically transported auxin is recycled into the basal auxin stream by inward lateral transport (blue arrows). (B) diagram showing expression domain and protein localization of PIN1 in the root meristem. (C) diagram showing expression domain and protein localization of PIN2 in the root meristem; apical localization in epidermal and lateral root cap cells, and basal localization in

cortical cells. (D) expression domains and protein localizations of PIN3, PIN4, and PIN7 in the root meristem. (E) the flow of auxin at the root tip. Adapted from (Ruiz Rosquete et al. 2012).

Fig. 1.9 depicts PIN protein localisation and auxin flux movement in the Arabidopsis root tip. Auxin is transported in the stele directionally to the root tip via AUX1 influx and PIN1 efflux carrier proteins. Auxin Directional auxin polarity polar movement corresponds with the apical position of AUX1 and the basal position of PIN1 within the cell. PIN4 funnels the auxin into the quiescent centre (QC) where the total auxin concentration maximum will occur. Meanwhile, PIN3 and 7 are localised in the columella, and transport auxin to both sides of the lateral root. Auxin is then transported back up the shoot (basipetally) via the epidermis and cortex via PIN2. This is referred to as the reverse fountain model (Mironova et al., 2010).

It is important this auxin distribution is a highly regulated process to induce appropriate growth responses for, for example, gravitropism which results in. Here a change in PIN3 distribution acts to asymmetrically change the concentration of auxin to one side of the root to induce directional growth change (Adamowski & Friml, 2015; Rakusová et al., 2011).

1.4.2 Ethylene

Ethylene is the smallest phytohormone with the simplest structure (see Fig. 1.8). The phytohormone is produced primarily in response to various stress factors. It has a well-understood role in plant defence response to pathogens, it is a gaseous hormone and allows plants to communicate with each other (Thao et al., 2015). More recent research has determined roles in regulation of organ development and growth and total yield under abiotic stresses. The main actors transcriptional regulators of ethylene signalling are the ethylene response factors (ERFs).

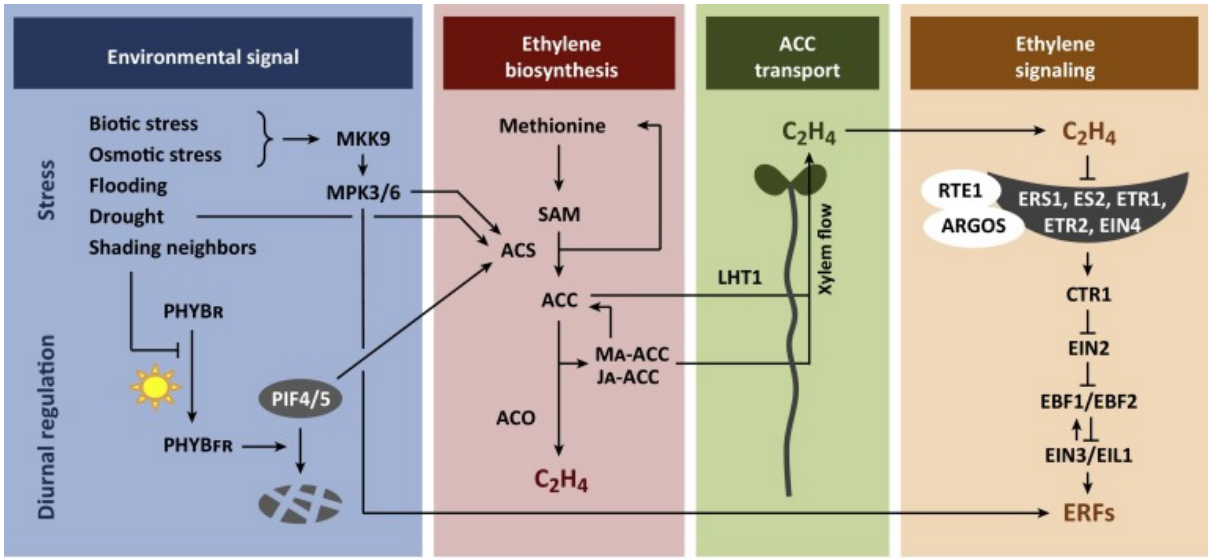

Figure 1.10: Summary of the biosynthesis and subsequent signalling pathways of ethylene (Dubois et al., 2018).

Ethylene is involved in the inhibition of root elongation, in the development of lateral roots as and in stimulating root hair formation (Dubois et al., 2018b). Ethylene stimulates the expression of auxin biosynthesis genes and members components of the auxin transport machinery (Péret et al., 2009; Swarup et al., 2007). This results in ethylene induced auxin accumulation and inhibition of cell expansion of cells exiting the root meristem (Swarup et al., 2007).

1.4.3 Reactive Oxygen Species

Reactive oxygen species (ROS) play a key role in the functional homeostasis of a plant. ROS describes a selection of molecules that are derived from oxygen (O_2). Whilst stable O_2 ROS are considered to be by-products of plant metabolic systems and can be generated in a number of different plant tissues organelles such as the peroxisomes (Sandalio & Romero-Puertas, 2015), chloroplasts (Dietz et al., 2016) and mitochondria (Huang et al., 2016). ROS can cause irreparable damage to DNA and trigger cell death in high concentrations, but it also has a function as a signalling molecule that can regulate standard plant responses to stress. It is likely ROS play different roles in the plant depending on concentration and area site of production (Miller et al., 2010).

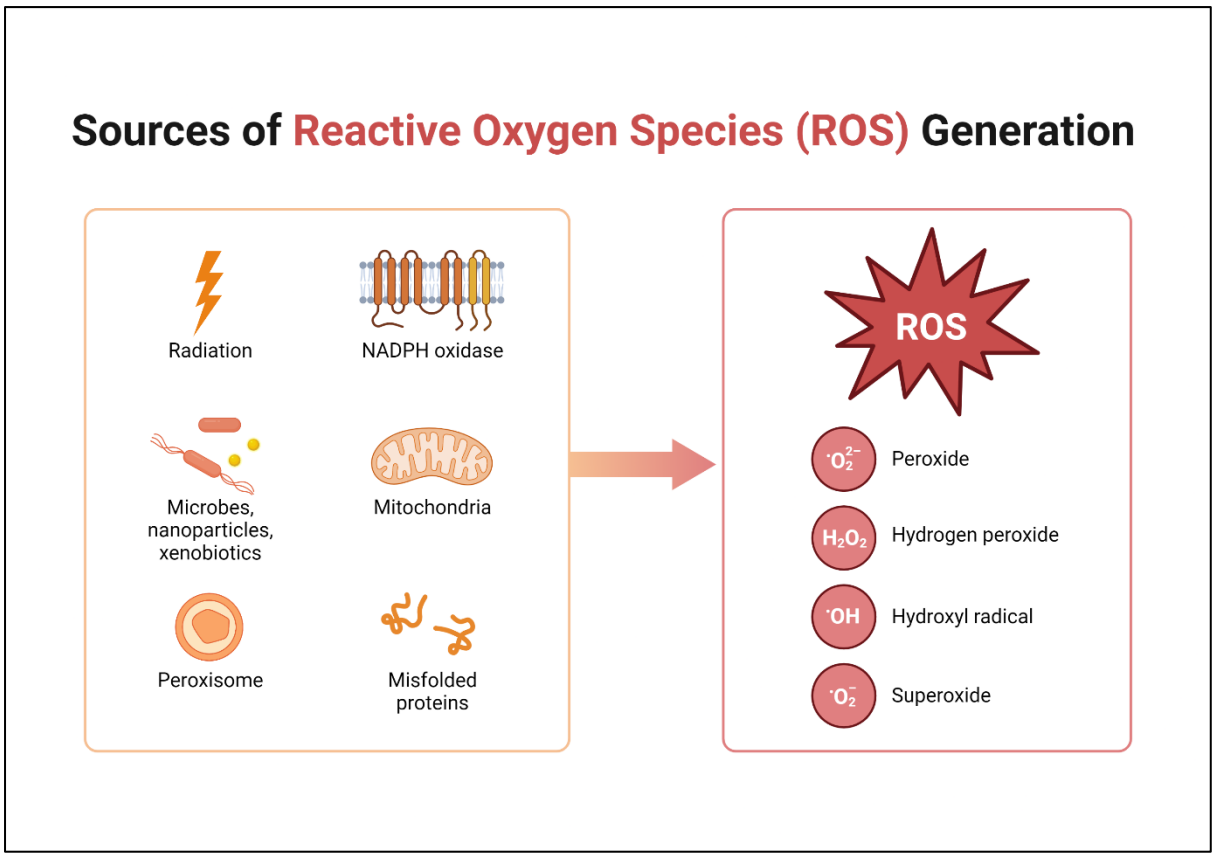

Figure 1.11: some of the causes of ROS production within cells through homeostatic processes.

Oxygen, the progenitor of ROS, is a highly stable molecule, and ROS are generated by excitation or reduction of atmospheric oxygen but can be caused by numerous internal homeostatic factors or by external influences (Figs. 1.11-1.13).

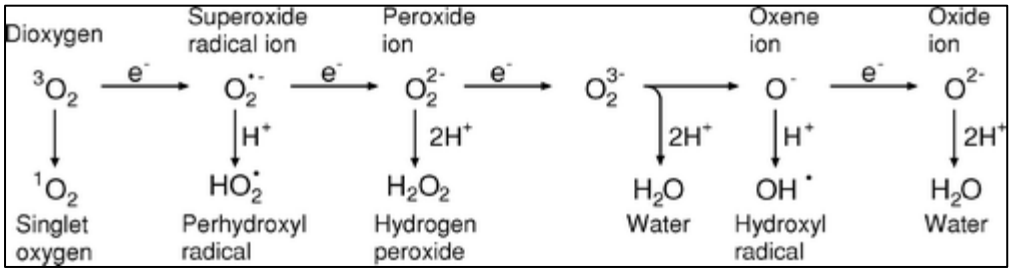

Figure 1.12 figure of formation of reactive oxygen species via oxidation or reduction of stable oxygen – adapted from (Waszczak et al., 2018)

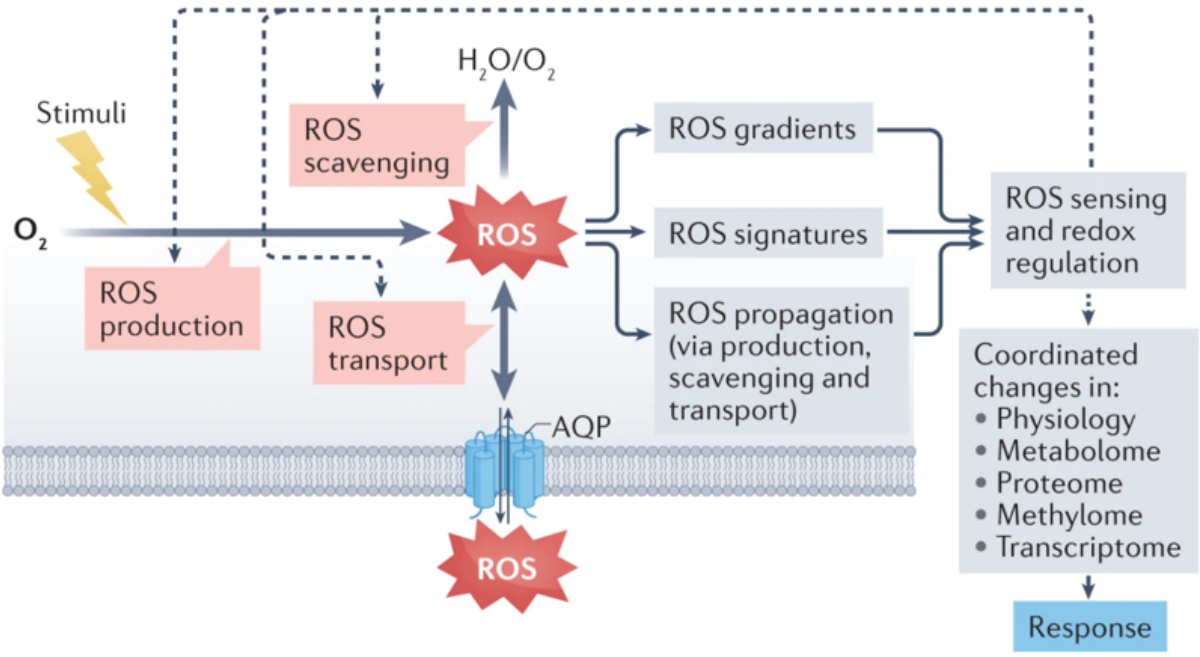

Figure 1.13: There are three processes to regulate ROS levels: production, its scavenging and transportation. ROS levels and gradients are dictated by the interplay of these processes. ROS operates as a signaller and responder to external and internal influences (Mittler et al., 2022).

The generation of reactive oxygen species (ROS) can result in the oxidation of cellular components such as lipids, proteins, RNA, DNA, and several other small molecules. This high reactivity is attributed to the altered chemistry of ROS, compared to O_2, which facilitates the donation of electrons or transfer of excited energy states to acceptor molecules. The predominant forms of ROS in cells include hydrogen peroxide (H_2O_2), superoxide ($O_2^{\cdot-}$), singlet oxygen (O_2), hydroxyl radical (HO.), and a variety of organic and inorganic peroxides, each of which exhibits distinct properties and levels of chemical reactivity (Fig. 1.11; Waszczak et al., 2018). High levels of regulation are required in order to prevent overproduction which may cause unintended cell damage, this is done by regulating the 3 processes illustrated in Figure 1.12, to keep ROS low and regulate ROS signal reactions.

As depicted in Fig. 1.11 ROS is produced during normal homeostatic processes as by-products of housekeeping or metabolic pathways by-products (respiration, photosynthetic processes). ROS can also be transported via aquaporins or AQPs, to other regions and tissues, to signal, for removal/dispersal or to accumulate and sequester. ROS therefore can be produced in a different region to its downstream function (Rodrigues et al., 2017; Mittler, 2017).

ROS accumulates via a different pathway as a result of exposure to pathogen stresses. Hydrogen peroxide is produced in the apoplast due to the activation of specific oxidases such as the RBOHs, it is also produced in chloroplasts due to the disruption of metabolic systems (Torres et al., 2002).

Most importantly there is evidence to suggest that ROS as a result of different stresses there are different kinds of ROS accumulation patterns that occur in different parts of the cell (Exposito-Rodriguez et al., 2017; Haber et al., 2021; Mizrachi et al., 2019); Marty et al., 2019; Nietzel et al., 2019).

Different ROS produced in different cellular components can trigger a stress specific response and signal transduction pathway that activates a specific acclimatization and defence mechanism (Fig. 1.14).

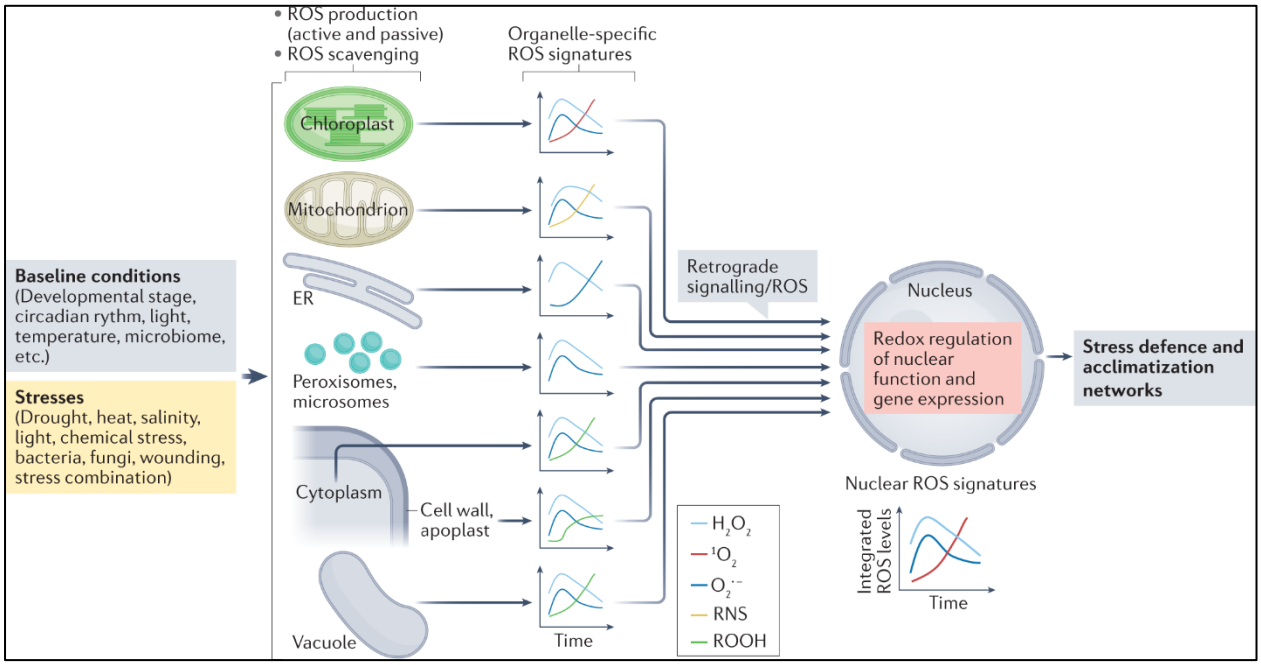

Figure 1.14: The generation and scavenging of reactive oxygen species (ROS) within distinct cell compartments, including the cell wall and apoplast, during stress conditions results in the formation of compartment-specific ROS signatures (as indicated on the right). These signatures are integrated with other retrograde signals that do not involve ROS and reach the nucleus, leading to alterations in the nuclear ROS signature and triggering of defence and acclimatization responses. Abbreviations: ER refers to the endoplasmic reticulum, ROOH refers to organic hydroperoxide, and RNS refers to reactive nitrogen species. Adapted from (Mittler et al., 2022).

1.4.3.1 ROS sensing

In plants, several proteins and enzymes can sense ROS levels such as transcription factors: Some transcription factors can directly or indirectly sense ROS levels. For example, NPR1 (NON-EXPRESSOR OF PR-GENES1) senses changes in the cellular redox state and regulates gene expression in response to ROS production (Wolf & Höfte, 2014). ROS can also modulate the activity of protein kinases, such as mitogen-activated protein kinases (MAPKs) and calcium-dependent protein kinases (CDPKs), which in turn initiate downstream signalling events (Meng & Zhang, 2013). Enzymes like catalase, superoxide dismutase (SOD), and peroxidases can sense ROS levels and help in ROS detoxification they are known as ROS scavengers.

In contrast to traditional signal transduction molecules like hormones or peptides, which typically have a specific set of receptors, variations in cellular ROS levels can affect the structure and function of numerous proteins, thereby influencing a wide range of signal transduction pathways. This capacity for ROS to act on multiple pathways is primarily facilitated by oxidative post-translational modifications (oxi-PTMs). As a result, ROS can serve as versatile and dynamic regulators of diverse stress responses (Mittler et al., 2022).

1.5 Nanoparticles

A focus of the work described in this thesis is the plant response to copper nanoparticles. A nanoparticle is a microscopic particle with at least one dimension that is less than 100 nanometers. Nanoparticles can be made of various materials, including metals, ceramics, polymers, and biological molecules. Small dimension sizes give them unique physical and chemical properties compared to larger but equivalent material counterparts, making them useful for a wide range of applications, including drug delivery, imaging, and sensing(Khan et al., 2019). Over the last several decades there's there has been significant interest in inorganic metal nanoparticles, the structures of which can display substantially novel and enhanced physical, chemical and biological properties, different phenomena and diverse functionality all down a consequence of to their nanoscale measurements. The ability and potential exists for these particles to achieve mediate significant processes and selectivity specifically in biological and pharmaceutical processes. (Pal et al., 2007a; Piao et al., 2011).

1.5.1 Aggregates and Agglomerates

Past innovations have showed that different properties of nanoparticles (optical, catalytic and electromagnetic) can be influenced by their shape and size (Burda et al., 2005). There have been increased motivations to synthesis methods that will allow for optimisation and control of the shape and size of the nanomaterial (Jana et al., 2001,Zhou et al., 1999;Sun et al., 2003). Different past innovations have shown that the shape and size can influence different properties of nanoparticles (optical, catalytic and electromagnetic) (Burda et al., 2005). There have been increased motivations to synthesise methods that will allow for optimisation and control of the shape and size of the nanomaterial. (Jana et al., 2001; Zhou et al., 1999; Sun et al., 2003).

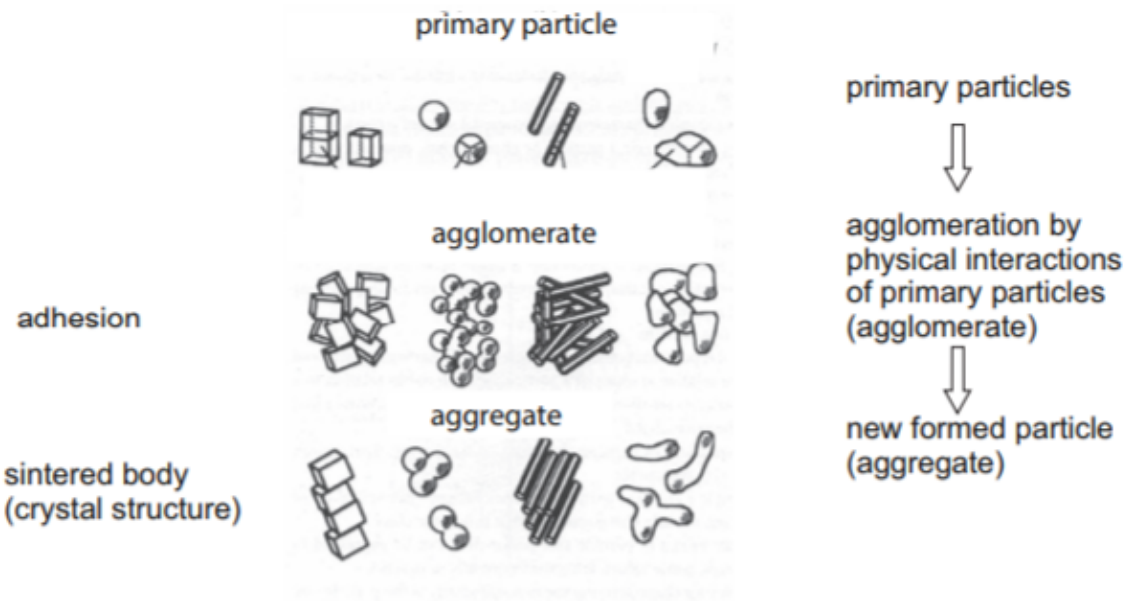

Figure 1.15: Relationships between primary particles, agglomerates and aggregates.(Walter, 2013)

Individual particles occur in different geometrical forms, example they can be spherical, cuboidal or have a 'rod-like' geometric shape or as a bulk material. These primary particles typically agglomerate to larger units (called agglomerates by adhesion, with low energy physical interactions).

An agglomerate is a large assembly of primary particle units (adhered at the corners of the edges), or aggregates with a total surface area not significantly different from the sum of the specific surface areas of primary nanoparticles.

Agglomerates are not fixed or constant units and are capable of alternating shape and size. If certain conditions in the surrounding medium are altered (such as pH, viscosity temperature or pressure) of the surrounding medium, this can result in more varied agglomerates, larger agglomerates can break down into smaller ones or vice versa. Density depends on the original particle unit size distribution (with an assumption of equal geometry and chemical composition) (Vollath, 2020).

Aggregates will form when primary particles begin to form a common crystalline structure. This resembles the formation of aggregates to the sintering process like the formation of compact ceramic solids from smaller primary particles (Ma et al., 2010).

Primary particles agglomerate by adhesion. When crystal growth begins, the agglomerate will be converted into a new larger formed particle (aggregate). Although the original geometry will still be apparent in the aggregate, the particles are fused together. The new surface area of this particle is reduced compared to the sum of its parts.

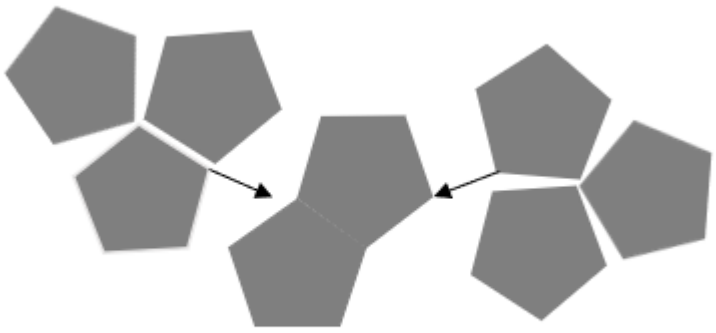

Figure 1.16 : Agglomerate consisting of two different aggregates. Number of original individual primary particles is still apparent in the aggregates.

Figure 1.16 illustrates how smaller aggregates may form agglomerates (Walter, 2013).

Click or tap here to enter text.

1.5.2 Methods for Characterising Nanoparticles

The best methods for characterising nanoparticles is X ray diffraction (XRD), a technique which is generally used to characterise solids.

For solids < 100 nm XRD measurements will not be particularly conclusive as a result of effects of scattering; in this case electron microscopy, and in particular transmission electron microscopy (TEM) with subsequent elemental analysis (EDX), is a suitable method (Kato et al., 2009).

On account of fairly sophisticated sample preparation required, TEM analysis is only of limited suitability for routine measurements.

1.5.3 Nanotechnology and Toxicology:

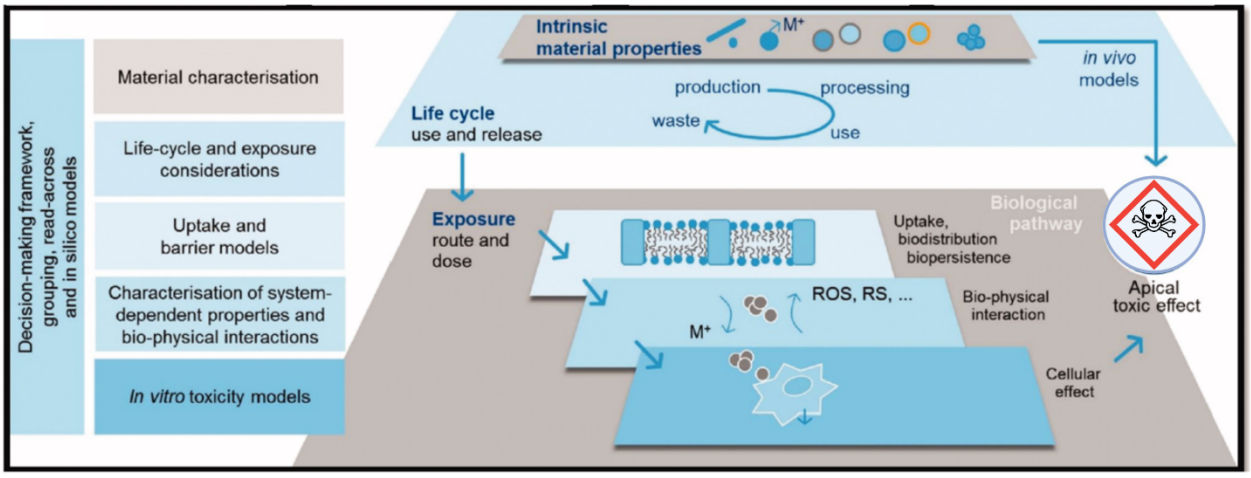

Figure 1.17: Illustration of some of the key scientific considerations to account for when developing a nanomaterial. The boxes on the left hand side detail the tools that are necessary towards a) ensuring that intrinsic properties and nanomaterial life cycle are considered in the prioritisation of nanomaterials taken forward into hazard testing, and b) the successful utilisation of non-animal, mechanistic approaches to predict apical toxic effects (Burden et al., 2017).

Nanomaterials offer numerous advantages across various applications, but concerns regarding human and environmental exposure remain. The UK's NC3Rs convened an expert working group of regulators, academics, and industry scientists to discuss advancing nano safety, aligning these advances with the 3Rs (Replacement, Reduction, and Refinement) in nanomaterial safety testing, and shifting risk assessment focus from hazard-based to exposure-driven approaches (Burden et al., 2017)

1.5.4 Effects of Copper Nanoparticles:

While many different metal nanoparticles have been demonstrated to possess toxic or carcinogenic properties, what is known about the effects of copper nanoparticles on the environment?

1.5.4.1 Copper effects on plant growth

Copper is an essential element that is necessary for vital biochemical processes in plants and animals (Services & Crawford, 2003). Concentrations of bioactive copper (non-bioactive copper is referred to as 'fixed' copper) exceeding a variable threshold can have inhibitory effects on plant growth. Growth inhibition is associated almost entirely with the roots, and negligible amounts of copper are translocated to other parts of the plant (Services & Crawford, 2003; Prantner & Scholler, 2014).

Copper's inhibitory effects have been known about for a long time and were utilised in the first fungicide sprays in the late 19th century. In 1882 Millardet realised grape vines that were sprayed with a mixture of copper sulphate and lime did not lose their leaves throughout a growing season, compared to untreated vines which lost their leaves. The conclusions were that this formulation could control and treat downy mildew in grapevines (Morton & and Staub, 2008).

Copper is usually present in the soil at low concentrations (< 100 ppm), as bioactive copper ions (Cu^{2+}) rapidly complex in the soil unless the pH is below 3, which is itself not very favourable for plant growth. Excess copper can result in copper-induced iron chlorosis. This is caused by competition between iron and copper ions and can be corrected by adding chelated iron fertiliser (Dimkpa, 2014). Copper uptake and concentrations that induce toxicity vary significantly between species (Cataldo & and Wildung, 1978; Heale & and Ormrod, 1982).

CuNPs impact growth and metabolism in different crop species. Germination and growth of rice are impeded by CuNPs, with concomitant oxidative damage (Shaw & Hossain, 2013; Shaw & Hossain, 2013), accompanying increases in the amount of enzymes involved in metal stresses, the reactive oxygen scavenging enzyme system (ascorbate peroxidase, catalase, superoxide dismutase), proline content and lipid peroxidation, in leaves as well as root tissues. Bioaccumulation of NPs has also been evaluated and the interrelated cascade of the enzymatic system with H_2O_2 production was identified. The uptake of NPs in plant leaves was confirmed by scanning electron microscopy, X-ray diffraction, and Fourier Transform Infrared Spectroscopy. Plant growth was found to be diminished with elevated levels of CuO NPs (Rao & Shekhawat, 2016; Kimet al., 2012; Fig. 1.18). Other studies of CuNPs on radish, ryegrass and buckwheat also demonstrate negative impacts on growth and DNA integrity (Atha et al., 2012; Lee et al., 2013).

Effects of NPs on plants can be both apparent and obvious such as in growth suppression or induction enhancement, or much subtler and more difficult to detect – such as effects at the metabolic or physiological levels. Ag and CuO NPs induce both effects, while other NPs such as CeO appear to not show obvious toxicity but generate subtle outcomes that can impact crop quality and safety for consumption (Xie et al., 2022).

Reductions in microbial biomass have been reported when exposed to CuO or ZnO NPs (Rousk et al., 2012). NPs are have also been shown to lower the rate of nitrogen fixation in root nodules of soybean (Priester et al., 2012)

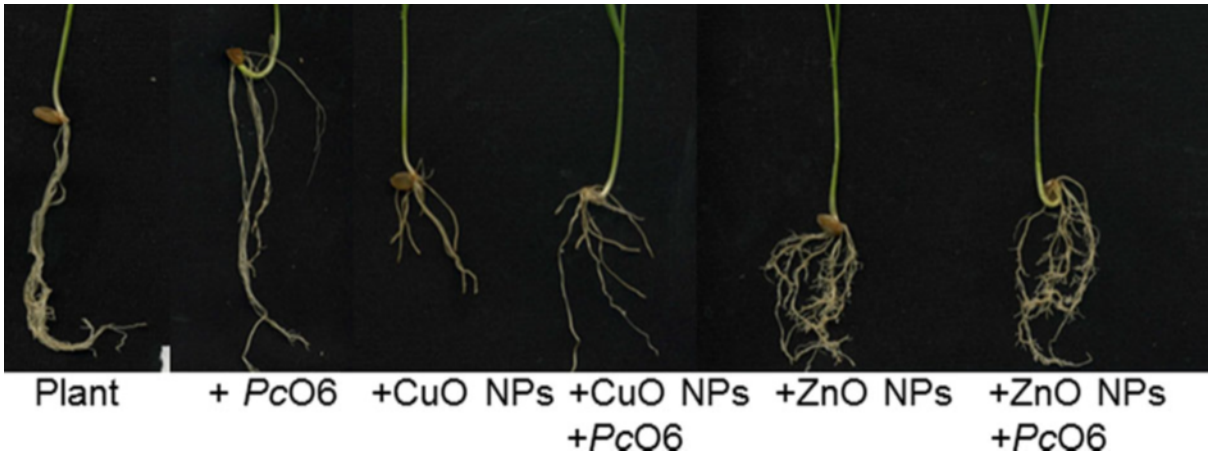

Figure 1.18. : Effect of CuO and ZnO NPs (500mg Cu or Zn/kg) on root growth in wheat (2 weeks after germination). Both NPs reduced root elongation, however, ZnO but not CuO NPs induced the proliferation of lateral roots. Inoculation of the roots with a soil bacterium Pseudomonas chlororaphis O6 (PcO6) has no effect on primary and lateral root growth of the control plants. Root colonization of the NP-exposed plants by PcO6 does not completely negate NP effects on the roots. Adapted from (Dimkpa et al. (2013).

Microarray studies with *E. coli* exposed to Ag NPs indicate that NPs could have transcriptome-wide ramifications in bacteria. Stimulation of expression of stress-related genes and genes for Fe, S and Cu balance was reported (McQuillan, 2012). Other processes affected included those involved in oxidative stress tolerance, metal detoxification, transcription and elongation processes, protein degradation, cytoskeleton remodeling, and cell division.

It was revealed that exposure of *Oryza sativa sativa* L. root to different concentrations of AgNPs resulted in an accumulation of protein precursors, indicative of the dissipation of a proton motive force. The identified proteins are involved in oxidative stress tolerance, Ca^{2+} regulation and signalling, transcription and protein degradation, cell wall and DNA/RNA/protein direct damage, cell division and apoptosis (Mirzajani et al., 2014).

In *Pseudomonas chlororaphis* O6 (Pc06) the expression of genes involved in periplasmic maturation and secretion of fluorescent pyoverdine siderophores was repressed by CuONPs, correlating with reduced production of siderophores in their presence (Dimkpa al. 2012a; 2012b).

NP properties may be altered by different bioenvironmental factors. Presence of organic matter (compost) in soil stimulated bacterial enzyme activities that were otherwise inhibited by Ag NPs (Peyrot et al., 2014).

There are potential adverse effects of NPs on mycorrhizal fungi that have a symbiotic association with plants, and potential larger scale impacts of introducing something like metal NPs to the environment will have on such microbial life, e.g. damage to the hyphal component of mycorrhizae - most trees possess some form of sheathing ectotrophic mycorrhizae (Functional ecology of woodlands and forests, 1992). Many tree species have been shown to

grow more quickly when infected with mycorrhizal fungi (Alexander & Lee, 2005), especially in nutrient deficient soil conditions such as low pH, toxic chemicals, and water stress.

Information of accumulation of NPs and/or component metal in plant tissues is poorly known, and effects on different crops have been studied mainly in vitro within aqueous suspensions (Lin & Xing, 2007; (Kumari et al., 2009; Stampoulis et al. 2009). Experiments have also been performed with agar culture media (Lee et al., 2008), while very few experiments have been carried out utilising soil (El-Temsah & Joner, 2012; Priester et al., 2012).

Toxicological experiments carried out using hydroponic systems and agar media can be enormously useful for understanding NP properties and outcomes in a conceptual experimental format, h. However, there may be unrealistic results since chemical and physical properties alongside biological microbiota ones in the soil can affect how much NPs are bio-actively available to soil biota and crops (Antisari et al., 2011; Antisari et al., 2015).

1.5.5 ROS activation in plants by nanoparticles

A large increase in reactive oxygen species (ROS) expression is a typical trope of exposure to both Ag and TIO_2NPs. Increased ROS activity doesn't always appear to be a negative trait for all species, in some plants it can result in seemingly positive phenotypic effects, particularly for AgNPs, for seed germination and root elongation studies all showing similar results (Cox et al., 2016).

Kaveh et al. (2013) exposed seedlings to silver nanoparticles (AgNPs) up to 20 mg/l (20 nm in size) or silver nitrate (AgNO3) for 10 days (Fig. 1.19). After this period, the leaves and roots were harvested, and the gene expression in the plants was analysed using microarray technology. The results revealed that the genes with increased expression were primarily related to responses to metals and oxidative stress, while down-regulated genes were mainly associated with responses to pathogens and hormonal stimuli.

Interestingly, plants treated only with AgNPs showed a unique up-regulation of specific genes. These genes were involved in various processes, such as salt stress response, defense against insects and pathogens, response to wounding, and the thalianol biosynthetic pathway. This indicates that the exposure to AgNPs had a distinct effect on the plants' gene expression

profile compared to those treated with AgNO3, highlighting the potential impact of nanoparticles on plant biology and stress responses (Geisler-Lee et al., 2013).

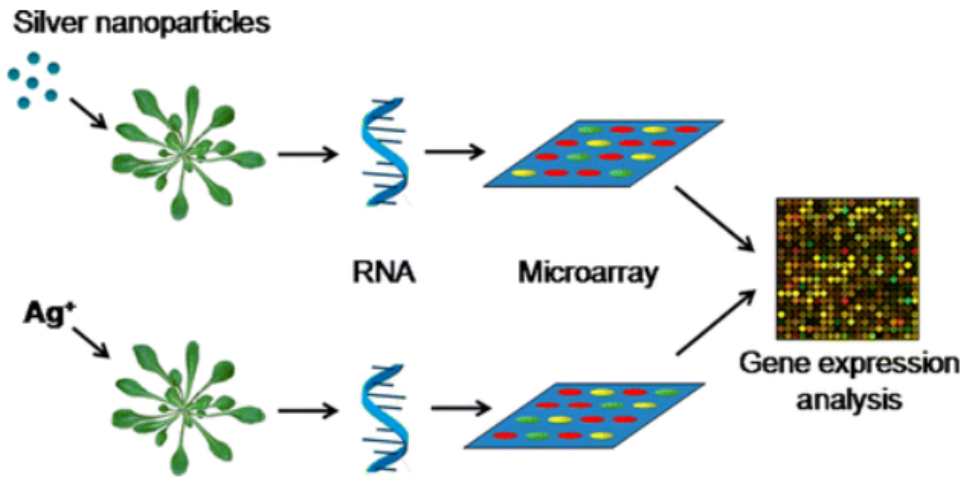

Figure 1.19: Experimental process undertaken by Kaveh et al. (2013) demonstrating treatment of Arabidopsis by silver nanoparticles and silver ions for transcriptome analysis.

In particular, the operon-like cluster of genes related to the thalianol pathway is of interest, because it is thought to be related to plant defense (Field et al., 2011). Interestingly, down-regulated gene expression caused by both Ag+ and AgNPs included genes related to ethylene signalling and response to pathogens and hormonal stimuli, such as systemic acquired resistance (SAR) against fungi and bacteria. Ag release from AgNPs was not explored specifically in this study, and thus it is unclear if results from AgNP treatment were due to the NPs in particular or the release of Ag from the AgNPs. Click or tap here to enter text.

Studies on gene and protein expression following AgNP exposure may reveal pathways involved in the cytotoxicity (Mirzajani et al., 2014). Proteomic studies on *Oryza sativa* (Asian rice) have revealed increased protein precursors for oxidative stress tolerance, calcium regulation and signaling, cell wall/DNA/RNA/protein direct damage, cell division, and apoptosis after AgNP exposure (up to 60 µg ml−1; 18 nm) for 21 days. While toxicity to the plant was not directly studied, these results would be useful for future investigations in determining toxic limits to this species. Based on the proteomic study the authors hypothesized that AgNPs can inhibit cell division by condensing the DNA/protein due to the effect of nanoparticles on the metabolic processes such as protein synthesis/degradation and

apoptosis, but this was not addressed directly in the study. It was not determined if these effects would be based solely on the AgNPs or the ion release, a topic that is widely debated, Mirzajani et al. (2014 and Qian et al., (2013) also showed that antioxidant gene transcripts increased in response to ROS at low levels of stress in *A. thaliana*, but continued levels of high concentration AgNPs (3 mg l^{-1}) was toxic to the seed. *A. thaliana* has shown up-regulation in the expression of sulfur assimilation, glutathione biosynthesis, glutathione S-transferase, and glutathione reductase genes upon exposure to AgNPs when compared to Ag ions. These studies indicate that AgNPs possess the ability to affect gene expression and cause cytotoxicity including genotoxicity, which may be a concern for the ecosystem. Interestingly, it was also demonstrated that AgNPs were more toxic than Ag+ in this experiment, adding new insight to the topic of NP versus ion effects.

1.5.6 Copper Ions Vs Copper Nanoparticles

The primary reason CuNPs were chosen for study was due to the novel nature, applications and commercial opportunities increased understanding of nanoparticles impact on plant growth. It is also easy to produce our own nanoparticles in house. There were 3 main reasons the project opted to proceed with CuNPs over copper ions artificially added to gel matrices.

Enhanced Bioavailability: CuNPs will have a higher surface area compared to larger particles or ions of copper. This increased surface area can enhance the bioavailability of copper, making it easier for plants to absorb and utilize. This improved bioavailability might result in more effective uptake by plants.

Controlled Release: CuNPs can potentially provide a controlled release of copper ions over time. This controlled release can help maintain a stable concentration of copper in the soil, preventing excessive accumulation that may be overly harmful to plants. This feature is particularly beneficial in avoiding toxicity issues associated with sudden releases of copper ions.

Reduced Environmental Impact: The use of nanoparticles can lead to a reduction in the overall amount of material required. This reduction may lead to lower environmental impact, as less copper may be needed to achieve the same desired effect. Additionally, the controlled release feature may reduce the risk of environmental contamination in potential field applications (Ma, 2010).

1.6 Gels / Crosslinkers

Crosslinking gels have garnered significant attention in recent years due to their unique ability to package and stabilize nanoparticles. As multifunctional, stimuli-responsive materials, gels offer numerous advantages in the fields of drug delivery, tissue engineering, and environmental remediation. By utilizing crosslinked polymer networks, customizable systems can encapsulate and release nanoparticles in a controlled manner (Piepenbrock et al., 2010).

Environmental remediation is yet another area where crosslinking gels have proven useful. These gels can be designed to encapsulate nanoparticles with photocatalytic, magnetic, or adsorptive properties, enabling the effective removal of pollutants from water or soil. Once the nanoparticles have captured the contaminants, the gel can be easily recovered and regenerated, allowing for repeated use in cleanup efforts. (Pivetz & Kovalick, 2001).

Despite their many advantages, the use of crosslinking gels to package nanoparticles also presents challenges. The design and synthesis of the gels and their crosslinked networks must be carefully optimized to ensure stability, biocompatibility, and the desired release kinetics (Zuo et al., 2015).

1.7 Aims and Objectives

This project was subdivided into primary aims with associated sub goals:

1) **Increase understanding of uptake and impact of copper nanoparticles into plants and growth impacts**
    a) Perform Growth analysis on wildtype Arabidopsis plants and associated hormone mutants to understand the genetic basis of the response to CuNPs.
    b) Carry out transcriptomic analysis to understand the transcriptonal basis of the response to CuNPs.
    c) Carry out proteomic analysis to understand the proteomic basis of the response to CuNPs.
    d) Carry out mass spec analysis to measure uptake of particles.

2) **Produce a minimal viable product (MVP) for the inhibition of root growth by copper nanoparticles for use in the water industry.**
    a) Experiment with different crosslinking agents to package copper nanoparticles.

b) Scale the experiments to replicate results in larger models (such as willow trees and rapeseed oil).
c) Gain environmental metrics (leakage rate into surrounding soil, other impacts on biome).
d) Investigate patenting product if sufficiently unique.
e) Carry out a larger pilot study outside the lab.

A project design figure template was drawn up (see figure 1.20).

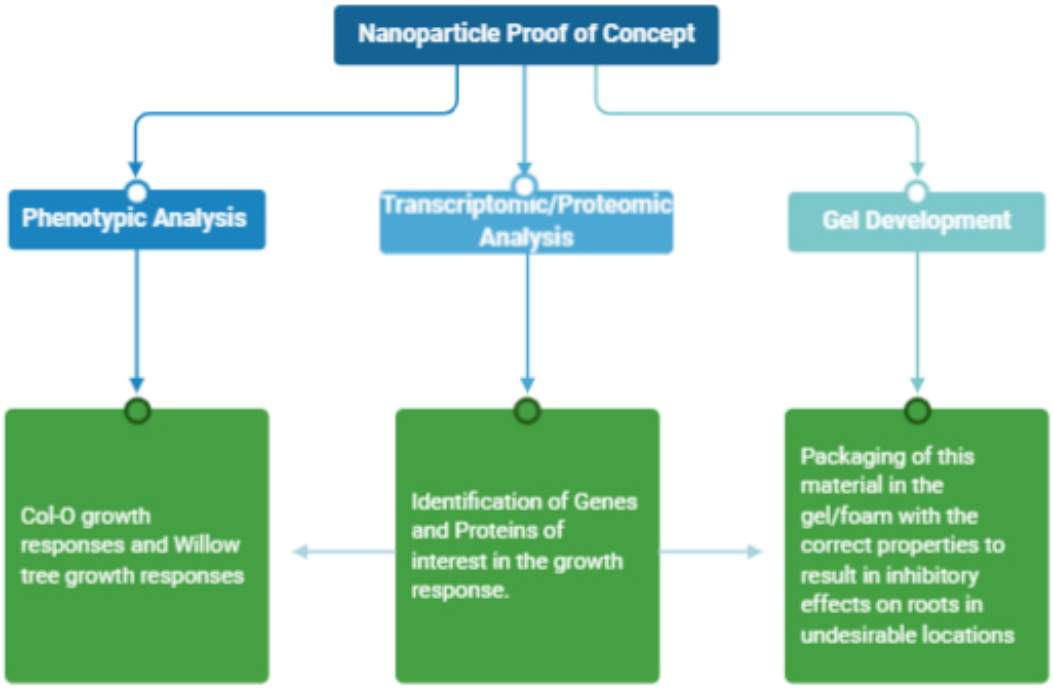

Figure 1.20: *The project pathway starting with the recognition of phenotypic implications of nanoparticle treatment, analysis from both a transcriptomic and proteomic perspective in order to understand the biological basis for the inhibition, feeding into our approach to develop a packaging concept for the gel*

Product design is intended to be circular so that results gathered in phenotypic and transcriptomic study can be fed into gel design and product development concurrently.

Chapter 2 Materials and Methods

2.1 Materials

2.1.1 Chemical Suppliers:

Chemicals/Nanoparticles were acquired from Sigma or Fisher Scientific unless otherwise stated. Gelling agents and supplies were provided by Intelligent Gels Ltd.

2.1.2 Plant Materials:

Seeds of *Arabidopsis thaliana* wild type (WT, Columbia (Col-0)) were supplied from existing lab stocks Arabidopsis thaliana seeds were obtained from laboratory stocks originally obtained from Lehle Seeds (Texas, USA).

Mutants were obtained from the Nottingham Arabidopsis Seed Centre (*Eurasian Arabidopsis Stock Centre (NASC)*) or existing lab stocks unless otherwise stated.

All mutants and reporter lines are in the Col-0 background and from lab stocks unless otherwise stated (Table 2.1).

2.1.2.1 Trees:

Salix viminalis (Common Osier Willow) 1-Year-Old Bare Root - 60-80cm was supplied by Hedge Nursery (Herefordshire). Clones from cuttings of these trees were produced for subsequent work.

2.1.2.2 Reporter Lines:

CYCB1;2::GUS lines were acquired from the Nottingham Arabidopsis Stock Centre (NASC) (http://arabidopsis.info/); *proPIN1: PIN1: GFP* (Benková *et al.*, 2003) and *proPIN2::PIN2::GFP* courtesy of Ben Scheres (Wageningen University, the Netherlands).

Hyper: Hyper consists of a circularly permuted YFP (cpYFP) inserted into the regulatory domain of the *Escherichia coli* hydrogen peroxide-binding protein (OxyR), and is a H_2O_2-specific ratiometric, and therefore quantitative, sensor (Hernández-Barrera et al., 2015; Belousov et al., 2006). The line was acquired courtesy of Marc & Heather Knight (Durham University, UK)

2.1.2.3 Mutant Lines:

SALK Lines (O'Malley et al., 2015) were acquired from NASC. The following list includes all the SALK mutants that were used in experimental work.

Uniprot ID	Gene	Name	NASC Code
Q9SRP6	At3G03420	Mitochondrial inner membrane protease ATP23	SALK_093517
Q9LD47	AT1G12520	Copper chaperone for superoxide dismutase, chloroplastic/cytosolic CCS	SALK_105330
Q39101	AT5G01600	Ferritin-1, chloroplastic FER1	SALK_055487
O78310	AT2G28190	Superoxide dismutase [Cu-Zn] 2, chloroplastic: CSD2	SALK_041901
P24704	AT1G08830	Superoxide dismutase [Cu-Zn] 1	SALK_109389
Q8LG89	AT2G02850	Basic blue protein	SALK_031458
Q39161	AT1G01580.1	Ferredoxin-nitrite reductase, chloroplastic NIR1	SALK_119575
Q96511	AT5G64100.1	Peroxidase 69, PER69	SALK_137991
Q42403	AT5G42980	Thioredoxin H3	SALK_112552
O82089	AT3G56240	Copper transport protein CCH:	SALK_042628
Q9ASR1	AT1G63440.1	HMA5 Heavy metal ATPase	SALK_030895

Table 2.1: Table of SALK lines utilised in this project

2.1.3 Genotyping Insertion Lines:

T-DNA insertion lines can be genotyped by carrying out two simultaneous PCR reaction mixtures utilising 3 different primers, a forward and reverse primer and a primer specific to the insertion region of the T-DNA (Fig. 2.1). The two different reactions were staged as follows: one with the forward and reverse primers, the second PCR with only the reverse primer and the insertion primer. In these reactions and primer setups, each band should be a different size, allowing a qualitative assessment to be made when visualised. Plants that are homozygous for the insertion would display one band whereas heterozygous reveals two different bands. There are details of the primers used included in Table 2.2. Primer sequences listed in Appendix I.

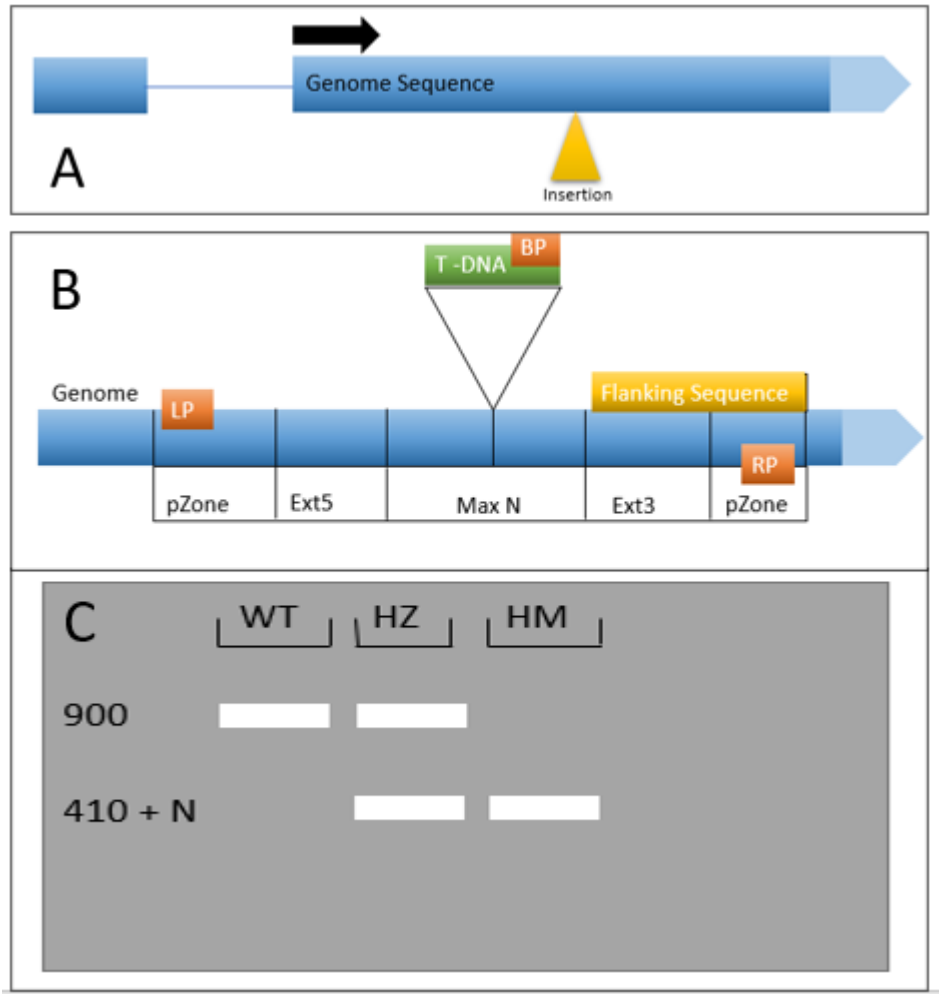

Figure 2.1: Pipeline for genotyping T-DNA insertion SALK lines. (A) The ID of the insertion site in the genome. (B) Primer design centres on using LP (left primer) and RP (right primer) and BP (T-DNA border primer) to amplify the specified region of the sequence. pZone is the region primers are picked up (approx. 100bp), Ext5 and Ext3 are regions that do not pick up primers between the pZone and MaxN, MaxN is the maximum number of base pairs in the primer which is 300bp. (C) This refers to the banding present in each situation, WT = wildtype, HZ = Heterozygous and HM = Homozygous, N = 0-300bp.

NASC Code	Gene	Associated Gene Name	Insertion Specific Primer	WT Band Size	Mutant Band Size
SALK_093517	AT3G03420	ATP23	LBb1.3	1104	491-791
SALK_105330	AT1G12520	CCS	LBb1.3	1070	509-809
SALK_055487	AT5G01600	FER1	LBb1.3	1186	556-856
SALK_041901	AT2G28190	CSD2	LBb1.3	1163	491-791
SALK_109389	AT1G08830	SOD1	LBb1.3	1176	503-803
SALK_031458	AT2G02850	ARPN	LBb1.3	1115	556-856
SALK_119575	AT1G01580.1	NIR1	LBb1.3	1121	487-787
SALK_137991	AT5G64100.1	PER69	LBb1.3	1184	597-897
SALK_112552	AT5G42980	Thioredoxin H3	LBb1.3	1032	458-758
SALK_042628	AT3G56240	CCH	LBb1.3	1035	493-793
SALK_030895	AT1G63440.1	HMA5	LBb1.3	1115	552-852

Table 2.2: Insertion lines with locus details, gene name, primers used for genotyping and expected bands if the insertion is present or absent.

2.2 Plant Tissue Culture

2.2.1 Seed Sterilisation:

To prevent contamination, seeds were sterilised in the following way. Seeds were decanted into Eppendorf tubes, labelled and dated. These were washed with a 70% v/v ethanol solution for 1 minute to de-wax the seeds. Ethanol was then removed (it's important to use separate pipette tips to avoid cross-contamination and transferring seeds to the wrong Eppendorf). The tubes were then filled with a bleach 20% v/v solution, inverted several times to dislodge seeds stuck at the bottom of the tube. The tube was left for 15 minutes. The bleach was then

removed, the seeds washed 4 times with sterile deionised water (sdH_2O) and left in 1ml sdH_2O. The seeds were then placed in the dark at 4°C to stratify, to encourage synchronous germination.

2.2.2 Culture Media

Plates of ½ Murashige & Skoog (MS) medium (Murashige & Skoog, 1962) contained 2.2g/L of MS, 8g/L of agar, pH adjusted to pH 5.7 with 0.1M or 1 M KOH. There was no sucrose in the mixture.

2.2.2.1 Copper Nanoparticle enriched MS media

To make up media containing 25 nm diameter CuNPs (obtained from Sigma) the weight of the media to which the CuNPs was being added was first determined. To make up a concentration of, for example, 20 µg/ml CuNPs in 235g of agar, the following calculation was made:

$235g\ x\ 0.02$ = 4.7

$\frac{4.7g}{150ml} * 200ml$ = 6.26ml needed to be added to make up the required concentration. This was then mixed using the ARE250 conditioning mixer on settings 2:30 spin at 1600 RPM and a 30 sec defoam at 400 RPM. Solutions containing 20, 40, 60 and 100 µg/ml of CuNPs were made.

2.2.2.2 Gels and Nanoparticles:

Copper nanoparticles of 25 nm diameter were utilised. Gels utilised in this project include:

Guar Gum
A17 (Platinum Base)
HD seal base (aluminium base)
Xanthan Gum

Table 2.3: Gels and crosslinkers used

CuNP concentrations in these gels were calculated as described in section 2.2.2.1.

The sample was then sonicated (in an RS pro ultrasonicator) for 3 minutes to ensure a homogenous suspension of CuNPs.

When analysing the particle size with zetasizer nano series for DLS (dynamic light scattering) a sample of particles dissolved in ethanol was prepared in a glass cuvette. The results of this were contrasted with TEMs results to ensure accuracy as DLS can be less accurate than TEMs is for quantifying size and morphology of nanoparticles.

2.2.3 Plant Growth Conditions:

All the CuNP assay and root architecture experiments were conducted utilising solid growth media in growth rooms or growth cabinets which were set under long-day conditions:

16 hrs light: 8 hours dark at 22ºC (c. 3000 lux).

Seeds were grown for 6-10 d.p.g. on vertical sterile 10x10 cm square Petri dishes containing 50 ml half-strength MS media and sealed with micropore tape.

CuNP-enriched media for assays used a vertical sterile 10x10cm square Petri dish with a strip removed and replaced with the copper NP media solution (Figs. 2.2, 2.3). A sterile scalpel was used to remove a section of the agar so it could be replaced with agar that was mixed with a different concentration of CuNPs.

Magenta pots were also used for some root architecture studies.

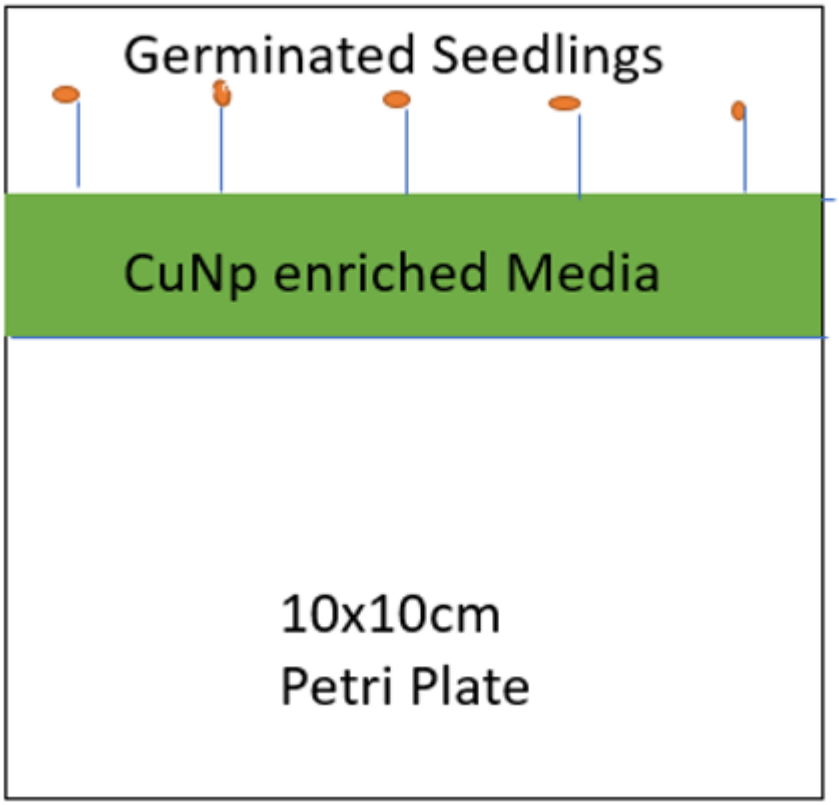

Figure 2.2: Diagram depicting CuNP-enriched strip 'barrier' for Arabidopsis seedlings

Arabidopsis seeds were germinated on these plates, using 3 replicate plates per experiment and one on control plate lacking CuNPs to observe the effects of the CuNPs on roots.

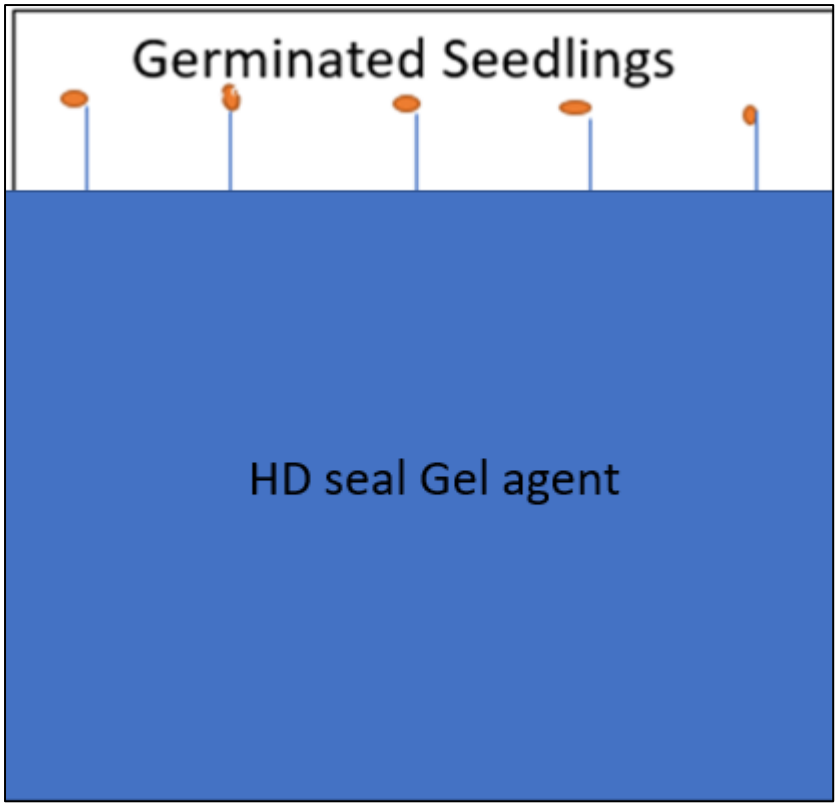

Figure 2.3: Diagram depicting growth setup for HD seal gel barrier on a 10x10 cm Petri dish.

2.2.3.1. Soil-grown seedlings

For soil growth, seedlings were grown in 24-well trays in a 5: 1 mixture of Gem multipurpose compost and horticultural silver sand (LBS Horticulture Ltd, UK). Plants were grown at 21°C, with a 16-h photoperiod. The systemic insecticide Intercept (Levington Horticulture Ltd, UK) was applied to all compost (60 mg per 24-well tray) before seeds were sown.

2.2.3.2 Hydroponics

For RNA seq analysis, plants were grown in a hydroponic setup as per Conn et al. (2013) using media and aeration techniques from Chivasa et al. (2005). Growth is comparable with standard media but allows easier separation of roots from shoot material and allows greater control of the time points for inoculation with copper nanoparticles.

Cultures were prepared in quadruplicate for each treatment, and every replicate contained at least six plantlets. Seeds were sown on 7 cm-diameter, 1 cm-thick polyurethane foam discs soaked in MS medium (0.22% w/v MS salts, adjusted to pH 5.7 with KOH/HCl). The discs were

placed in sterile phytatrays (Sigma-Aldrich) and incubated under a 16-h-light/8-h-dark cycle at 22°C. One week later, when the seeds had germinated, and the roots had penetrated the foam, 30 mL of sterile MS medium was added to the phytatray, which caused the foam discs to float. The trays were transferred to a shaking platform (25 rpm) under the same environmental conditions. During the second week, the plant roots had emerged through the other side of the foam and submerged in the nutrient-rich medium. Media changed each week. After 14 d of culture, uniform plants selected to be treated with CuNPs treated and harvested at 3 h and 24 h.

2.3 Root Architecture Analysis

2.3.1 Primary and Lateral root length

Vertical plates were placed onto an Epson Expression 1680Pro flatbed scanner (Epson, UK) set at a resolution of 800 dpi. Measurements were taken of the primary root length (PR), lateral root (LR) number, quantified using ImageJ software (Schneider et al., 2012) alongside a plugin for ImageJ UI called 'smartroot' (Shahzad et al., 2018). The software tool is designed around the quantitative analysis of the root system architecture (RSA). ImageJ data were utilised in both R and Excel to generate figures.

2.4 Statistical Analysis

All statistical analysis was carried out using R. 0.05, and 0.01 significance levels were used for data significance. Graphics were produced in R, biorender and graphpad prism.

2.5 Proteomics

A quantitative proteomic analysis was carried out to quantify the change in protein content of plant tissues following treatment with 20 µg/ml CuNPs (Sigma), outlined in Fig. 2.4.

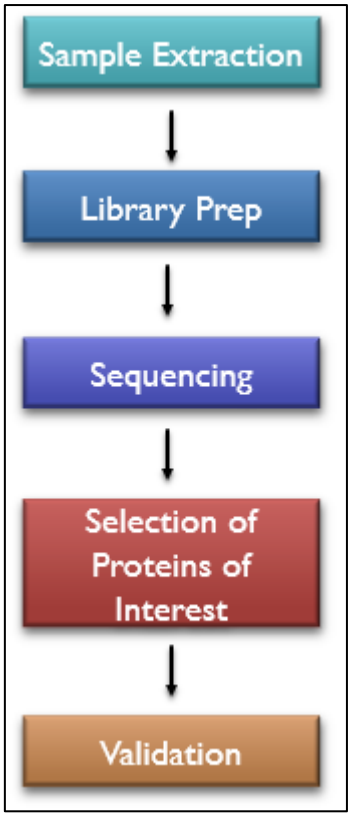

Figure 2.4: Pipeline of SWATH Proteomics process

Three biological replicates for each treatment (20 µg CuNPs and controls lacking CuNPs at 6 and 8 days) were carried out. Plants were treated as follows: two series of seedlings were collected, one before reaching the CuNP layer at 6-days and the second collection when the seedling roots touched the CuNP-containing bottom layer (at 8-days). Roots were cut from the seedlings and then transferred into new microcentrifuge tubes. These tubes were stored at -20°C until protein extraction.

2.5.1 Protein Extraction and Purification

During the protocol, care was taken to avoid sample contamination. Gloves were worn and open tube time minimised. Roots were kept frozen while the urea/SDS extraction buffer was added, to minimise the time for proteases to be active before denaturation in detergent/urea. Mortars and pestles were cleaned in detergent and rinsed, or soaked in 1M NaOH for 30 min and rinsed thoroughly in deionised water; and dried before use.

Root samples were stored in liquid nitrogen until just before grinding. Tubes were kept on ice until the addition of buffer. Grinding was carried out while the material was thawing out and

still frozen. To 0.1g root tissues was added 200 µL of extraction buffer (EB, 4 M urea, 1% SDS) and the tissues were ground. No sand was added. When the tissue was dispersed/ground, the pestle was rinsed with 120 µL of EB and added into the same tube. Tubes could be stored at room temperature in this solution since proteins are denatured. The solution was centrifuged at 20,000 x g for 5 min at RT and the supernatant removed to a new tube. The protein concentration was quantified using a Bradford assay (Bradford, 1976). Samples were then snap-frozen, and the pellets were stored at -20°C until further analysis. Prior to proteomic analysis samples were warmed to room temperature.

2.5.2 Sequencing

Three replicate SWATH-MS runs were performed for each extracted sample, giving 36 LC-MS acquisitions in total. 4757 proteins were detected and quantified using PeakView software (Sciex) across all samples. The SWATH library used for identification and relative quantification was generated using PeakView from a ProteinPilot.group result file. This combined data from 20 data-dependent acquisitions of fractionated peptides resolved by high pH reverse phase chromatography from Arabidopsis root extracts +/- copper nanoparticles. More than 7000 proteins were identified from an Arabidopsis database (SwissProt 0217) at 1% global FDR by ProteinPilot 5.0 during library construction.

For each experimental treatment, nine extracted fragment-ion chromatogram peak area values were obtained for identified proteins. MarkerView 1.2.1 software (Sciex) was used to perform multiple pairwise comparisons of replicate peak areas for two states using t-tests. False discovery rates (FDR) in resulting SWATH-experiment outputs was controlled by applying the Benjamini- Hochberg procedure for multiple comparisons (*Multiple comparisons - Handbook of Biological Statistics*). This was done automatically using R code to order P values, calculate Benjamini-Hochberg critical values and select proteins with resulting significant P values. The FDR (false positive discovery rate) values were set at 5%, 10% and 20% in separate calculations and results tabulated. Comparisons of Cu-8-day to control. Non-significant proteins were removed from further analysis, and the resulting list of proteins was ordered on fold-change between the states, highest to lowest.

It can vary between different experiments what fold-change of protein expression is considered significant but for this work the fold change threshold of >2.0 or <0.5 for up- and down-regulated proteins was considered significant

Proteomic global experiments are considered to indicate pathways or avenues of interest for further research. GO ontology over-representation, compared to whole database entries using software such as Panther (Thomas et al., 2003) was the method used to highlight biochemical pathways that respond to treatment.

2.5.3 Validation: Western Blotting

Seedlings were grown as per the hydroponic methodology described in section 2.2.3.2. 50 mg tissue samples were taken and then homogenised with bugbuster reagent and a 2-minute run in the Tissuelyser. This method was modified for tree samples of *Salix virminalis*, as these samples were significantly harder to break down and lyse due to higher levels of lignin in their cell walls compared to small leafy plant tissues. These structural components provide rigidity and support to the plant, making them more resistant to mechanical disruption, also as a result of differing cell size and density: Tree tissues tend to have larger, thicker-walled cells with a higher density compared to herbaceous plant tissues. This makes it more difficult to break open the cells and release their contents, including proteins.

Western blotting (Fig. 2.14) is a widely used technique in molecular biology and enable specific proteins in a sample to be detected. Western blots can be used to confirm the presence and abundance of proteins that have been previously identified such as in proteomic analyses. To perform a western blot, proteins are first separated by size using gel electrophoresis. The proteins are then transferred onto a membrane (transfer blot) and probed with a specific antibody that recognizes the protein of interest. The antibody binds to the protein and following a second incubation with a visualisation antibody, allows it to be visualized using a mechanism of detection such as chemiluminescence

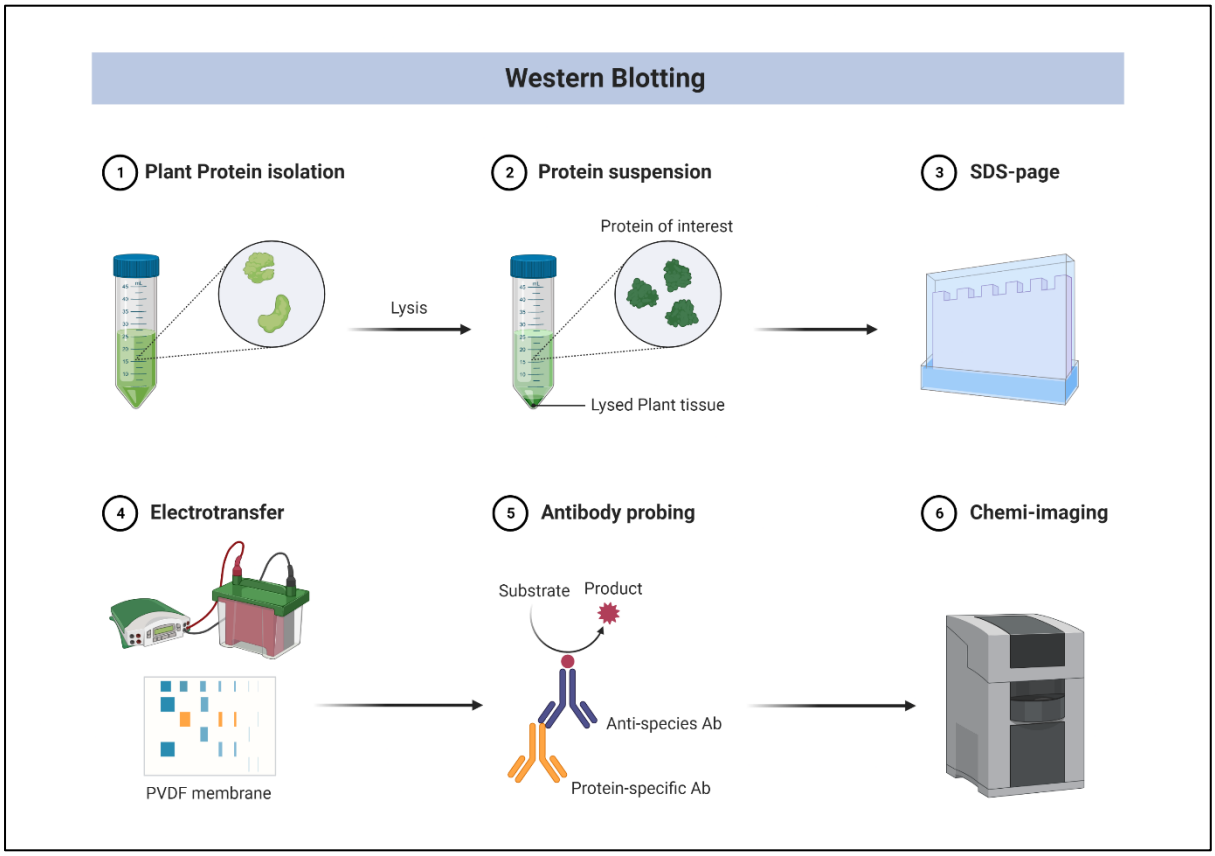

Figure 2.14: The western blot process – homogenisation followed by suspension and SDS-Page, followed by a transfer process and a primary then secondary antibody incubation process.

By comparing the results of western blots with the results the SWATH analysis, validation of the identity and abundance of proteins is possible. If the western blot confirms the presence and abundance of a protein that was identified. it provides additional confidence in the accuracy of the proteomic analysis. If the western blot shows a different result than what was predicted by the proteomic analysis, it can signal potential issues with the mass spectrometry-based method and may warrant further investigation.

For validation of proteomic results, several identified proteins were targeted for detection using western blotting.

Seedlings were grown as previously described in the proteomics experiment (Section 2.5). Proteins were extracted using the same methodology described in, followed by SDS PAGE electrophoresis.

Western blotting was carried out according to the Sigma protocol (*Western Blot Protocol | Immunoblotting Protocol | Sigma-Aldrich*). Membrane transfer was carried out using tank transfer, followed by immunodetection. Primary antibodies used are listed in Table 2.4, all primary antibodies are anti-rabbit, secondary antibodies are chicken anti-rabbit. Dilutions ranged between 1 to 10 in 1000 depending on commercial instructions for each antibody; for the secondary antibody the concentration was always 1 in 1000.

Antibodies:

UNIPROT ID	**Gene/Protein Name**
Q9LD47	CCS Copper Chaperone
P21276	FSD1 Superoxide Dismutase
O78310	CSD2 Superoxide Dismutase 2
Q8LG89	ARPN Basic Blue Protein
E3TC62	ACT2 Actin

Table 2.4: List of Antibodies used.

After induction with the primary antibody for one hour with agitation, the blot was washed with PBS twice for 10 min before being placed in a secondary antibody solution, incubated with agitation for one hour at room temperature. The blot was then washed in PBS for 10 min and repeated twice with fresh buffer. After this step, the blot was visualised with fluorescence detection chemiluminescence. Images at a range of exposures were taken between 15 seconds and 120 seconds.

2.6 Histochemical Staining

2.6.1 GUS Staining:

The reporter gene beta-glucuronidase (GUS) was utilised as a histochemical reporting gene to visualise the location of promoter activity in transgenic plants (Jefferson et al., 1987). Enzyme activity was localised by incubating plant tissue in the substrate X-Gluc, which converts to an easily visualised blue precipitate in cells expressing the GUS enzyme.

Seven day-old seedlings were incubated in a staining solution of 1 mM N-N dimethylformamide in 100 mM sodium phosphate (buffer solution pH 7.0), 10mM EDTA, 0.5mM potassium ferrocyanide, 0.5mM potassium ferricyanide, 0.1% v/v Triton X buffer in a 1.5ml Eppendorf tube as described in Topping and Lindsey (1997). Seedlings were incubated for up to 16 h at 37°C. The GUS reaction was halted by adding 100% ethanol solution (which also washes out the chlorophyll in the plant). Seedlings were rehydrated with deionised water, then placed on a microscope slide with chloral hydrate solution as a clearing agent (Hoyer's solution (Berleth & Jurgens, 1993)). A coverslip was placed on top of the tissue and slides before imaging.

2.6.2 DAB staining

In vivo imaging of H_2O_2 formation in shoots was investigated by histochemical staining with 3,3 – diaminobenzidine (DAB) (Thordal-Christensen et al., 1997). DAB forms a water-insoluble brown precipitate when it is oxidised. In the presence of hydrogen peroxide, DAB can readily oxidise, and hydrogen peroxide is produced when a plant produces ROS. The protocol followed is '*DAB-Peroxidase Substrate Solution (Brown) | Protocols Online*'. DAB solution was added to plants grown on standard 1/2MS medium in the presence of different concentrations of CuNPs. The entire seedling was soaked in DAB (50 µM concentration) for approximately 5 min and vacuum infiltrated. Seedlings were washed with PBS and set on a slide for later visualisation.

2.6.3 NBT staining

In vivo detection of ROS generation in the shoot and the roots was done by staining with nitroblue tetrazolium (NBT) (Sigma Aldrich) which forms dark blue insoluble formazan when it reacts with superoxides (Fryer et al., 2002). As described in Section 2.6.2, seedlings were harvested and placed in a solution of NBT for 3-5 min before being removed and fixed for visualisation.

2.6.4 Clearsee technique

A useful technique for clearing and visualising plant material under the microscope has been described by Kurihara et al. (2015). Tissues were vacuum infiltrated with 4% paraformaldehyde solution for 30 min. Clearsee solution (urea 25%, sodium deoxycholate 15%, xylitol 10%) was then added to the seedling after it was washed in PBS and incubated at

room temperature for 4 d. The seedling was then fixed in PFA, added to the slide and visualised.

2.6.5 Cellrox staining

Cellrox deep red was used to visualise ROS. 500-1000 nM (50 to 1 dilution) was added to roots and vacuum infiltrated for 30-60 min before two washing steps with PBS. Samples fixed with PFA before setting on slides for visualisation.

2.7 Nucleic Acid Isolation

2.7.1 Genomic DNA Extraction

A crude and rapid extraction is all that is necessary for genotyping DNA, this was done as per the method described by Edwards et al. (1991). All steps were completed at room temperature: The lid of a 1.5 ml Eppendorf tube was used to pinch out a disc from a young leaf into the tube. A small pestle was utilized to grind the leaf material in the tube without buffer for approximately 15 seconds. Then, 400 µl of extraction buffer (200 mM Tris-HCl pH 7.5, 250 mM NaCl, 25 mM EDTA, 0.5% w/v SDS) was added, and the mixture was vortexed for 5 seconds. The tube was spun for 1 minute at full speed in a microfuge to pellet the debris. Next, 300 µl of the supernatant was transferred into a fresh 1.5 ml Eppendorf tube (avoiding debris from the pellet). After that, 300 µl isopropanol was added, mixed, and left at room temperature for approximately 2 minutes. The mixture was spun for 5 minutes at full speed in a microfuge to pellet the DNA. All the supernatant was removed, and the pellet was dried gently (for instance, by incubating the open tubes at 37°C for a few minutes). The pellet was not allowed to get too dry, as it would have been challenging to redissolve the genomic DNA. Then, 100 µl T10E1 was added, and the pellet was dissolved by gentle shaking (vortexing was avoided). After resuspending in 30µl sterile water, the DNA pellet could be stored at -20°C until needed.

2.7.2 RNA Extraction, Library prep and Sequencing Protocol

RNA extraction, use Dynabead Protocol: below

RNA extraction was carried out according to the Dynabead® protocol (ThermoFisher).

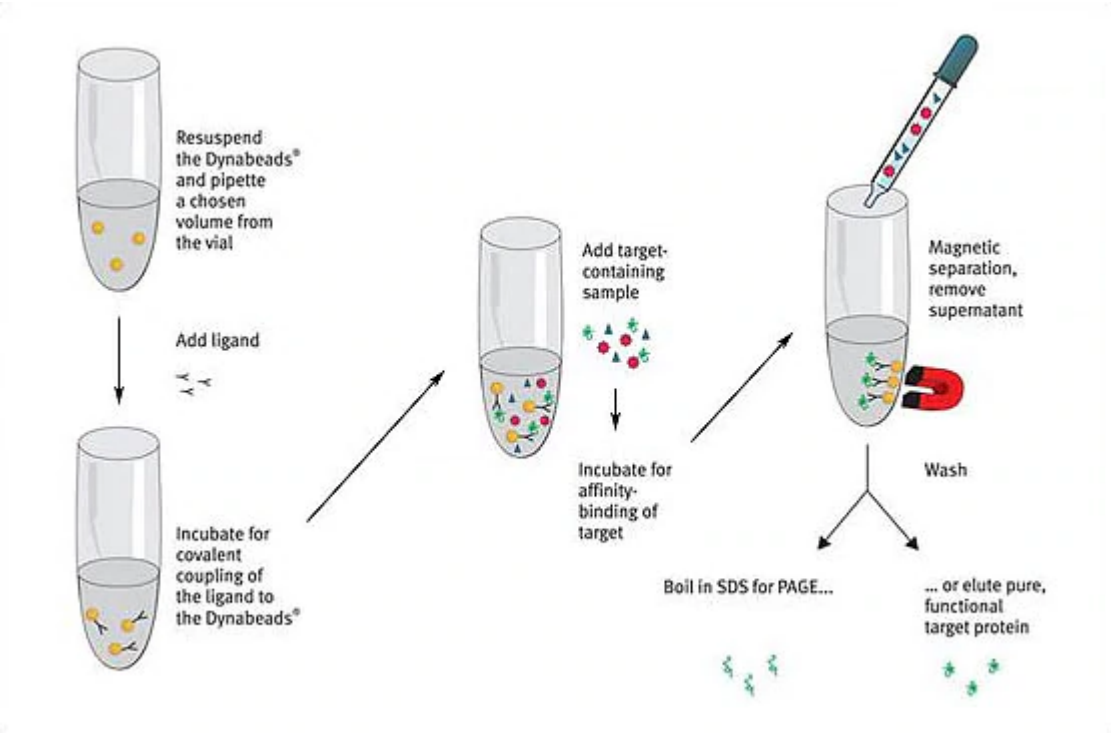

Figure 2.5: Diagram of Dynabead extraction protocol principle.

2.7.2.1 Protocol Wash and Resuspend Dynabeads®

Dynabeads® were suspended in the vial by vortexing for 1 minute. The desired volume of beads was transferred to a falcon tube. An equal volume of binding buffer (at least 1ml) was added and mixed. The tube was placed in a magnet for 1 minute and the supernatant was discarded. The tube was removed from the magnet and the now washed beads were resuspended in the same volume of binding buffer from the first washing step.

2.7.2.2 Preparation of Lysate from Animal Tissues, Plants, and Cells

This protocol was optimized for approximately 20-50 mg of plant material. The amount of was aliquoted while frozen. Using more than the recommended amount would reduce the mRNA yield and purity. The frozen tissue was ground up in liquid nitrogen. The tissue material was kept frozen at all times to avoid RNA degradation. The still frozen powdered plant material was transferred to a homogenizer with 1ml of Lysis/Binding buffer and used for 1-2 minutes until the tissue was completely lysed. Rapid and efficient lysis in the buffer prevented unnecessary mRNA degradation. The lysate was centrifuged for 1 minute in a microcentrifuge to remove debris. The lysate could then be used for mRNA purification and isolation; at this step, the lysate could also be frozen and stored at –80°C for later use.

2.7.2.3 Isolation of mRNA from Crude Lysate

Using the Dynabeads described in section 2.7.2.1, the solution was removed from the tube and the lysate (section 2.7.2.1) was added. The beads and the lysate were mixed. Time was allowed for binding by rotating on a mixer for 5 minutes at room temperature. The annealing time was increased if the mixture was particularly viscous. mRNA annealed to the oligo dT sequence during this step. The tube was placed on a magnet for 2 minutes and the supernatant was removed at this point. The beads were washed twice at room temperature using the magnet, one time with 1ml washing buffer A, and again with 1ml washing buffer B. The beads were thoroughly resuspended in washing buffers to avoid any possible contaminants, and the supernatant was completely removed between washing steps. The bead-bound isolated mRNA was used in solid-phase cDNA synthesis, so one extra wash with Washing Buffer B (500 µL) was performed followed by one wash with the enzymatic buffer used in cDNA Synthesis.

2.7.2.4 Verification of RNA Purity

mRNA sample purity was analysed a NanoDrop® ND-1000 spectrophotometer (ThermoFisher Scientific) and Agilent 2200 TapeStation. RNA samples with RNA integration number equivalent (RIN^e) above 7.0 were utilised downstream for library preparation.

2.7.2.5 Library Prep and Sequence

Library preps were completed utilising NEBNext® Ultra™ Directional RNA Library Prep Kit for Illumina® protocol for use with NEBNext Poly(A) mRNA Magnetic Isolation Module (NEB #E7490) following the manufacturer's instructions (NEB, Hitchin, UK). The total mRNA starting material of between 100 ng and 1 µg was used. The isolated mRNA was fragmented and primed, cDNA was synthesised, and end prep was performed. Samples were packaged and sent to Novogene for Agilent QC and sequencing.

2.8 Plant Stress Assays

2.8.1 Plant growth measurements:

After 14 days of treatment, the plants were carefully removed from their plates and washed with deionised water to remove the remains of the growth media. The primary root length of

the control and CuNP-exposed plants were measured using a scale. The fresh weights of the roots were calculated using a digital balance.

2.8.2 Chlorophyll detection:

As per Lichtenthaler (1987), leaf samples (50 mg) were incubated in 10 ml ethanol (95% v/v) under dark conditions at 4ºC for 48hr. The absorbance of the supernatant was measured at 664.2 nm (A664.2) and 648.6 nm (A648.6) with a UV spectrophotometer. The experiment repeated 3 times and total chlorophyll content expressed as mg g^{-1} fresh weight (FW).

2.8.3 β Carotenoids

Carotenoid content was determined according to Lichtenthaler (1987). Leaf tissue (50 mg) was homogenised in 5 ml chilled methanol (100%) and the homogenate was centrifuged for 15 min. The absorbance was recorded at 470 nm and content was expressed as mg g^{-1} FW

2.8.4 Peroxidase Enzyme activity:

100 mg tissue was homogenised in 1 ml 10 mM phosphate buffer, centrifuged at 14,000 rpm for 20 min. 25 µl of supernatant was mixed with 25µl 50 mM H_2O_2, 5µl of 250 mM guaiacol, 195 µl of 125mM dimethylglutaric acid. This was incubated at room temperature for 15 min. Sample absorbance at 470 nm was then recorded using a spectrophotometer. Results were expressed as MDA mg^{-1}FW. Malondialdehyde (MDA) is a common biomarker used to measure lipid peroxidation, a process that occurs when reactive oxygen species (ROS) attack polyunsaturated fatty acids in cell membranes, resulting in cell damage. MDA is a by-product of lipid peroxidation and is often used as an indicator of oxidative stress and cell damage in various biological systems (Sevanian & Hochstein, 1985).

2.8.5 Lipid Peroxidation

Lipid peroxidaiton (LP) was measured according to Heath & Packer (1968). 100 mg plant tissue samples were homogenised in 5 ml of 0.1% (w/v) trichloroacetic acid (TCA) solution and then centrifuged at 7000 x g for 10 min at room temperature. Approx. 2 ml of supernatant was then mixed with 2 ml of 0.67% (w/v) thiobarbituric acid (TBA) and subsequently heated to boiling for 30 min, then immediately cooled by running cold water on the flask. Absorbance of the supernatant was recorded at 532 nm and 600 nm using a UV-spectrophotometer. The MDA concentration was calculated using the extinction coefficient 155 mM/cm.

2.8.6 In vivo detection of hydrogen peroxide

Quantitative measurement of hydrogen peroxide content in shoots and roots of the control and CuNP-exposed plants were determined using the hyperline mutants (Hernández-Barrera et al., 2015) and quantifying hydrogen peroxide content under confocal microscopy. Seedlings were first cleared using the above mentioned Clearsee technique (Kurihara et al., 2015) and then fixed with PFA for visualisation by confocal microscopy.

2.8.7 In vivo detection of superoxide

The in vivo detection of superoxide content in roots of the control and CuNP exposed plants was done by treating with dihydroethidium (DHE Sigma,) as described by (Feigl et al., 2013). H202 content was detected by treating with a 3' (p-hydroxyphenyl) fluorescein (HPF Invitrogen)

2.8.8 ICP-MS – Determination of CuNP uptake

Typically 30 mg of root material and 60 mg of shoot material, sampled following CuNP or control treatment, was digested with H_2O mixed with 800 µL of 65% Suprapur HNO_3 (Merck Millipore), before dilution (1 in 5) with 2.5% Suprapur HNO_3 for analysis. Quantitative analysis of metal content was determined using an X-SERIES-2 ICP mass spectrometer (Thermo Fisher Scientific) following calibration with elemental standards that were matrix-matched to the sample. Internal standards (beryllium, silver, and indium) were used to correct for any variations in analytical performance. Mean and SD values were determined from three biological replicates for each treatment. Graphs were made in R and graphpad.

2.9 Microscopy

2.9.1 TEM

Transmission electron microscopy (TEM) was utilised to quantify and visualise the size and morphology of CuNPs, including those that were bought from Sigma Aldrich and those that were synthesised in-house in the Chemistry Department (Prof. Chris Greenwell).

Samples suspended in ethanol were placed on the TEM grid and visualised. A dilute suspension of the metal nanoparticles was prepared in ethanol to ensure that particles were well-dispersed. A few drops of the nanoparticle suspension were placed onto a TEM grid allowing the liquid to evaporate, and leaving a thin layer of nanoparticles on the grid. Negative

staining with heavy metal salts (uranyl acetate) can be performed to enhance contrast but this is optional.

ImageJ tools was used to measure the size and morphology of the nanoparticles. Parameters such as particle diameter, shape, and size distribution were considered (Schneider et al., 2012).

2.9.2 Light Microscopy:

Histological tissue sections were examined using a Zeiss Axioskop compound microscope (ZEISS International) alongside a QImaging Retiga-2000r camera using a x10 or x20 objective.

2.9.3 Confocal Laser Scanning Microscope

Either a Zeiss 800 or 880 with Airyscan software (*Imaging Biological Samples with ZEISS LSM 800 and LSM 880 - Microscopy*) was used for visualising fluorescent markers in seedlings. Hyperline seedlings were subject to the Clearsee infiltration method. Whole seedlings were removed from plates with forceps and either stained or placed directly onto microscope slides. The hypocotyl and cotyledons were removed with a razor and root tips suspended in sdH20 before placement of a cover slip (22x22mm, 0.16-0.19mm thick). Cover slips were sealed and secured with clear nail polish. To prevent damage of the specimen by compression of the lens on the cover slip, two additional thinner cover slips (22x22mm, 0.13-0.17mm thick) were placed either side of the root before placement of the top cover slip to act as a buffer. Imaging was done using the x20 and x40 objective lenses and appropriate excitation wavelengths for the fluorophores.

2.9.4 Analysis of Confocal Images

Images were exported as TIFF files and opened using ImageJ (Schneider et al., 2012). Fluorescence differentials were measured using quickdraw and analysis tools with the protocol referenced. (*Measuring cell fluorescence using ImageJ — The Open Lab Book v1.0*,). Images from at least 3 repeats were analysed for each sample.

The following table explains the different laser settings utilised for the different stains and lines used in confocoal microscopy

Dye / Flurophore	**Laser Setting**
Calcofluor White	405nm HeNe
HyPer	405nm and 488nm (blue + green channels)

CellRox Deep Red	633nm HeNe

Table 2.5: Laser settings for different dyes or flurophores

2.9.4.1 Analysis of Hyper reporter lines

Hyper consists of a circularly permuted YFP (cpYFP) molecule inserted into the regulatory domain of the Escherichia coli hydrogen peroxide (H2O2) sensor. When exposed to H_2O_2 the excitation peak of the attached cpYFP is shifted from a max of 420 to 500 nm, while the emission peak remains unchanged at 516 nm (Belousov et al., 2006). Due to this H_2O_2-induced change in excitation wavelength, Hyper can be used as a ratio-metric biosensor. For Hyper analysis, images were acquired with two channels, one using the 405nm laser excitation (blue channel) and one at 488 (green channel). Separate TIFF files of each channel were exported for analysis in ImageJ. Image Calculator was used to generate a ratio-metric image of green channel to Blue channel for analysis

2.9.4.2 Analysis of CellRox DeepRed

Images of CellRox DeepRed stained roots were obtained for both the root tip A brightfield image was also taken using the Electronically Switchable Illumination and Detection module (ESID) to reveal cellular organisation of the root and aid with analysis. Fluorescence was measured as mean grey value in 32-bit images containing only the DeepRed channel. Images containing both DeepRed fluorescence and ESID image were used as a reference and to select regions of interest.

2.10 ICP-MS

Intercoupled plasma mass spectrometry (ICP-MS) was used to quantify the level of copper nanoparticles present in the media in which plants are grown, it was also used to quantify Cu uptake from the environment and how well those Cu particles were translocated from root tissue to shoot tissue. It is a powerful analytical technique used for the detection and quantification of trace elements, ICP-MS offers high sensitivity, accuracy, and a wide dynamic range.

The resulting mass spectrum contains information about the elements present in the sample, including their isotopes, and their concentrations. By comparing the sample's mass spectrum to calibration standards, the concentrations of trace elements in the sample can be accurately determined (Mittal et al., 2017).

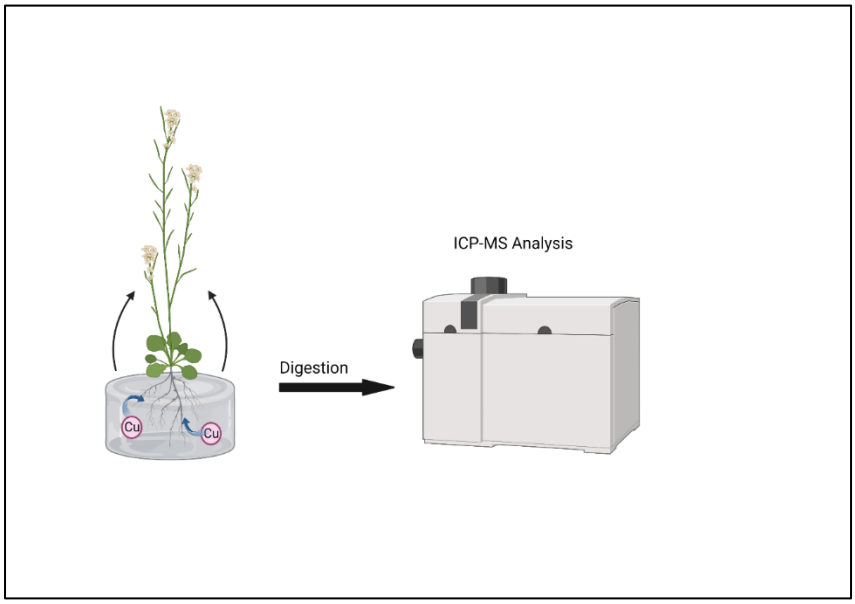

Figure 2.6: Depicting ICP-MS experimental design – growing Arabidopsis seedlings in Cu-enriched media before digestion and analysis in the ICP-MS facility.

2.10 Polymerase Chain Reaction (PCR) assays

2.11.1 Primers

Primers were designed using the SALK primer design tool (*T-DNA Primer Design*). Primers synthesised by IDT (*Custom DNA oligo products*).

Salk Line	**LP**	**RP**
SALK_093517	CTTCTCGAAGACACGTTTTGC	TGATTCCAAAACCCTAAACCC
SALK_105330	AGTAGCAGAATTCAAAGGCCC	GCAGCACATAACATTTCACATG
SALK_055487	TCCTCACGTTCACACTATCCC	GAGACAGAGCCAACTCCATTG
SALK_041901	TTCACCATACCAAGCCATCTC	CAATTGAGAGAGACGGACCTG
SALK_109389	TCTTCTGAAGATGCCTTGACC	GTCATTACCCTTTCCGAGGTC
SALK_031458	AGGGAATTGCTTCACAAAATG	ATCAGCCAATCGTGTTCTTTG
SALK_119575	ACCGGGTAAAGCTCTTGAATC	AACAGCCATGCTGGTATTCAG
SALK_137991	AAAAAGAAAAATGGGTCGTGG	TCATTTTGACCATCGACTTCC
SALK_112552	TTCGCTGGTAAATCCATCAAC	TTACATTGGAAGCTTTGGGTG
SALK_042628	ACTGGTCGGCTTGGTCTTTAC	TCAGGAGAACTGAAACCTTGG
SALK_030895	TGGAGGAATCTCCATGTTCTG	AACAAATTTAAGCCAGCATCG

Table 2.6: List of SALK primers used and sequences for both left (LP) and right (RP) primers

2.11.2 Standard PCR

Conditions of PCR amplification and gel electrophoresis can vary from one gene to another, but the standard setup was as in Table 2.7, which indicates a MyTaq™ (Bioline) mix.

10' Reaction Buffer	**4 µl**
Bioline Taq	0.1 µl
Forward Primer	0.5 µl
Reverse Primer	0.5 µl
Template	0.4 µl
RNase/DNase free water	14.5 µl

Table 2.7: PCR mix

The following program was run using a Proflex PCR system from applied biosystems.

	Temperature (°C)	**Time**	**Number of cycles**
Initial denaturation	95	1 min	1
Denaturation	95	15 s	25–60
Annealing	(variable depending on primer sets)	15 s	
Extension	72	15 s	
Final extension	72	1 min	1
Refrigerate	4	Hold	1

Table 2.8: Program used for the standard PCR reaction

2.11.3 Gel Electrophoresis

After completion of PCR reactions, DNA samples were separated by size using gel electrophoresis to identify PCR products.

A 3% agarose gel (1.5% regular agarose, 1.5% low melting agarose) was prepared in 1 x TAE (242 g Tris, 37.2 g Na2EDTA.2H2O, 57.1 ml glacial acetic acid, in 5 L) and contained ethidium bromide (0.5µg/ml) for DNA staining. This produced a 1% w/v gel. To allow good resolution of the bands, thin (0.7mm) combs were used for the wells. From the PCR reaction, 5µl was taken, and 2µl of loading dye was added. The electrophoresis gel was run for approximately 40 minutes at 80 Volts. Finally, the gel was photographed in the transilluminator BioRad Gel-Doc 1000.

2.11 Bioinformatics

2.12.1 Analysis of RNA Seq Data

Illumina HiSeq2500 data were processed according to a trimming and data annotating workflow pipeline starting with Trimmomatic (Bolger et al., 2014), which cuts and trims out lower quality reads from the raw data. TopHat2 (Kim et al., 2013) was utilised to align reads against the TAIR database.

After this step, SAMtools was used (Li et al., 2009). This tool indexes and sorts binary sequence alignment files (BAM) and then converts them into accessible (SAM) files. HTseq 0.6.1 (Anders et al., 2015) was used to quantify and estimate gene counts, followed by Edge R (McCarthy et al., 2012; Robinson et al., 2009) normalised gene counts and estimated differential expression patterns between different sample groups. P values of ≤ 0.05 and $\log_2$ fold change in excess of ≥ 0 were taken to be significant.

2.12.2 Software and online tools used in Analysis of Transcriptomic and Proteomic Data

Tool	Reference / Website	Function
BioVenn	(http://www.biovenn.nl/index.php) (Hulsen *et al.*, 2008)	Comparison and visualisation of biological lists using area-proportional Venn diagrams
AgriGO	(http://bioinfo.cau.edu.cn/agriGO/) (Du *et al.*, 2010; Tian *et al.,* 2017)	Gene Ontology analysis tool
REViGO	(http://revigo.irb.hr/) (Supek *et al.*, 2011)	Summarisation and visualisation tool for long lists of gene ontology terms
Plant Reactome	(http://plantreactome.gramene.org/) (Naithani *et al.*, 2017)	Database of plant metabolic and regulatory pathways, allowing analysis of gene sets
AtTFDB-Arabidopsis transcription factor database	(http://arabidopsis.med.ohio-state.edu/AtTFDB/) (Yilmaz *et al.*, 2011)	Identification of transcription factors & links to interaction tools (GRG-X)

GSEA	(https://www.gsea-msigdb.org/gsea/index.jsp	interpreting gene expression changes in the context of known biological pathways, gene ontologies
STRING	(https://string-db.org/) (Szklarczyk *et al.*, 2017)	Database of known and predicted protein-protein interactions
PANTHER GO	http://www.pantherdb.org/(Thomas et al., 2003)	Annotation software for Gene ontology aimed explicitly at the proteomic data input
TAIR (The Arabidopsis Information Resource)	(https://www.arabidopsis.org/)	Database of genetic and molecular biology data for the model higher plant *Arabidopsis thaliana*
UniProt	(http://www.uniprot.org/)	Comprehensive, high-quality and freely accessible resource of protein sequence and functional information.
Biorender	https://app.biorender.com/biorender-templates/figures	Creating visual diagrams

Table 2.9: list of tools used in the analysis.

2.12 Model Pipe Experimental Setup

To set up a suitable growth model to measure the effectiveness of gels on root growth and ingress in pipe systems, it was decided to coat pots with different gel materials and quantify root biomass and root architecture after 12 weeks.

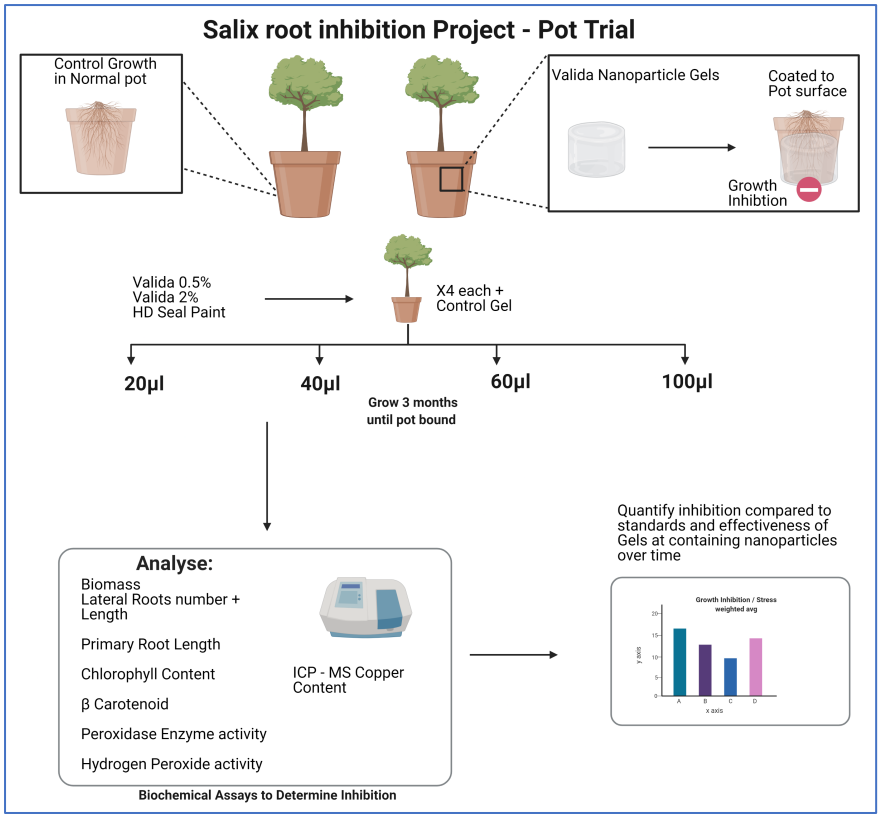

Figure 2.7: Diagram of experimental procedure for willow tree growth trial.

Experiments carried out on Arabidopsis roots were also performed on the willow root tissue, to gather comparable results. Modifications such as additional grinding time were used, given the different properties of woody roots.

Chapter 3 Effects of CuNPs on Root Phenotype

3.1 – Introduction

Root architecture is most simply defined as the spatial configuration of a plant's root system in the soil (Fitter, 1987). This geometric arrangement is made up of plant variables including the root type, how each root is spatially positioned and oriented via modulation in root angle, rate of growth and degree of lateral root branching; and is regulated by a number of gene networks (Kochian, 2016). When plants are exposed to quantities of copper nanoparticles there is an impact on root architecture that appears to be a dosage-dependent response. When present in minute quantities there have been measured benefits to the growth of the plant, while higher concentrations can have an inhibitory growth effect (Nair & Chung, 2014). At these inhibitory concentrations primary root (PR) growth in Arabidopsis is decreased and there is an increase in lateral root (LR) density in the seedling. Biomass is also decreased in treated plants while several other indicators of plant stress and reactive oxygen species production are upregulated.(Xie et al., 2022)

Arabidopsis thaliana accession Col-O was chosen primarily for this analysis in this part of the prject due to consistent root architectural configuration and the wealth of genetic resources available. This chapter describes the analysis phenotypic effects of root development in treated plants alongside indicators of plant stress and ROS production to verify existing literature (Nair & Chung, 2014; Shaw & Hossain, 2013; Jia et al., 2020). The effect of CuNP exposure was also investigated through the use of ROS system mutant SALK lines and in willow tree root systems.

Aims:

To understand the impact of different concentrations of CuNPs on the phenotypic growth of *Arabidopsis thaliana*.

3.2 Results

3.2.1 Root growth changes in the PRs in response to treatment by CuNPs

To determine the effects of CuNPs on Arabidopsis root growth, plants were grown for 14 days post-germination (d.p.g.) in different concentrations (up to 100 μg/ml) of CuNPs. Untreated seedlings show a reduction in primary root growth rate at day 8 (Fig. 3.1). In response to CuNPs, Col-0 seedlings show reduced primary root growth at all concentrations tested over a growth period of 12 days compared to untreated controls (Fig. 3.1). The rate of CuNP-treated root growth slowed more than controls by the 8th day, which was shortly after coming into contact with a CuNP-enriched medium on day 7.

As seen in Fig. 3.1 every treatment with CuNPs resulted in significant inhibition of primary root growth. While 20 μg/ml treatment partially restored growth after 10 d, the higher concentrations completely inhibited primary root growth. There is a point of the plateau of inhibition, where an increase of CuNP concentration achieves diminishing returns in phenotypic effect. Fig. 3.2 shows growth expressed as a percentage of the total previous day's growth and indicates the rate of growth drops off for most of the treated plants but with indications of some recovery in the case of 20 μg/ml treatment. Plants treated with high concentrations of CuNPs show little or no growth by 10 days.

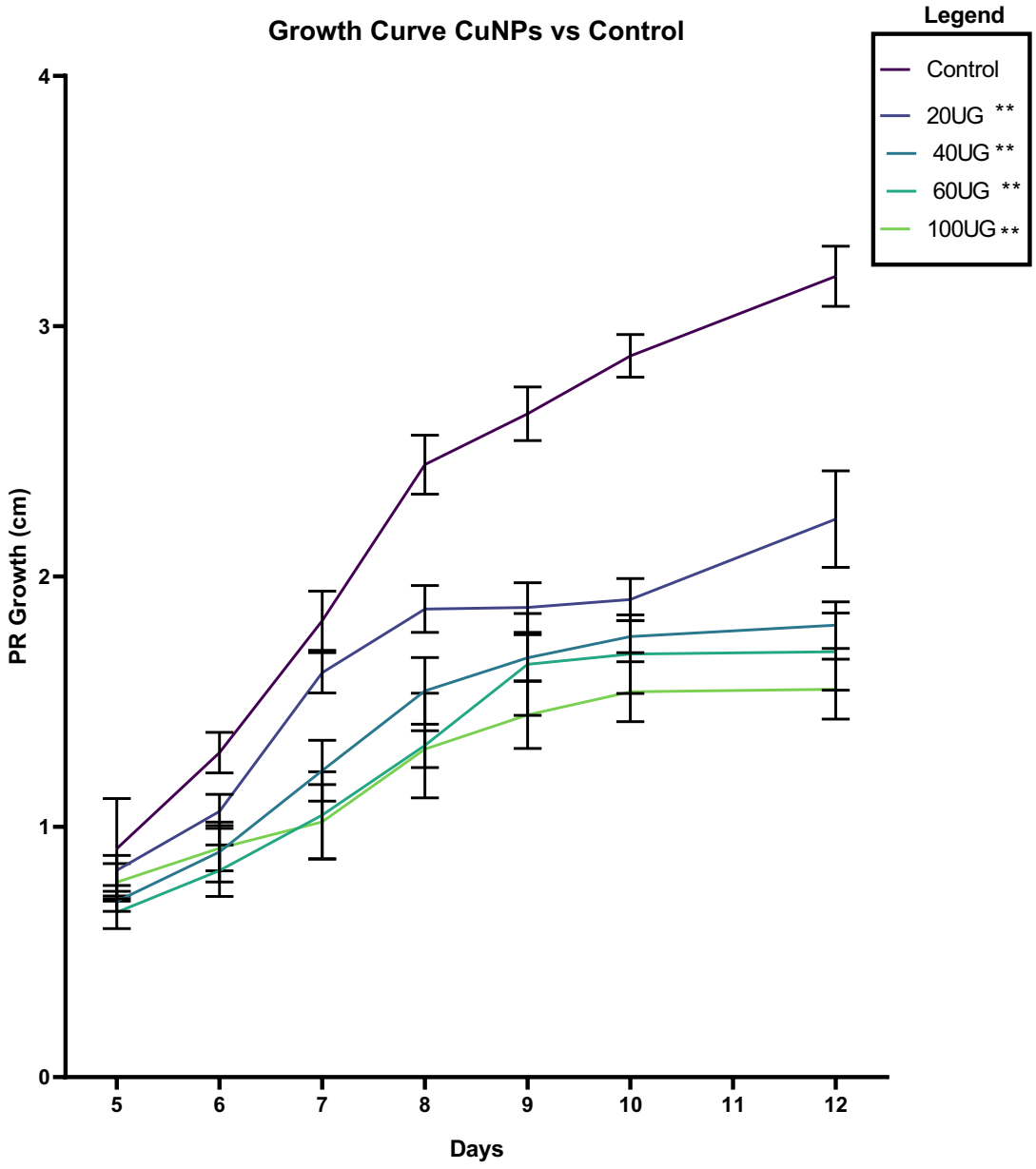

*Figure 3.1: Primary Root growth measurements of Arabidopsis with different treatments of copper nanoparticles (CuNPs). The minimum sample size is 7. * Represents P value < 0.05. ** represent P value <0.01. (B) Image of seedlings at 21 days on 0, 20 and 40 µg/ml CuNPs.*

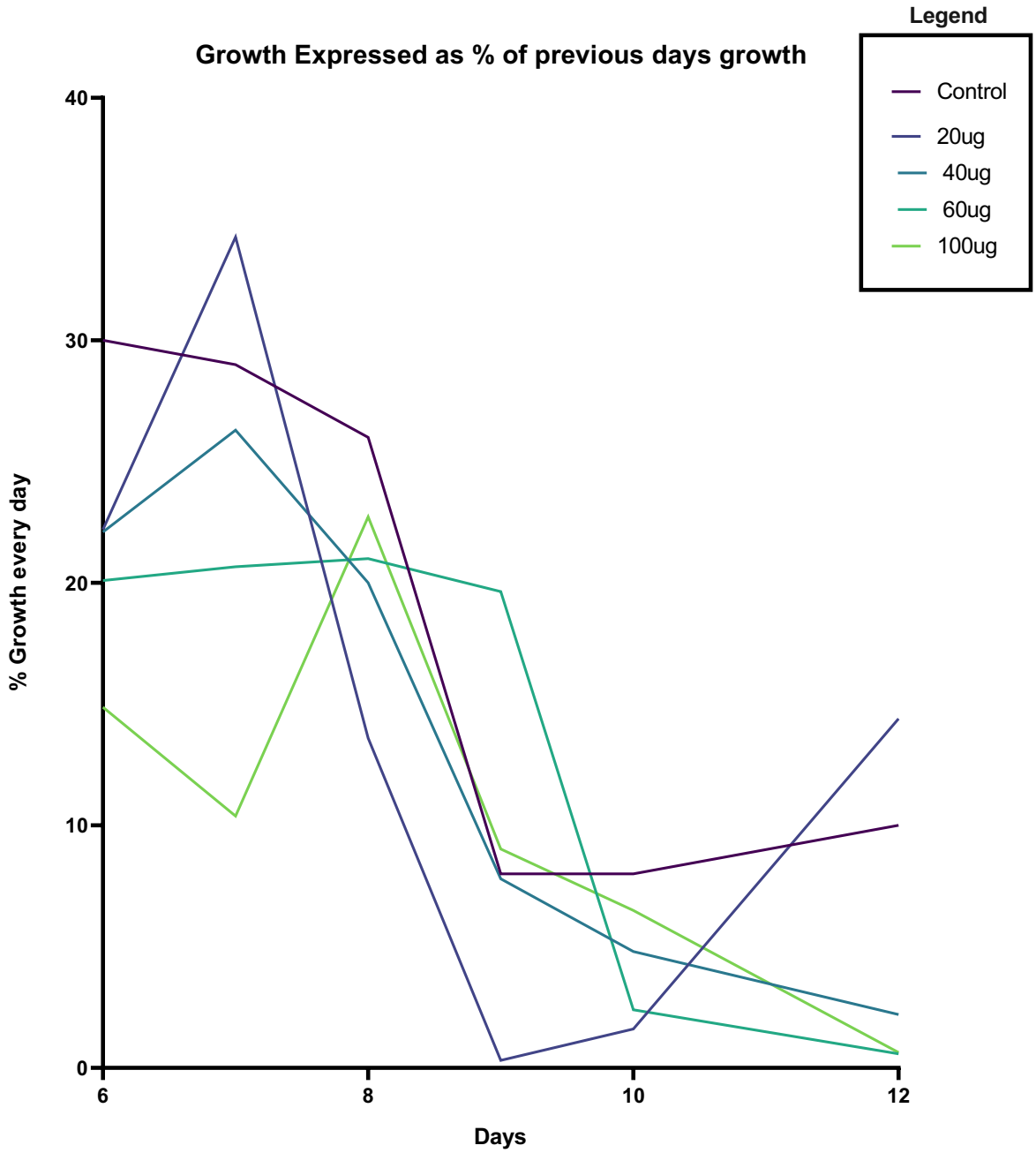

Figure 3.2: Primary root growth expressed as a percentage of previous day's growth.

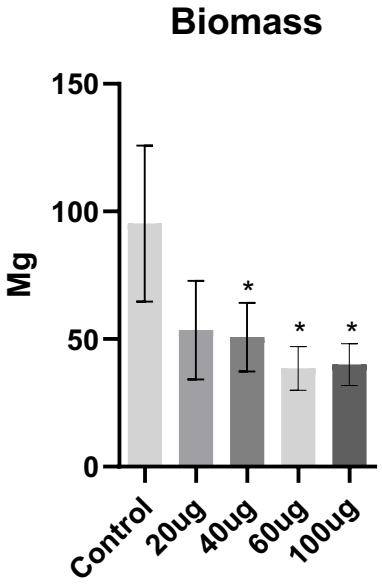

*Figure 3.3 Mean biomass of each seedling at 14 days old, including treatment with CuNPs (0 - 100 ug/ml) for 7 d. 40 ug * P = 0.0373, 60 ug * P= 0.0117, 100ug * P = 0.0130*

Biomass was measured after seedlings had been grown in the presence or absence of CuNPs. By 14 d.p.g. the roots of treated seedlings had been exposed to CuNPs for 7 days.The results in Fig. 3.3. show that CuNPs at 40 - 100 ug/ml significantly affected total biomass as root growth is inhibited at these concentrations.

3.2.2 Root growth changes in the LRs in response to treatment by CuNPs

The number of LR and their length was measured at 14 days of growth in vertical plates in the presence and absence of CuNPs. This was done in order to determine if primary root inhibition had an impact on lateral root development and would provide evidence of a hormonal redistribution. At 14 d.p.g. the roots had been exposed to CuNPs for 7 days. As seen in Fig. 3.4 (A) the number of lateral roots initiated was relatively unchanged compared to untreated controls when grown at different CuNP concentrations. However, Fig. 3.4 (B) shows a clear increase in lateral root length in treated plants at all CuNP concentrations compared to control. In Fig. 3.4 (C) and Figure 3.5 we see an proportional decrease in the length of root hairs as the concentration of CuNPs increases.

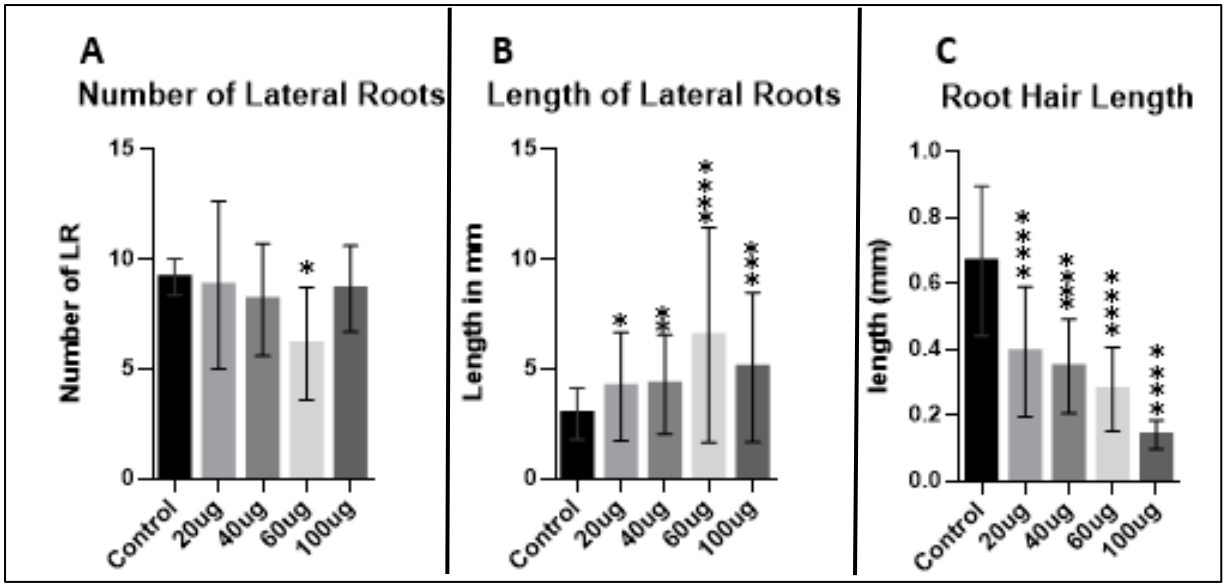

*Figure 3.4 Phenotypic metrics of plants grown in Cu enriched media : (A) Mean number of lateral roots in seedlings either untreated (control) or treated with different CuNP concentrations. (B) Mean lateral root lengths in seedlings either untreated (control) or treated with different CuNP concentrations (C) Mean root hair lengths in seedlings either untreated (control) or treated with different CuNP concentrations. All measurements were taken at 14 d.p.g. Sample size minimum 15. * indicates P <0.05. ** = P <0.01. *** = P<0.005. **** = P<0.0001*

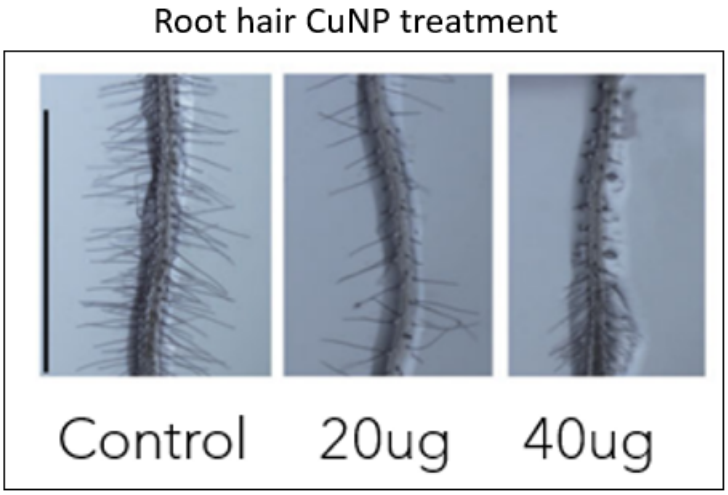

Figure 3.5: Light microscopy image of root hairs Exposure to 0, 20 or 40 ug/mL CuNPs; higher concentrations alter the root hair length and density of the root significantly at 14 d.p.g.

3.2.3 Biochemical Assays

Biochemical assays are essential tools for studying plant responses to abiotic stress. By measuring various biomolecules and enzymatic activities, we can assess the physiological status of plants and determine their tolerance and adaptation mechanisms.

Hydrogen peroxide is a ROS produced in plants under stress conditions. High levels of H_2O_2 can damage cellular components, while its accumulation can indicate oxidative stress. H_2O_2 assays, such as the colourimetric assay using potassium iodide, are used to measure H_2O_2 content in plant tissues. This information can help assess the level of oxidative stress experienced by the plant.

Lipid peroxidation is a process by which ROS attacks unsaturated fatty acids in cellular membranes, resulting in the production of the compound malondialdehyde (MDA). Lipid peroxidation is an indicator of oxidative stress and cellular damage. The thiobarbituric acid reactive substances (TBARS) assay is a widely used method for measuring MDA levels, which reflects the extent of lipid peroxidation in plant tissues(Tsikas, 2017).

Peroxidases are enzymes that help neutralize ROS, playing a key role in the plant's antioxidant defence system. Peroxidase activity can be measured using colourimetric assays, such as the guaiacol peroxidase assay. By assessing peroxidase enzyme activity, researchers can determine the plant's ability to cope with oxidative stress and evaluate its stress tolerance mechanisms (Kwasniewski et al., 2013; May et al., 1996).

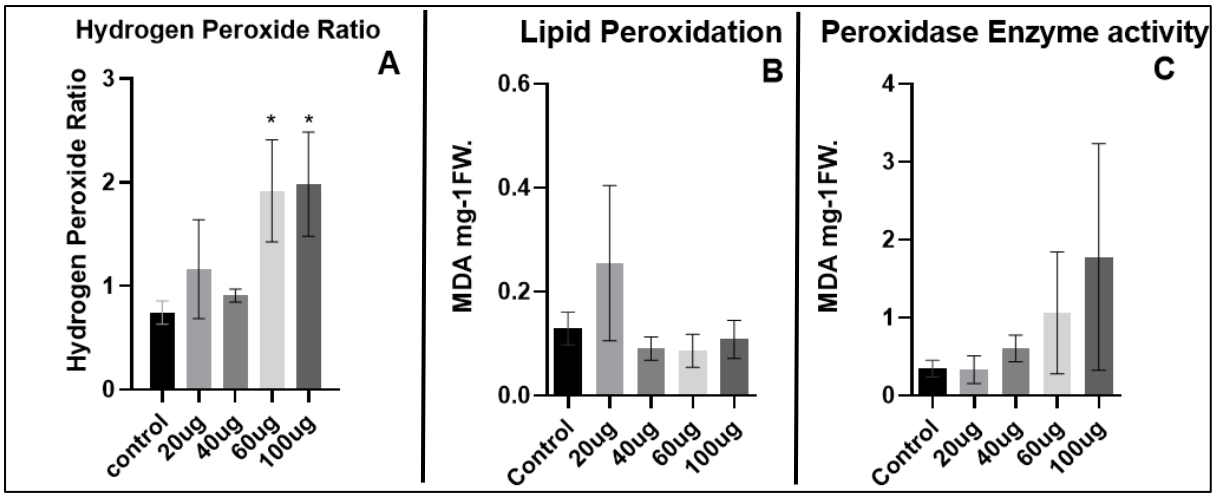

*Figure 3.6 (A) Hydrogen peroxide content as measured via HyPer line confocal microscopy. * indicates P <0.05. (B) Indicates peroxidase enzyme activity in the extracted seedlings – measured in MDA mg-1*

FW. One way Anova = 0.1717. (C) Indicates lipid peroxidation levels measured in MDA mg1 FW. One way Anova results = 0.0424. Mean values for each seedling at 14 days old, including treatment with CuNPs (0 - 100 ug/ml) for 7 d. n = 10 seedlings.

In Fig 3.6 hydrogen peroxide production progressively increased as CuNP concentration increased in the experiment, indicating one of the key metabolites in the stress response was being produced. Lipid peroxidation results stayed relatively constant within the margin of error but Peroxidase activity was significantly increased.

Chlorophyll is the main pigment responsible for photosynthesis in plants. Abiotic stress, such as drought, salinity, or temperature fluctuations, can affect chlorophyll content and lead to reduced photosynthetic efficiency. Chlorophyll assays are used to measure the amount of chlorophyll a and b in plant tissues, often via spectrophotometric methods. Reduced chlorophyll content can be an indicator of stress-induced damage to the photosynthetic apparatus (Lichtenthaler, 1987).

Carotenoids are accessory pigments found in the chloroplasts of plants. They play a vital role in photosynthesis, photoprotection, and scavenging reactive oxygen species (ROS) generated during stress. Carotenoid content can be determined spectrophotometrically or via high-performance liquid chromatography (HPLC). Changes in carotenoid levels can evaluate the plant's response to stress and its antioxidant capacity (Lichtenthaler, 1987).

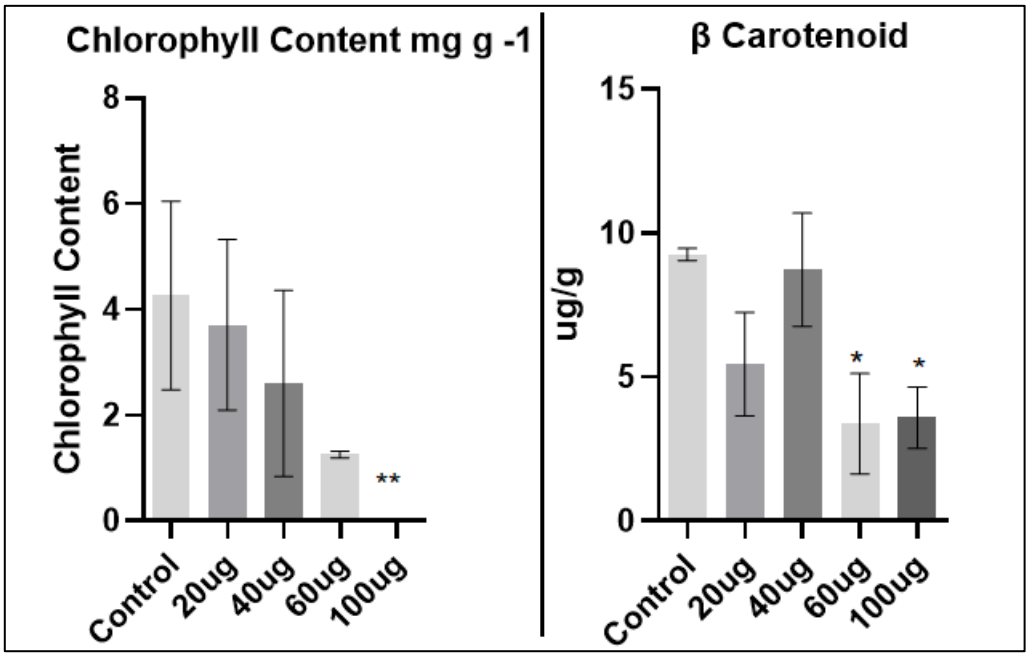

Figure 3.7 Chlorophyll content and β Carotenoid content (n=10 seedlings). 100 ug/ml P value =0.0043. B carotenoids 60 ug vs control p = 0.0419 100 ug vs control P = 0.0179. Mean values for each seedling at 14 days old, including treatment with CuNPs (0 - 100 ug/ml) for 7 d.

In Fig 3.7 chlorophyll content decreased progressively with greater concentrations of CuNP, β Carotenoid activity significantly decreased only at the 60 ug/ml and 100 ug/ml concentrations.

3.2.4 GUS, DAB and NBT Staining

There are several ways to visualise the effects of different treatments on Arabidopsis roots, a commonly used technique is with DR5-GUS hybrid seedlings, a reporter system which allows the visualisation of auxin gradients inside the plant tissue (3,3'-diaminobenzidine), GUS (β-glucuronidase), and NBT (nitroblue tetrazolium) staining are widely used techniques in plant research, each with its specific utility in studying different biological processes or markers.

The GUS staining technique is based on the expression of the reporter gene β-glucuronidase (uidA) from Escherichia coli, which is often used in plant research to monitor gene expression patterns or promoter activity. GUS staining relies on the enzymatic conversion of a colourless substrate (X-Gluc) into a blue precipitate by the β-glucuronidase enzyme. The blue staining can then be visualized and analysed under a light microscope to determine gene expression patterns (Jefferson et al., 1987).

DAB is commonly used for the detection of reactive oxygen species (ROS), particularly hydrogen peroxide (H2O2), in plants. This is useful for studying plant responses to biotic and abiotic stresses. DAB reacts with H2O2 in the presence of peroxidase enzymes, forming an insoluble brown precipitate that can be visualized under a light microscope. Areas of accumulation of the precipitate in different plant tissues indicate the stress response and identify areas of oxidative stress (Daudi & O'Brien, 2012).

NBT staining is used to detect superoxide radicals in plant tissues. Superoxide radicals are another type of ROS, which play a crucial role in plant responses to stress conditions. NBT staining involves the reduction of the colourless NBT salt to a dark blue, insoluble formazan precipitate in the presence of superoxide radicals. This technique allows us to localise and quantify superoxide production in plant tissues, providing insights into the plant's response to stress factors (Chandler, 2009).

3.2.4.1 CYCB1;2::GUS and DR5::GUS Microscopy

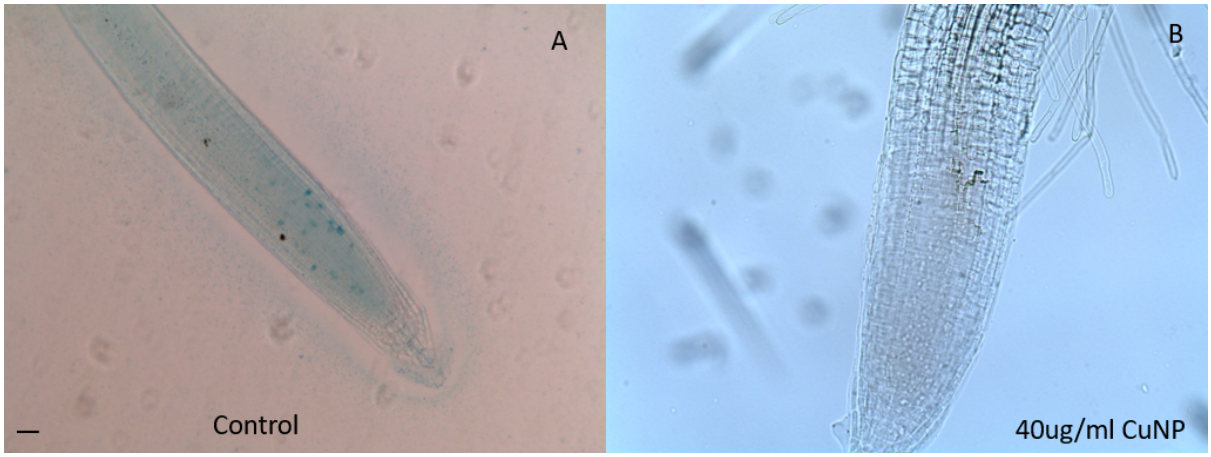

Figure 3.8 – CYCB1;2::GUS expression in the (A) control image and (B) after treatment with CuNPs for 7 days exposure. Scale bar = 1mm

As can be seen in Fig 3.8 there is normal cell division in the root tip of the control root, in the 40ug/ml root there is no discernible *CYCB1;2::GUS* expression indicating no cell division activity following CuNP treatment.

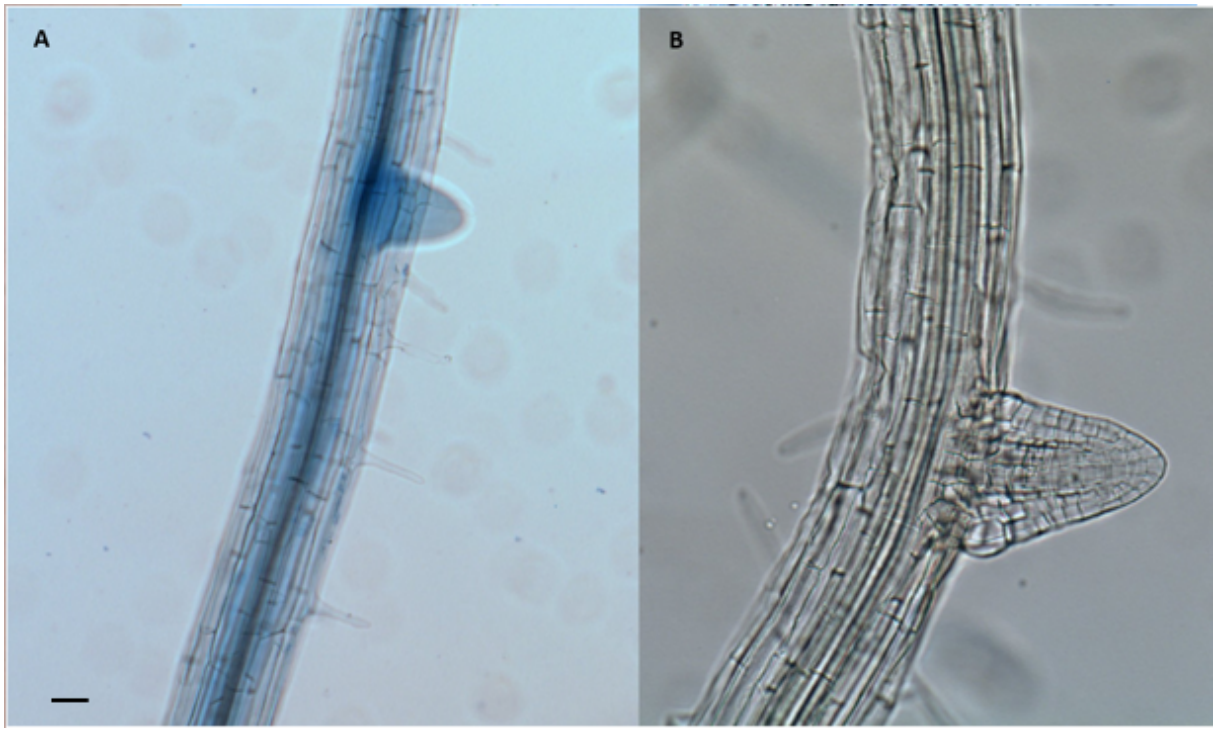

Figure 3.9: DR5::GUS seedlings with (A) showing normal development of a lateral root, (B) showing a treated plant (40ug/ml) and disrupted auxin transport. 7 days post treatment. Scale bar = 1mm

In Figs. 3.9 and 3.10 we see no discernible DR5::GUS activity in the lateral root that has been exposed to CuNPs compared to the control, indicative of a reduced auxin response following CuNP treatment.

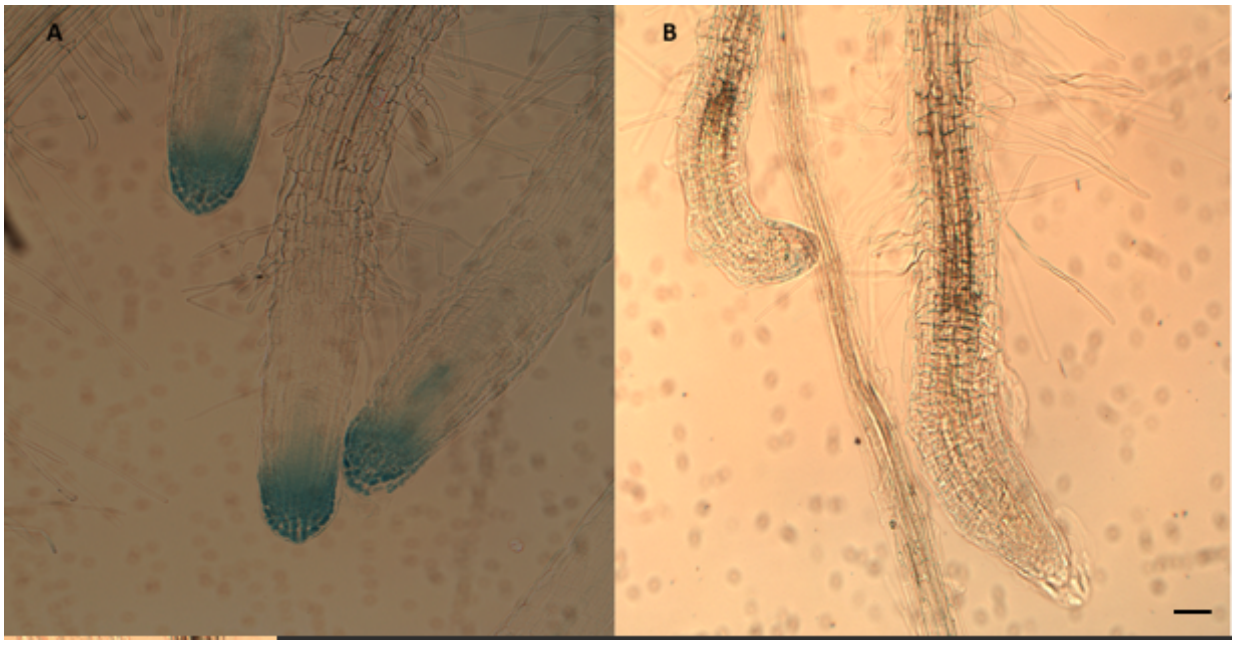

Figure 3.10 : DR5::GUS expression in lateral roots: (A) Lateral roots in untreated plants vs (B) treated plants 20ug/mg with CuNPs lateral roots. Taken after 7 days. Scale bar = 1mm

Fig. 3.10 shows very clear signal in control group lateral roots and practically no activity in exposed lateral roots.

3.2.4.2 DAB Microscopy

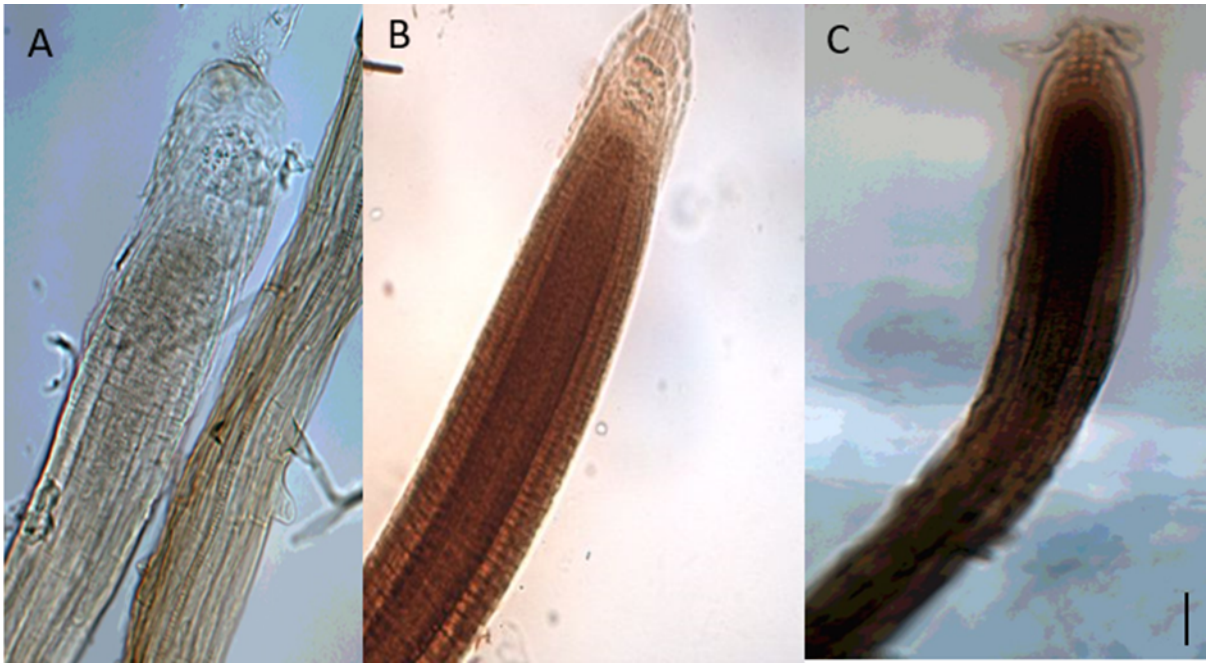

Figure 3.11: DAB staining of (A) control root tip, (B) 20ug/ml CuNP treated root, (C) 40ug/ml treated root. Treatment post 7 days, scale bar = 1mm

Increasing concentration of brown precipitate following DAB staining was seen until the density of it made visualising the roots challenging at higher concentrations of treatment with CuNPs. DAB staining was increased significantly over controls (A), indicating the activation of the stress response in the CuNP-treated roots (B) and (C).

3.2.4.3 NBT Microscopy

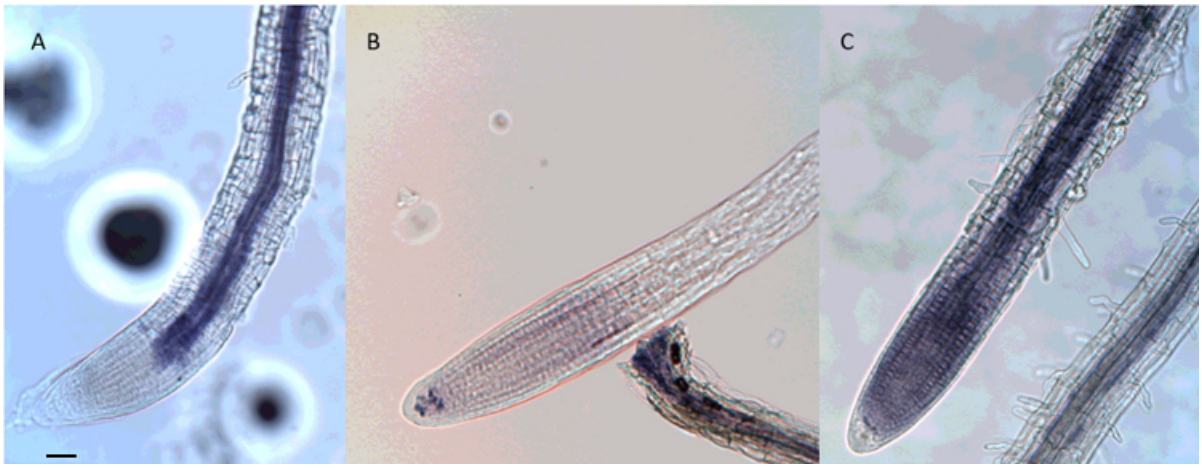

Figure 3.12 NBT staining of (A) control primary root, (B) 20ug/ml (C) 100ug/ml treated CuNP roots. Increased staining in the quiescent centre and elongation zone compared to control. Scale bar = 1mm

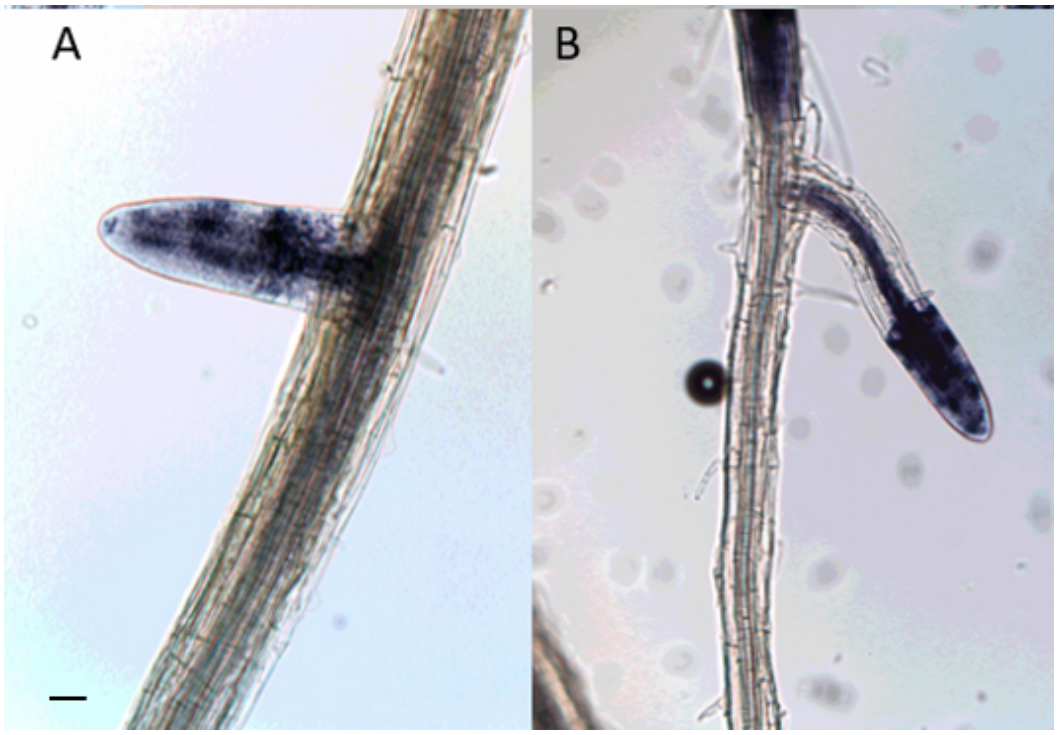

Figure 3.13: NBT staining of lateral roots: (A) Control vs (B) 40ug CuNP treated seedlings. 7 days post treatment, scale bar = 1mm.

As seen in fig 3.11-3.13 there is a basal level of oxidation activity occurring within the plant root as ROS activity is a common part of cell division and metabolism (Mittler, 2017). High ROS activity is however seen in any root that has been treated with even low concentrations (from 20 ug/ml) of CuNPs, with accumulation in the tip of primary and lateral roots.

3.2.5 Confocal Microscopy

3.2.4.2 HyPer

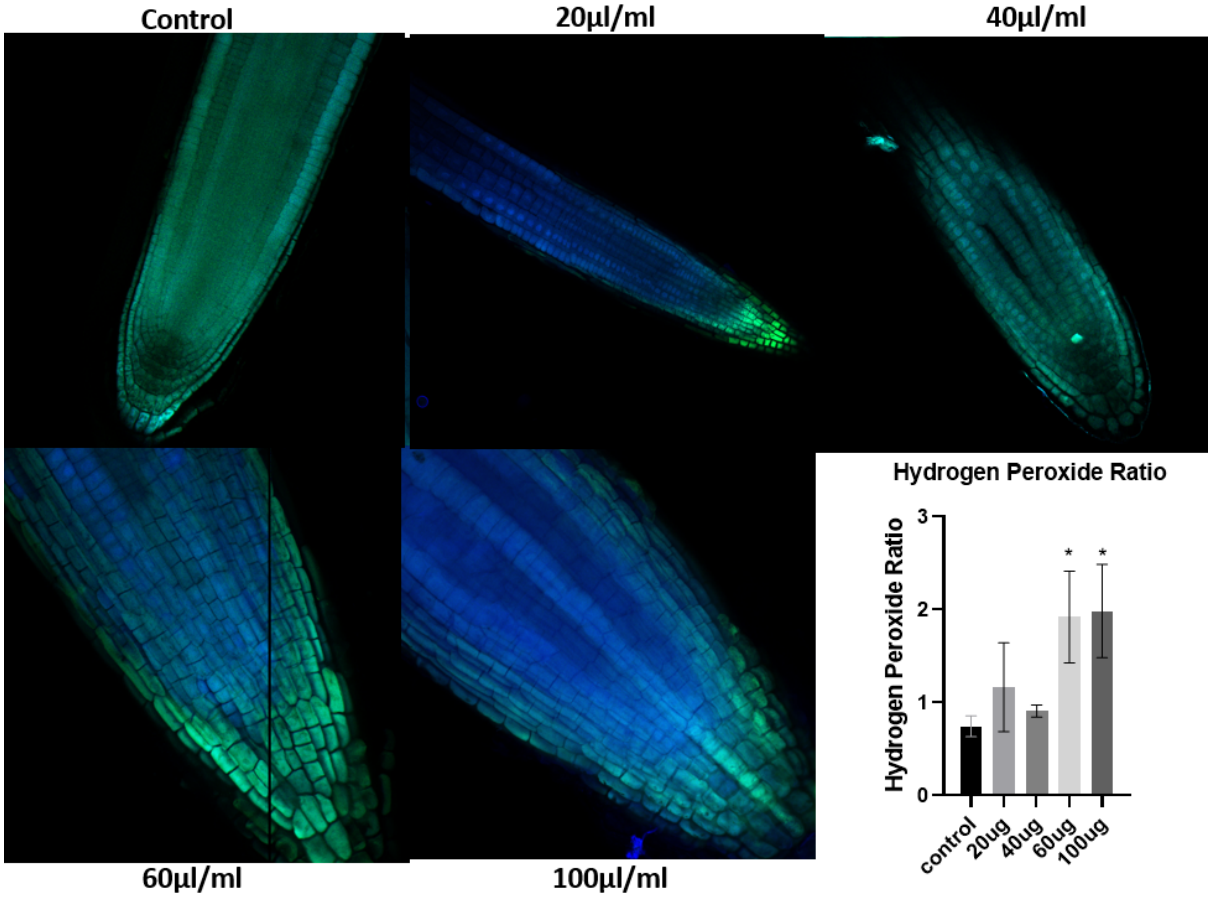

Figure 3.14: Hyperline Arabidopsis imaging of plant roots exposed to varying quantities of CuNPs. The ratio of blue to green channel indicates Hydrogen Peroxide Activity (Hernández-Barrera et al., 2015). Scale bar: control + 40ul/ml= 75um, 20ul/ml = 100um, 60 and 100ul/ml = 50um. HyPerline confocal microscopy indicates strong hydrogen peroxide production in the meristematic zone of the root compared to the control.

Hyper imaging reveals hydrogen peroxide levels in plant tissues, abd can be quantified using confocal imaging. The hydrogen peroxide ratio indicated in Fig. 3.14 is the quantified hydrogen peroxide measurements that indicate a consistent increase in hydrogen peroxide accumulation as the exogenous concentration of CuNPs increases.

3.2.4.3 CellROX Stains

CellROX stains are a class of fluorogenic probes used for detecting ROS in cells. These dyes are cell-permeable and non-fluorescent in their reduced state. Upon oxidation by ROS, they

become highly fluorescent, allowing for the visualization of ROS production in living cells. Confocal microscopy can be used in combination with CellROX stains to study the spatial distribution of ROS in plant cells under stress conditions (Celeghini et al., 2021).

CellROX dyes are available in different excitation/emission wavelengths, making them compatible with various confocal microscope setups. Using a confocal microscope, the stained samples can be imaged with appropriate excitation and emission settings for the CellROX dye and any other fluorophores used. Image analysis software can be employed to quantify fluorescence intensity, measure colocalization between different fluorophores, and calculate various cellular parameters. This information can provide insights into the role of ROS in plant physiology, stress responses, and developmental processes. CellROX stains are valuable tools for studying ROS dynamics in plant cells using confocal microscopy. This approach can reveal essential information about the spatial distribution and function of ROS in living plant cells, helping understand their roles in stress responses, development, and other physiological processes.

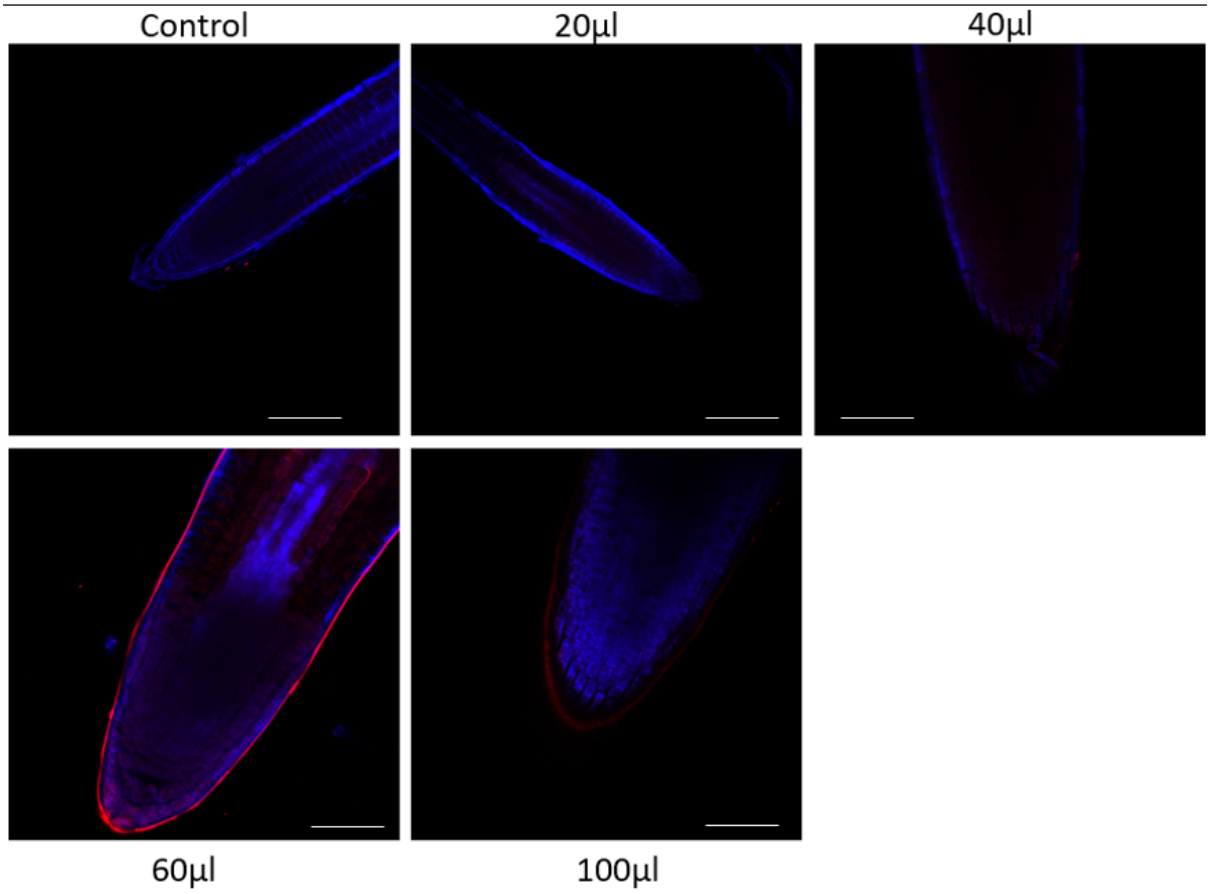

Figure 3.15: Cellrox stained to fluoresce in presence of ROS allowing areas of high enzymatic activity to be visualised in the root. Compared to controls treated plants fluoresced significantly in the meristematic centre and in the vascular tissue. Scale bars = control, 20ul/ml = 100um, 40, 60 and 100ul/ml = 50um.

In Fig. 3.15 increasing levels of cellrox signal is seen in seedlings treated with up to 60 ug/ml of CuNPs, consistent with the observed increased in ROS shown above using other methods.

3.2.6 ICP-MS

Intercoupled plasma mass spectrometry (ICP-MS) was used to quantify the level of copper nanoparticles present in the media the plants were grown in and to quantify Cu uptake from the environment into the seedlings, and how well those Cu particles were translocated from root tissue to shoot tissue (Mittal et al., 2017).

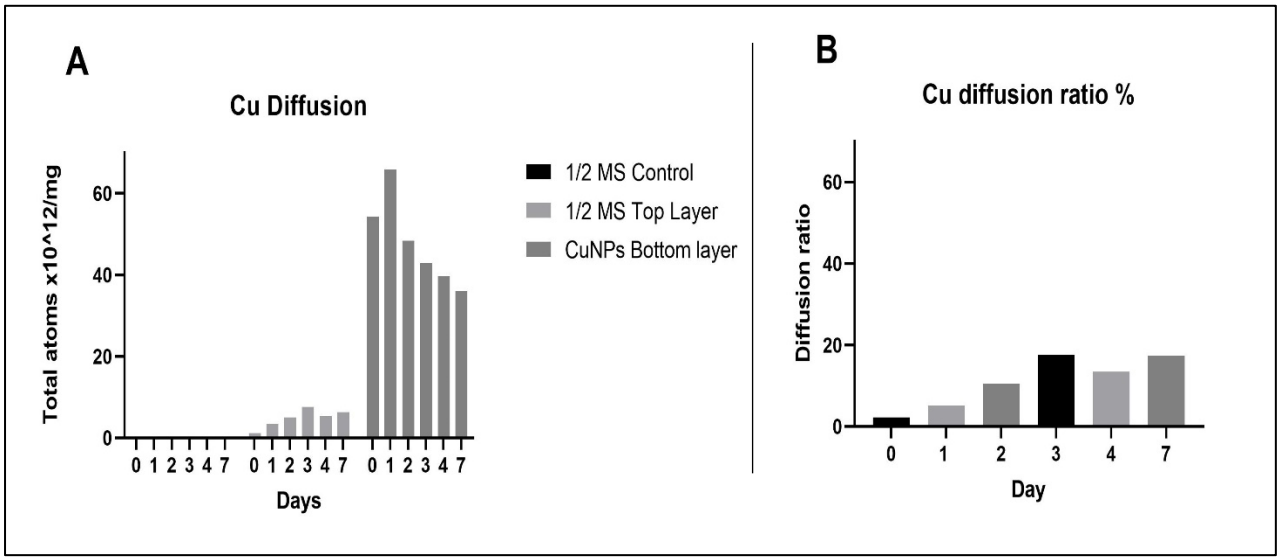

Figure 3.16: (A) Measurement of Copper ions present in the cell media post diffusion of CuNPs in control plates (no CuNPs) and split plates with no CuNPs (Top Layer) and with CuNPs (Bottom Layer), indicating little movement of Cu into the upper plate later from the lower CuNP-containing layer. (B) The ratio of diffusion from the loeer to the upper layer as a percentage.

Results in Fig. 3.16 show that the control media (A) had negligible quantities of Cu, while split plates mostly retained CuNPs (with Cu eventually leaking in over the course of a week). The diffusion ratio of Cu from the treated layer of the plate to the untreated layer of the plate was approximately 20% over the course of a week.

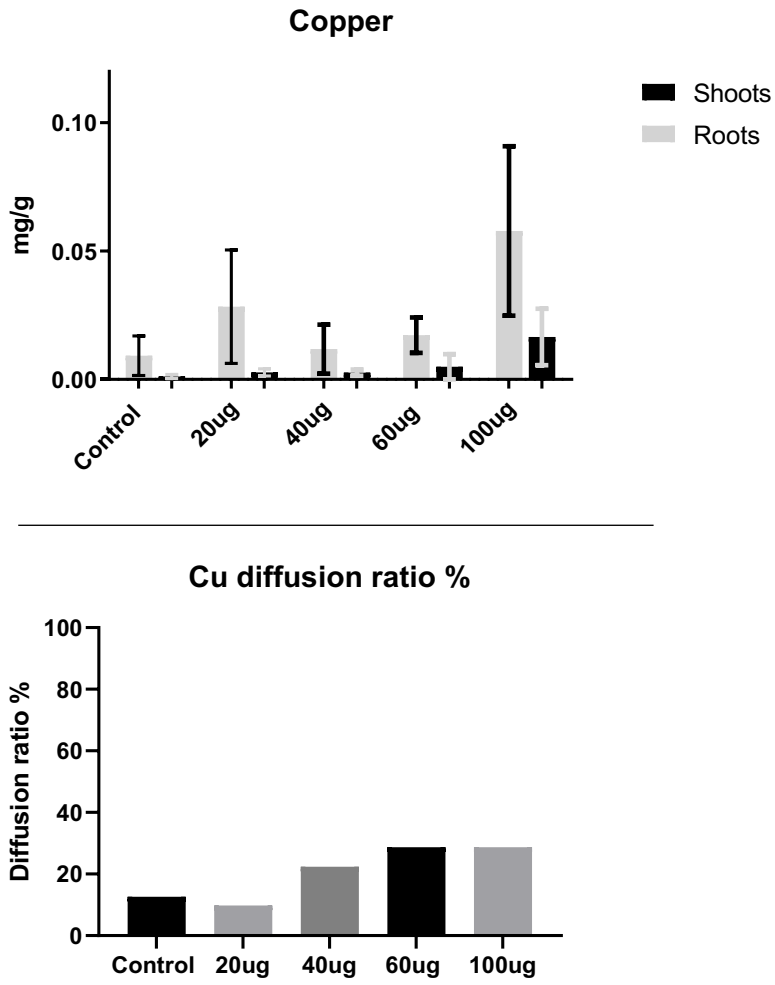

Figure 3.17 depicting the Cu content in roots vs shoot material in 14 day old Arabidopsis seedlings after treatment with Cu enriched media at different concentrations. The diffusion ratio indicating what proportion of Cu material successfully translocated from the root tissue to the shoot tissue.

Figure 3.17 indicates a low percentage of copper successfully translocates from root to shoot and that absorption of copper achieves an upper threshold between the 40-60ug range.

3.2.7 TEM Microscopy

Transmission electron microscopy (TEM) can be a useful way to visualise the internal structure of plant cells. TEM has proven to be a powerful tool for analysing the uptake of nanoparticles, their biodistribution and relationships with cell and tissue components (Malatesta, 2021; Tizro et al., 2019).

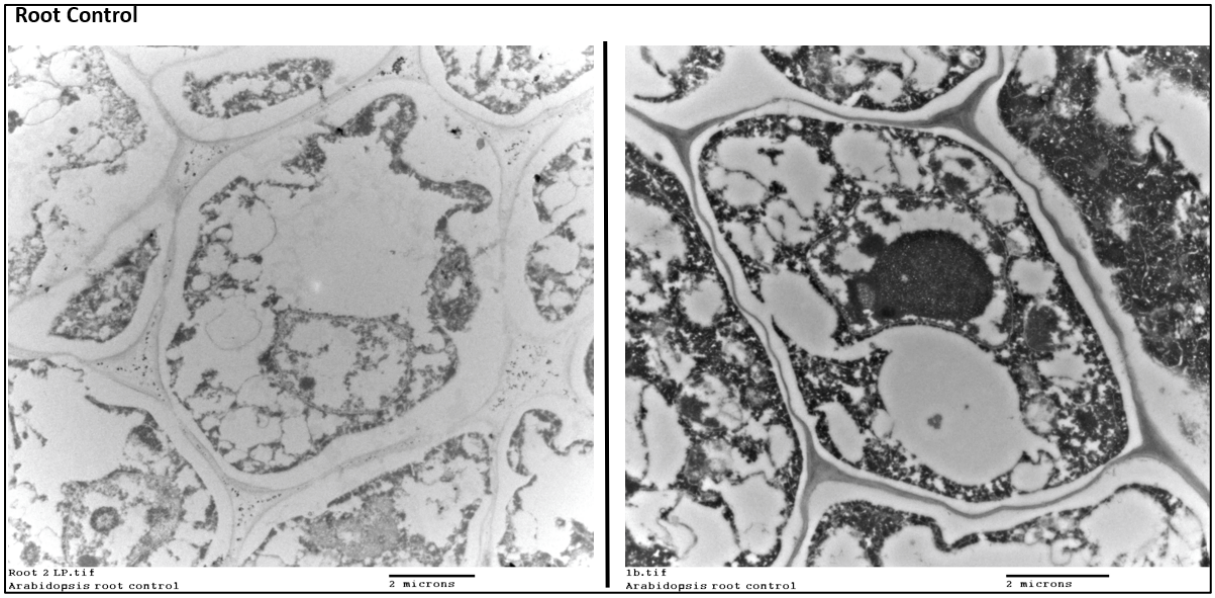

Figure 3.18 : Two different control plant root cells with no CuNP exposure.

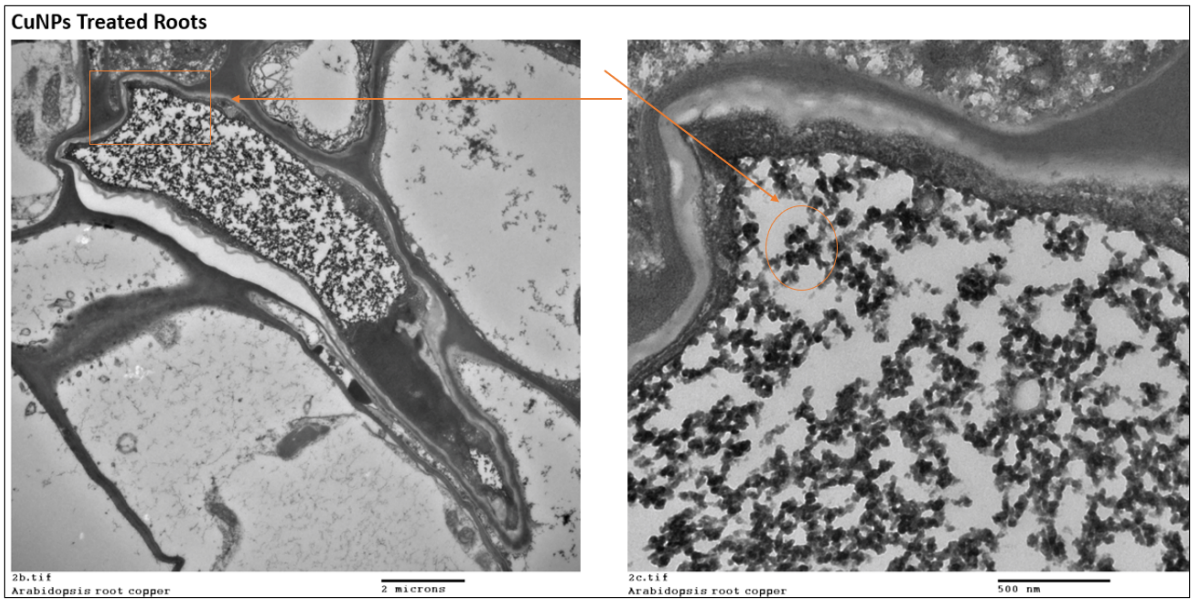

Figure 3.19: The presence of CuNPs in the root tissue of Arabidopsis at scales of 2 microns and 500 nm. Orange rectangle indicating zoomed in region, orange circle indicating area containing nanoparticles.

TEM analysis identified no CuNPs in control cells (Fig. 3.18) but found the presence of CuNPs in the extracellular matrix and cytoplasm after exposure (Fig. 3.19).

3.3 Summary

This chapter focused on quantifying the phenotype observed when Arabidopsis is exposed to excess CuNPs in its environment. Primary root length is significantly decreased and has a positive correlation with increased concentration of CuNPs, this also affects overall plant biomass. Additionally, while the number of lateral roots remained relatively constant, CuNPs led to increases in length, suggesting possible auxin redistribution.

Root hair formation is significantly disrupted. Furthermore, it has been demonstrated by biochemical means and by visual stains that enzymes and indicators of ROS activity are significantly upregulated in the plant post-treatment.

TEM and ICP-MS microscopy indicate that CuNPs are likely to stay located within the cytoplasm or cell wall of the plant – The translocation rate is less than 20% from root to shoot. The vast majority of uptaken CuNP appears to stay localised to the cytoplasm.

We have observed CuNPs make an impact on the observed phenotype of plants, and the next objectives were to investigate transcriptome and protein changes following CuNP treatment.

Chapter 4 Changes in Gene Transcription in response to CuNPs

4.1 Introduction

In the late 2000s several academic publications introduced the idea of an innovation technique to map only the transcribed 'coding' areas of an organism's genome utilising next generation sequencing (NGS) technology.

The method was referred to as RNA sequencing or RNA-Seq for short (Cloonan et al., 2008; Honys et al., 2003; Lister et al., 2008; Mortazavi et al., 2008; Nagalakshmi et al., 2008). Prior to the innovations of NGS, microarrays were mainly used to elucidate high throughput gene expression, however NGS has important advantages as it sequences a full transcriptome it does not necessitate prior knowledge about gene sequences for hybridisation tagging, and so the technique can be used on non-model species or where there is little or no previously available data (Wang et al., 2009).

A greater description of the technique and method used for RNA extraction and library preparation, and parameters used, can be found in the methods section (Chapter 2).

This chapter will first describe how sufficient root material was gathered to allow to root specific RNA extraction, and will also include RT-qPCR data that allowed the experimental parameters to be optimised to allow the optimised acquisition of differential expression results – this was made possible due to pre-existing proteomic data compiled. The next parts of the chapter will be a description of the differentially expressed genes (DEGs) found at two different timepoints and the categorisation of these with gene ontology (GO) software. A hypothesis is formed that is tested in the following chapter.

Aims :

Analysing the transcriptomic profile of plants treated with CuNPs, verifying with qPCR at different timepoints, and utilising GO software to categorise the transcriptomic profile of treated plants.

4.2 Hydroponics

In order to generate sufficient root material to carry out transcriptomic analysis it was necessary first to implement a hydroponic growth system that encouraged root growth and allowed easy separation of roots and shoots.

Hydroponics is an innovative technique for growing plants without soil, typically using nutrient-rich water solutions to deliver essential elements directly to plant roots. This method has the potential to generate more plant biomass than traditional growth methods, offering several key advantages such as in efficient nutrient delivery. Plants receive nutrients directly through the water, which allows for precise control of nutrient concentrations and pH levels. This targeted approach can result in faster growth rates and higher yields compared to traditional methods.

Hydroponics setups can also reduce disease and pest issues. Soil-based pathogens and pests are less likely to affect hydroponic systems. faster growth cycles: The precise control of nutrients and environmental conditions in hydroponic systems can lead to faster growth and shorter crop cycles, enabling more harvests in a given timeframe (Manos & Xydis, 2019).

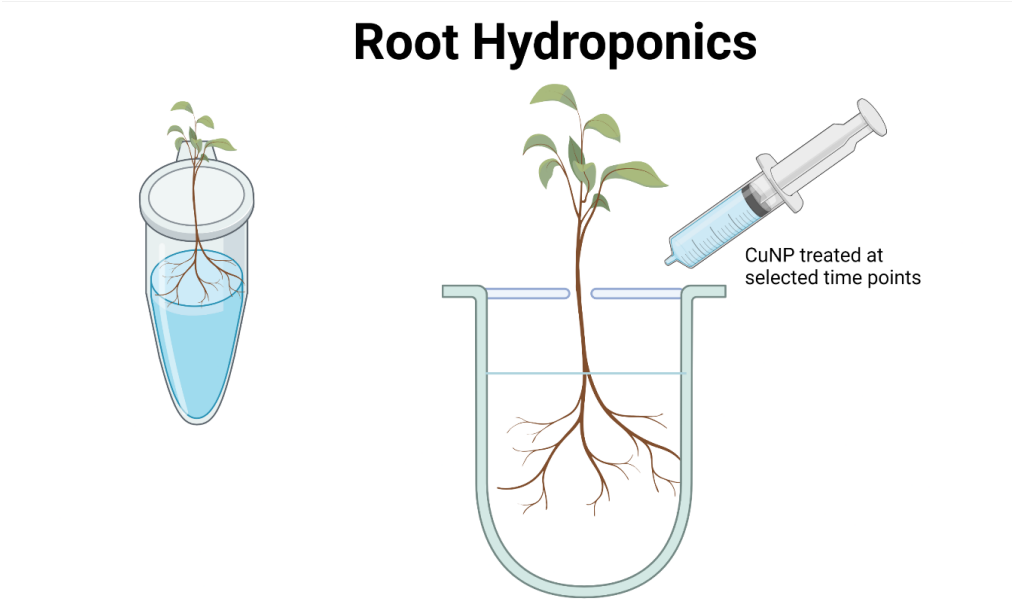

Figure 4.1: Hydroponics experimental setup indicating ability to control timepoints of CuNP delivery.

The system utilised was a modification of a hydroponic setup as per Conn et al. (2013) using media and aeration techniques described by Chivasa et al. (2005). Growth is comparable with standard media but allows more natural separation of roots from shoot material and allows greater control of the time points for inoculation with CuNPs.

Cultures were prepared in quadruplicate for each treatment, and every replicate contained at least six plantlets. Seeds were sown on sterile 7 cm-diameter, 1 cm-thick polyurethane foam discs soaked in MS medium (0.22% [w/v] MS salts, adjusted to pH 5.7 with KOH/HCl). The discs were placed in sterile Phytatrays (Sigma-Aldrich) and incubated under a 16-h-light/8-h-dark cycle at 22°C. One week later, when the seeds had germinated, and the roots had penetrated the foam, 30 mL of MS medium was added to the Phytatray, which caused the foam discs to float. The trays were transferred to a shaking platform (25 rpm) under the same environmental conditions. During the second week, the plant roots had emerged through the other side of the foam and submerged in the nutrient-rich medium. Medium was changed each week. After 14 days of culture, uniform plants selected to be treated with CuNPs were treated and harvested at 3 hours and 24 hours.

This experimental setup allowed optimal sample generation speed and a greater organic mass to work with as well as greater ease and cleanliness of root and shoot extraction and separation.

The results of plant growth using hydroponics are presented in Fig. 4.2. There is significantly higher plant biomass overall, almost double the standard control. In addition the primary root grew on average nearly 2 cm more than standard 1/2MS media grown controls.

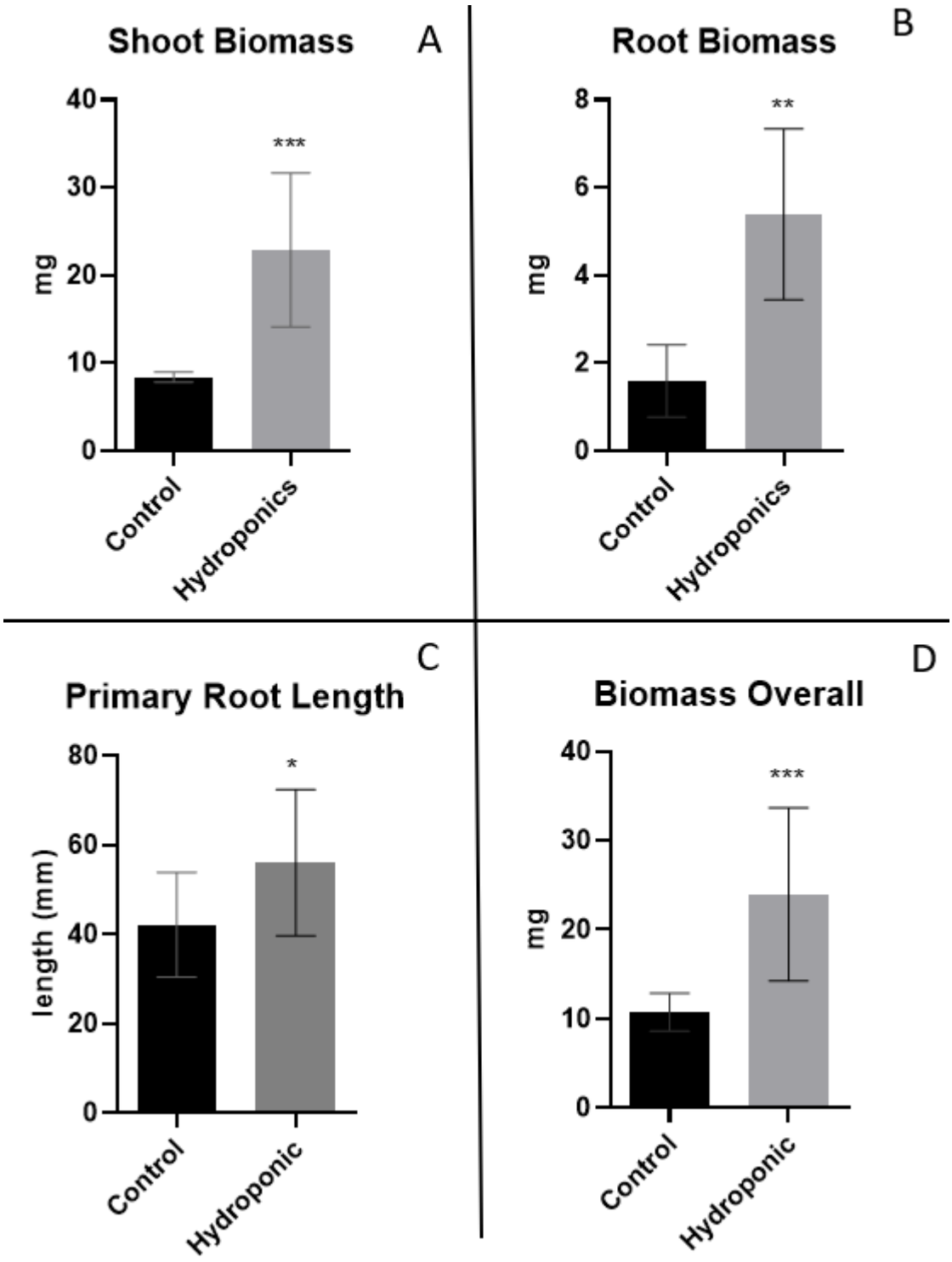

Figure 4.2: Comparative growth metrics between Arabidopsis grown for 21 days in standard ½ MS media vs the Hydroponic media setup. (A) Shoot biomass, p = 0.00945. (B) Root biomass p = 0.00254. (C) Primary root length p = 0.0442 (D) total Biomass compared to controls p = 0.00355. Hydroponic growth comparatively grew faster across all recorded metrics, with a

greater volume of root material being the most essential aspect for downstream applications. N= 10 plants,

4.3 RT-qPCR

In order to determine optimum time points for revealing differential gene expression, RT-qPCR was performed. Five genes expected to change under CuNP stress (encoding CCS copper chaperone, Basic Blue ARPN, RBOH D, RBOH F and PIN2) and 4 timepoints (1 h, 2 h, 3 h and 24 h) were chosen in order to determine the best differential expression, compared to expression levels at time 0 (Fig. 4.3). The Delta-delta CT was calculated after RT-qPCR amplification to determine relative expression compared to a housekeeping gene (*ACTIN2*), according to the method and software developed by Ruiter et al. (2009).

The results show significant increase in differential gene activity from the 3 hour and 24hour timepoints. *ARPN* 3hr time point stood out significantly (Fig 4.3). *CCS* had a progressively increasing relative expression pattern from the 1 hour timepoint onwards (Fig 4.4). *RBOH D* and *RBOH F* both have significant upregulation in the 3 hour time point and relatively marginal increase at the 1,2 and 24 h time points.

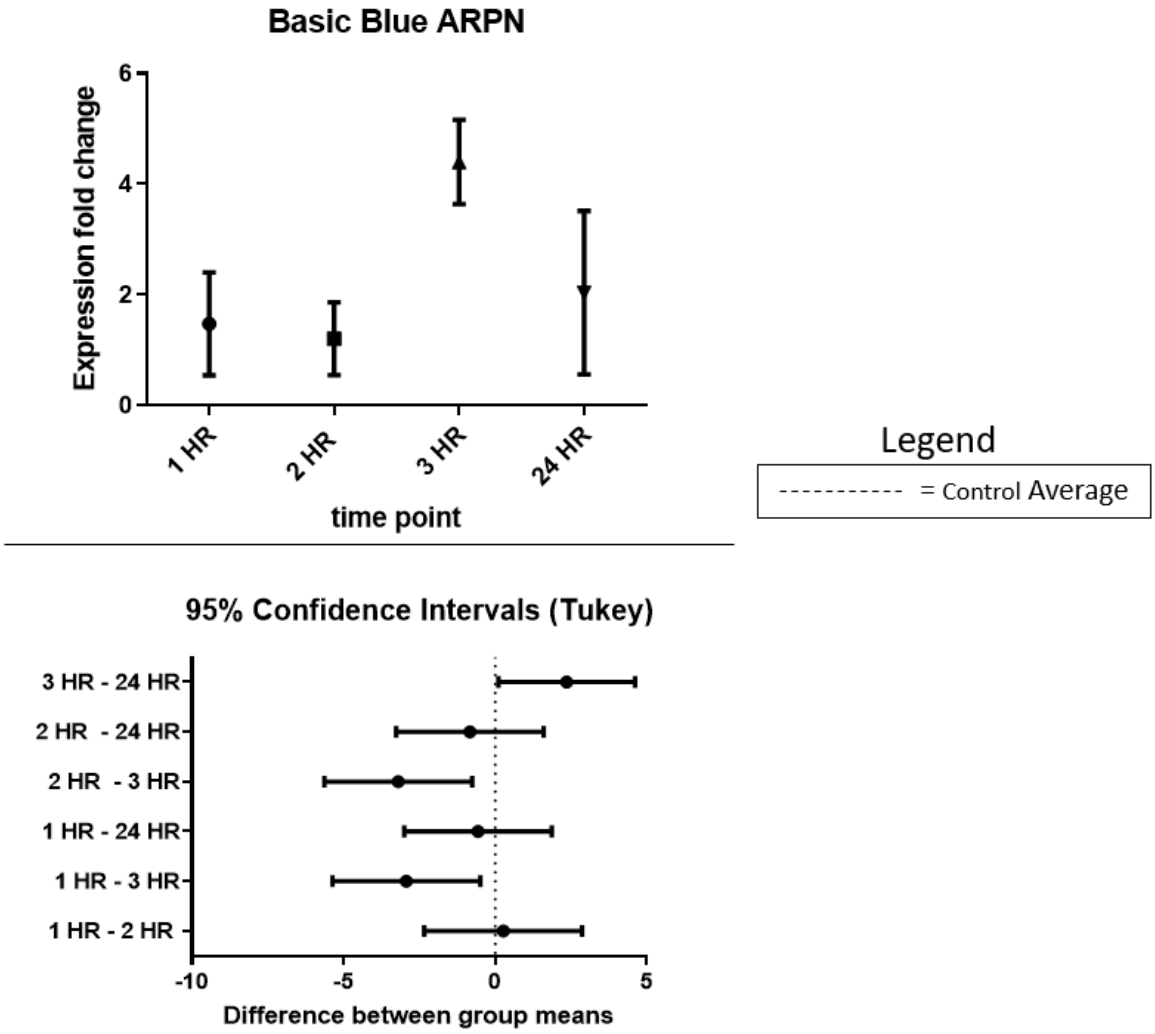

Figure 4.3: Expression fold change for the BB ARPN gene at different time points compared to an untreated sample. One-way Anova indicates P value of 0.0075 indicating a significant difference between means, this is further characterised in the 95% confidence tables where it is clear the most significant mean difference is between the 3-hour timepoint and the others.

The Tukey confidence interval is commonly used after performing an ANOVA test, which determines if there are statistically significant differences among the means of three or more groups. If the ANOVA indicates that there are significant differences, post hoc tests like Tukey's range test are often conducted to identify which specific pairs of group means are significantly different from each other. Fig. 4.3 demonstrates 3hr and 24hr time points are significantly different from the control.

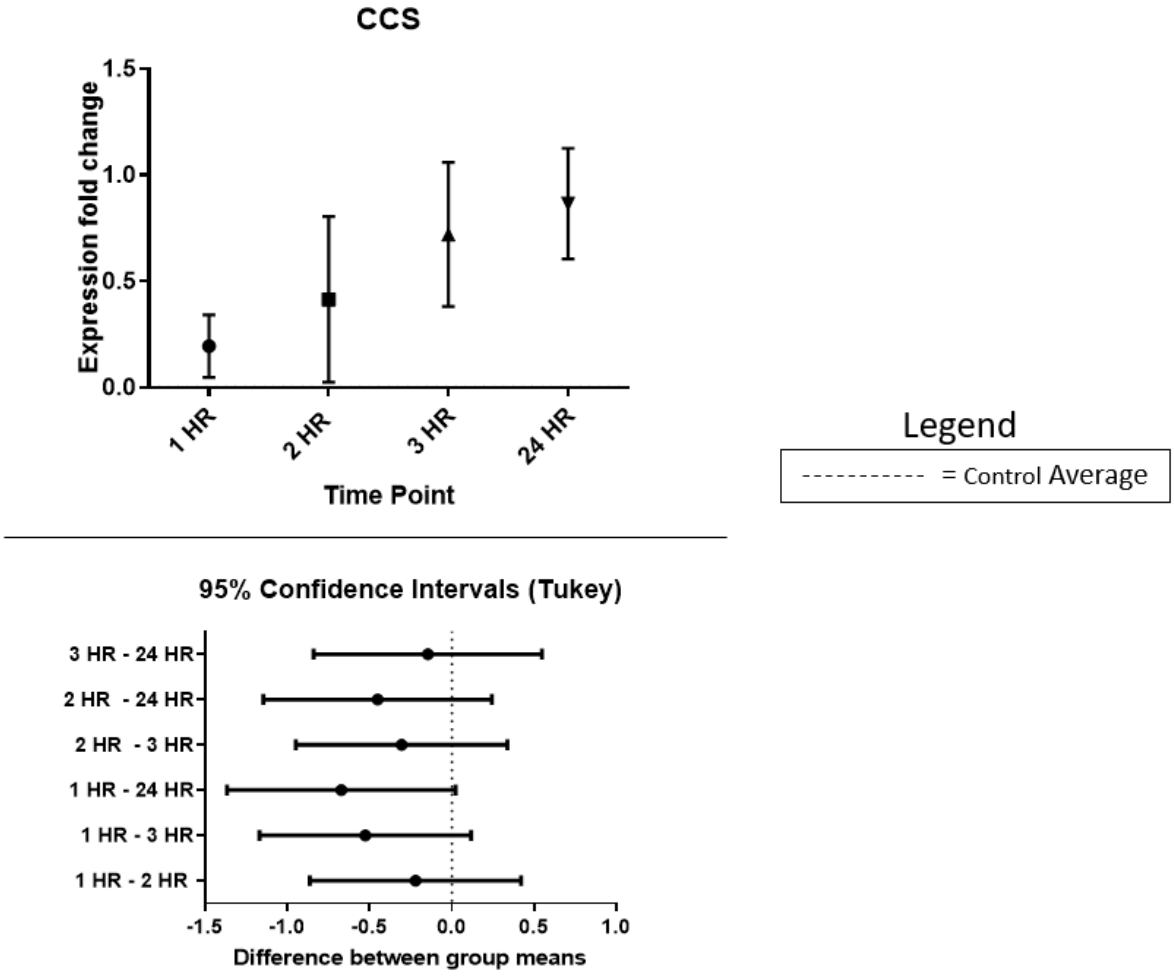

Figure 4.4: Graph of expression fold change amongst the BB gene at different time points compared to an untreated sample, one-way Anova indicates P value of 0.0494 indicating a significant difference between means, this is further characterised in the 95% confidence tables.

No dataset is significant for the *CCS* gene in this tukey analysis (Fig. 4.4) although we do see an increase in gene expression from baseline in the progressively from 1hr up to 24hrs.

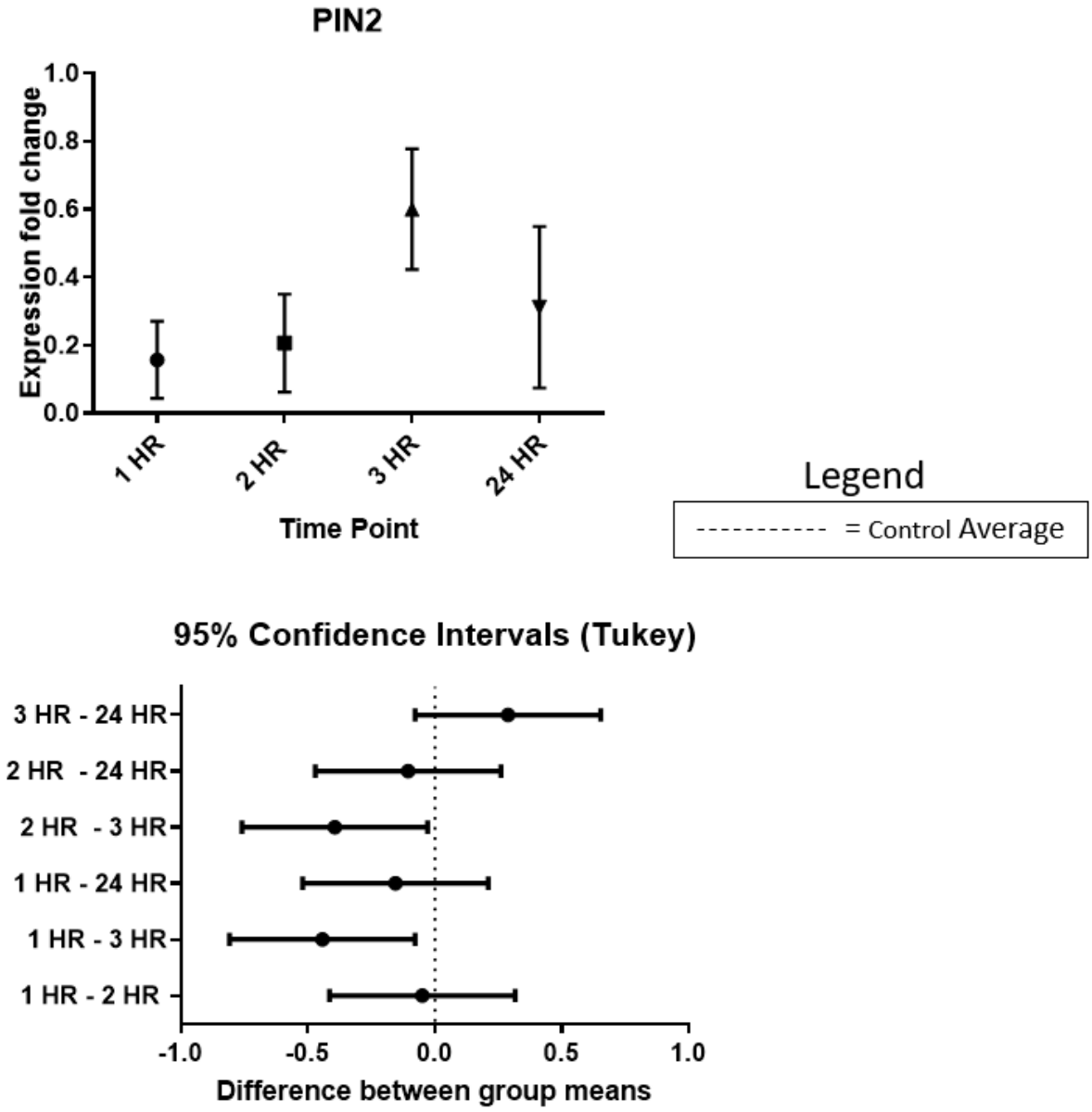

Figure 4.5 : Graph of expression fold change amongst the PIN2 gene at different time points compared to an untreated sample, one-way Anova indicates P value of 0.0158 indicating a significant difference between means, this is further characterised in the 95% confidence tables which show significant differences between the 3hr timepoint and the 1 and 2 hour timepoints.

For PIN2 expression, the 2-3hr and 1-2hr timepoints are significant in this tukey confidence ratio, we also see a significant increase in expression at the individual 3hr timepoint compared to baseline (Fig. 4.5).

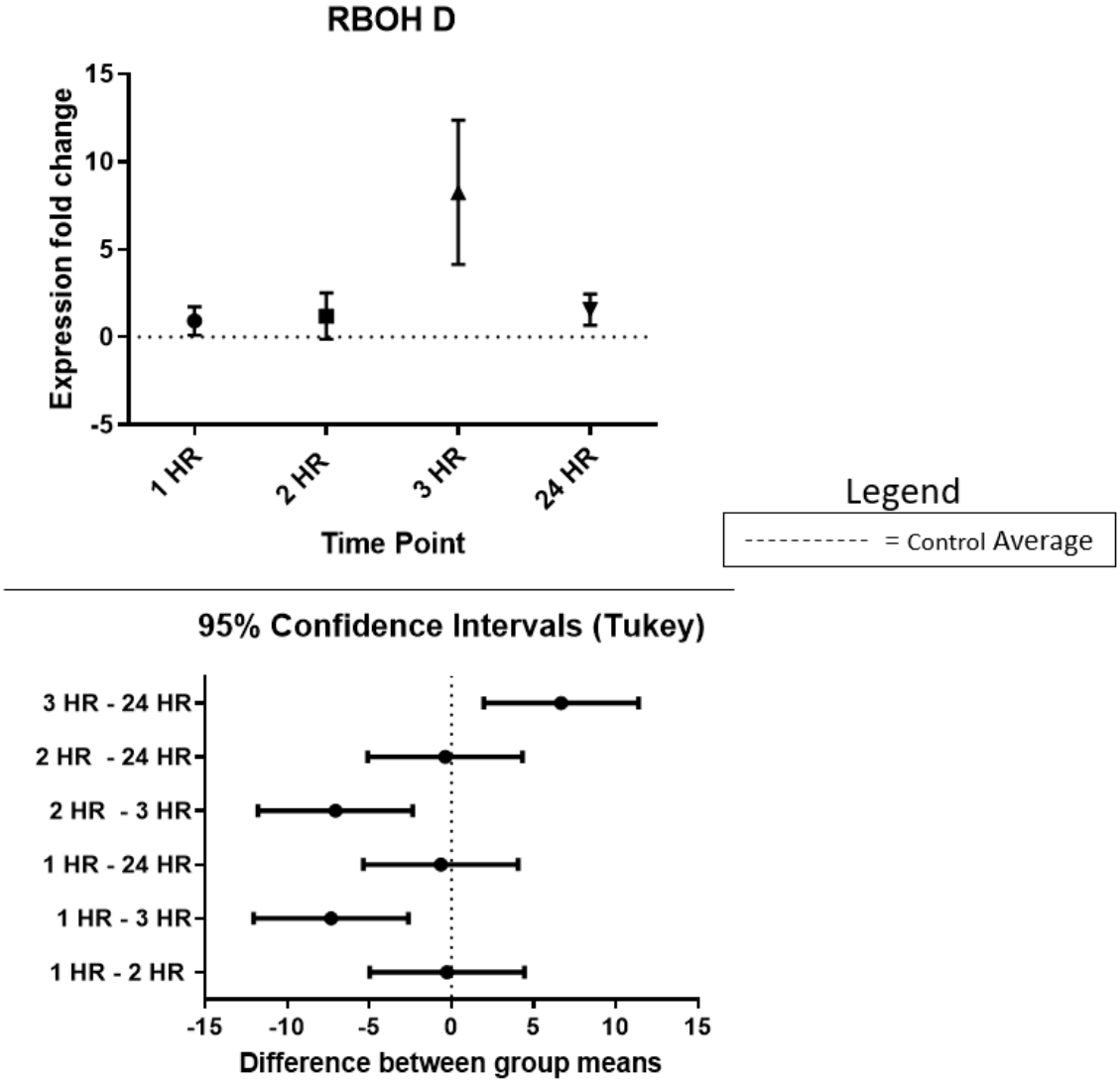

Figure 4.6: Graph of expression fold change amongst the RBOH D gene at different time points compared to an untreated sample, one-way Anova indicates P value of 0.0015 indicating a significant difference between means, this is further characterised in the 95% confidence tables which show significant differences between the 3hr timepoint and the 1 and 2 hour timepoints.

Fig. 4.6 shows the response of the *RBOH D* gene to CuNPs. The 3hr timepoint is considerably upregulated from the control, and the Tukey assessment shows 1-3hr, 2-3hr and 3-24hr are all significantly different from the control baseline expression – although the 3hr timepoint has likely significantly influenced the dataset.

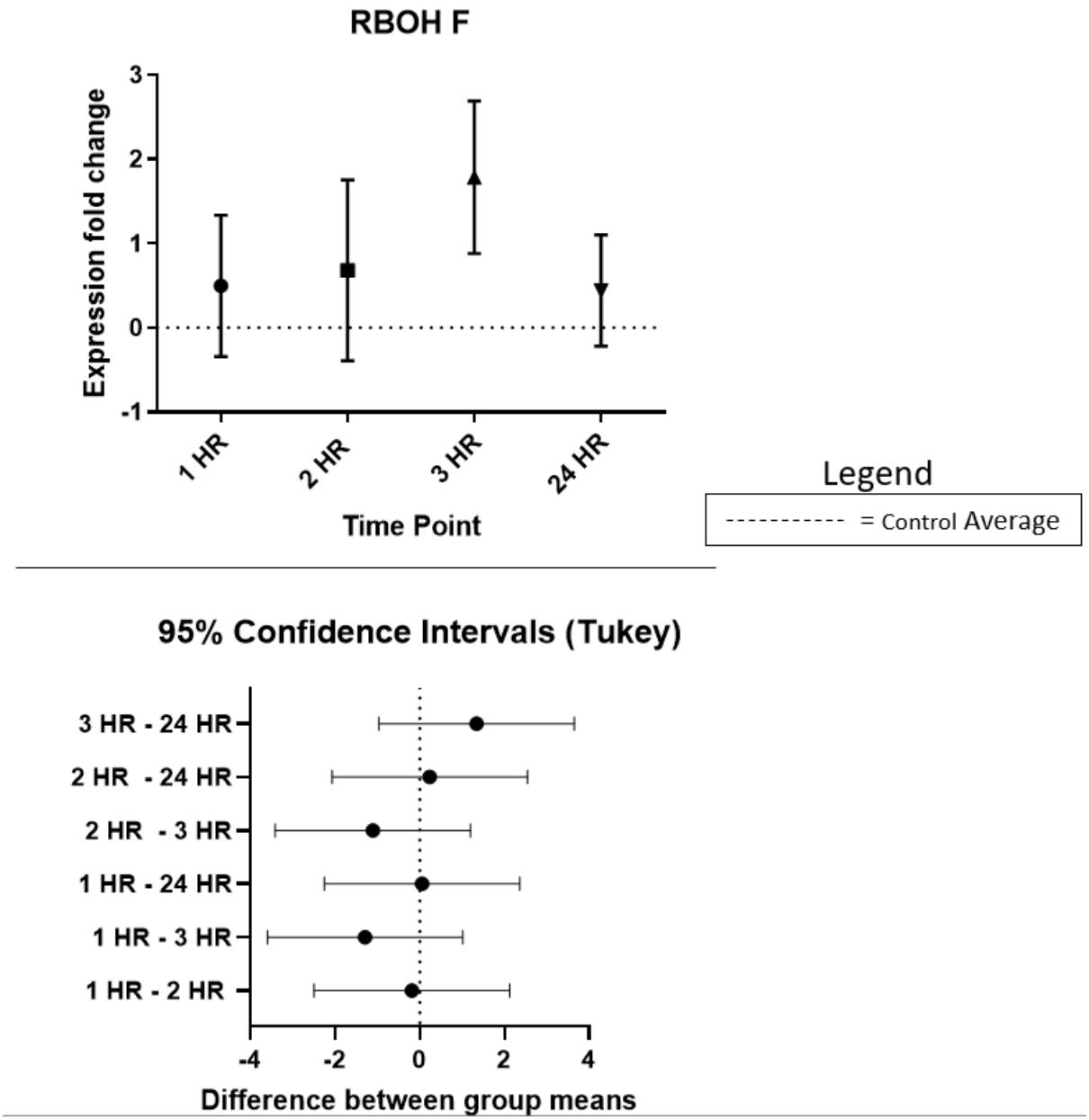

Figure 4.7: Graph of expression fold change amongst the RBOH F gene at different time points compared to an untreated sample, one-way Anova indicates P value of 0.2778 indicating there is no significant difference between means, this is further characterised in the 95% confidence tables.

In Fig. 4.7 we see that the 3hr time point for *RBOH F* expression is significantly upregulated.

4.4 RNA-SEQ

The results of the RT-qPCR analysis indicated that the 3-hour timepoint demonstrated significant differential expression – so it was chosen alongside the 24-hour timepoint for RNA

sequencing to gather more information on global gene expression changes following CuNP treatment. Time point expressional transcriptomics was carried out in order to characterize the temporal patterns (upregulation, downregulation), providing insights into the underlying regulatory processes. This would allow us to construct gene regulatory networks to understand the relationships and interactions between genes and identify key regulatory hubs and transcription factors that play crucial roles in orchestrating temporal gene expression changes. It was also an objective to conduct functional enrichment analysis to identify biological processes, molecular functions, and pathways associated with temporal changes in gene expression and understand how specific pathways are activated or suppressed at different time points.

Multiple time-point RNA-seq studies are particularly powerful for unravelling the dynamic nature of biological processes and understanding the temporal coordination of gene expression events. The analyses mentioned above contribute to a deeper understanding of molecular mechanisms, help identify key regulatory players, and guide subsequent experimental investigations.

4.4.1 Differential Expression Analysis – Generation of List of DEGs

An adjusted *P*-value of ≤ 0.05 and a $\log_2$ fold change ($\log_2$fc) of ≤-0.5 and ≥0.5 were selected to identify differentially expressed genes (DEGs) between the control and CuNP treated conditions at each of the timepoints.

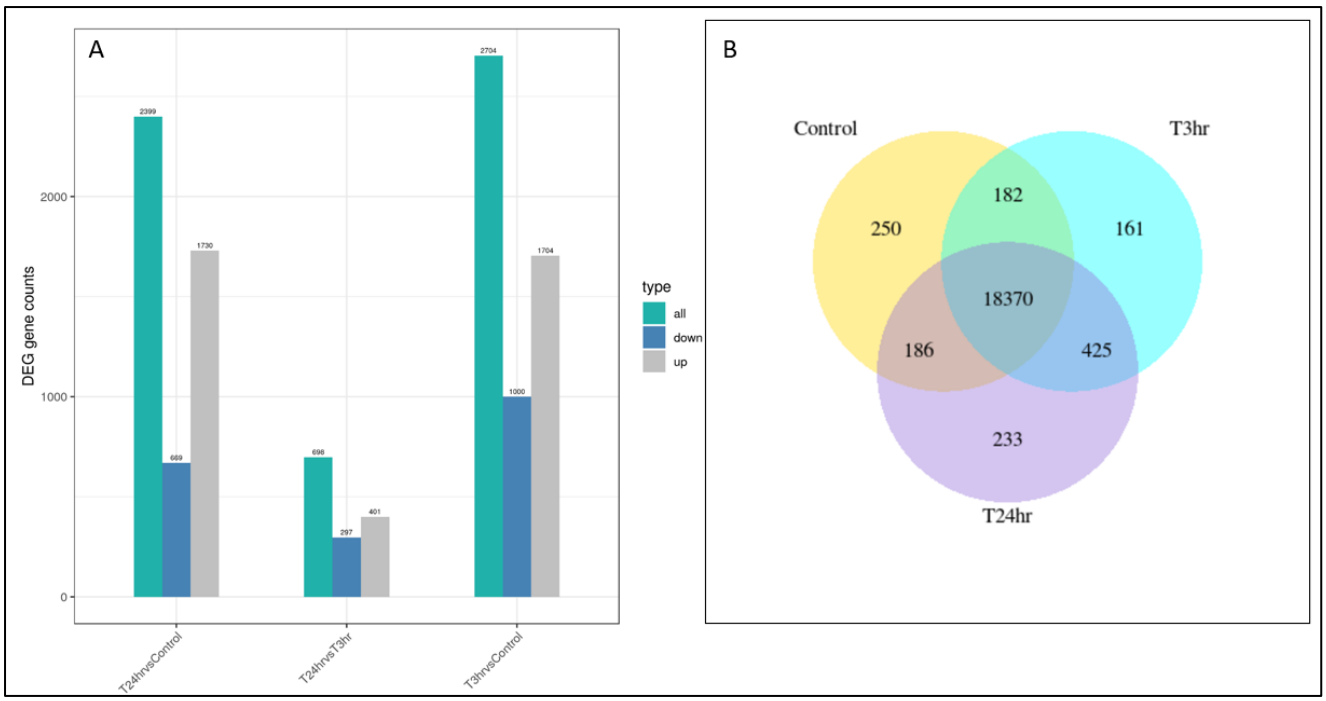

Figure 4.8 (A) Histogram indicating numbers of up and down regulated genes detected for the 24hr post treatment, 3hr post treatment and differential between 24hr and 3hr. $p \leq 0.05$ and log 2-fold change ≥ 0.5 *(B) Venn diagram indicating the difference in up and down regulated genes between the three data sets.*

Results show the greatest amount of differential expression occurring in the treated groups compared to control with a much smaller amount of differentially expressed genes between the two timepoints indicating a lower amount of differential activity based on timepoint from treatment compared to the control vs treatment datasets.

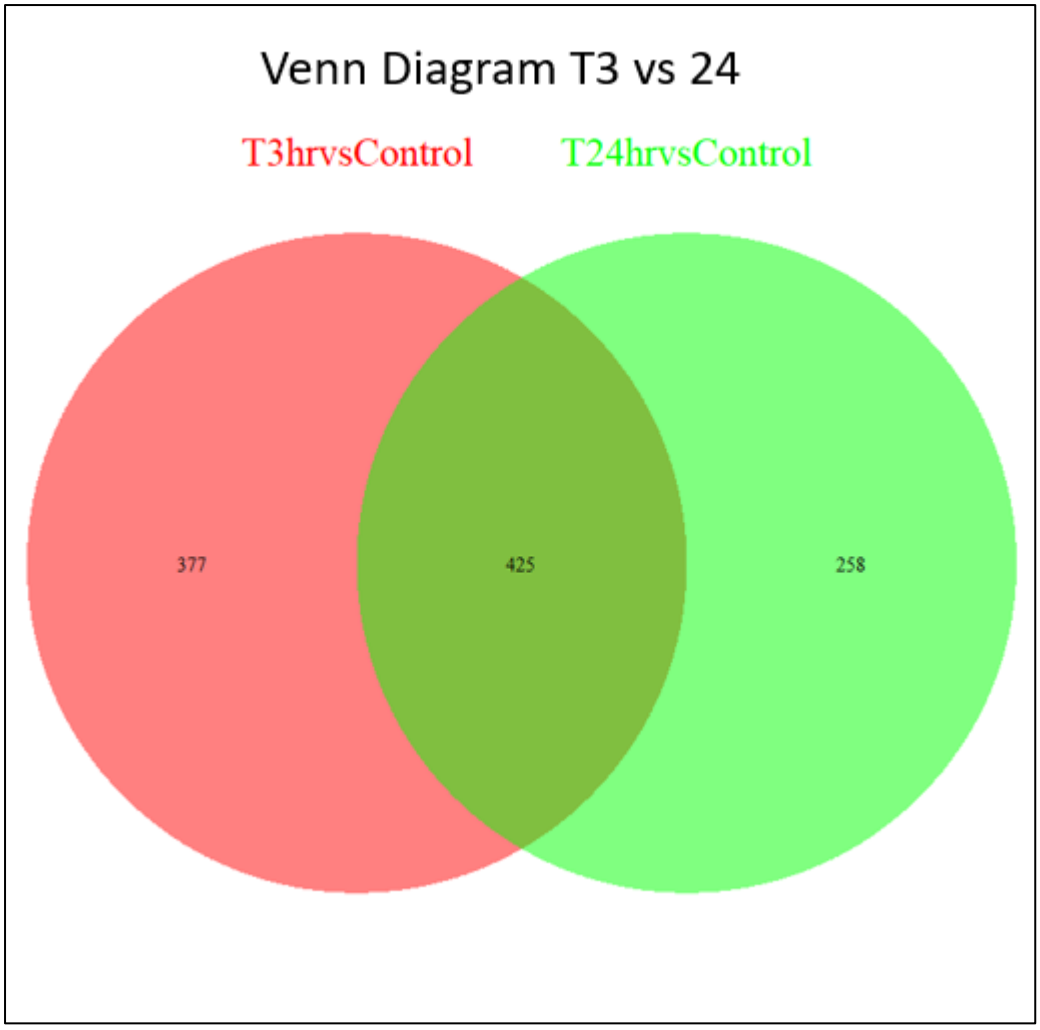

Figure 4.9 2 data groups, 3hrs DEG from Control, 24hrs vs Control. P adjust and P value = 0.05. Fold change >1 Venn diagram created with Biovenn (Hulsen et al., 2008)

Under these parameters a total of 1060 protein coding exons were found to be differentially expressed.

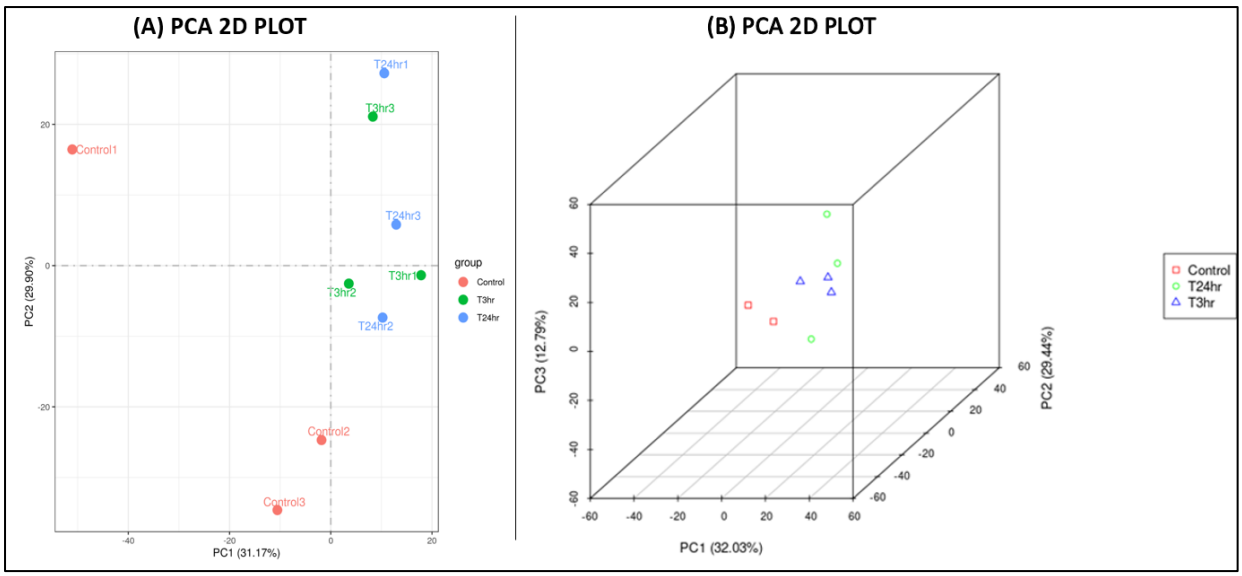

Figure 4.10: Principal Component Analysis of the triplicate data sets for control, 3hr and 24hr timepoints displaying the disparity in expression data between control and treated samples. 3hr and 24hr do cluster in the same quadrant of the plot while there is one errant control dataset.

Principal Component Analysis (PCA) visualised in Fig. 4.10 is a valuable statistical tool for the analysis of transcriptomic data. PCA helps simplify and visualize these datasets by reducing the dimensionality. Transcriptomic data is typically high-dimensional, containing expression levels of tens of thousands of genes across multiple samples. This can make it difficult to identify meaningful patterns and trends. PCA reduces the dimensionality of the data by projecting it onto a lower-dimensional space, which maintains most of the original data's variation. This simplification enables us to more easily identify and interpret biologically significant patterns in the data (Ringnér, 2008). When visualised in a 2D and 3D plot as in Fig. 4.11 the treated datasets (blue and green) are clearly separately clustered from the control sample dataset (although there is an errant sample that does not match the precision of transcriptomic expression the other two have).

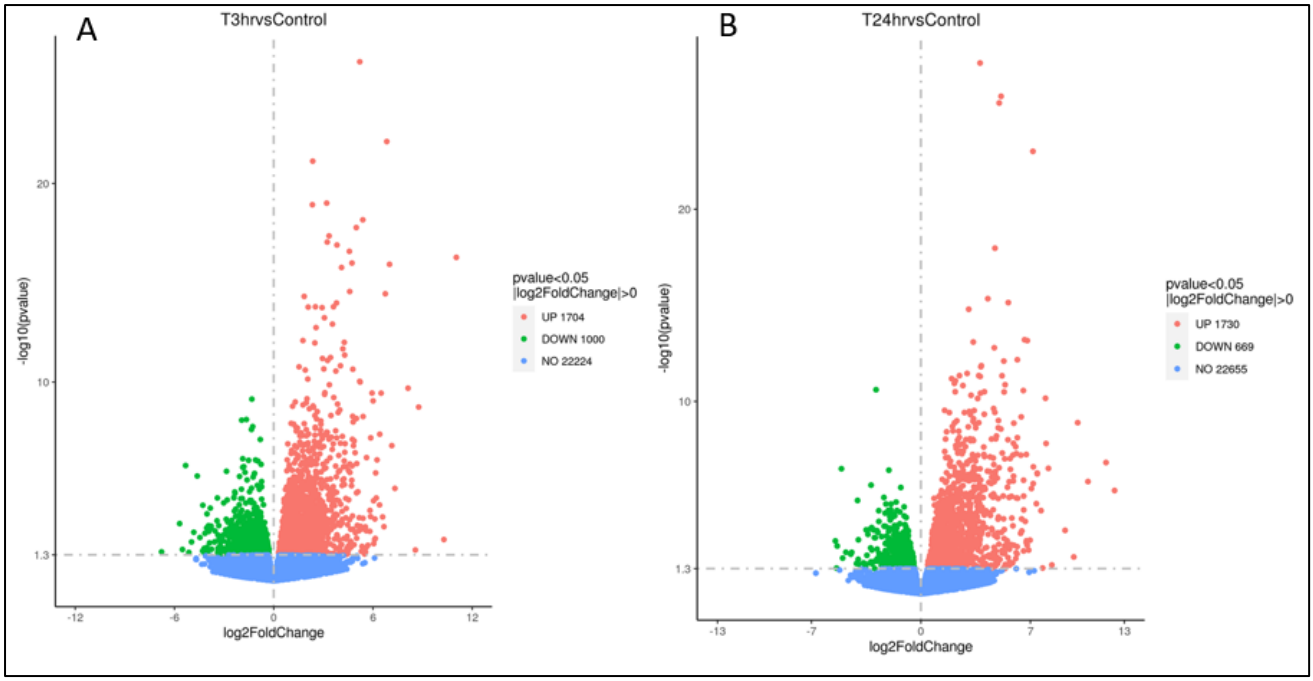

Figure 4.11: Volcano plot demonstrating the up regulated (green) and down regulated (red) of the fold changed genes (>0) and a p adjusted value < 0.05. (A) 3-hour dataset, (B) 24-hour dataset. This data is the volcano plot representation of the Venn diagram Figure 4.9.

A volcano plot displays the relationship between the fold-change in gene expression (e.g., treatment vs. control) and the statistical significance of that. This is a macro top-down visualisation style for the entire dataset and helps us to with identification of DEGs as they highlight genes with both significant fold-changes and high statistical significance. They also assist in simultaneous visualization of fold-change and significance: By plotting both the fold-change and statistical significance on the same graph, we can simultaneously assess the magnitude and significance of gene expression changes. Most important it allows a clear visual representation of gene expression patterns of the overall pattern of gene expression changes between two conditions. which can be used to identify trends or global effects, such as a general upregulation or downregulation of gene expression in response to a treatment (McDermaid et al., 2019).

In Fig 4.11 the x-axis shows the fold change of genes in different samples. The y-axis shows the statistically significant degree of changes in gene expression levels. The smaller the corrected p-value, the bigger -log10 (corrected p-value), the more significant the difference. The points represent genes, blue dots indicate no significant difference in gene expression,

red dots indicate upregulated differentially expressed genes, green dots indicate downregulated differentially expressed genes.

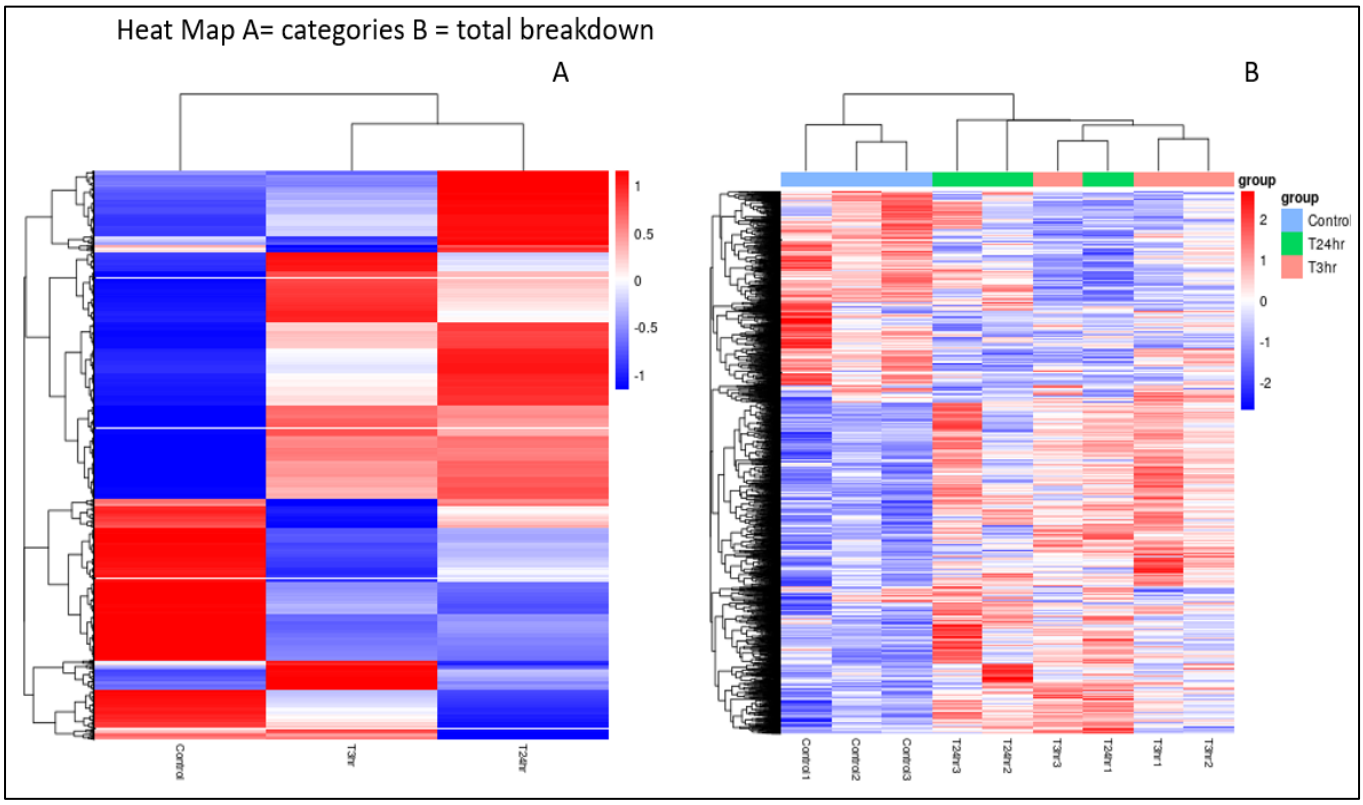

Figure 4.12 Heat map categorising up and down regulation and (B) visualisation of the total breakdown of each gene's up and down-regulation. The overall results of FPKM cluster analysis, clustered using the log10(FPKM+1) value. Red denotes genes with high expression levels, and blue denotes genes with low expression levels. The colour ranging from red to blue indicates log10(FPKM+1) value from large to small.

Heatmaps are a widely used and valuable visualization tool for displaying gene expression patterns across multiple conditions in transcriptomic data. They represent data in a matrix format, where rows correspond to genes, and columns represent different experimental conditions or samples. The expression level of each gene in a particular condition is represented by a coloured cell, with the colour gradient indicating the magnitude of expression (e.g., low to high). Heatmaps provide a clear and concise visual representation of gene expression patterns across varying conditions (such as no metal stress, 3hr post and 24 post metal stress). Heatmaps incorporate hierarchical clustering or other clustering algorithms to group genes with similar expression patterns and/or conditions with similar

gene expression profiles. This clustering can reveal important relationships between genes and conditions (McDermaid et al., 2019).

There is an obvious and clear difference between the control and treated samples for up and down-regulated gene expression (blue and red colour on chart). There is a particular up regulation in two thirds of the represented genes compared to the control and a down-regulation in the other third of treated samples. (A and B are inverted in Fig. 4.13 but represent the same data.)

4.4.2 Gene Ontology (GO) Analysis of DEGs

To further interrogate the list of DEG data generated from the RNA-Seq experiment, a gene ontology (GO) analysis was carried out using R script and the novosmart analysis tool (Kim et al., 2013). This enables us to identify GO terms and categories that occur most frequently in the DEG list, which can reveal biological processes that are differentially regulated, the cellular components in which these processes are occurring (localisation) and the molecular functions that are specifically affected by treatment with CuNP in the root system of the plant. The data generated from R script and novosmart analysis was further analysed by an online analytics tool called REVIGO (Supek et al., 2011), which can summarise and decrease the number of functional redundancies in categorisations, allowing easier and more coherent visualisation. Treemap outputs can display each cluster which are grouped further by colour into larger clusters, and the larger the cluster the more significant the P-value. The analysis allows a better overview of the data which can be utilised for downstream identification of pathways and biological processes over represented.

There are three major classifications for GO:

- **Biological process:** refers to the biological role involving the gene or gene product, and could include “transcription”, “signal transduction”, and “apoptosis”. A biological process generally involves a chemical or physical change of the starting material or input.
- **Molecular function:** represents the biochemical activity of the gene product; such activities could include “ligand”, “GTPase”, or “transporter”.

- **Cellular component:** refers to the location in the cell of the gene product. Cellular components could include “nucleus”, “lysosome”, and “plasma membrane”.

4.4.2.1 3-Hour Dataset GO analysis.

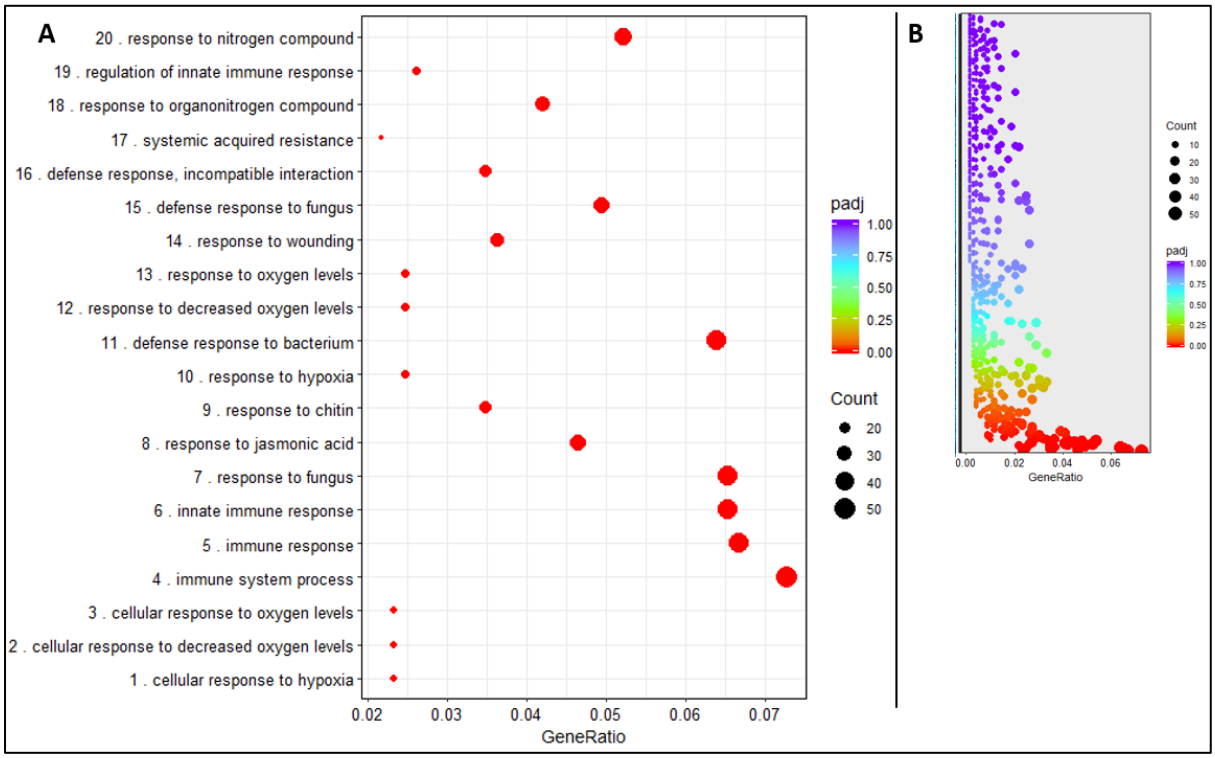

Figure 4.13: (A) GO dot plot depicting the top 20 represented BP categories in the 3-hr data set. Padj values indicate significance and size of circle indicates number of genes associated with category detected. (B) A more macro depiction of the total number of categorised genes including every detected BP category. Figure generated with Goplot (R plug in)

In Fig. 4.13, highly represented BP categories are linked to stress responses in the plant, such as immune responses and low oxygen responses as well as hormone responses. A colour gradient is used to highlight high confidence p scores, dark blue = low confidence, dark red = high confidence. The larger the circles the larger the number of detected DEGs associated with it.

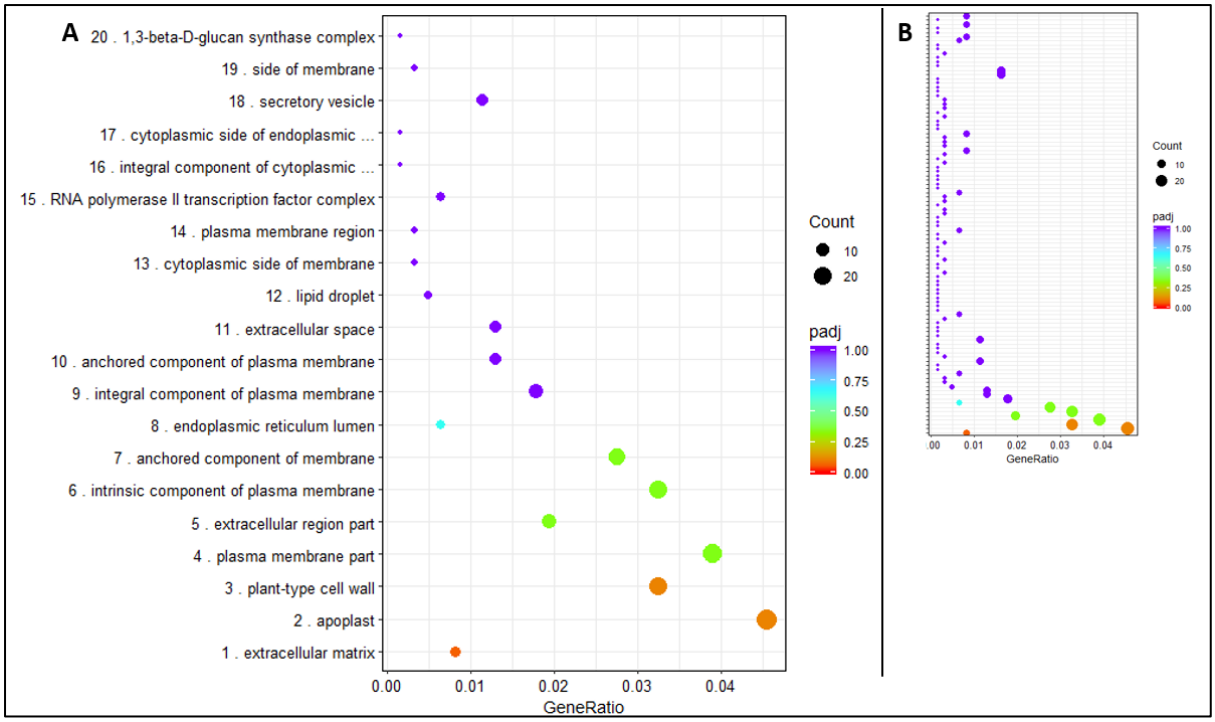

Figure 4.14: (A) GO dot plot depicting the top 20 represented CC categories in the 3hr data set. Padj values indicate the significance and the size of the circles indicates the number of genes associated with the category. (B) Macro depiction of the total number of categorised genes. Figure generated with Goplot (R plug in)

In figure 4.14 the highly represented localised areas of upregulation include genes encoding components of the extracellular matrix, cell wall and plasma membrane. This response is in line with observations made in Chapter 3 results where CuNPs were imaged localised within the extracellular space of the plant. There is a strong localisation in very few locations within the plant cell, primarily the apoplastic space indicating most of the differential activity and transcriptional change occurred in genes linked to the outer face of cell organelles.

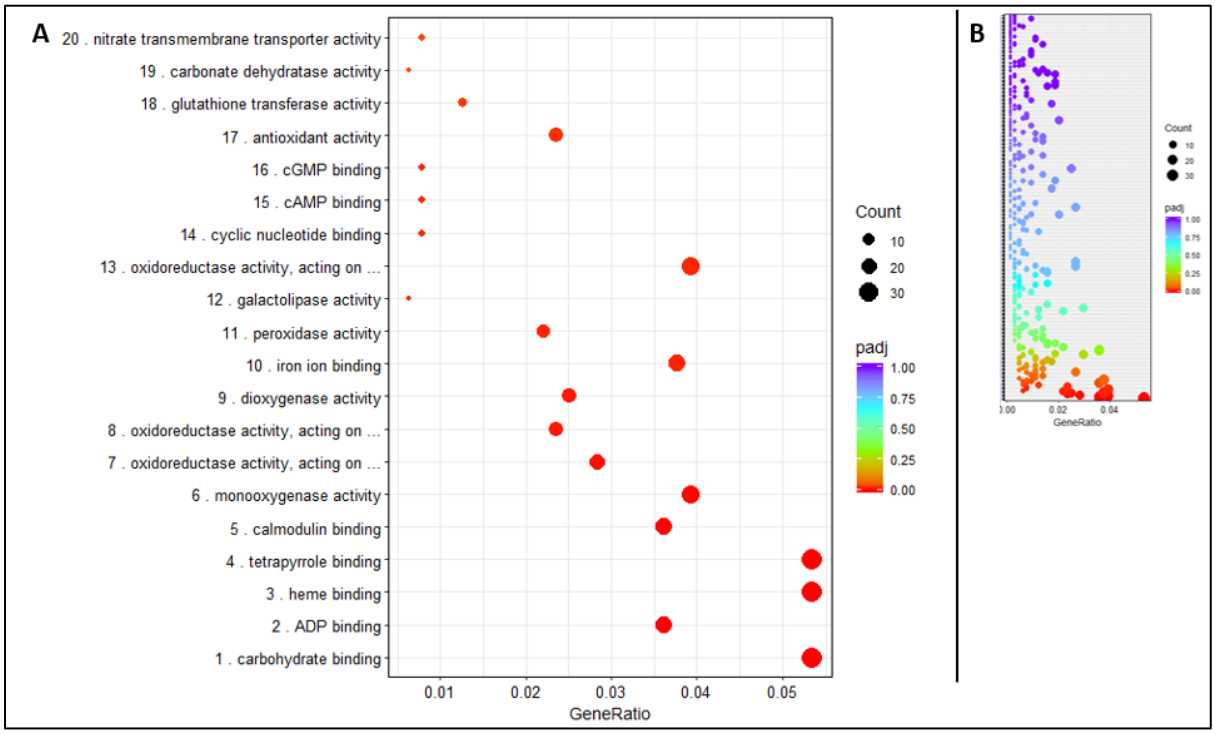

Figure 4.15: (A) GO dot plot of Molecular function (MF) category displaying the top 20 represented in 3 hr dataset. Padj values indicate significance and size of circles indicating number of genes associated with the category. (B) Macro depiction of total number of categorised genes. Figure generated with Goplot (R plug in)

Figure 4.15 shows the top 20 MF categories associated with differential regulation, and include a significant amount of binding and sequestering processes as well as several ROS-associated processes.

4.4.2.2 24-hour Dataset GO analysis

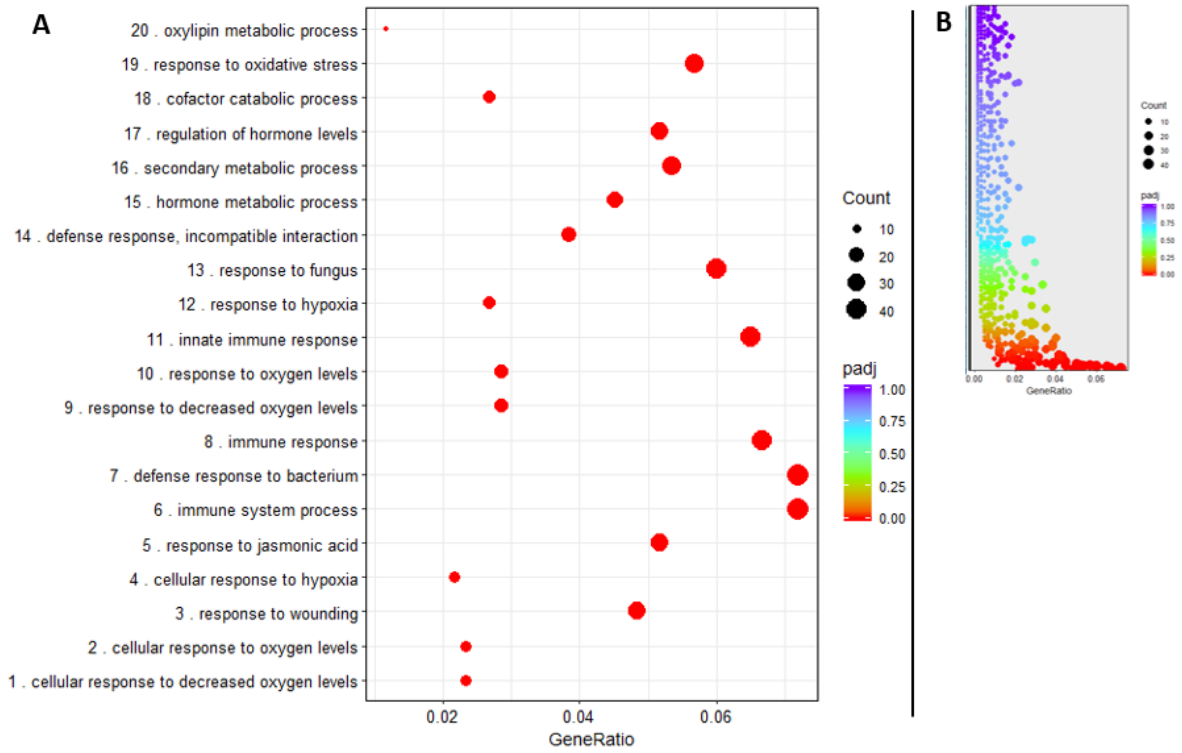

Figure 4.16 *(A) GO dot plot of Biological Process (BP) category displaying the top 20 represented in 24 hr dataset. Padj values indicate significance and size of circles indicating number of genes associated with the category. (B) Macro depiction of total number of categorised genes. Figure generated with Goplot (R plug in)*

Figure 4.16 displays the BP processes of the 24hr dataset and with significant upregulation of genes associated with the immune system and ROS.

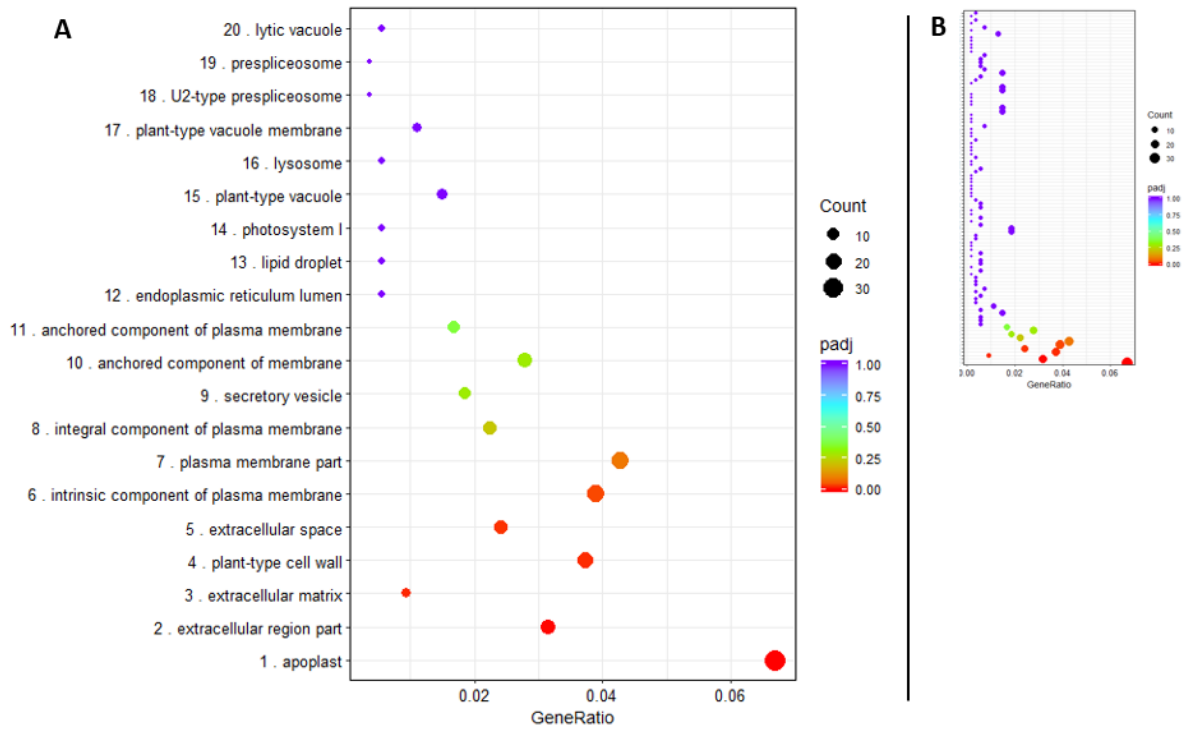

Figure 4.17 (A) GO dot plot depicting the top 20 represented CC categories in the 24-hr data set. Padj values indicate the significance and the size of the circles indicates the number of genes associated with the category. (B) Macro depiction of the total number of categorised genes. Figure generated with Goplot (R plug in)

Like the 3 hr dataset, Fig. 4.17 CC data show that DEGs are associated with proteins linked to the apoplast, cell wall and plasma membrane, more significantly and more highly represented than for any other cellular compartment.

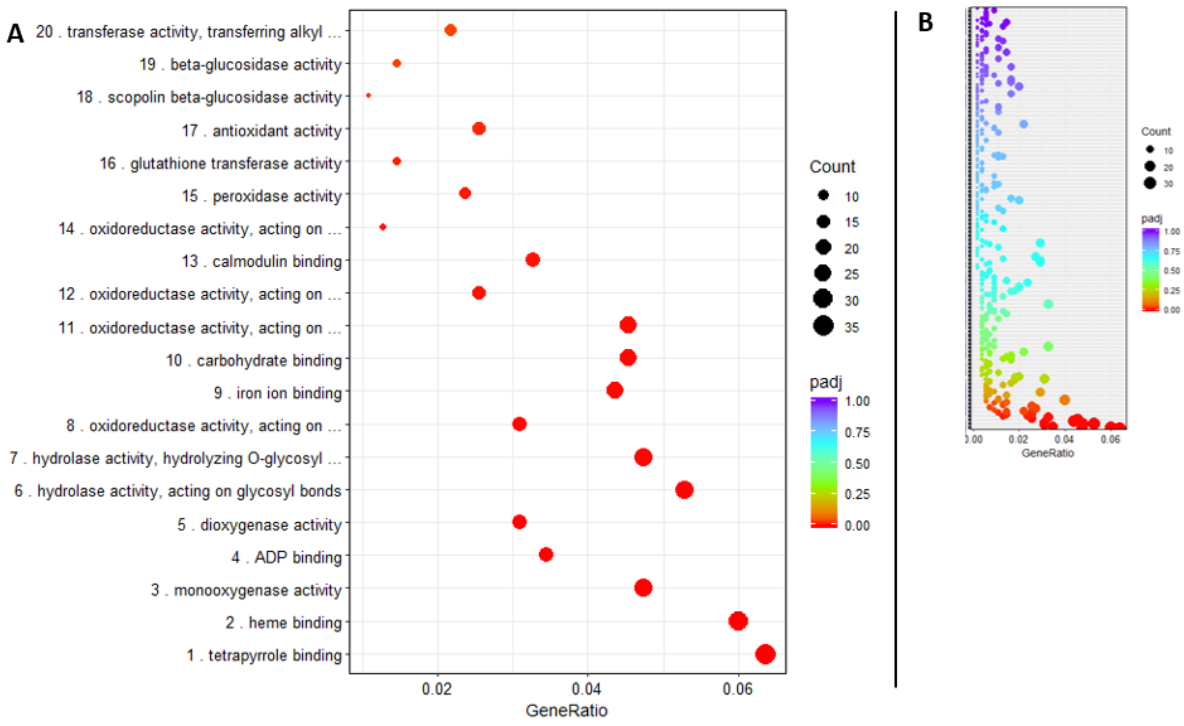

Figure 4.18: (A) GO dot plot of Molecular function (MF) category displaying the top 20 represented in 24 hr dataset. Padj values indicate significance and size of circles indicating number of genes associated with the category. (B) Macro depiction of total number of categorised genes. Figure generated with Goplot (R plug in)

Very similarly to the 3-hr dataset most of the same MF categories are seen represented at 24 h (Fig. 4.18), including metal binding, redox processes and hydrolases.

4.4.3 Functional Analysis – GO enrichment

Figures 4.13 - 4.18 indicate the biological process, molecular function and cellular component categorisations for both up- and downregulated genes. It is likely that there will be substantial redundancies from the outputs of GO analyses which can cause challenges in interpretation as multiple categories overlap or are including the same regulated genes (Supek et al., 2011). Further analysis of the data was conducted using REVIGO, an online tool that summarizes a list of GO terms and reduces functional redundancies, enabling the visualization of the data in a user-friendly format (Supek et al., 2011). The tool achieves this by grouping semantically similar GO terms into clusters and identifying a single GO term as the representative for each cluster, thus reducing the lengthy list of GO terms into a more manageable format. The treemaps (Figures 4.19 -4.23) present each cluster as a rectangle and further group them,

based on colour, into superclusters, with the size of the rectangles representing the corresponding P-values. This analysis provides a concise overview of the data and facilitates the identification of potential pathways and processes.

4.4.3.1 3hr Dataset

Figure 4.19 CC REVIGO plot of 3 hr dataset. P-value ≤ 0.05 and a log_2 fold change (log_2fc) ≥1. Each rectangle represents a gene ontology (GO) term cluster and each colour represents a supercluster of related clusters. The superclusters are listed in the key below the treemap. Sizes of rectangles reflect the –log10 P-value of each cluster.

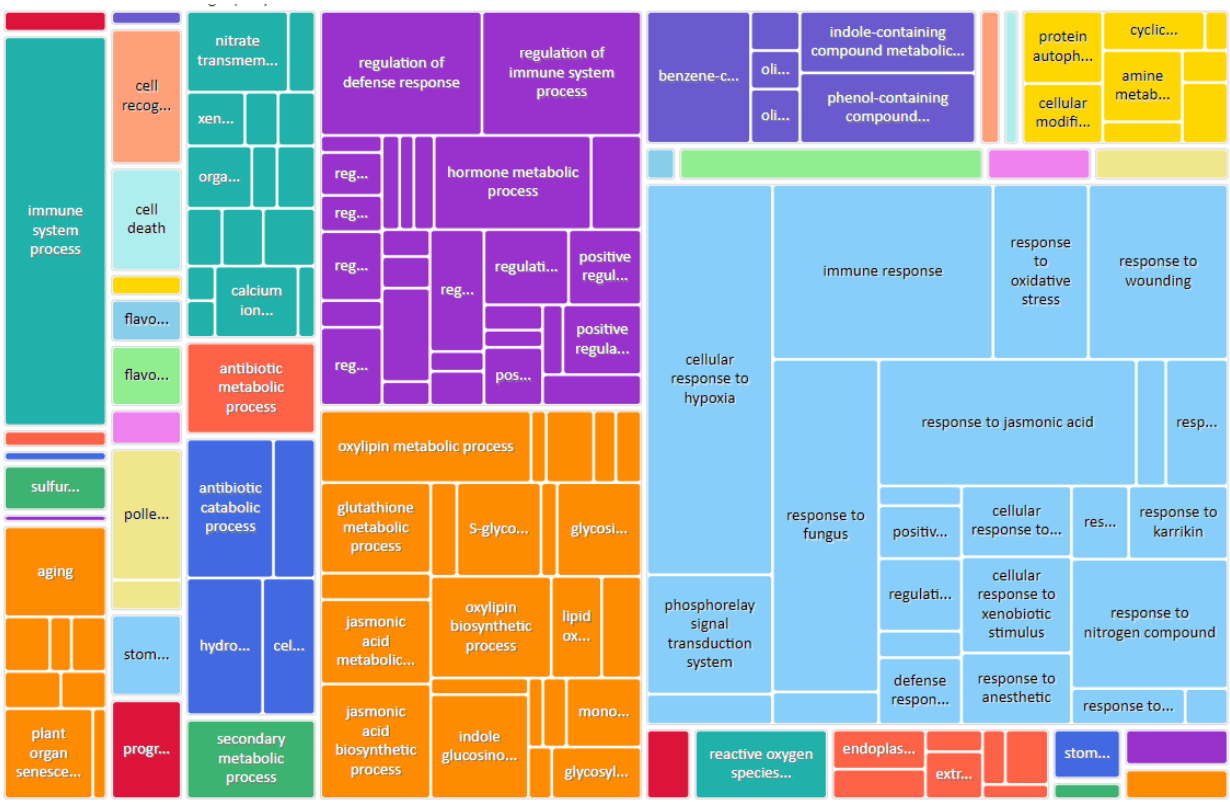

Figure 4.20 BP REVIGO plot of 3hr dataset. P-value ≤ 0.05 and a log_2 fold change (log_2fc) ≥1. Each rectangle represents a gene ontology (GO) term cluster and each colour represents a supercluster of related clusters. The superclusters are listed in the key below the treemap. Sizes of rectangles reflect the –log10 P-value of each cluster.

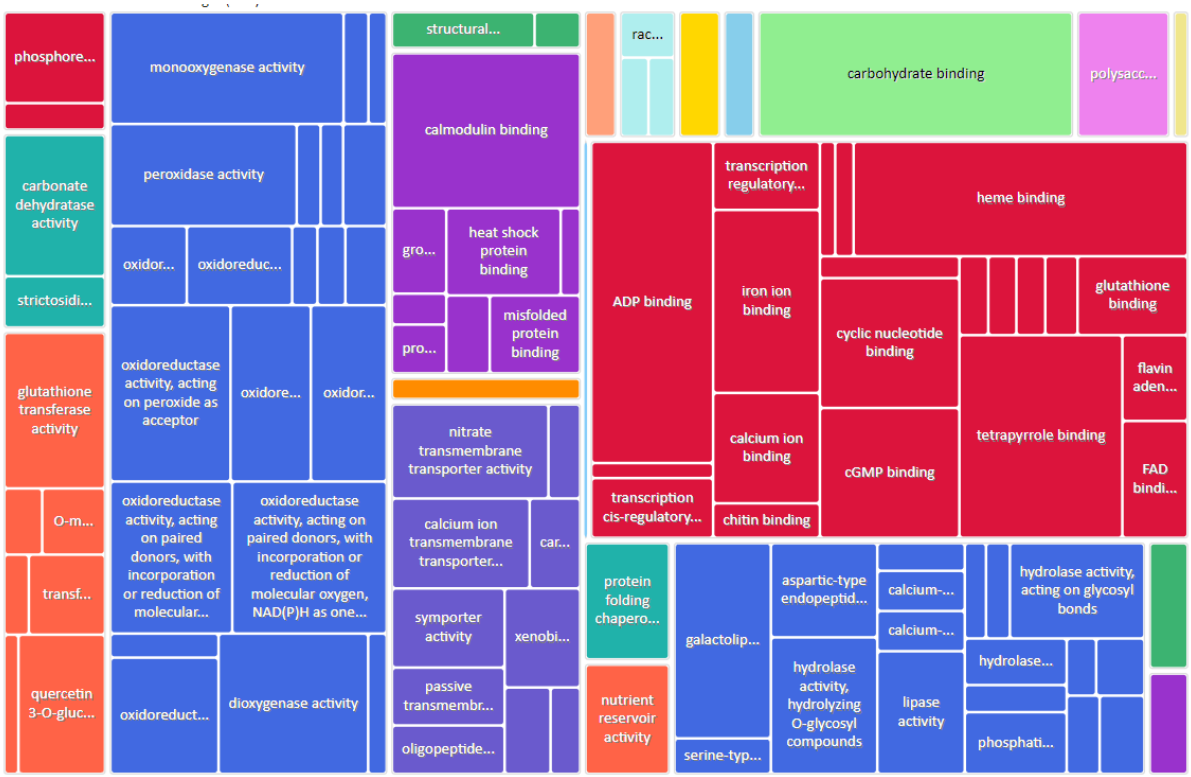

Figure 4.22: MF REVIGO plot of 3hr dataset. P-value ≤ 0.05 and a log_2 fold change (log_2fc) ≥1. Each rectangle represents a gene ontology (GO) term cluster and each colour represents a supercluster of related clusters. The superclusters are listed in the key below the treemap. Sizes of rectangles reflect the –log10 P-value of each cluster.

4.4.3.2 Analysis of 3hr dataset TREEMAP visualisation

We can see from the CC dataset that activity is located in the plasma membrane and other membrane-associated GO terms (red) Apoplastic space (purple) and extracellular matrix (green). CuNPs. Very few other cellular components were significantly differentially expressed which gives us confidence in the location of the expressional changes. BP processes included metabolic changes (orange), hormone signal transduction (blue) and an immune system response (purple). MF big categories include binding (red), oxidoreductase activity (blue),

4.4.3.3 24hr Dataset

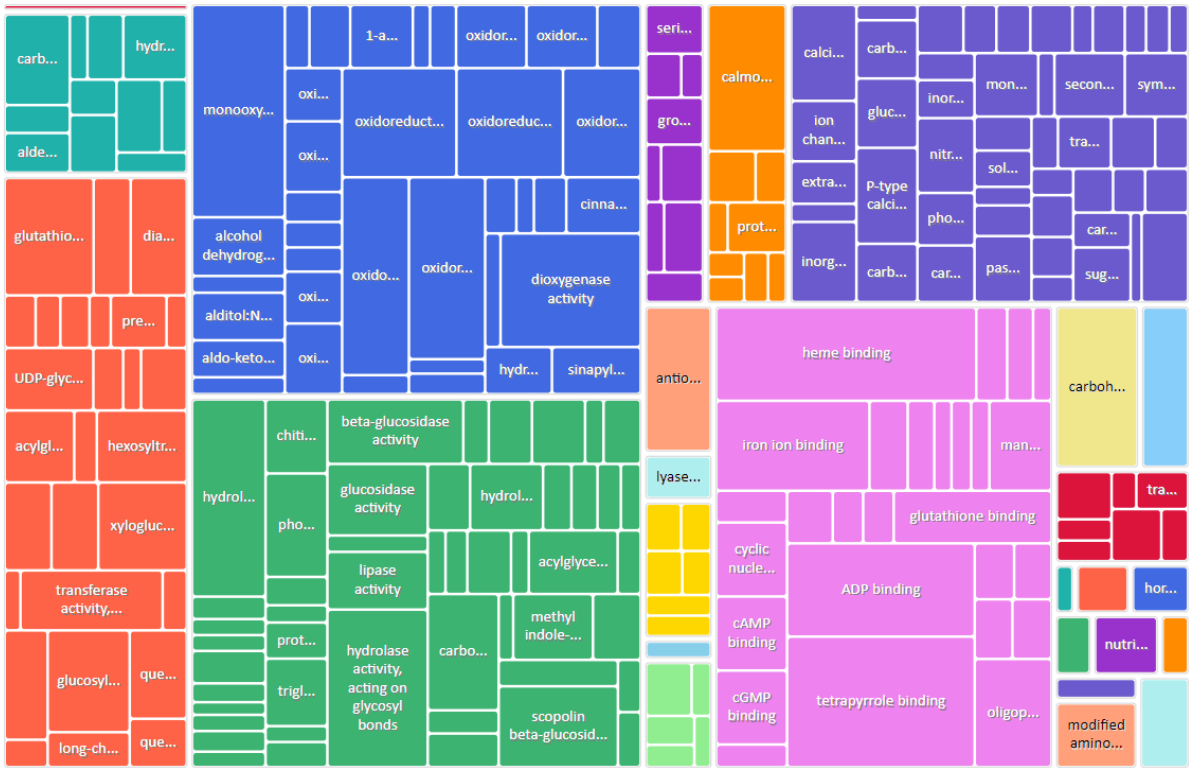

Figure 4.21: MF Revigo plot of 24hr dataset. P-value ≤ 0.05 and a log_2 fold change (log_2fc) ≥1. Each rectangle represents a gene ontology (GO) term cluster and each colour represents a supercluster of related clusters. The superclusters are listed in the key below the treemap. Sizes of rectangles reflect the –log10 P-value of each cluster.

Figure 4.22: BP REVIGO plot of 24 hr dataset. P-value ≤ 0.05 and a log_2 fold change (log_2fc) ≥1. Each rectangle represents a gene ontology (GO) term cluster and each colour represents a supercluster of related clusters. The superclusters are listed in the key below the treemap. Sizes of rectangles reflect the –log10 P-value of each cluster.

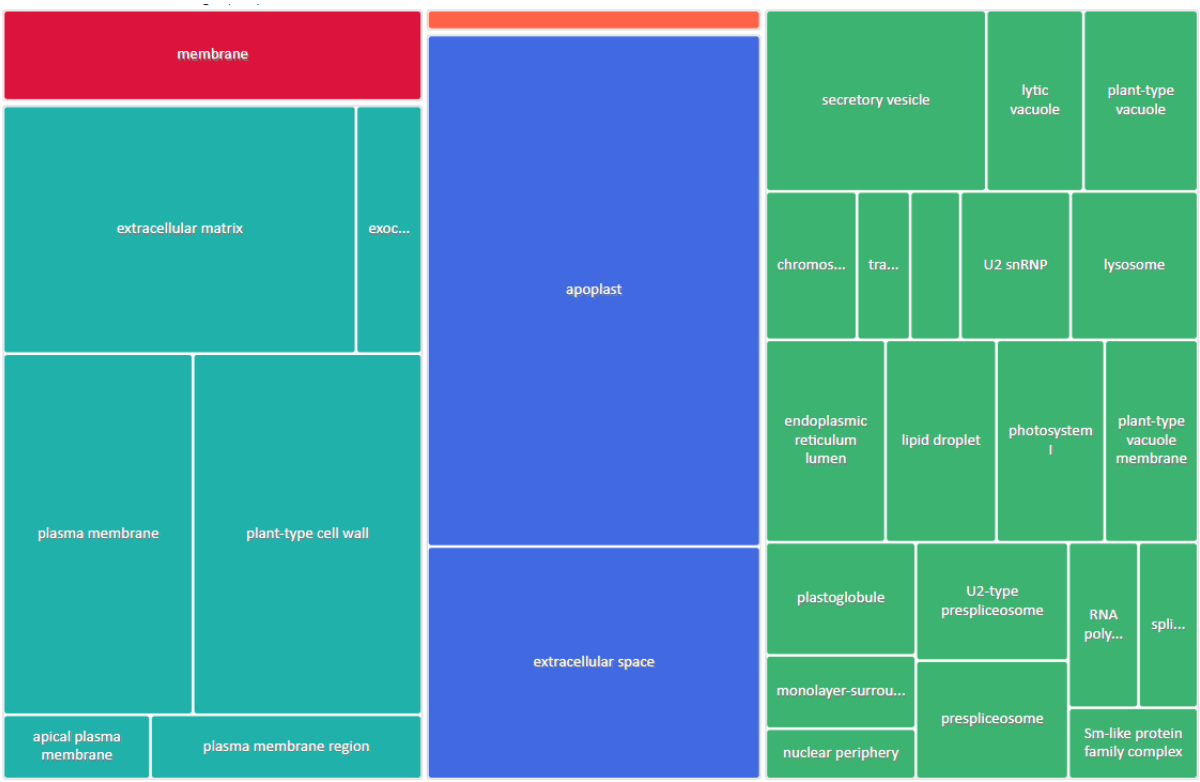

Figure 4.23: CC REVIGO plot of 24hr dataset. P-value ≤ 0.05 and a log_2 fold change (log_2fc) ≥1. Each rectangle represents a gene ontology (GO) term cluster and each colour represents a supercluster of related clusters. The superclusters are listed in the key below the treemap. Sizes of rectangles reflect the –log10 P-value of each cluster.

The results show there is a clear overlap in the GO expression data for both the 3 and 24 hr datasets. In terms of the localisation in the CC category there is clearly a significant expressional change occurring within genes encoding components of the extracellular and apoplastic space in response to uptake of CuNP particles, and there are superclusters present for membrane and intermembrane vesicular transport genes. BP from both datasets indicates a significant increase in the genes involved in responses to external stresses, in particular pathogen response (response to fungus, response to wounding). Superclusters strongly represented are under the category of immune system process (Fig. 4.24). There are also superclusters associated with hormone signal transduction (Figs. 4.27, 4.24). Molecular function (MF) has a particular supercluster around oxidative 'ROS' response in both the 3 and 24 hr datasets. Additionally, there is a supercluster in both datasets centred on ion binding and transport. The significant impact on ROS pathways and hormone signalling is a significant

indication of an important biological shift in the plants developmental response to the stress caused by CuNP addition.

4.5 KEGG Analysis

Kyoto Encyclopaedia of Genes and Genomes (KEGG) annotates genes to pathway level. Taking the previously explored information and expanding upon the pathways they act upon gives us greater insights into specific implications of DEG expression in response to CuNPs, and its impact upon the macro biological processes of the plant (KEGG PATHWAY Database).

4.5.1 3 Hr KEGG analysis

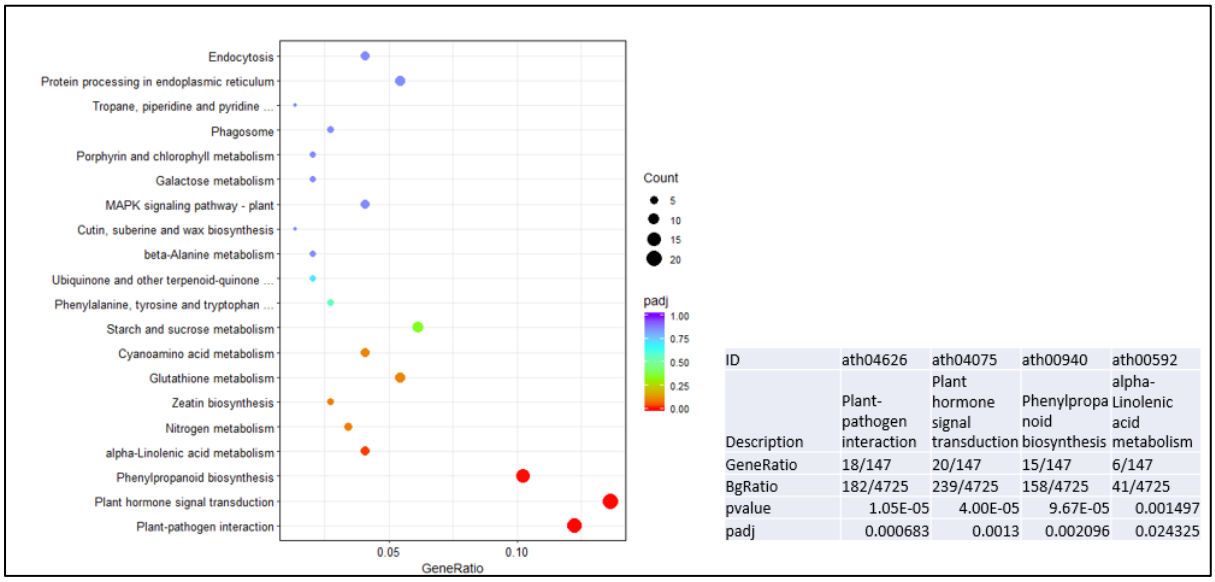

ID	ath04626	ath04075	ath00940	ath00592
Description	Plant-pathogen interaction	Plant hormone signal transduction	Phenylpropanoid biosynthesis	alpha-Linolenic acid metabolism
GeneRatio	18/147	20/147	15/147	6/147
BgRatio	182/4725	239/4725	158/4725	41/4725
pvalue	1.05E-05	4.00E-05	9.67E-05	0.001497
padj	0.000683	0.0013	0.002096	0.024325

Figure 4.24: KEGG dot plot of pathways differentially regulated following CuNP treatment. Top 4 KEGG pathways identified that meet the p-value and gene ratio requirements for significance in this study. Plot generated with Go plot (R plugin)

The gene list is attached to Fig. 4.24 and demonstrates some of the most commonly occurring KEGG pathways that have been upregulated in this experiment, and these were analysed further.

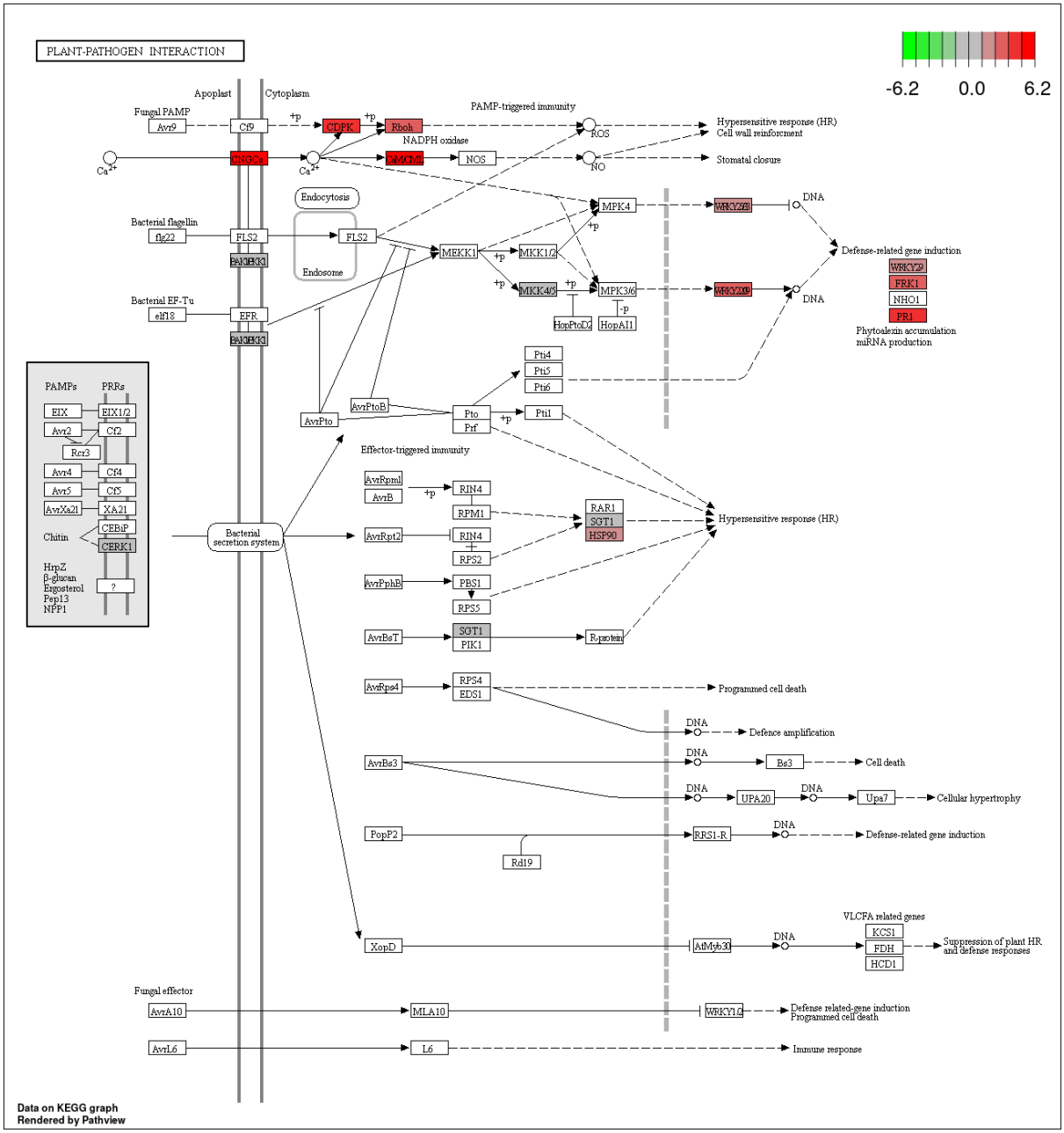

Figure 4.25 : The Plant Pathogen pathway with up and down-regulated transcriptomic data at 3 hr CuNP treatment included – upregulated genes colour coded increasingly red while downregulated are colour-coded green. as depicted in the KEGG database (KEGG PATHWAY Database).

As can be seen from Figs 4.25, there is significant upregulation of genes involved in the recognition of PAMPs, Ca^{2+} signalling and defence-related gene induction.

Plant Pathogen Interaction	log2 Fold Change
CNGC19	2.756787
CPK22	2.604251
CML37	2.594689
SIRK	2.513054
CML12	2.34014
HSP90-1	2.301658
CML39	2.20379
CPK27	1.868966
CNGC13	1.716775
CML44	1.61704
WRKY29	1.606503
RBOHD	1.416518
CNGC10	1.363213
RBOHA	1.112725
CNGC20	0.869834
CNGC2	-1.6098

Table 4.1: Genes involved in the plant pathogen response pathway and their expressional fold change compared to the control dataset.

An examination of the differentially expressed transcripts led to the identification of 17 genes with known functions, some of which play a role in plant responses to pathogen infection, and changes in expression of stress-related genes. For example, *RbohA* and *D* are associated with the ROS response system (See Chapter 1 ROS). These findings suggest that plants perceive exposure to CuNPs in part at least as a biotic stress factor comparable to pathogen or herbivore attack. This upregulation of plant pathogen response genes reflects results from other metal nanoparticle research, notably exposure to titanium and silver nanoparticles (García-Sánchez et al., 2015).

CNGC2, *10*, *13*, *19* and *20* are differentially regulated. Cyclic nucleotide-gated ion channels (CNGCs) are a family of ion channels that play a crucial role in various physiological processes in both animals and plants. These channels are non-selective cation channels that are activated by the binding of cyclic nucleotides, such as cyclic adenosine monophosphate (cAMP) and cyclic guanosine monophosphate (cGMP). CNGCs are involved in various physiological processes, such as nutrient uptake, pollen tube growth, and response to biotic

and abiotic stress. In plant models 20 CNGC genes are known which are grouped into four major groups (I-IV).

Group I: This group consists of six members (CNGC1-6). Members of this group are primarily involved in plant development and nutrient uptake. CNGC2 has a role in pollen tube growth and guidance. but is down regulated here.

Group II: This group contains CNGC7-10. Group II CNGCs have been implicated in various physiological processes. CNGC10 has a role in the regulation of plant growth and development, as well as in the response to oxidative stress so is substantially upregulated here.

Group III: This group is composed of CNGC11-16. Group III CNGCs are associated with plant development and stress responses. CNGC13 has been implicated in response to salt stress.

Group IV: This group consists of four members CNGC17-20. Members of this group have diverse functions, including roles in plant development, nutrient uptake, and stress responses. CNGC19 plays a role in the response to biotic stress, and CNGC20 is associated with abiotic stress responses, particularly in the regulation of stomatal closure (Duszyn et al., 2019).

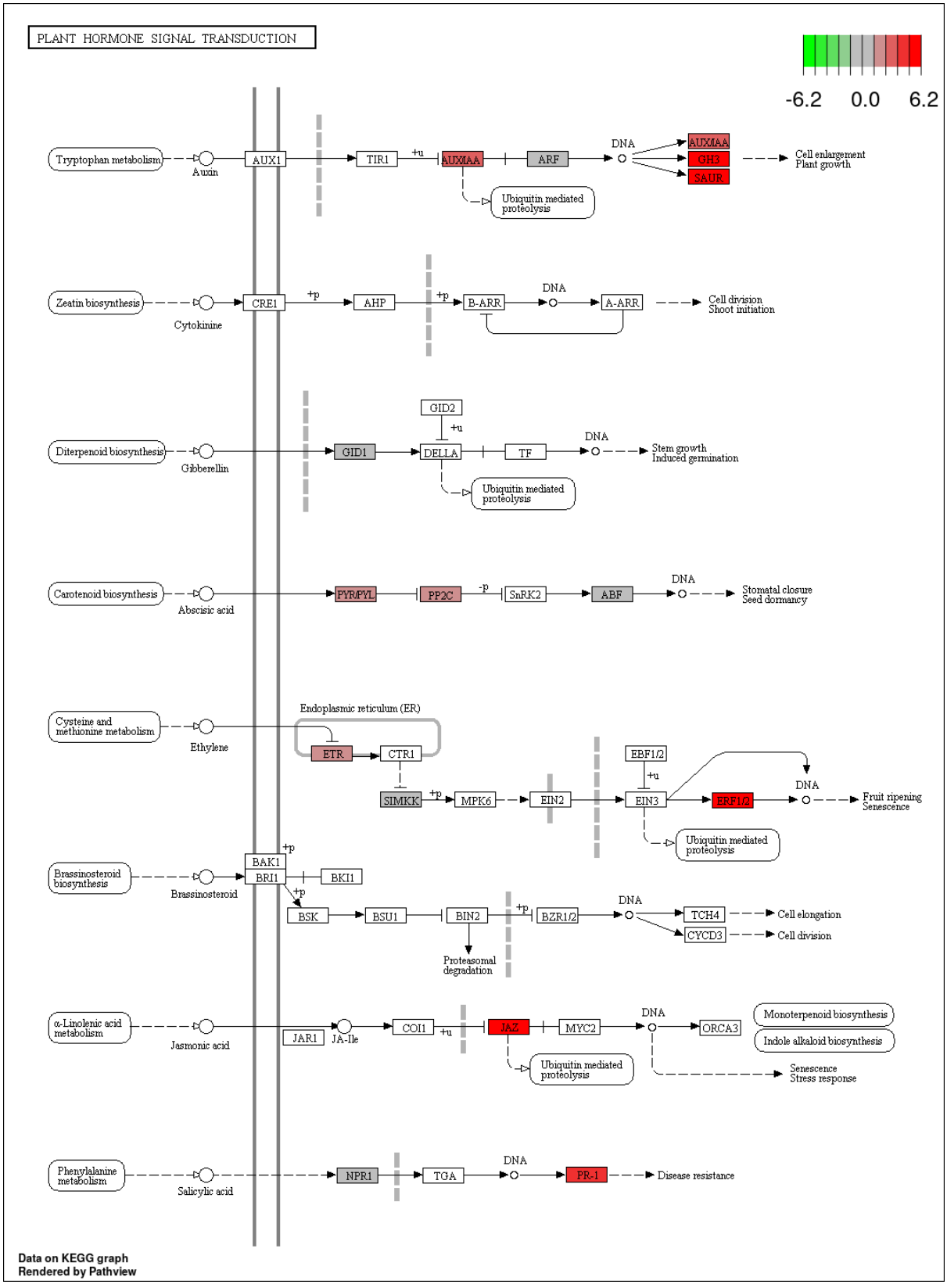

Figure 4.26: Plant Hormone Signal Transduction pathways as depicted by KEGG pathway (KEGG PATHWAY Database). with 3 hr upregulated genes colour coded in red through the pathviewer visualising software. Organism-specific pathway: green boxes are hyperlinked to

GENES entries by converting K numbers (KO identifiers) to gene identifiers in the reference pathway, indicating the presence of genes in the genome and also the completeness of the pathway. a red highlight indicates a disease-causing gene or disease associated variants (KEGG PATHWAY Database,)

Plant Hormone Signal Transduction	Log2 Fold Change
PBS3	4.29578
SAUR71	3.759186
JAZ10	3.064139
ERF1B	3.051736
TIFY11A	2.07444
ERF2	1.979565
PYL6	1.773044
SAUR41	1.550903
GID1B	1.142129
IAA10	0.988825
IAA18	0.717054
EEL	0.541283
ARR9	-0.86955
ABF1	-1.3455
ARR5	-1.65092
ARR6	-1.6722
SHY2	-2.06563

Table 4.2: 17 Genes up and down-regulated in the KEGG pathway at the 3hr time point compared to the control dataset.

There are numerous differential expression points in the plant hormone signal transduction pathway in this dataset. Most notable is the tryptophan metabolic pathway associated with auxin biosynthesis cell enlargement and plant growth. We also see moderate increase in carotenoid biosynthesis, associated with synthesis of the stress hormone ABA (something identified in biochemical assays in Chapter 3). Cysteine and Methionine metabolism linked to ethylene signalling is also upregulated, and in particular the ERF1/2 gene associated with increased senescence in the plant. α-linoleic acid synthesis metabolism is strongly upregulated, linked to jasmonic acid, ROS response and terpenoid synthesis. These represent

plant defence and immune responses through mechanisms involving respectively, the phytohormones jasmonic acid, auxin, ABA and ethylene pathways. Results in Chapter 3 that describe the phenotypic response to CuNPs show there is significant primary root growth inhibition as well as significant impact on the growth and development of the root hairs. Hormonal signalling, such as described above, is an important regulator of root development. ABF1 (a protein that binds abscisic acid responsive elements in target gene promoters) has been shown to be involved in readjustment of root morphology in the event of abiotic stress conditions (Galvan-Ampudia & Testerink, 2011; Wang et al., 2008).

Some genes regulating hormonal stimuli and stress response were also identified as responsive to CuNP treatment and linked with systemic acquired response (SAR), an enhanced immunity in tissues remote from the initial infection site. SAR is triggered upon challenge by certain pathogens and occasionally by mechanical damage such as damage by insects (Raza et al., 2022).

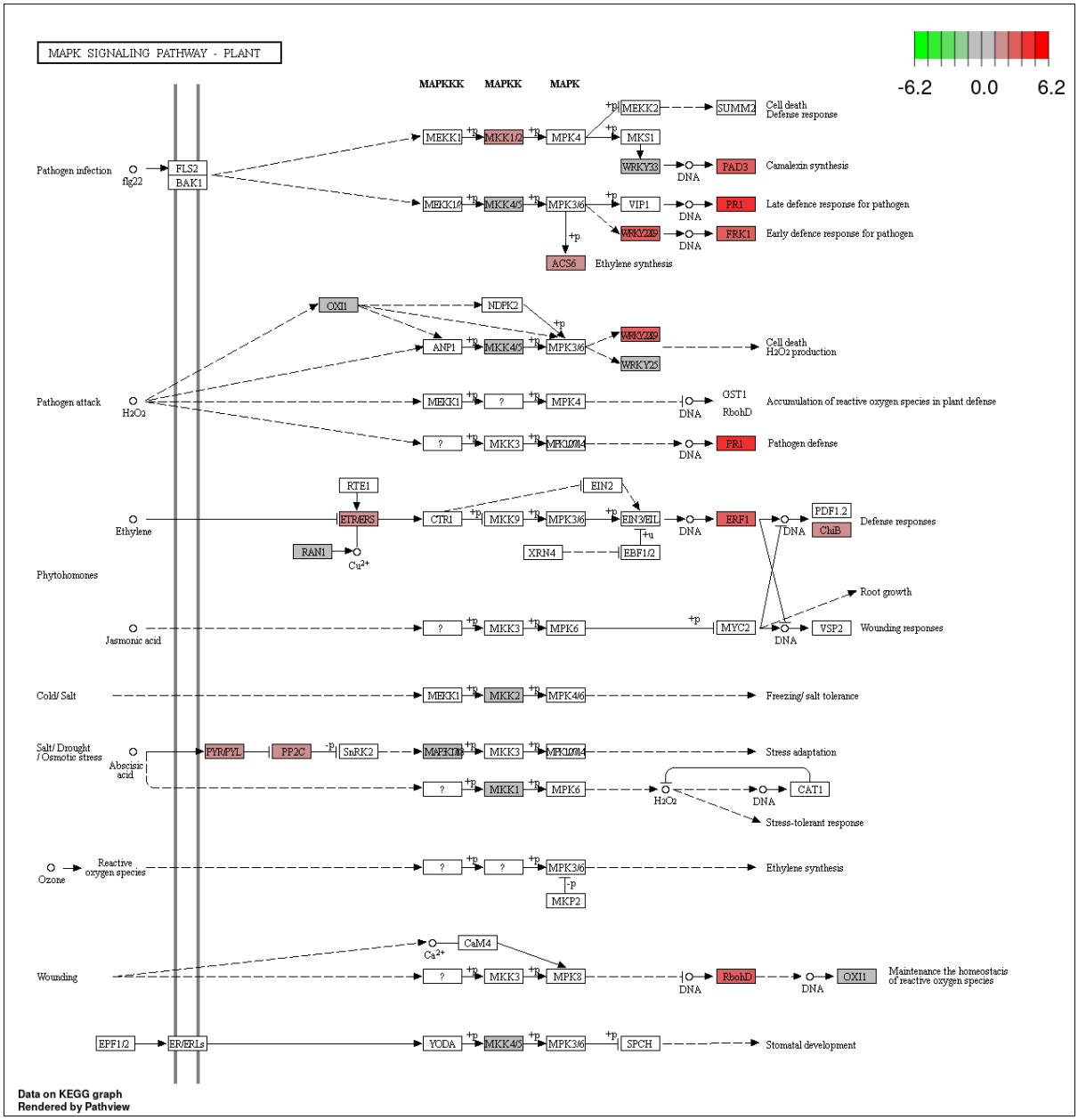

Figure 4.27: MAPK signalling pathway – Mitotic activated protein kinase pathway is crucial to regulated transcription and cellular proliferation (KEGG PATHWAY Database). *3hr upregulated genes colour coded in red through the pathviewer visualising software.*

The response to CuNPs also leads to activation of genes associated with ethylene, ROS and other stress-induced signalling pathways. The MAPK cascade (Fig. 4.27) leads to phosphorylation of downstream target proteins, including transcription factors, which ultimately regulate gene expression, resulting in diverse cellular responses. The MAPK signalling system is a crucial mechanism in plants for sensing and responding to environmental changes (Meng & Zhang, 2013). ERF1 activates the MAPK pathway by phosphorylating the MAPKKK (Mitogen-Activated Protein Kinase Kinase Kinase) protein CTR1

(CONSTITUTIVE TRIPLE RESPONSE1), leading to its inactivation. This, in turn, activates the downstream MAPK cascade, ultimately leading to the phosphorylation of various downstream target proteins and transcription factors, which regulate gene expression and plant responses to stress and to the ethylene signalling response (Meng & Zhang, 2013).

PR1 (PATHOGENESIS-RELATED PROTEIN 1) is a known marker gene for the salicylic acid (SA) signalling pathway and is commonly used as a readout for SA-mediated plant defence responses. *PR1* expression is regulated by the transcription factor NPR1 (NONEXPRESSER OF PATHOGENESIS-RELATED GENE 1) and is induced in response to pathogen attack and other stress signals (Meng & Zhang, 2013). PR1 may also play a role in the MAPK pathway in plants. PR1 has been shown to be a downstream target of MPK3 and MPK6, two key components of the MAPK cascade in plants (Meng & Zhang, 2013). MPK3 and MPK6 can phosphorylate a transcription factor, WRKY33 that activates the expression of PR1 and other defence genes There is a possibility that the MAPK pathway and the SA pathway are not independent of each other, but rather interact through cross-talk in the plant defence response.

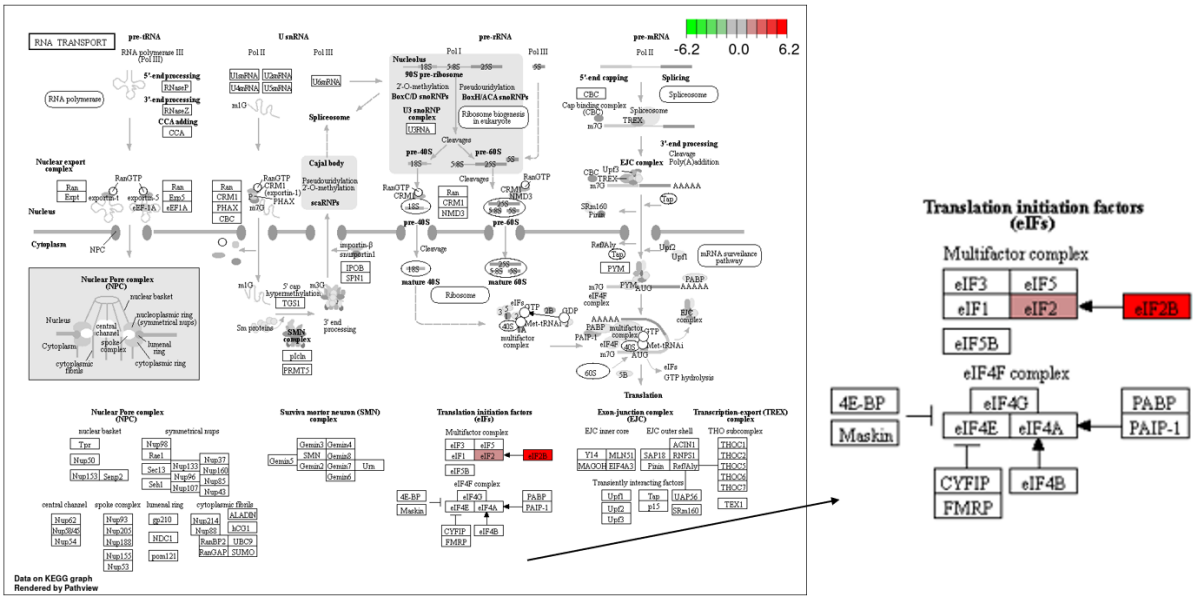

Figure 4.28: Upregulation at 3hr of EIf2/B in the RNA transportation pathway in seedlings treated with CuNPs (KEGG PATHWAY Database).

eIF2/B (Eukaryotic Initiation Factor 2/B) is a protein complex that plays a role in the regulation of protein synthesis initiation in eukaryotic cells. While eIF2B is primarily known for its function in translation initiation, in eukaryotic cells RNA molecules are synthesized in the nucleus and then transported to the cytoplasm for translation. This process involves the

binding of specific RNA-binding proteins, such as EXPORTIN 1 (XPO1) protein, to the RNA molecules, which then facilitates their transport through the nuclear pore complex. eIF2B can bind to XPO1 and promote its nuclear export, leading to an increase in the transport of RNA molecules from the nucleus to the cytoplasm (Kelen et al., 2009).

Therefore, eIF2B may have a broader role beyond translation initiation, as it could contribute to the regulation of cellular processes that rely on proper RNA transportation (Azmi et al., 2021). and thus may be enhanced in response to CuNPs.

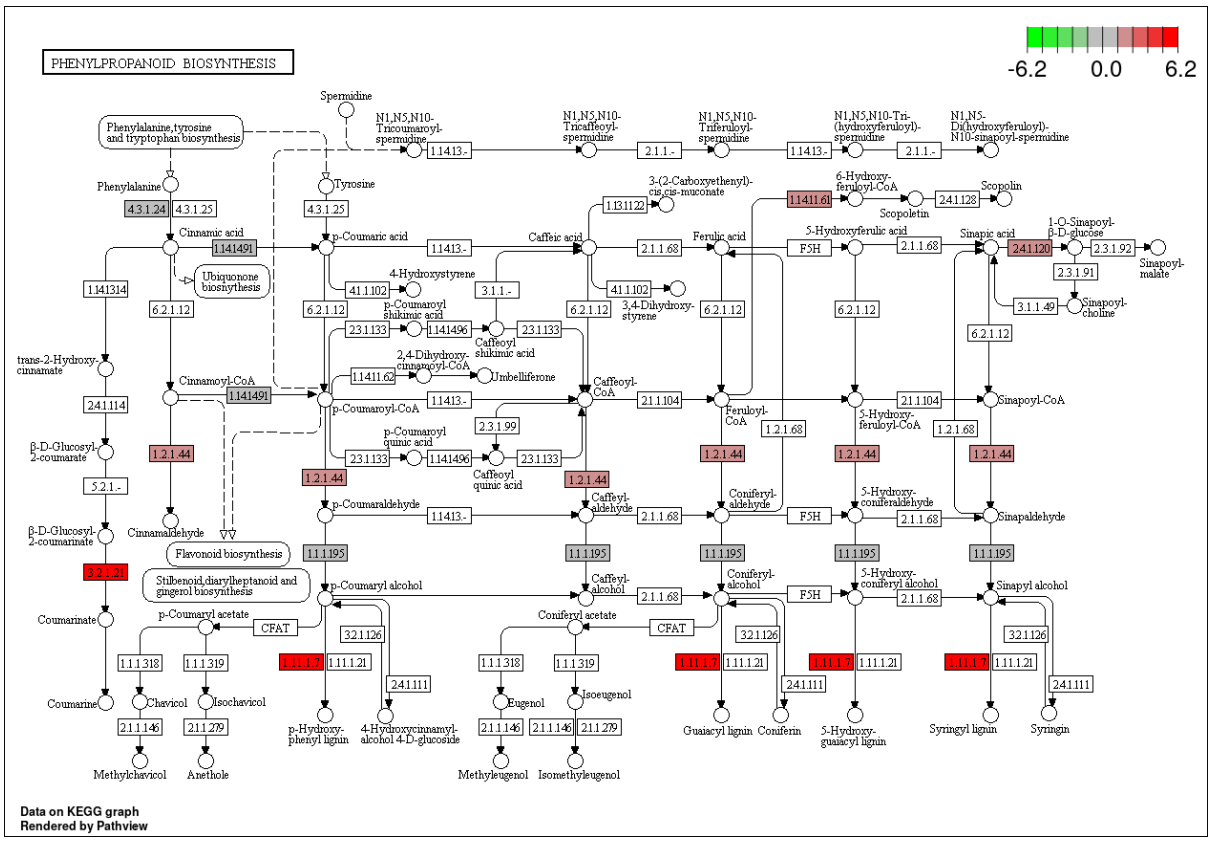

Figure 4.29: KEGG pathway showing phenypropanoid synthesis pathway (KEGG PATHWAY Database)*. Genes upregulated at 3hr are colour coded in red.*

Phenylpropanoid biosynthesis	Log2 Fold Change
PER28	4.575691535
PER33	5.000725256
BGLU27	3.786149753
PER62	2.115091969
PER12	1.734114031
PER4	1.865744832
BGLU46	2.225420865

BGLU24	3.431649147
PER37	2.980777595
PER10	2.467045484
PER38	2.712321248
BGLU32	4.588295273
PER5	2.915688165
PER25	0.879649211
PER59	3.053864956

Table 4.3: Table of most significantly upregulated genes in the phenylpropanoid biosynthesis pathway in seedlings treated with CuNPs.

Phenylpropanoids are an important group of plant secondary metabolites that have roles in plant growth and development, as well as in plant defence against biotic and abiotic stresses (Govender et al., 2017). The results in Fig. 4.29 show that the pathway is activated in response to CuNPs. The main pathway for phenylpropanoid synthesis in plants is the general phenylpropanoid pathway, which starts with the conversion of phenylalanine to cinnamic acid by the enzyme phenylalanine ammonia-lyase (PAL). Cinnamic acid is then converted to p-coumaric acid by cinnamate 4-hydroxylase (C4H), and then to a variety of different phenylpropanoids, including flavonoids, lignins, and stilbenes, by different enzymatic reactions (Vogt, 2010).

The lignin biosynthesis pathway is another important branch of the general phenylpropanoid pathway, these provide structural support to plant cell walls. The key enzymes involved in the lignin biosynthesis pathway include cinnamoyl-CoA reductase (CCR), cinnamyl alcohol dehydrogenase (CAD), and peroxidase (POD). Peroxidase is significantly upregulated in this pathway from the data in Table 4.3 and Figure 4.29. Peroxidases play an important role in the phenylpropanoid pathway. Peroxidases catalyse the polymerization of monolignols, which are precursors for the biosynthesis of lignin (Ralph et al., 2019). The polymerization of monolignols into lignin involves the oxidative coupling of monolignol radicals, which is catalysed by peroxidases. These peroxidases use hydrogen peroxide and other ROS as co-substrates to oxidize the monolignols and promote their polymerization into lignin. In addition to their role in lignin biosynthesis, peroxidases are also involved in the biosynthesis of other phenylpropanoid compounds, such as flavonoids and anthocyanins. peroxidases are involved in the final step of anthocyanin biosynthesis; they catalyse the polymerization of anthocyanidins into condensed tannins or proanthocyanidins. They play a role in plant

defence against biotic and abiotic stresses, and these data show also in response to CuNPs. Peroxidases are also involved in the processing of ROS through the Fenton reaction pathway (Govender et al., 2017; Lüthje et al., 2011).

The other significantly upregulated genes are beta glucosidases. They have two main functions, namely the release of phenylpropanoid aglycones which are a crucial part of many secondary metabolites, and in plant defence against pathogens and herbivores. Plants can induce the expression of beta-glucosidases, which hydrolyse the glycosides that are present in the cell wall of the pathogen, releasing toxic aglycones that can kill the pathogen (del Cueto et al., 2018).

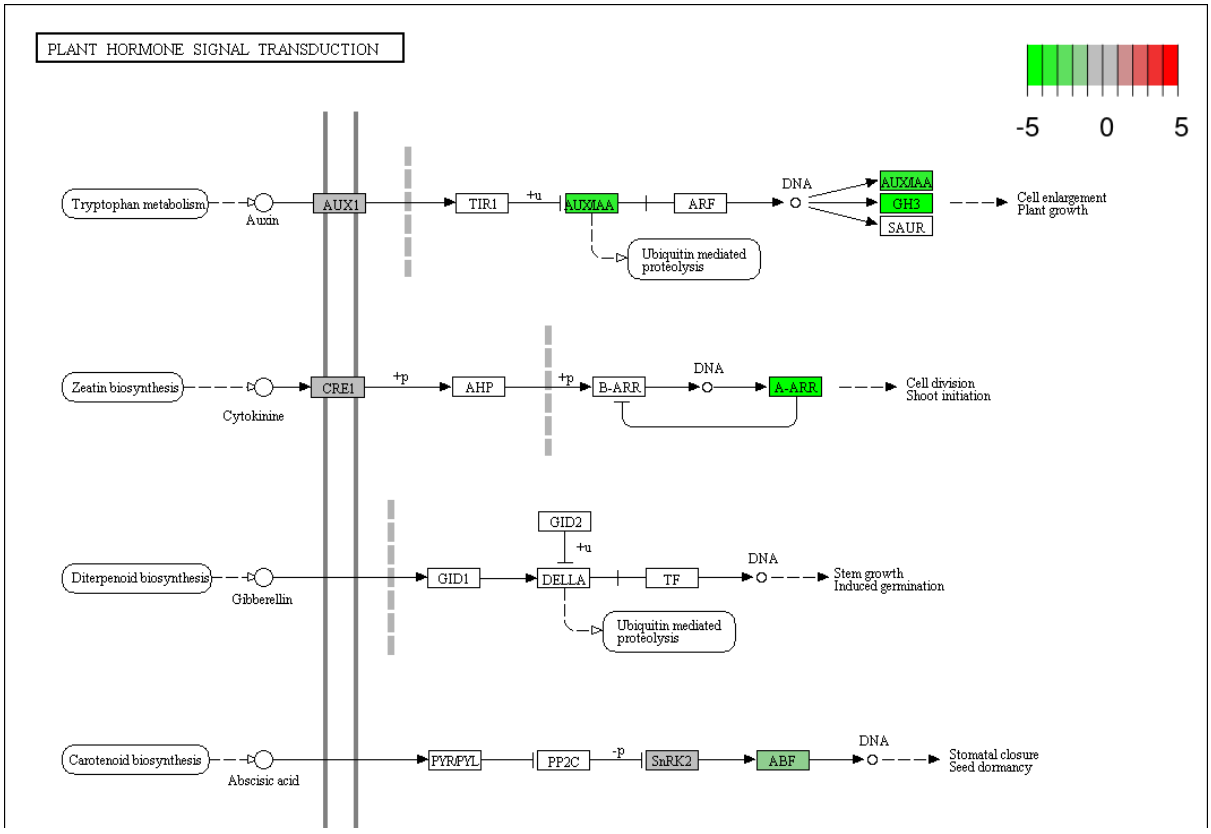

Figure 4.30: 3 hr dataset showing A-ARR down regulation associated with decrease in cell division and shoot initiation in seedlings treated with CuNPs.

Figure 4.30 shows KEGG analysis that reveals a downregulation of both auxin, cytokinin and ABA signalling pathways, consistent with the phenotypic evidence of root tip growth disruption and the inhibition of primary root growth in response to CuNPs.

4.5.2 24 hr dataset

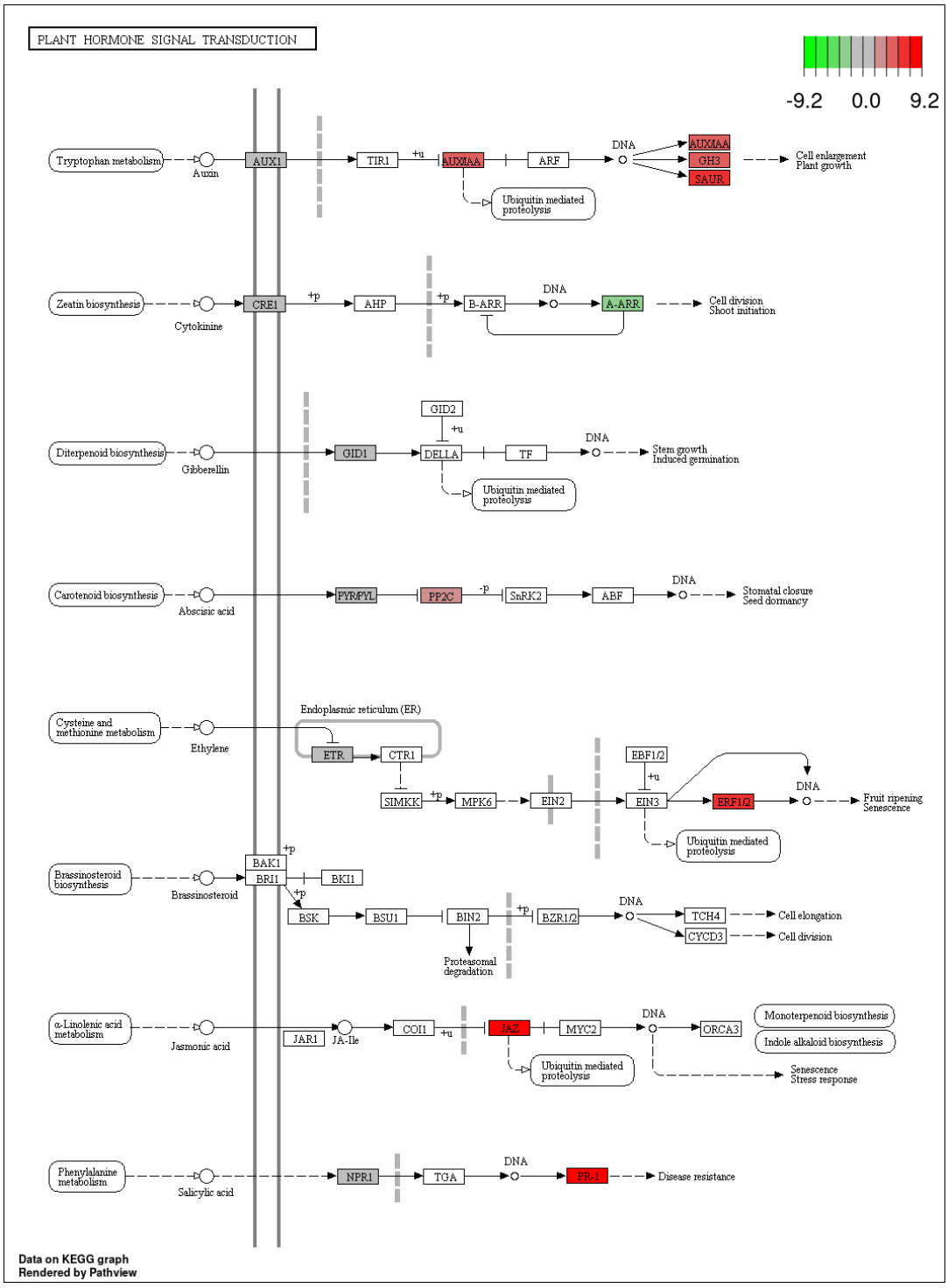

Figure 4.31: KEGG analysis at 24 hr after CuNP treatment, showing up and down-regulation of genes, colour coded red and green respectively.

At 24 hr of CuNP treatment (Figure 4.31) there is seen a similar change in expression pattern to that seen in the 3hr datasets.

4.5.3 Comparisons between 24 hours and 3 hours

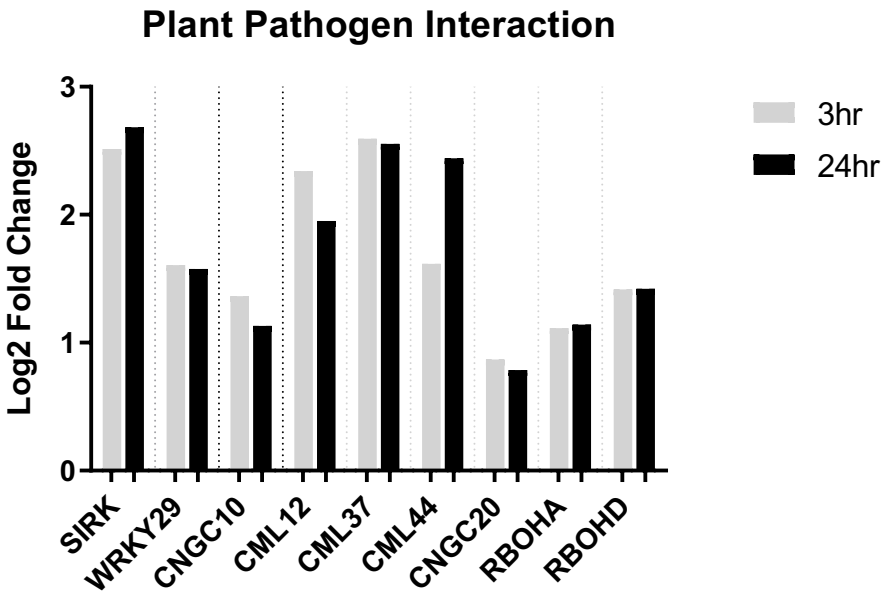

Figure 4.32: Comparison of gene expression levels at 3 hr and 24 hr after CuNP exposure.

The general trend revealed in Fig. 4.32 was a slight increase in the expression of most measured genes between 3 to 24hrs, however there are decreases in *WRK29*, *CNGC10*, *CML12* and *CML37*. Data expressed as mean RE log2Foldchange.

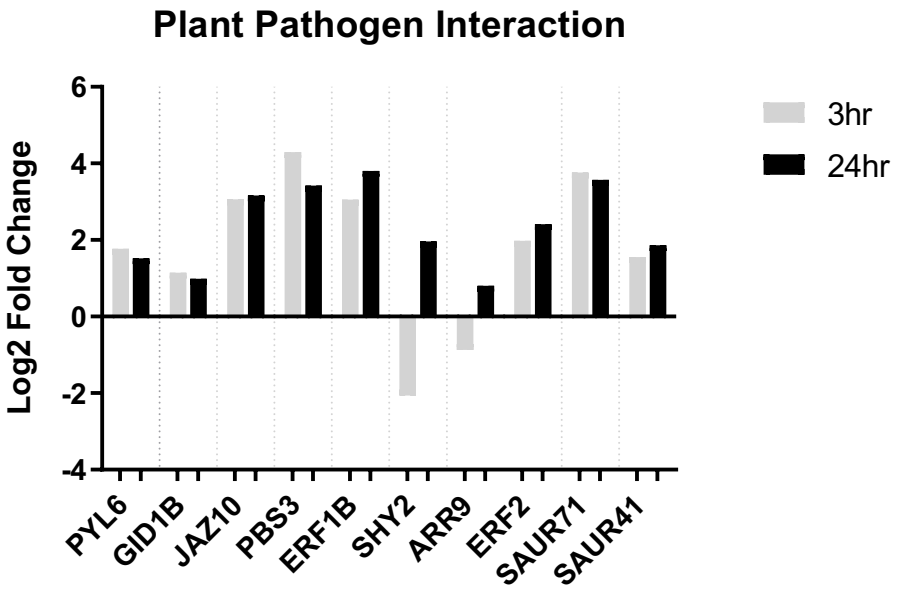

Figure 4.33: Comparison of expression levels for plant pathogen interaction genes at 3 hr and 24 hr after CuNP exposure.

In Fig. 4.33 there is seen a substantial increase in expression levels of *SHY2*, *ARR9*, *SAUR41* and *SAUR71* genes between 3 h and 24 h CuNP treatment, alongside smaller increases in *ERF2* and *JAZ10*.

SHY2 is a transcriptional repressor and plays a role In plant-pathogen interactions, and has been implicated in the regulation of defence-related gene expression(Li et al., 2020). It also regulates auxin-cytokinin balance effects on the function of the root meristem (Moubayidin et al., 2010), and has been shown to interact with the ERF transcription factor ORA59 (Yang et al., 2021). This is activated and induces the expression of various defence-related genes, including those involved in the biosynthesis of plant hormones jasmonic acid and ethylene. SHY2 negatively regulates ORA59 activity, thereby modulating the expression of defence genes in response to pathogen attack. SHY2 has also been shown to interact with other components of the plant defence signalling pathway, such as MPK6 (mitogen-activated protein kinase 6) and WRKY33 (a member of the WRKY family of transcription factors) (Li et al., 2020). Both ERF2 and JAZ10 are upregulated further in 24-hour dataset implicating a systemic defence transcriptional change has started to occur in the plant in response to CuNP exposure.

SAUR41 and *SAUR71* (*SMALL AUXIN UP RNA*) are plant genes that belong to the auxin-responsive gene family. They are strongly induced in plants after infection with the bacterial pathogen *Pseudomonas syringae* and are both directly activated by the plant defence hormone salicylic acid. *SAUR71* is also upregulated in response to treatment with jasmonic acid. The study also showed that SAUR71 was involved in regulating JA-responsive gene expression and that plants overexpressing SAUR71 displayed enhanced resistance to a fungal pathogen.

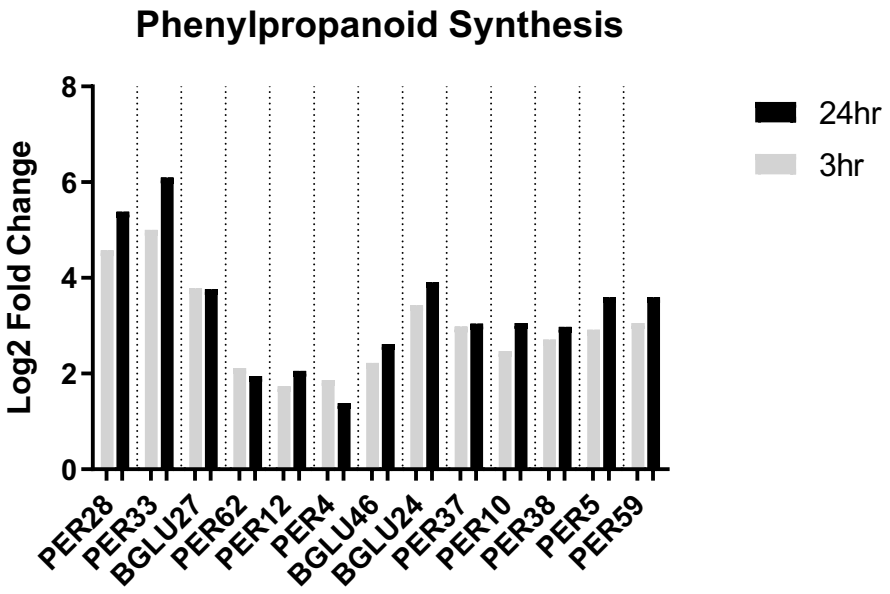

Figure 4.34 Comparison of expression rates for phenylpropanoid synthesis genes in seedlings treated with CuNPs.

There is a general increase in both peroxidase and glucosidase gene activity as the defensive lignification response intensifies between 3 hrs and 24 hours after CuNP treatment in figure 4.34. This is further evidence of the activation of stress responses in response to CuNP exposure.

4.6 Summary

The main aim of this chapter was to increase understanding of the transcriptional changes that occur in response to exposure to CuNPs in Arabidopsis over both a short time span (3 hrs) and a longer timeframe (24 hrs). These time points were identified by an initial qPCR analysis to determine most significant changes in expression of stress-related genes. An RNA-Seq experiment was carried and significantly differentially regulated genes were identified after statistical analysis. Gene ontological analysis and KEGG pathway analysis was used to quantify and assign significance to affected pathways. The objective of understanding the underlying changes in root architecture and phenotype in treated plants was pursued. Changes in genes associated with plant pathogen response and phytohormone signalling have been identified as well as increases in the phenylpropanoid biosynthesis pathway, and other stress factors such as ROS have been identified.

Data from RNA-Seq suggest the plant response to CuNP treatment involves changes in expression of auxin response factors, an increase in the production of jasmonic acid and ethylene biosynthesis as well as an increase in the production of salicylic acid and ROS which produce a potential systemic response to copper uptake that resembles the response seen by biotic stress factors. The results of this chapter indicate that the response to CuNP involves gene transcriptomic regulation that may be mediating the observed phenotypic response.

Chapter 5 Proteomic Expression

5.1 Introduction

The proteomic analysis aims to identify the full set of proteins in a sample: identifying, quantifying, and characterizing the proteins present. Proteomic analysis can give us useful insights into protein expression levels, post-translational modifications, interactions, and functions; while in the previous chapter transcriptomics is the study of the full set of RNA transcripts produced by the plant. While proteomics and transcriptomics are related fields, there are some key differences between them. Transcriptomics studies the intermediate product of gene expression, while proteomics studies the final product of gene expression. Proteomics can also provide information about protein modifications, which would not be detected from the RNA transcript. Proteomics can also provide information about protein interactions and functions, which are not directly evident from the RNA transcript(Chantada-Vázquez et al., 2022) Proteomic analysis and transcriptomics are complementary approaches that can be compared and contrasted for further knowledge of the changing biological expression patterns of a plant under a new environmental stress (Jafari-Raddani et al., 2022).

The specific aim of the work described in this Chapter was to use proteomics to understand and categorise the expression profile of proteins in Arabidopsis plants exposed to copper nanoparticles, and to verify changes with western blotting.

5.2 SWATH Proteomics

SWATH (Sequential Window Acquisition of All Theoretical Mass Spectra) is a proteomic technique that combines data-independent acquisition (DIA) mass spectrometry with targeted data analysis.

In SWATH, a protein sample is digested into peptides, and the resulting peptides are separated using liquid chromatography (outlined in Fig. 5.1). The eluting peptides are then ionized and subjected to mass spectrometry analysis. During the mass spectrometry analysis, instead of selecting specific ions for fragmentation as in data-dependent acquisition (DDA), the mass spectrometer acquires mass spectra for all peptides in sequential windows across the mass-to-charge (m/z) range. This results in a DIA dataset containing fragment ion spectra for all detectable peptides in the sample. The DIA dataset is then analysed using software that

matches the acquired fragment ion spectra to a spectral library of reference spectra generated from reference samples. This targeted data analysis allows for the quantification of a large number of peptides and proteins in the sample with high accuracy and reproducibility. A significant advantage to SWATH is that it allows for a comprehensive and reproducible quantification of thousands of proteins across large sample cohorts. This makes it a powerful tool for biomarker discovery and validation, as well as for studying complex biological systems and disease mechanisms (Birhanu Kitata et al., 2022).

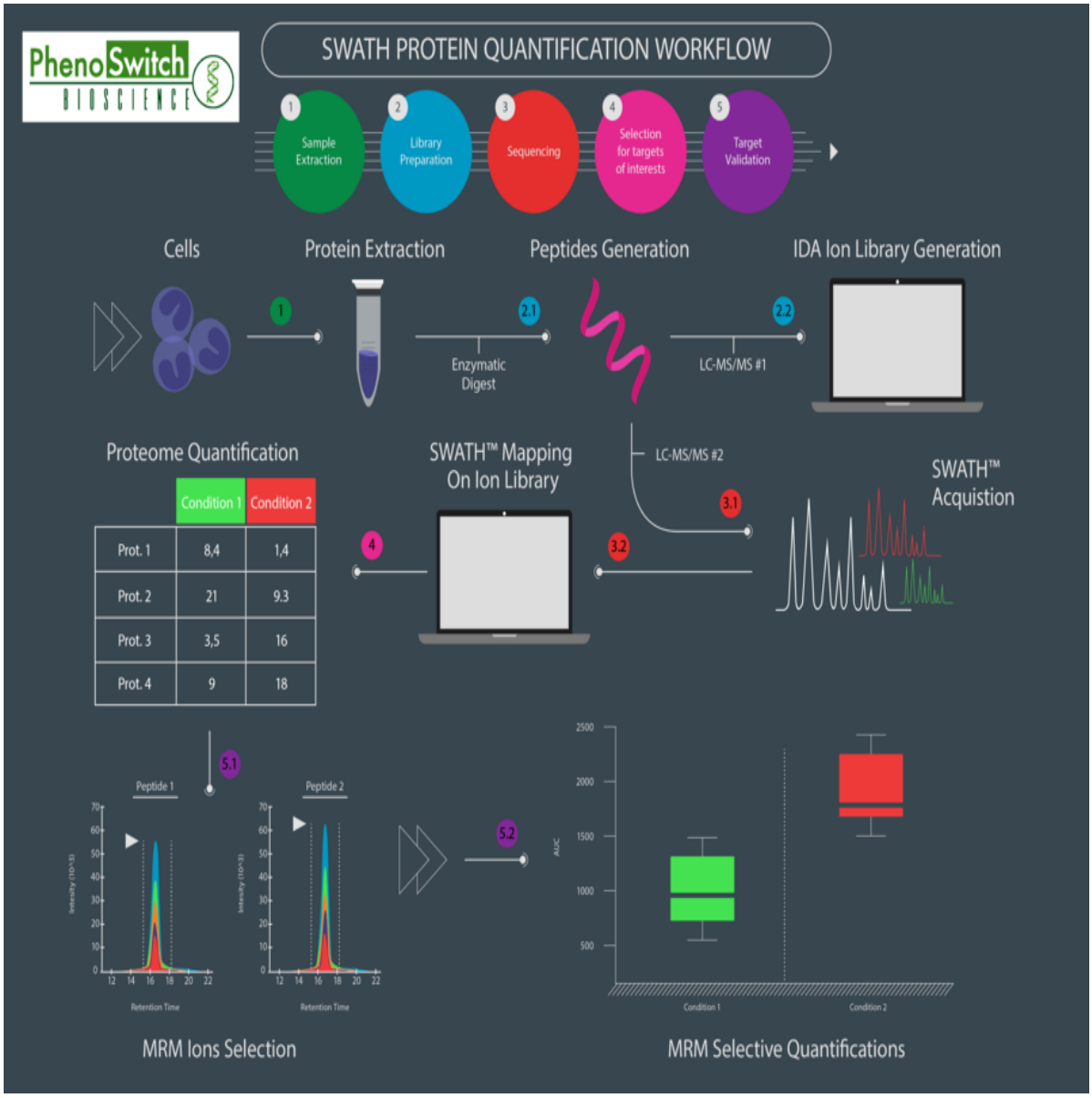

Figure 5.1 SWATH proteomic workflow (adapted from phenoswitch biosciences)

SWATH is a robust and sensitive proteomic technique that combines the advantages of DIA mass spectrometry with targeted data analysis, enabling the accurate and comprehensive quantification of proteomes.

In the work described in this Chapter, three biological replicates for each treatment (± CuNP treatment) were carried out and three replicate SWATH-MS runs were performed for each resulting digest, giving 36 LC-MS acquisitions in total. 4757 proteins were detected and quantified using PeakView software (Sciex) across all samples. The SWATH library used for identification and relative quantification was generated using PeakView from a ProteinPilot.

This information was analysed using Panther software for gene ontology analysis and filtered to only express information with a significant P value, and was also ordered according to the magnitude of up or down-regulation. Arabidopsis encodes up to ca. 35,000 protein-coding genes but the functions and annotations of a substantial number of these genes remain unknown, even by homology (Rhee & Mutwil, 2014). This combined data from 20 data-dependent acquisitions of fractionated peptides resolved by high pH reverse phase chromatography from Arabidopsis root extracts +/- CuNPs. More than 7000 proteins were identified from an Arabidopsis database (SwissProt 0217) at 1% global FDR by ProteinPilot 5.0 during library construction.

For each experimental treatment, nine extracted fragment-ion chromatogram peak area values were obtained for identified proteins. MarkerView 1.2.1 software (Sciex) was used to perform pairwise multiple comparison of replicate peak areas for two states using t-tests. False discovery rates (FDR) in resulting SWATH-experiment outputs was controlled by applying the Benjamini- Hochberg procedure for multiple comparisons (*Multiple Comparisons - Handbook of Biological Statistics*, n.d.) This was done manually using an Excel spreadsheet to: order *P* values, calculate Benjamini-Hochberg critical values and select proteins with resulting significant *P* values. The FDR (false positive discovery rate) values were set at 5% and results tabulated. The purpose of performing a p-adjust statistical analysis, such as the False Discovery Rate (FDR) correction, when analysing proteomic data and their P values is to account for the possibility of false positive results. When performing multiple statistical tests simultaneously, there is a higher chance of detecting false positives or Type I errors. By applying the FDR correction, overall rate of false positives can be controlled while maintaining a high level of sensitivity for detecting truly significant results.

5.2.1 Effect of treatment by CuNPs on the Arabidopsis total seedling proteome.

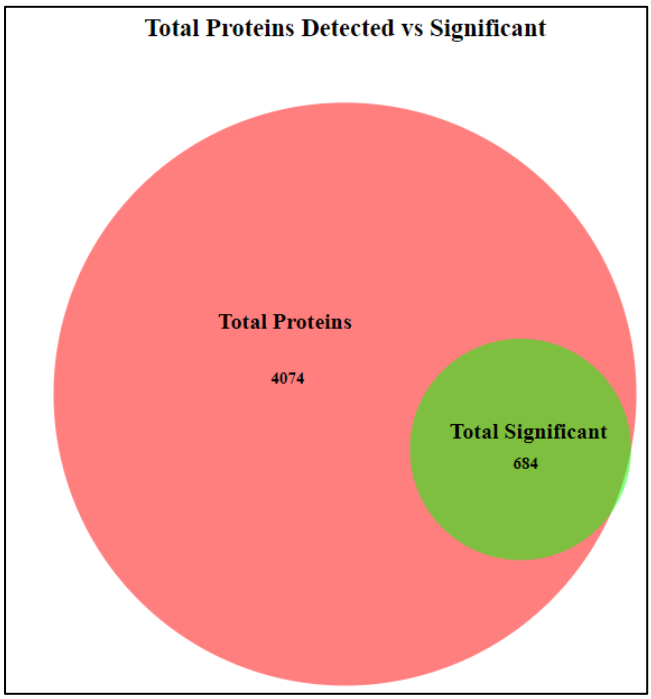

Figure 5.2: Total proteins detected in the SWATH analysis vs total significant at 5% FDR (Hulsen et al., 2008)

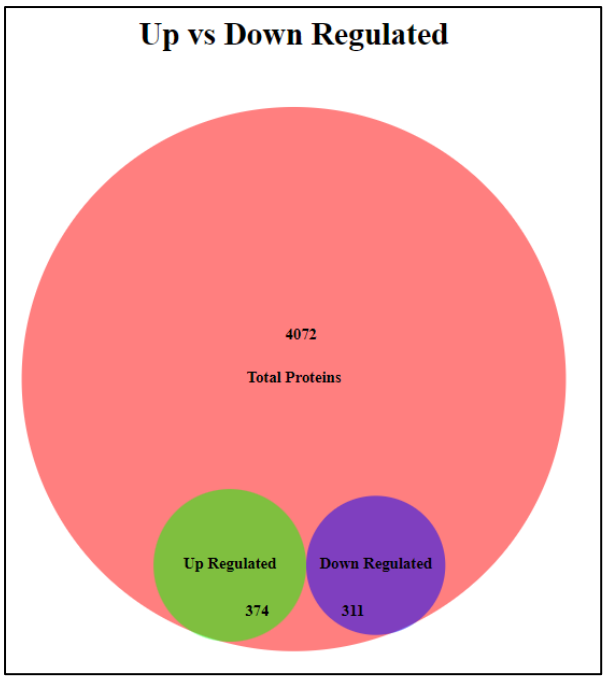

Figure 5.3: Biovenn chart indicating the proportion of proteins up and down-regulated (Hulsen et al., 2008)

Seedlings were grown in the presence of absence of 20uM CuNPs for 8 days and proteins were extracted from whole seedlings (Figs. 5.2-5.4). Non-significant protein changes were removed and the resulting proteins were ordered on fold-change between the treatments, highest to lowest. A Log2 Fold change of <0.1 for up- and down-regulated proteins was considered significant.

Proteomic global experiments are considered to indicate pathways or avenues of interest for further research (e.g. genetic analysis of candidates to determine function). GO ontology over-representation, compared to whole database entries, is a method used to highlight biochemical pathways that are responding to treatment.

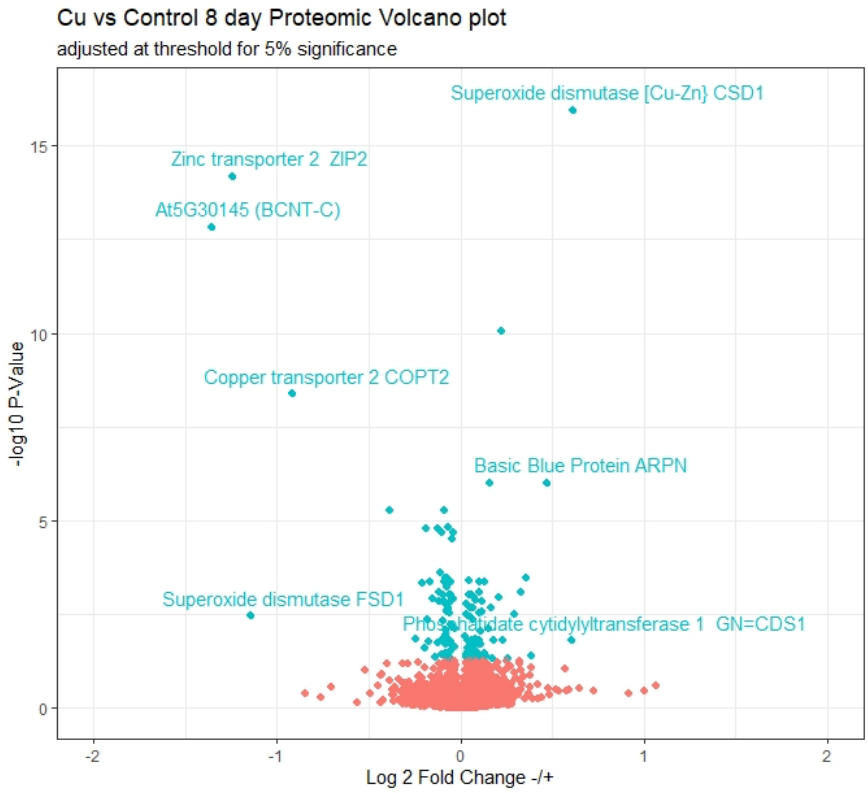

Figure 5.4: Volcano plot of up and down-regulated protein expression with log2fold change >0.5 and adjusted P score below 0.05 some highly expressed and high p value proteins are labelled.

At the 5% confidence ratio and the 0.5 log2 fold change criteria only approx. 200 proteins were identified as changing significantly (labelled blue in volcano plot).

Basic Blue Aspartate-Rich N-terminal Domain Protein (ARPN) forms a family of small, acidic proteins found in a wide range of organisms, including plants. The basic blue subgroup of ARPNs, also known as bARPNs, is characterized by a conserved domain that contains a cluster of basic amino acids and binds to negatively charged molecules, such as DNA or RNA. Additional to their potential role in gene expression, bARPNs have also been implicated in other cellular processes, including being involved in DNA replication and may play a role in coordinating the timing of DNA synthesis during the cell cycle. bARPNs may also be involved in the response to abiotic stress, such as drought, salinity or metal stress (Kim et al., 2003b).

Zinc transporter 2 (ZIP2) is a member of the ZIP family of transporters that are responsible for the uptake and translocation of zinc in plants. Studies in Arabidopsis have shown that *ZIP2* expression is induced not only by zinc deficiency, but also by copper deficiency. This suggests

that ZIP2 may play a role in the uptake and transport of both zinc and copper in plants. It has been demonstrated that Arabidopsis plants overexpressing *ZIP2* exhibit increased copper uptake and tolerance to copper toxicity, indicating that ZIP2 may play a role in copper uptake and homeostasis, however in this experiment we see a decrease in expression levels from the control (Fig. 5.4) (Maeshima, 2014).

COPT2 is expressed in various tissues, including roots, shoots, and flowers, and is involved in the uptake and distribution of copper in the plant. COPT2 is upregulated in response to copper deficiency, indicating that it plays a role in the uptake of copper from the soil. In Arabidopsis, COPT2 has been shown to be important for copper transport to developing seeds, where copper is required for photosynthesis and respiration. COPT2 has been shown to be involved in copper homeostasis in Arabidopsis roots, where it regulates copper uptake and transport to avoid excess copper accumulation and toxicity (Arora et al., 2016). Like ZIP2 this protein is also downregulated in the CuNP treated samples (Fig. 5.4).

5.2.2 GO Pathway Classification

To further interpret the list of differential expression data generated from the proteomics study, a GO ontology analysis was carried out using R script and REVIGO, as was done in Chapter 4 for transcriptomic changes. This enables us to identify GO terms and categories that occur most frequently in the list (Supek et al., 2011).

These are again classified under the 3 major GO classifications:

- **Biological process**
- **Molecular function**
- **Cellular component**

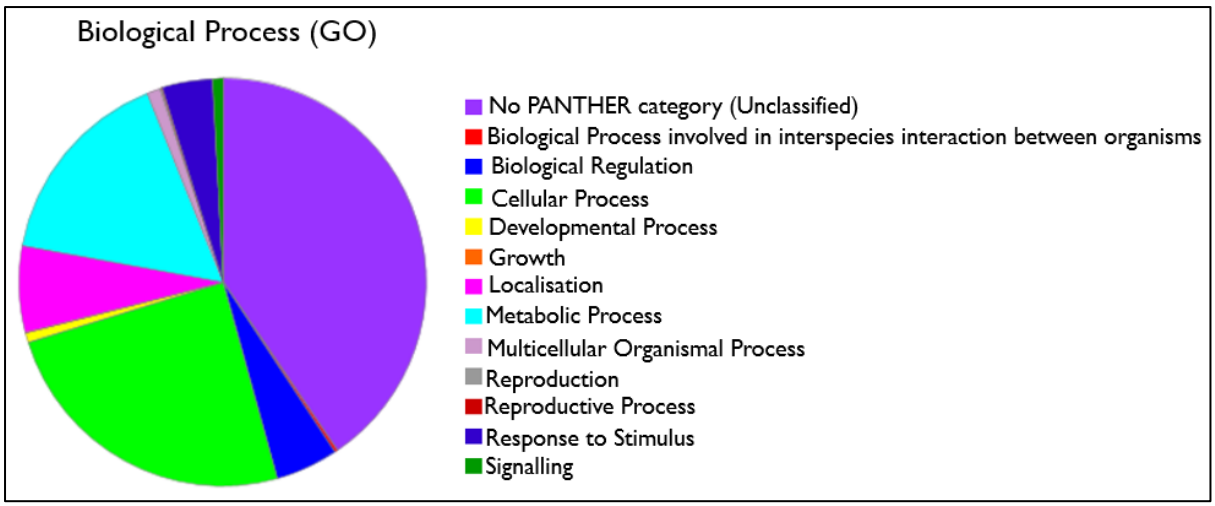

Figure 5.5: Biological processes Gene Ontology, showing a substantial number of detected proteins are not classified to a process but we do see significant protein changes in Cellular Processes, Localisation and Metabolic Process. This graph was generated using the PANTHER Arabidopsis reference genome and the list of 684 differentially expressed proteins.

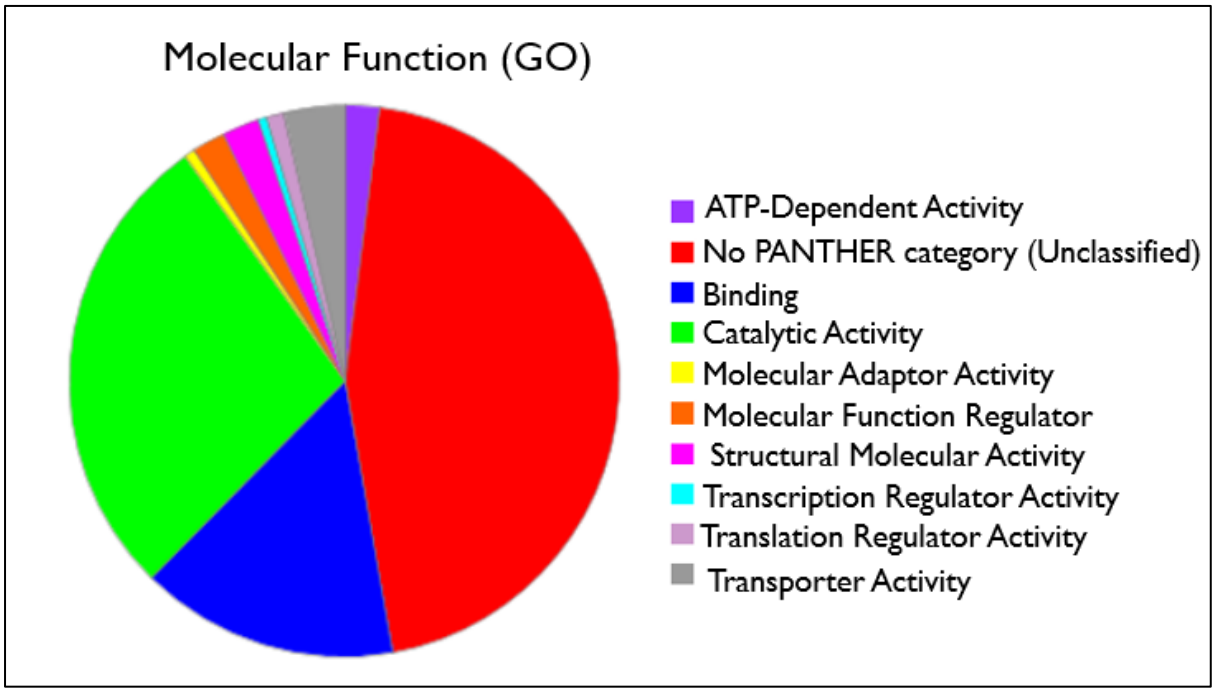

Figure 5.6 : Molecular Function Gene Ontology graph indicating a substantial proportion of activity under the category of binding and catalytic activity. A significant number of protein changes remain unclassified. This graph was generated using the PANTHER Arabidopsis reference genome and the list of 684 differentially expressed proteins.

'Binding' category in Gene Ontology refers to the selective, non-covalent, often stoichiometric interaction of a molecule with one or more specific sites on another molecule. Under abiotic stress conditions, plants may experience various challenges, such as drought, salinity, extreme temperatures, and heavy metal toxicity. The molecular response to these conditions often involves proteins that bind to other molecules, such as: Transcription factors: These proteins can bind to specific DNA sequences, regulating the expression of stress-responsive genes that help plants acclimate to the stress. Chaperones: During abiotic stress, proteins may misfold or become damaged. Molecular chaperones, such as heat shock proteins, bind to these proteins to stabilize and refold them, maintaining cellular homeostasis. Ion transporters and channels: Proteins that bind and transport ions play a vital role in maintaining cellular ion homeostasis under stress conditions, such as high salinity or heavy metal toxicity.

Catalytic activity (GO:0003824) in Gene Ontology refers to the activity of a molecule, usually a protein, that speeds up a specific chemical reaction. Enzymes with catalytic activity are essential for various metabolic processes, which can be modulated in response to abiotic stress. Such as in ROS detoxification: Under abiotic stress, plants produce excessive ROS, which can cause cellular damage. Enzymes such as SOD, catalase (CAT), and peroxidases help neutralize ROS. There is also scope for hormone biosynthesis and signalling: Enzymes involved in the synthesis and metabolism of plant hormones like ABA, ethylene, and gibberellins, play a role in regulating the plant response to abiotic stress.

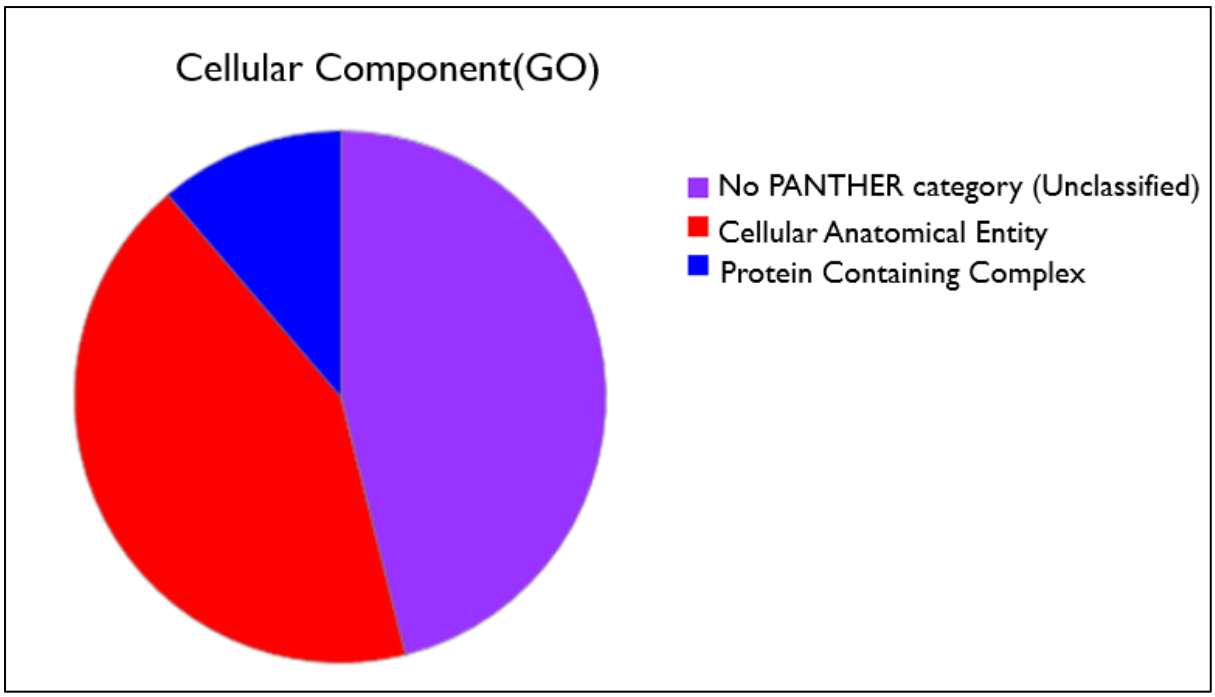

Figure 5.7: Cellular Component Gene Ontology graph – While there is a substantial unclassified section of proteins in the PANTHER directory, the other two significantly present categories are Cellular Anatomical Entity and protein containing complex, the breakdown of these constituted mostly cytoplasmic and intermembrane spaces. This graph was generated using the PANTHER Arabidopsis reference genome and the list of 684 significantly expressed proteins

Cellular Anatomical Entity (GO:0110165): The 'Cellular Anatomical Entity' category in Gene Ontology refers to the structural components of a cell, such as organelles, cellular compartments, and other structural entities within the cell. In response to CuNP stress, changes in cellular anatomical entities can play a crucial role in plant survival and adaptation. These include chloroplasts, vacuoles (under abiotic stress conditions, such as metal toxicity, vacuoles help maintain cellular homeostasis by sequestering ions and toxic metals), and cell walls.

Protein Containing Complex (GO:0032991): The 'Protein Containing Complex' category in Gene Ontology refers to any stable assembly of two or more proteins that function together. Protein complexes play a vital role in various cellular processes, and their formation and regulation are essential for plant stress responses. Photosystem I and II: These protein complexes are part of the photosynthetic machinery in the chloroplasts ROS scavenging

complexes, (ROS) can accumulate under abiotic stress and cause oxidative damage. Protein complexes, such as the NADPH oxidase complex, can modulate ROS production, while other complexes, such as the ascorbate-glutathione cycle components, help in ROS detoxification.

The above PANTHER directory breakdowns for GO in MF, BP and CC unfortunately failed to categorise a substantial number of proteins detected above the significance threshold. Significant changes were subject to further analysis to break down category redundancy in the listed GO subsets (Fig. 5.8).

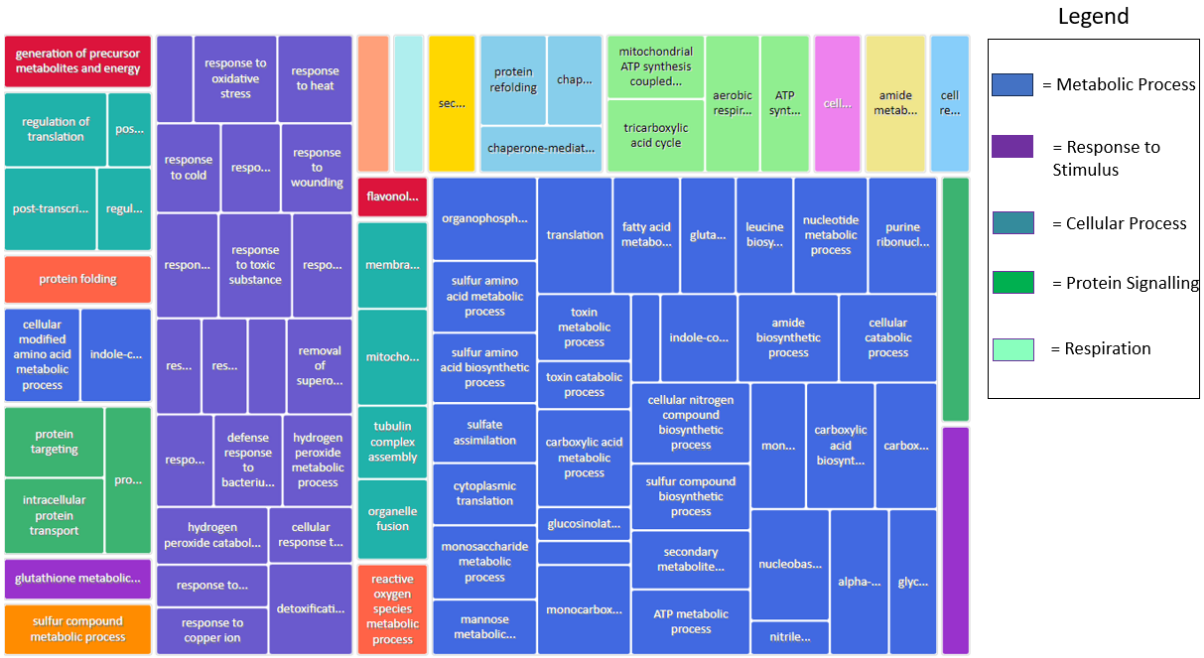

Figure 5.8 : Biological Process treemap processed with REVIGO to further classify the GO terms detected and reduce redundancy in category generation. Generated with the 684 significantly expressed proteins. Legend including the top represented BP categories.

In the REVIGO treemap in Fig. 5.8 analysed for up or down regulation we see two biological processes significantly present which is response to abiotic stress (Purple) and metabolic processes (blue), but we also see some smaller categories upregulated too such as membrane and organelle

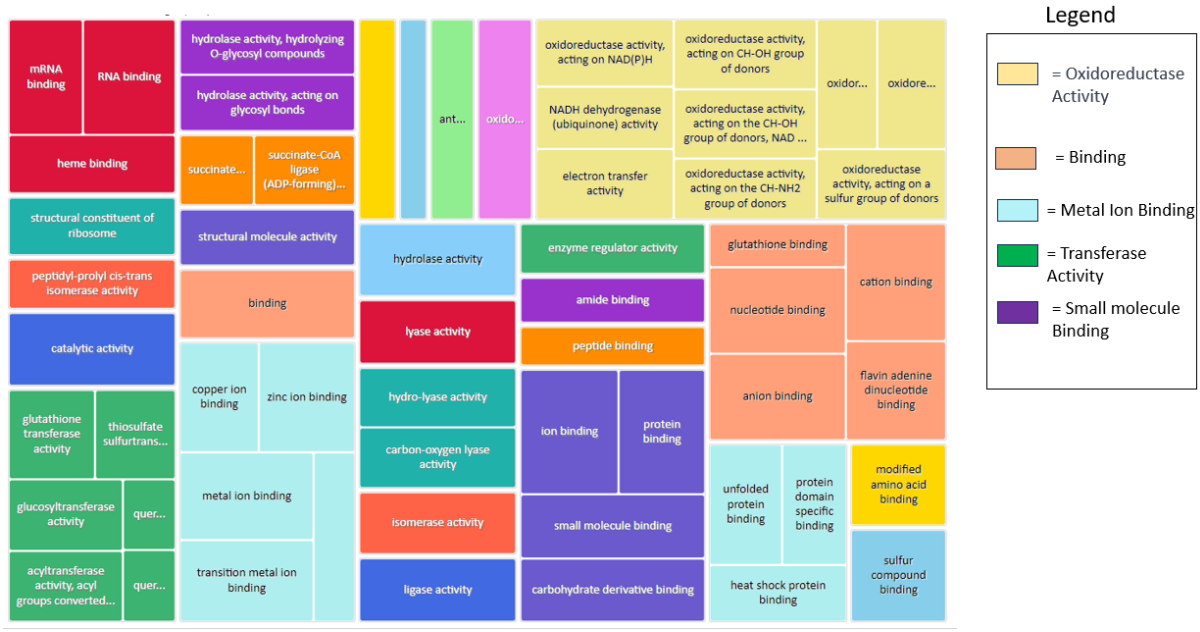

Figure 5.9: MF Molecular Function treemap processed with REVIGO including up and down-regulated proteins to further classify the GO terms detected and reduce redundancy in category generation. Generated with the 684 significantly expressed proteins.

There are multiple molecular function categories that are clearly significantly represented the 'chelation' group (copper ion binding, zinc ion binding, metal ion binding etc) represented by light blue. Oxidoreductase activity is an enzymatic activity that involves the transfer of electrons from one molecule to another in a redox reaction. These enzymes catalyse the oxidation of one molecule by the reduction of another molecule (yellow). There are many diverse types of oxidoreductases, including dehydrogenases, oxidases, reductases, and peroxidases. These enzymes differ in their substrate specificity and the type of reaction they catalyse. Dehydrogenases catalyse the removal of hydrogen atoms from a substrate, while oxidases catalyse the transfer of electrons to molecular oxygen. Other significant categories identified in this figure include transferase activity (green). Glutathione transferase activity is an important enzymatic activity that plays a key role in the detoxification of xenobiotics and endogenous compounds in living organisms. Also seen is the category binding (purple): ion binding, protein binding, small molecule binding. We see a clearly highly upregulated catalytic activity binding – chelation activity across the proteome here.

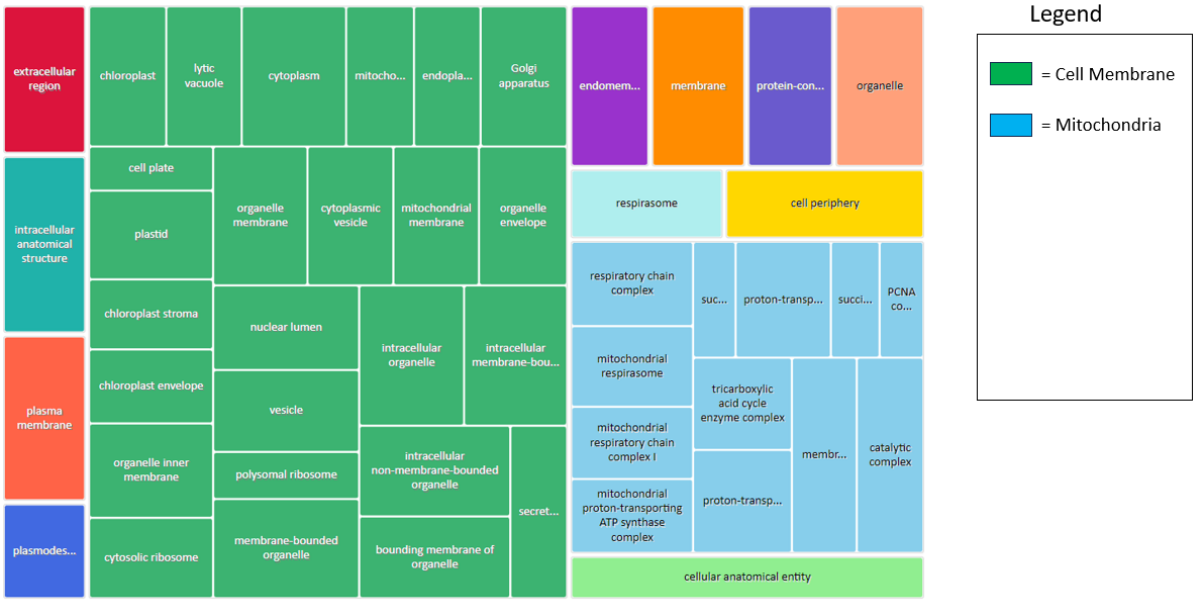

Figure 5.10: CC *Cellular Component treemap processed with REVIGO to further classify the GO terms detected as up-regulated and reduce redundancy in category generation. Generated with the 684 significantly expressed proteins.*

The upregulation of genes involved in membrane and chloroplastic space components suggests that the corresponding cellular processes are highly active in the cell in response to CuNP treatment. For example, upregulation of genes involved in vesicle transport may indicate that the cell is actively secreting or taking up molecules. The vast majority of all proteomic differential activity is clearly occurring in two main locations which is the intermembrane space and within the mitochondria (Green and light blue on this chart).

5.3 Western Blots

The results of the proteomics analysis necessitated validation through physical assay work in both Arabidopsis and to see if related proteins were expressed in willow tree samples that had also been used in CuNP assays.

By comparing the results of western blots with the results the SWATH analysis, validation of the identity and abundance of proteins is possible. If the western blot confirms the presence and abundance of a protein that was identified. it provides additional confidence in the accuracy of the proteomic analysis. If the western blot shows a different result than what was predicted by the proteomic analysis, it can signal potential issues with the mass spectrometry-based method and may warrant further investigation.

5.3.1 Actin

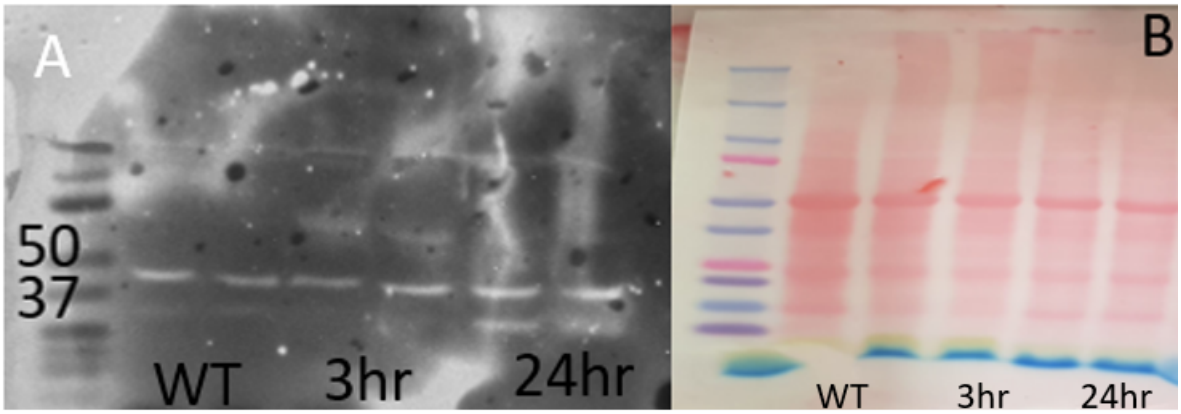

Figure 5.13 : (A) Actin control labelled with ladder kda numbers, first two columns are wild type control at 0 h, next two columns are 3 hr post-treatment with 20 uM CuNP and final two columns are final 24 hr 20uM CuNP treatments. (B) Ponceau stain indicating total protein content in the samples after SDS PAGE electrophoresis. Actin estimated Kd antibody = 41-45Kda

Actin is a highly conserved, abundant, and ubiquitous protein that plays a key role in the structural support and movement of cells. In this Western blot, actin is used as a housekeeping protein or loading control to normalize for variations in protein loading and transfer between different samples. Including actin as a control in Western blotting experiments, can ensure that differences in protein expression or detection are not simply due to differences in the amount of protein loaded or transferred. Actin is particularly useful as a housekeeping protein because it is expressed at relatively constant levels across many different cell types and tissues, and it is resistant to changes in cellular or environmental conditions. The intensity of the actin band can then be used to normalize the intensity of the protein of interest band, allowing for an accurate comparison of protein expression levels between different samples. In this experiment, we do see a higher expression of ACT2 in the 24-hour samples (Figs. 5.13, 5.14) but with this experiment, we can normalise expression levels before doing comparisons for relative expression (Zhang et al., 2012)

5.3.2 Fe Sod (Iron Superoxide Dismutase)

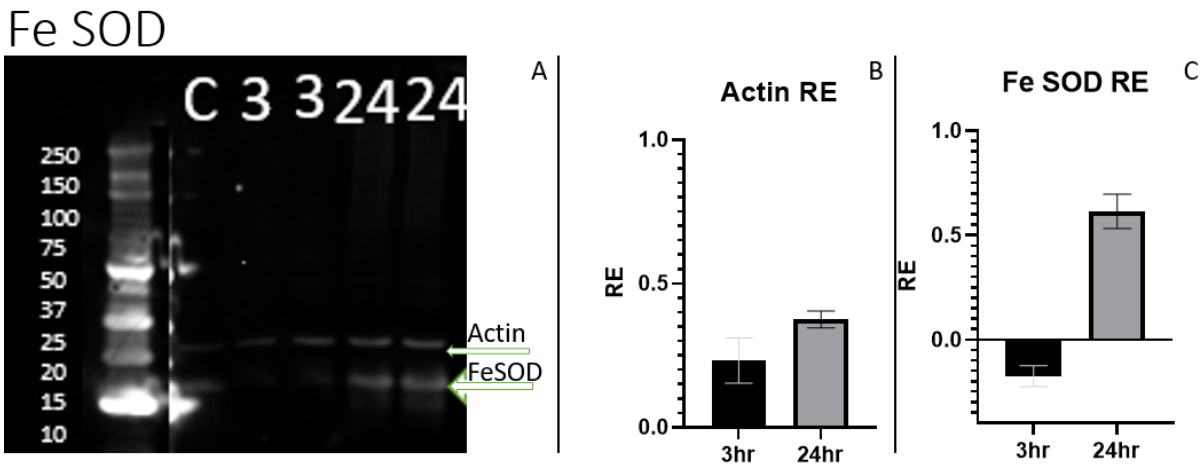

Figure 5.14: (A) Western blot of Actin and FeSOD bands in control lanes, two 3-hour treated lanes and two 24-hour treated lanes. (B) Actin relative abundance, (C) Iron Superoxide dismutase relative abundance

5.3.3 Cu/Zn Sod (Copper/Zinc Superoxide Dismutase)

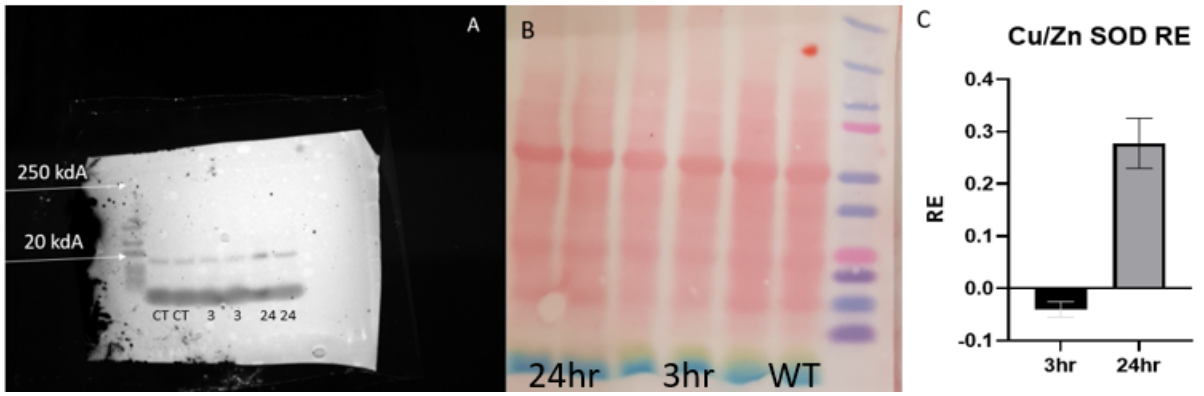

Figure 5.15: (A) Cu/Zn SOD staining with WT Control (CT), 3 hr Cu Treatment and 2 4hr treatment, two sample repeats. (B) Ponceau stain indicating relative protein extracted. (C) Relative abundance of Cu/ZN SOD. Bars represent relative expression compared to control (Wt).

Copper/Zinc Superoxide Dismutase (Cu/Zn SOD) is an important antioxidant enzyme found in many different types of cells in various organisms, the primary role of which is to protect cells from the toxic effects of ROS by converting superoxide radicals into less harmful hydrogen peroxide and molecular oxygen. Cu/Zn SOD is one of the key enzymes involved in cellular defence against ROS. This process requires the presence of copper and zinc ions as cofactors in the active site of the enzyme. Results presented in Fig. 5.16 show that while the abundance

of Cu/ZN SOD is reduced after 3 hr of treatment with CuNPs, it increased dramatically after 24 hr treatment.

5.3.4 CSD2 / CCS (Copper Superoxide Dismutase / Copper Chaperone)

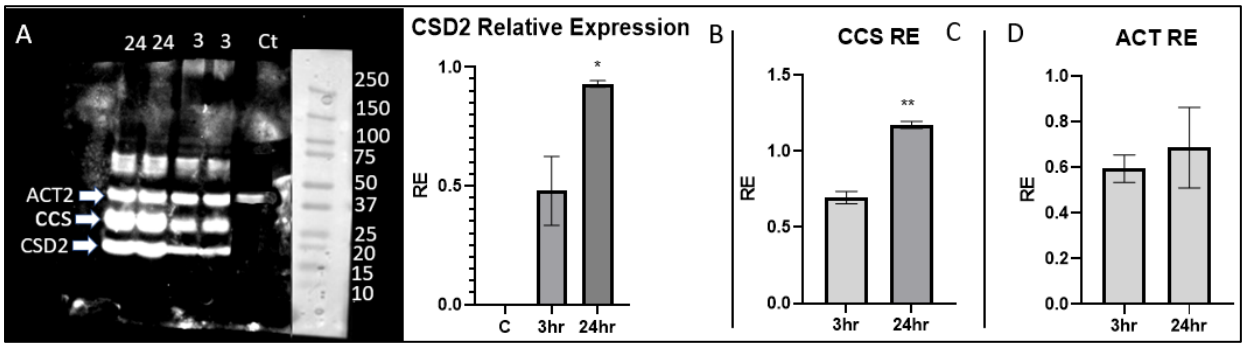

Figure 5.16 (A) CSD2 and CCS staining with 24hr and 3 hr timepoints. (B)Relative expression of CSD2, (C) Relative expression of CCS, (D) relative expression of ACT2.

CCS (Copper Chaperone for Superoxide Dismutase) plays an important role in the copper uptake pathway in plants. It is involved in the transport of copper ions from the cytosol to the plastids, where they are needed for the biogenesis of chloroplasts and the assembly of photosynthetic proteins. The CCS protein functions as a copper chaperone, which means it binds to copper ions and helps transport them to their final destination in the cell. CSD2 (Copper-Zinc Superoxide Dismutase 2) is another protein involved in the copper uptake pathway in plants. CSD2 belongs to the superfamily of antioxidant enzymes called superoxide dismutases (SODs) that catalyse the dismutation of superoxide radicals into molecular oxygen and hydrogen peroxide.

In the copper uptake pathway, CSD2 works together with CCS to ensure proper copper transport and utilization. CSD2 binds to CCS and helps stabilize it, thereby enhancing the efficiency of copper delivery to the plastids. Together, CCS and CSD2 ensure proper copper transport and utilization in plant cells. They work synergistically to protect plant cells from oxidative damage and maintain the cellular redox balance.

Results presented in Fig. 5.16 show that, when adjusted for ACT2 expression levels, the relative expression of both CSD2 and CCS is found to substantially increase from 3 hr to 24 hr after treatment with CuNPs.

5.3.5 Willow tree sample (Cu/ZN SOD)

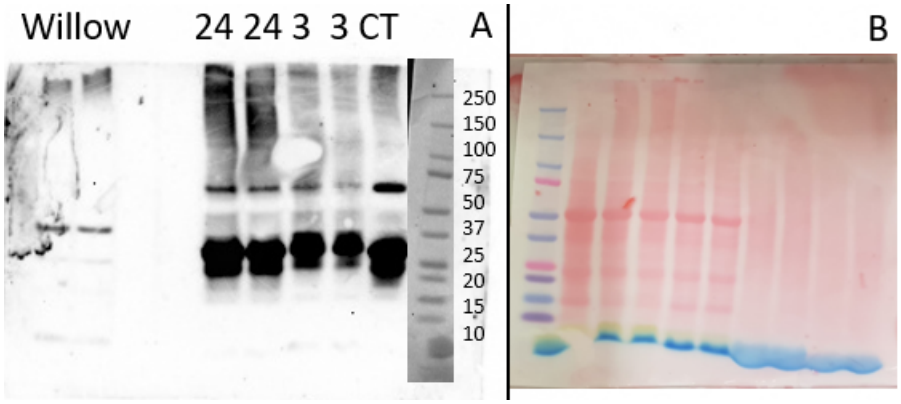

Figure 5.17: (A) Willow tree and Arabidopsis (untreated, CT and CuNP-treated samples, 24 h, 3 h) samples; (B) Ponceau Stain of Willow ((A) far left) and Arabidopsis (untreated, CT and CuNP-treated samples, 24 h, 3 h)untreated (CT) and treated samples (24 h, 3 h), showing the smaller amount of protein extracted from the willow samples

To understand something of the conservation of proteomic response to CuNPs between species, a comparative analysis was carried out between Arabidopsis and willow. Willow roots were sampled after 3 hr and 24 hr of CuNP treatment, and proteins were extracted for Western blot. The amount of protein extracted protein was low based on Ponceau staining compared to Arabidopsis samples (Fig. 5.17), presumably due to the lignin content of the root tissue, which caused problems with the extraction process. Cu/ZN SOD was detected only after ling (120 sec) blot exposures (Fig. 5.17, Willow lanes), but very little total protein was extracted and detected (Fig. 5.17B), and so this aspect of the analysis was not taken further.

5.4 Comparisons to Transcriptomic Data

Comparing proteomic and transcriptomic data can be challenging due to the non-linear relationship between gene expression and protein accumulation; and the complexity of post-transcriptional regulation and protein turnover. However, integrating both datasets can potentially provide a more comprehensive understanding of plant responses to stresses.

An approach is to look for genes that show consistent changes in both datasets, which could indicate a direct link between changes in gene expression and protein levels - identifying genes/proteins that are significantly upregulated or downregulated in both datasets and

performing a pathway analysis on these common targets. It is important to keep in mind that differences between the datasets may arise due to differences in sensitivity and dynamic range of the two technologies.

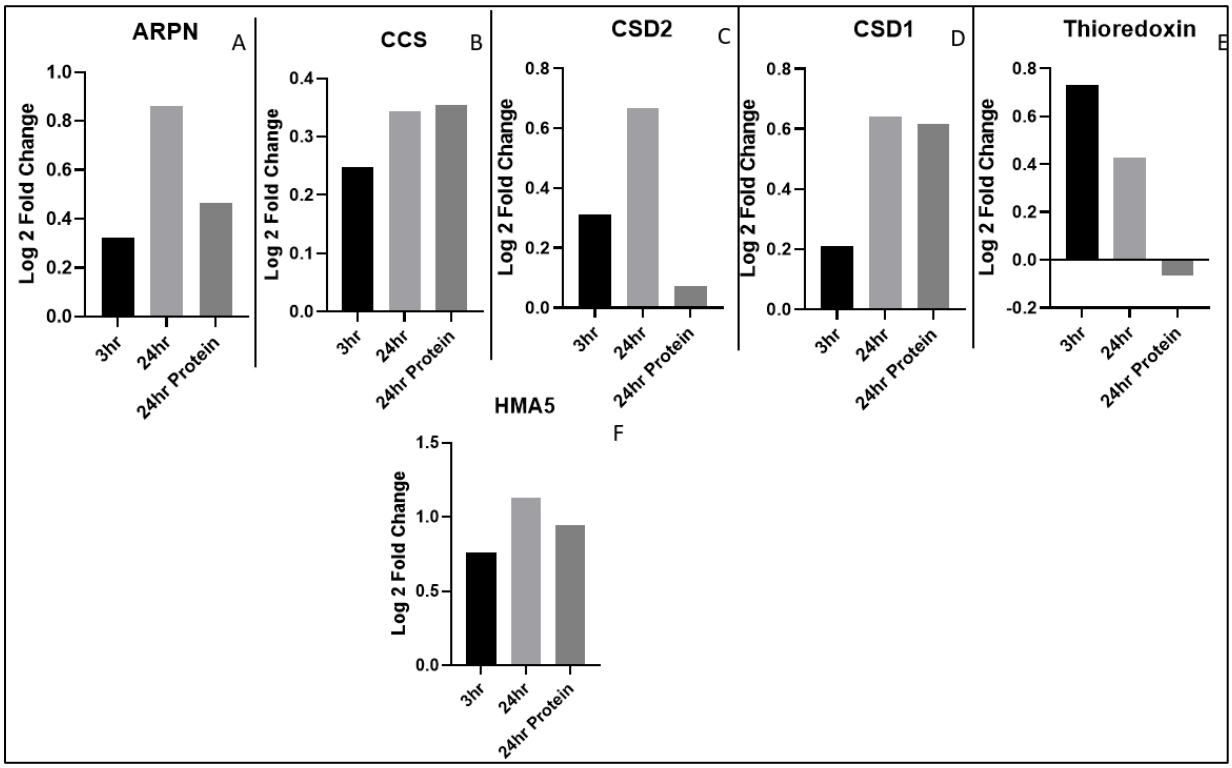

Figure 5.18: *Log2 Fold changes for 6 up-regulated genes and proteins taken from transcriptomic and SWATH MS proteomic data for expression comparison. Black bar represents 3 hour transcriptomic time point, light grey bar represents 24hr, dark grey proteomic 24hr dats*

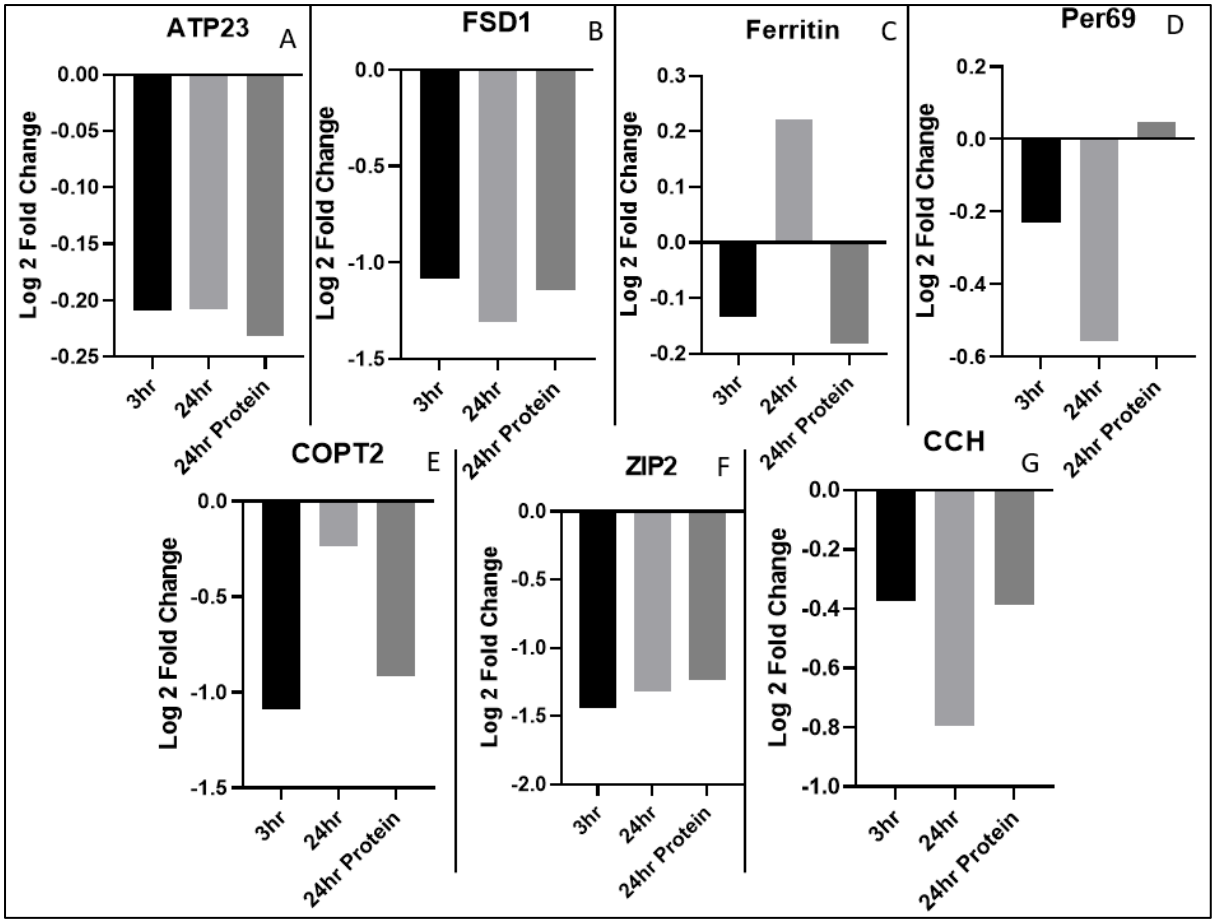

Figure 5.19: Log2 Fold changes for 7 down-regulated genes and proteins taken from transcriptomic and SWATH MS proteomic data for expression comparison. Black bar represents 3 hour transcriptomic time point, light grey bar represents 24hr transcriptomic, dark grey proteomic 24hr data

While most of the genes and proteins detected and quantified for fold change had up or down regulations that verified the other datasets, some were contrary – such as thioredoxin and ferritin or Per69.

Several post-transcriptional processes can significantly impact the final protein abundance, leading to inconsistencies between transcriptomic and proteomic data. Some examples of different mechanisms of such action include alternative splicing: This process allows a single pre-mRNA to generate multiple mRNA transcripts by selectively including or excluding exons, resulting in different protein isoforms (Halbeisen et al., 2008). mRNA stability: The stability of mRNA molecules affects the level of proteins produced. Regulatory elements, such as microRNAs (miRNAs) or RNA-binding proteins, can cause mRNA degradation or stabilization,

impacting protein expression (Uchida et al., 2019). RNA editing: The nucleotide sequence of an mRNA molecule can be altered post-transcriptionally, leading to changes in the amino acid sequence of the encoded protein (Mino & Takeuchi, 2018). Translation regulation: The efficiency of translation initiation, elongation, and termination can impact protein expression levels. Regulatory elements, such as upstream open reading frames (uORFs) and riboswitches, can modulate translation rates (Duarte-Conde et al., 2022; Halbeisen et al., 2008).

Post-translational modifications (PTMs): Modifications to proteins after translation, such as phosphorylation, acetylation, or glycosylation, can affect protein stability, localization, and function (Duarte-Conde et al., 2022).

5.5 Mutant Growth Analysis

Several genes of interest were identified through the analysis of transcriptomic and proteomic data, consistently up- or downregulated. SALK lines were obtained and growth studies were performed to determine and validate if they played a significant function in the plant's response to copper stress (O'Malley et al., 2015; Alonso et al., 2003).

5.5.1 Basic Blue ARPN

Plantacyanins are blue copper proteins belonging to the larger family of phytocyanin's, which are plant-specific proteins that are involved in various physiological processes(Dong et al., 2005). They are characterized by their ability to bind to a single copper ion, giving them a blue colour and the ability to participate in redox reactions. Although plantacyanins have been identified in a wide range of plant species, their exact roles in plants are not fully understood but there is evidence to suggest some potential function such as electron transfer during stress responses: Plantacyanins have been implicated in the plant's response to drought, high salinity, and heavy metal exposure (Nersissian et al., 1998a). They may function as antioxidants, protecting cells from damage caused by ROS that are generated under stress conditions. They may also play a role in plant growth and development, including cell differentiation, elongation, and expansion, and may also be involved in hormone regulation, influencing processes such as germination, root growth, and flowering (Kim et al., 2003a). Plantacyanins might participate in cell-to-cell communication by functioning as signalling

molecules. They could facilitate the transport of signals between cells or act as ligands for specific receptors, modulating cellular responses to various stimuli. In some plant species, plantacyanins are found in reproductive tissues, such as pollen and the pistil, where they might play a role in the pollen tube growth, guidance, and fertilization process. (Dong et al., 2005; Kim et al., 2003b; Nersissian et al., 1998a, 1998b; Mascarenhas et al., 1964; Chae & Lord, 2011).

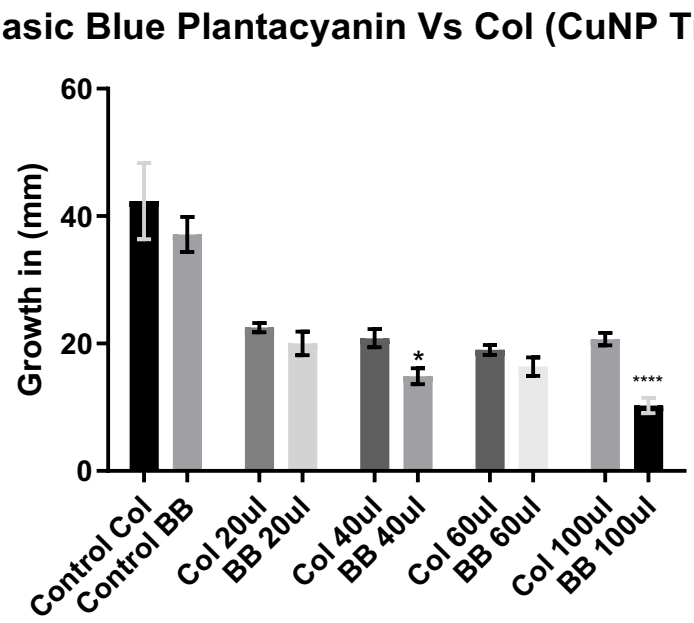

Figure 5.20: Basic blue plantacyanin mutant (BB) growth at 14 days vs WT Col-0. N= 10. The 40ul and 100ul growth responses were statistically significant. P = 0.0364 and <0.0001 respectively for significant data points.

To investigate the possible function of the basic blue plastocyanin protein a loss-of-function mutant (*bb*) was obtained and its growth was determined in the presence and absence of 20-100 ug/ml CuNPs. After growth for 14 days total primary root length was measured (Figs. 5.21, 5.22). While many of the comparisons were not statistically significant it can be observed that *bb* grew less resiliently than the control. The 40 ug/ml and 100 ug/ml datasets showed a significant difference in primary root growth between mutant and wildtype, suggesting the BB gene is required for the maintenance of root growth under CuNP stress.

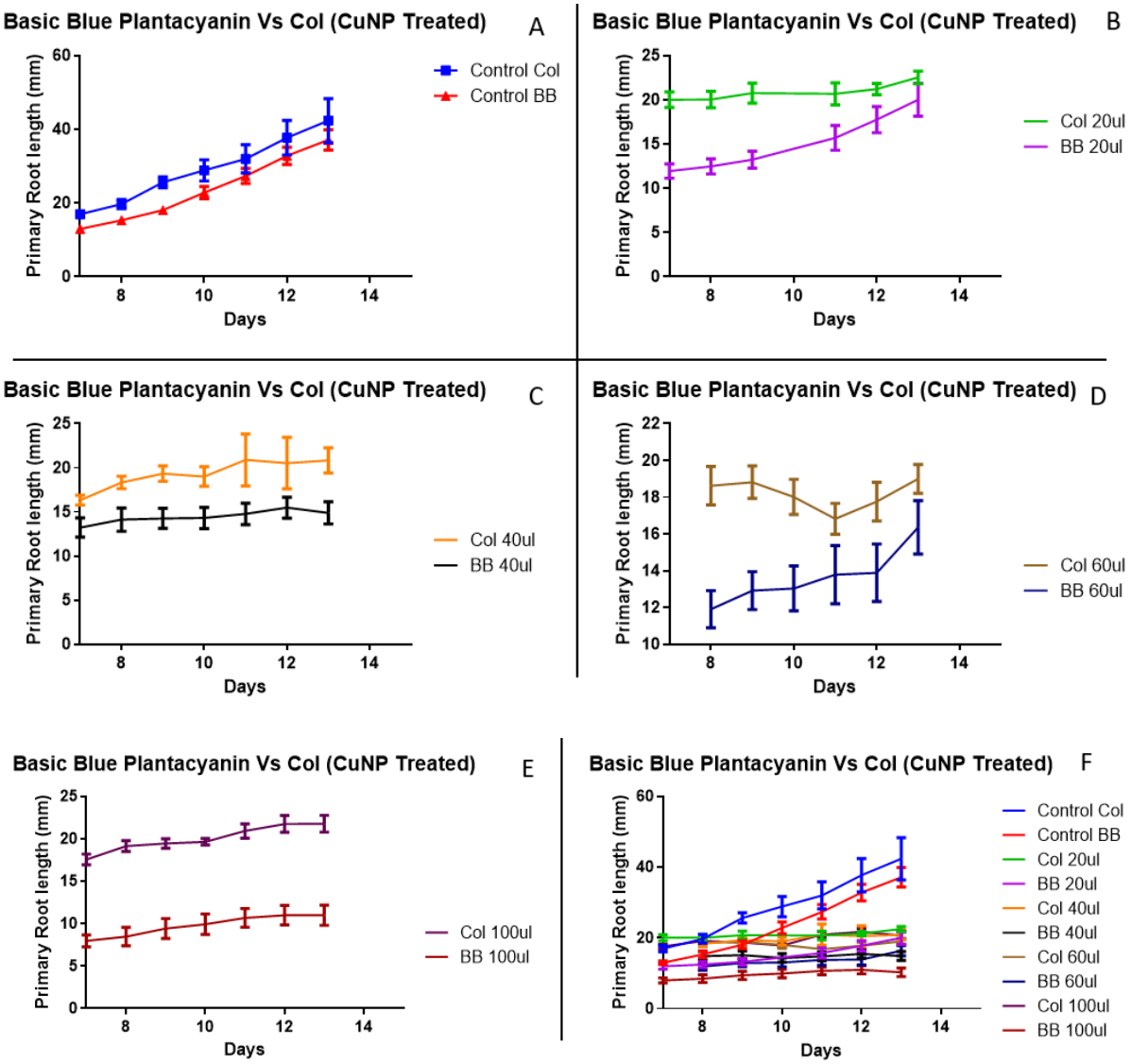

Figure 5.21: Basic Blue ARPN mutant (BB) growth curve comparisons with wildtype (Col) between 7 and 12 days under the same conditions. (A) Control media, (B) treated with 20 ug/ml CuNPs, (C) treated with 40 ug/ml CuNPs, (D) treated with 60 ug/mlCuNPs, (E) treated with 100 ug/mlCuNPs, (F) all samples graphed together. N = 10 seedlings measured per data point.

5.5.2 RBOH

To investigate the possible function of RBOHD a loss-of-function mutant (*rbohd*) was obtained and its growth was determined in the presence and absence of 20-100 ug/ml CuNPs. RBOH D (Respiratory Burst Oxidase Homolog D) is a type of NADPH oxidase enzyme that is involved in the production of ROS in plants. In addition to its role in ROS production, RBOH D has been

implicated in various cellular processes such as cell wall synthesis, hormone signalling, and programmed cell death. Dysregulation of RBOH D activity has been associated with various plant diseases and disorders.

.

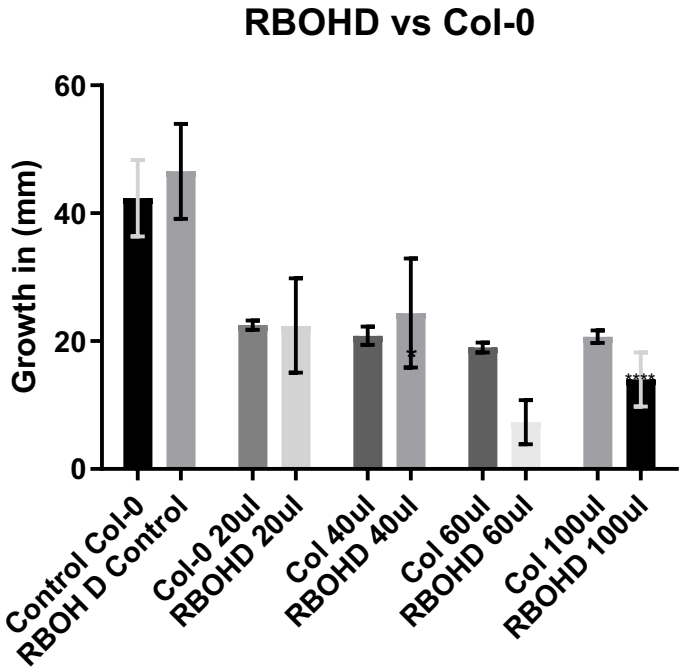

Figure 5.22 RBOH mutant growth at 14 days *vs WT Col-0. N= 10. The 60 and 100ul were significant at p= >0.00477 and p = 0.0455 respectively*

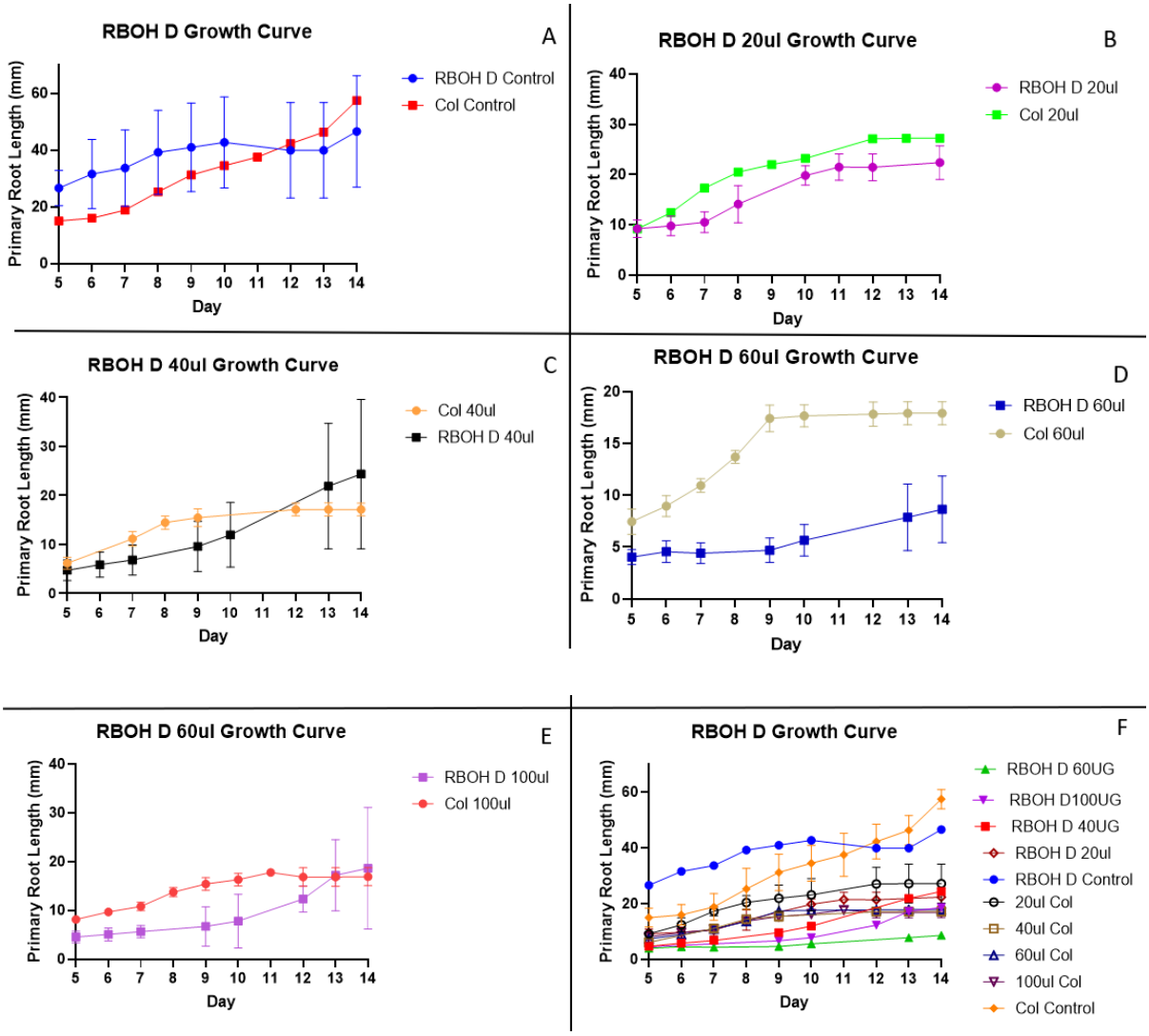

Figure 5.23 (A-E) RBOH D vs Col-0 growth curves from 5 to 14 days n = 10 seedlings. (F) All growth curves together.

While *rbohd* had far higher variance in root growth results (as evidenced by the substantially larger error bars seen in Figs. 5.23 and 5.24) compared to wildtype, there was no significant effect of the mutation on the ability of the plant to grow in the presence of CuNPs. When grown on 0, 20 ug/ml and 40 ug/ml CuNPs, the mutant had a higher mean growth rate (albeit with a substantial error margin) while only the 60 ug/ml and 100 ug/ml samples were less resilient to treatment with CuNPs than the control. This does not necessarily mean RBOH does not have an important role to play but there are multiple redundant and homologous genes in this family (Huang et al., 2019) so one knockout will not always cause a phenotype.

5.6 Chapter Summary

In this chapter, a SWATH proteomic analysis of Arabidopsis root extracts treated with CuNPs was conducted, and 684 proteins were found to be significantly differentially expressed. GO ontology analysis was carried out to identify GO terms and categories that occur most frequently in the list, which were then classified under the three major GO classifications: Biological process, Molecular Function and Cellular Component. The results showed that the significantly upregulated biological processes represented responses to abiotic stress and metabolic processes. The significantly upregulated molecular function was binding and enzymatic catalysis, and the significantly upregulated cellular component was a cellular anatomical entity and protein-containing complex. Overall, SWATH proteomics combined with GO ontology analysis provides useful information for studying the changing biological expression patterns of a plant in response to CuNPs. Protein-protein interaction networks (PPINs) were constructed using experimental results from SWATH loaded into the STRING program. STRING can identify direct or indirect interactions between proteins, provide information on the strength and dynamics of these interactions and can perform functional enrichment analysis on a set of proteins. Western blots were performed to validate the proteomic data obtained. A comparison of proteomic and transcriptomic data was made to provide a more comprehensive understanding of gene expression and protein regulation. Several genes of interest were identified through the analysis of transcriptomic and expressional data, consistently up and downregulated. Growth studies of mutants in candidate genes/proteins were performed to determine and validate if they played a significant function in the plant's response to CuNP stress. The study identified that Basic blue plantacyanin, which is a plant-specific protein involved in various physiological processes, had a statistically significant role in maintaining root growth in response to CuNP exposure.

Chapter 6: Gel Formulations

6.1 Introduction

Aims: The intended commercial output of this project is a bioengineered coating to halt root ingress into built civil infrastructure, particularly water effluent pipe systems. This chapter describes work on the testing, design and optimisation of a minimally viable product to be used in an industrial setting utilising the phenotypic effects described in Chapter 3.

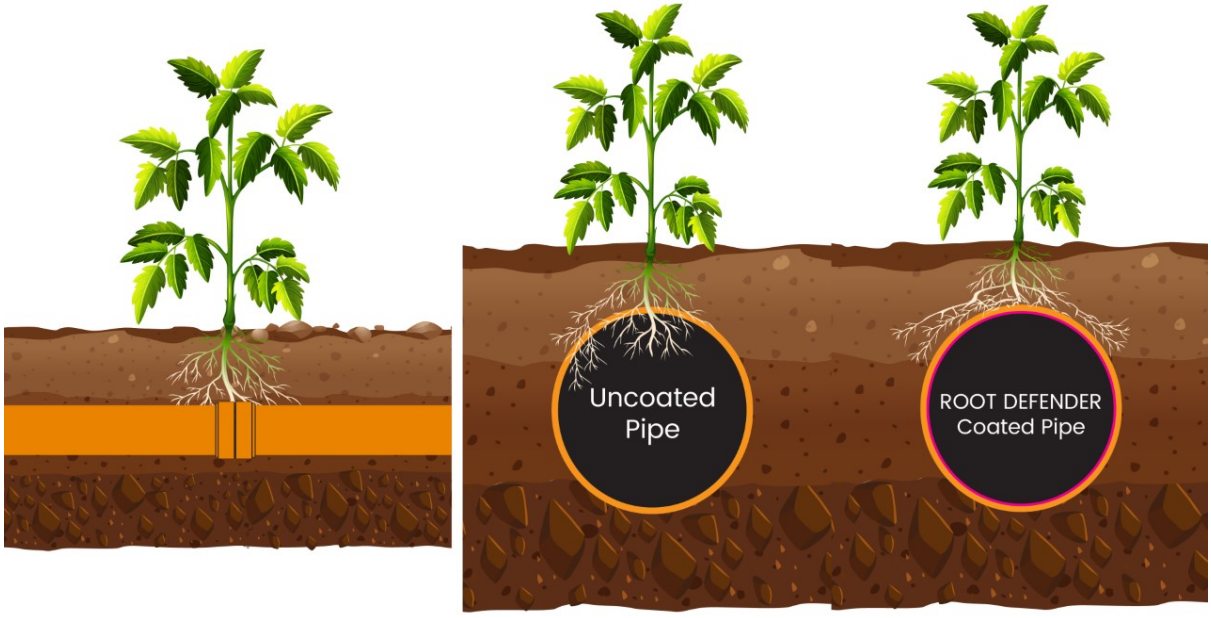

Figure 6.1: Illustration of root ingress into pipe systems vs a protected water pipe utilising a commercial application of CuNP packaged into a protective coating to redirect ingressing roots away from important infrastructure.

In order to establish a useable formulation and packaging material for CuNPs, it was first important to establish the parameters required that would be practical, affordable and commercially viable to use in an industry setting.

The first objective was to understand the nature of the material required for pipe application and to to test the materials and determine compatibility and costs appropriately. Parameters to be considered include those set by the material of pipes to be coated, pH levels, moisture levels, gel adhesion, necessity to reapply in a particular time frame, leakage of Cu ions, mechanical strength to higher pressure water flows, ability to be applied by spray or pig and the ability to be made from sustainable materials.

	Function required	Implication
	Up to 5 years effective life	
1.	Ability to deter root ingress	Steady dissolution of Cu from Cu Nanoparticles. ➔ Retention of Cu Nanoparticles
2.	Ability to remain in place	➔ Adhesion to substrates (ceramic/concrete/PVC pipes?). ➔ Resistance to dissolution in water. ➔ Sufficient mechanical strength to resist periods of high flow. ➔ Remains adhered even is dried out.
3.	i. Application by spray	➔ Highly shear thinning rheology (+ post application liquid ➔ solid phase change)
4.	ii. Application by pig	High strength? ➔ Need to resist water immediately after application.
5.	SHE	Low toxicity (acceptable to water companies) Preferably biodegradable?

Table 6.1: List of requirements of any packaging material for nanoparticle delivery to water efflux pipe system.

Table 6.1 was developed by the stakeholders of our project and its definitions are not necessarily exhaustive.

6.2 Dispersion of Nanoparticles

A key objective is understanding the effects of CuNP inhibition of plant roots and applying a CuNP formulation in a bio-sustainable and effective manner, to ensure the inhibitory effects are maintained over a useful period of time. The first challenge was deciding on a mixing strategy to mix and disperse the nanoparticle solution into an aqueous solution - as described in the introduction, nanoparticles have a tendency to agglomerate (I. Khan et al., 2019)

1. Surfactants: Added to the aqueous solution, surfactants can help disperse the nanoparticles by reducing their surface tension and preventing agglomeration. The choice of surfactant will depend on the properties of the nanoparticles, such as their size, surface charge, and chemical composition. Common surfactants used in the industry include Tween 20, Triton X-100, and sodium dodecyl sulfate (SDS) (Khan et al., 2022; Verma et al., 2023)

2. Sonication: Ultrasonic energy can help break up agglomerates and disperse nanoparticles in the aqueous solution. Sonication can be carried out using a bath or probe sonicator. The duration and power of sonication should be optimized based on the specific properties of the nanoparticles.

3. High-speed mixer: High-speed mixing can be used to disperse nanoparticles in an aqueous solution. The duration and speed of mixing should be optimized based on the specific properties of the nanoparticles.

Strategies, therefore, include using a powerful mixing unit, adding surfactants, sonication and ultimately a combination of these methods to produce the most viable outcome (Bhawana et al., 2011; Soumya et al., 2013)

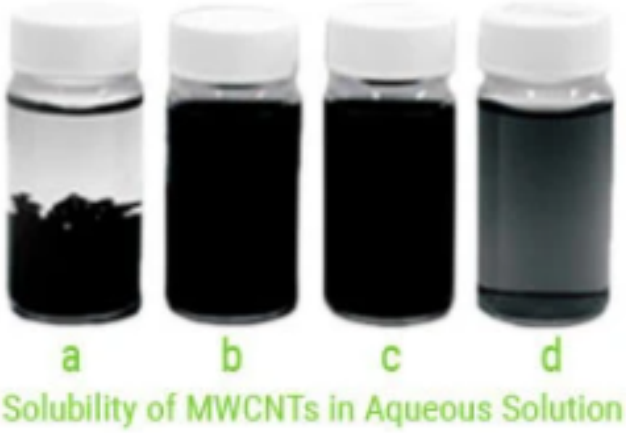

Figure 6.2: Samples of carbon nanotube dispersions in vials (a) showing coagulated carbon nanotubes in the body and at the bottom following bath sonication for 8 hours, (b) free-homogenous following probe sonication for 3 minutes; (c) maintained free-homogenous after 4 months of room temperature storage. The concentration of Multi-Walled Carbon Nanotubes (MWCNTs) is 2500 mg/L and the Multi-Walled Carbon Nanotubes (MWCNTs)/SDS ration is 1:10. (d) Multi-Walled Carbon Nanotubes (MWCNTs) of (c) diluted to 25 mg/L with deionized water. Adapted from (*Q700 Sonicator | Ultrasonic Homogenizer & Emulsifier | Qsonica*, n.d.)

As a result of work with Q700 ultrasonicator and surfactant addition, a usable methodology for mixing nanoparticles was developed. This however needed to be modulated depending on the properties of the gels being tested. Gels with greater viscosity tended to need longer pulse cycles in the sonicator for example.

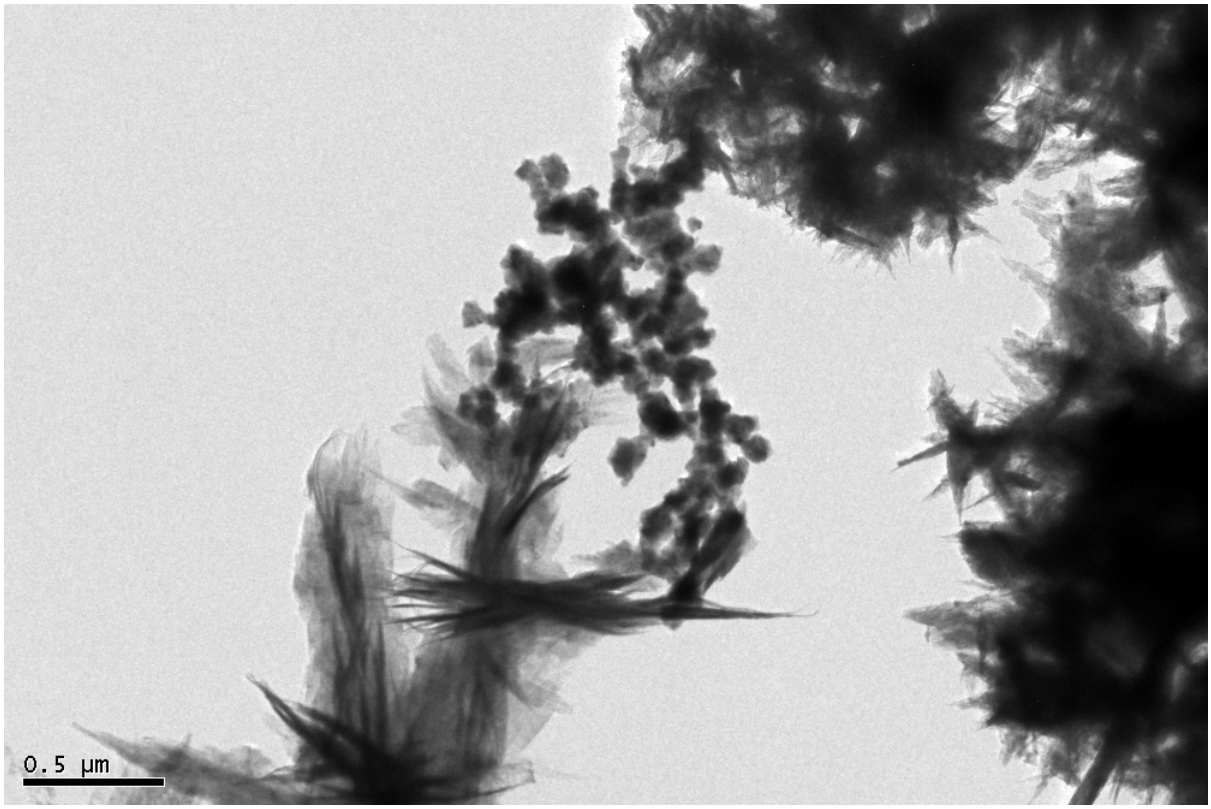

Figure 6.3: TEM image of CuNP suspension in aqueuous solution without surfactant or sonication – black particles in centre of image show the agglomeration that particles are prone to without sufficient mixing and dispersion in solution.

Figure 6.3 shows substantial agglomeration in the nanoparticle suspension following homogenisation into a water solution

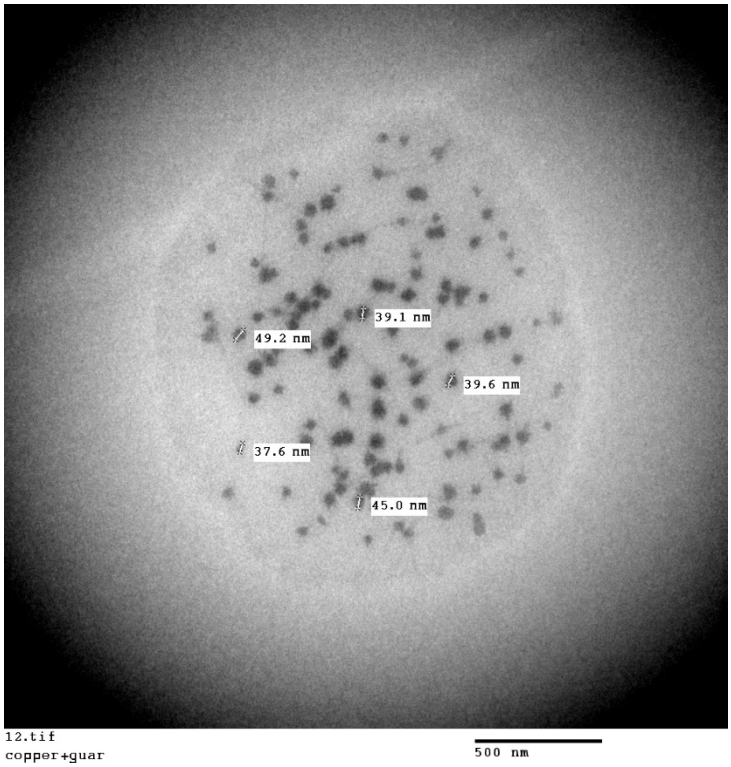

Figure 6.4:TEM of Copper nanoparticles suspended in guar gum crosslinked gel indicating more dispersion and suspension of particles when mixed and sonicated. Particle diameters are labelled (particles from Sigma are advertised as 25 nm in diameter, so there is still some agglomeration occurring).

Figs. 6.3 and 6.4 show the effects of dispersion methods. Nanoparticles dispersed via probe sonication into a crosslinked gel (Valida) (Fig. 6.5) an impact on the dispersion of the nanoparticles, which may influence bioavailability, especially considering the differing impacts of different sizes and morphologies on bioavailability discussed in the introduction (Geisler-Lee et al., 2013b)

Dynamic Light scattering (DLS) measurements were allowed the determination of the degree of homogeneity within the mixed solutions. (DLS) is a commonly used technique for measuring the size distribution of nanoparticles in solution. DLS analysis can be completed rapidly on a small sample volume with a wide variety of particle sizes ranging from a few nanometres to several microns in diameter (Kato et al., 2009b)

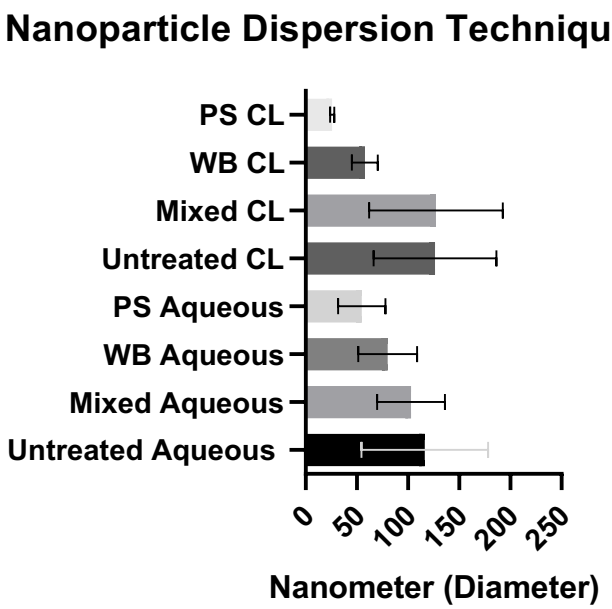

Figure 6.5: Comparison of measured particles sizes (n=7) in differently mixed and sonicated samples. Aqueous vs Crosslinked, WB = water bath sonication, CL = crosslinked, PS = Probe Sonication. Nanoparticles designated size = 25nm, larger results indicate some form of agglomeration occurring with larger measurements. N=10 samples per dataset.

Data shown in Figure 6.6 reveal that probe-sonicated nanoparticle dispersion is the most effective way to mix and disperse particles. Suspension in crosslinked material can help reduce rapid diffusion and sedimentation, although this is a process influenced by viscosity of the gel, temperature conditions and size of the nanoparticle, with larger nanoparticle sizes being correlated with reduced diffusion. Water has a viscosity of 1.05 CPS at 18^0 C vs agar at 10 to 100 CPS (depending on % used, increasing with crosslinking; (Kato et al., 2009b).

6.3 Gel Types

6.3.1 Aluminium and platinum-based crosslinked gels (A17 and HD Seal)

Aluminium-based sealant gels can provide a stable and protective environment for metal nanoparticles, which can improve their stability and prevent degradation over time. The gel matrix can act as a physical barrier against external factors such as light, heat, and moisture. Aluminium-based sealant gels can reduce the oxidation of metal nanoparticles. Metal

nanoparticles are prone to oxidation, which can degrade their properties and reduce their effectiveness and their bioavailability. Aluminium-based sealant gels can provide a low-oxygen environment for metal nanoparticles, which can reduce their oxidation and improve their stability. Aluminium-based sealant gels can enhance the barrier properties of packaging materials. The gel matrix can reduce the permeability of gases and liquids, which can prevent the ingress of contaminants and extend the shelf-life of the packaged nanoparticles. This can be particularly relevant for food packaging applications, where the barrier properties of the packaging material can impact the safety and quality of the food product. aluminium-based sealant gels are lightweight and easy to process, which can reduce the cost and complexity of packaging metal nanoparticles. They can also be easily moulded into different shapes and sizes, which can increase their versatility and applicability(Liu et al., 2021).

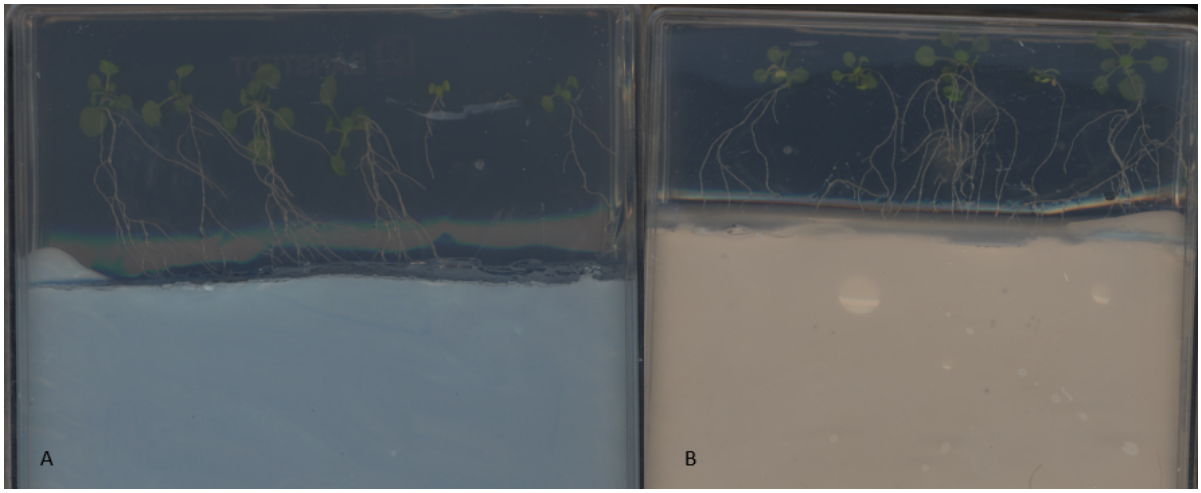

Figure 6.6: (A) Gel HD seal an aluminium crosslinked gel and (B) A17 a platinum-based gel sealant.

Trials investigating effects on plant growth were carried out with both A17 and HD seal gels. These gels are already used in industry to coat pipelines for a range of purposes and show good resilience and adherence.

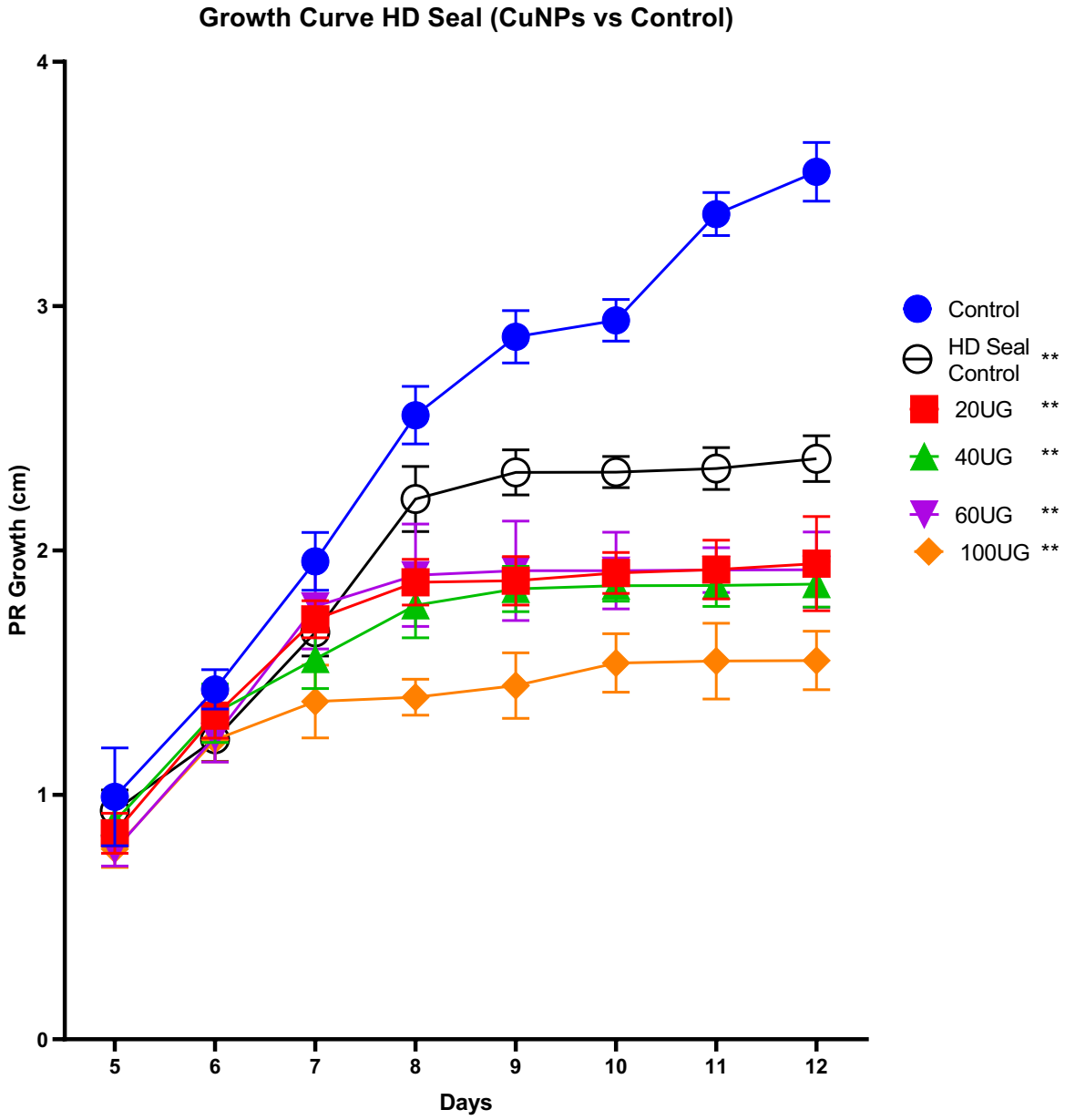

Figure 6.7: Growth Curve graph comparing A. thaliana primary root (PR) growth with no HD Seal gel (control) or HD Seal gel ± CuNPs (20, 40, 60, 100 ug/ml) over a period of 12 days..

It was found that there is a significant inhibition in the HD seal gel lacking CuNPs compared to control (*P* value of one-way ANOVA = 0.0047). Observations of the root making contact with the gel media suggest). It also appears to induce some stress responses in the plant without the necessity of having CuNPs added. This is due to the HD seal control having

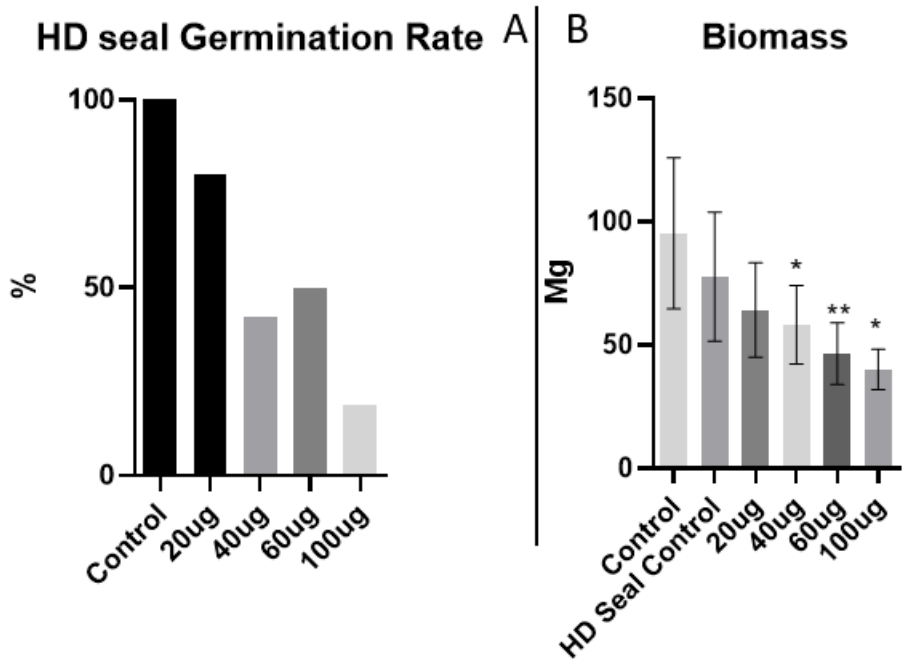

Figure 6.8 (A) Germination rates after 4 days in growth media; (B) total biomass after 7 days of growth.

HD seal control and 20 ug/ml were not significant when tested to the control but, 40, 60 and 100 ug/ml were has p values of 0.0178, 0.0041 and 0.0130 respectively. While not always statistically significant a reduction in growth metrics was regularly observed in the HD seal control media in the absence of CuNPs. However, there was full germination in HD seal media which suggests that the gel was largely non-toxic to the plant – in a way that the nanoparticles weren't. The CuNP-enriched media had progressively decreasing biomass correlated with increased dosage. Germination rates also trended downwards with increased concentration.

6.3.1.1 Biochemical Assays

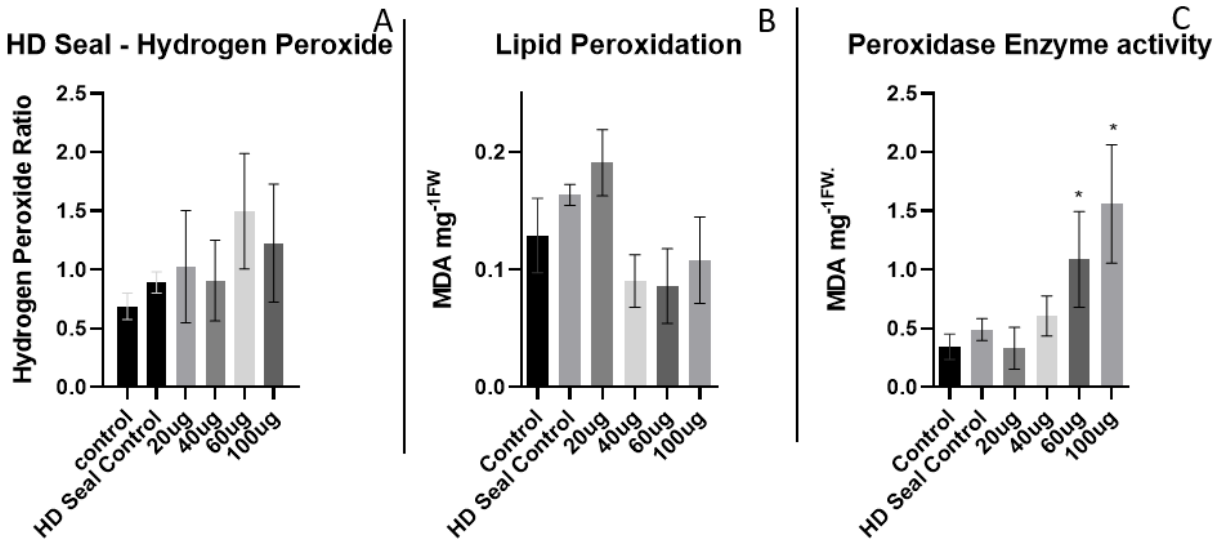

Figure 6.9 (A) Hydrogen peroxide ratio; (B) lipid peroxidation in mg^{-1} FW ; (C) peroxidase enzyme activity in plants grown on media with no HD Seal gel (control) or HD Seal gel ± CuNPs (20, 40, 60, 100 ug/ml) for 14 days.

The data points 60ug and 100ug are statistically significant P = 0.380 and 0.0151 respectively.

Malondialdehyde (MDA) production is used as a marker of lipid peroxidation and occurs when ROS is produced and damages the unsaturated fatty acids in cellular membranes (Tsikas, 2017). Peroxidases are enzymes that use hydrogen peroxide to oxidize various substrates, and peroxidase production is a later event in the ROS pathway and occurs as a response to the increased production of ROS (Tsikas, 2017).

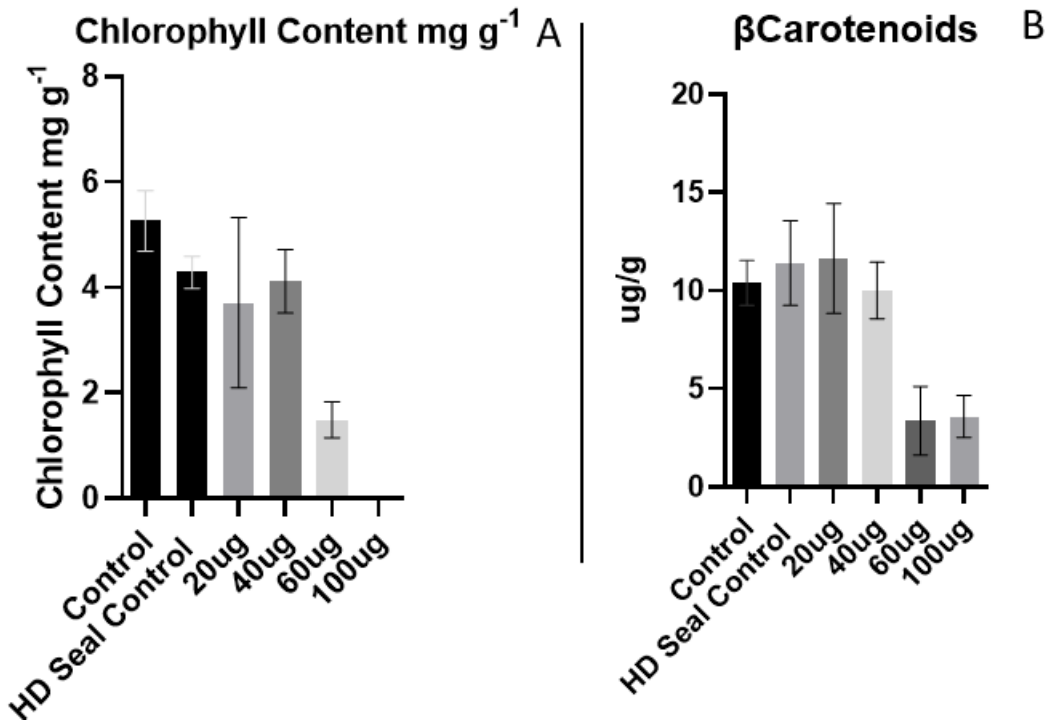

*Figure 6.10: (A) Chlorophyll content, (b) β carotenoid content in plants grown on media with no HD Seal gel (control) or HD Seal gel ± CuNPs (20, 40, 60, 100 ug/ml) for 14 days. N = 20 One way Anova: Chlorophyll – p < 0.0001 **** carotenoids - p < 0.0001 ****.*

Beta carotenoids are important pigments in plants that play a role in various physiological processes, including photosynthesis, photoprotection, and stress responses. Beta carotenoids act as antioxidants and help to prevent the harmful effects of excess light and oxidative stress on plant cells.

Under stress conditions, such as high light, drought, or salinity, plants often experience an increase in the production of reactive oxygen species (ROS), which can lead to oxidative damage to cellular components. Beta carotenoids can scavenge ROS and protect plant cells from oxidative stress by donating electrons and quenching singlet oxygen and other free radicals.

Important to note the plants seedlings entered death spirals as a result of very high exposure to CuNPs which resulted in very low levels of Chlorophyll and Beta Carotenoids in the plant shoot tissue.

6.3.1.2 Root Architecture

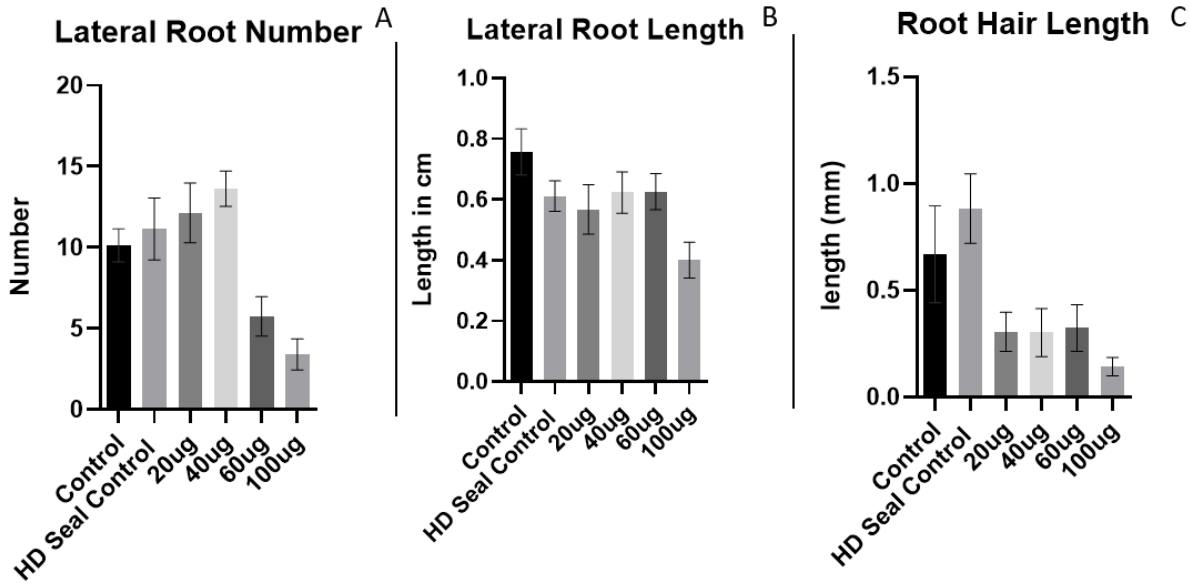

*Figure 6.11: (A) number of lateral roots, (B) Lateral root length (C) Root hair length One-way Anova p < 0.0001 ****. Lateral root number – p < 0.0001 ****. Lateral Root Length – p < 0.0001 ****

Root architecture was altered by treatment with HD seal CuNPs, progressively increasing LR number until 60+ CuNP. LR length did not vary as dramatically (except for 100ug treatment) but was decreased compared to the control, RH length was decreased significantly in all CuNP treatments.

6.3.1.3 HD Seal ICP-MS Analysis

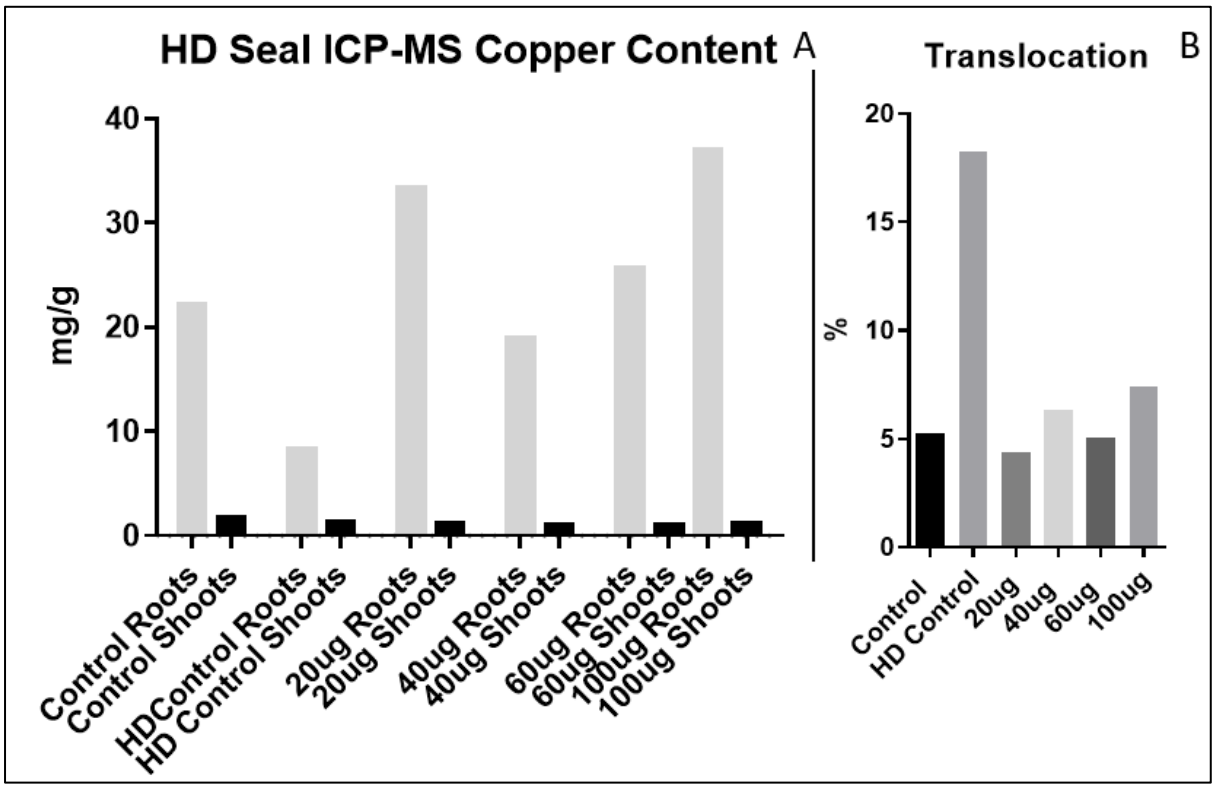

Figure 6.12: (A) ICP-MS measurements of Cu uptake into 14 day-old seedlings grown for 7 days in the absence (controls) and presence of CuNPs. (B) Copper translocation rate measured as averaging 5-7% although HD control skews the average.

Translocation refers to the process by which metal ions or compounds are absorbed, moved, and distributed within the plant system. This movement occurs from one part of the plant to another, such as from the roots to the shoots or from older leaves to younger ones. Translocation plays a crucial role in the uptake, distribution, and regulation of essential metal nutrients, as well as the detoxification of non-essential or toxic metals (Zhu et al., 2008). The uptake and translocation of Cu ions by 14 day old plants after 7 days of contact with the HD seal enriched gel is shown in Fig. 6.12. The results show that translocation rate stays around the 5-7% level, this is an expression of how much of the total metal uptaken was transported to the leaf tissue. Due to the lower uptake of Cu measured in the control HD Seal plants the subsequent measurement of the shoot content of Cu leads to a significantly larger translocation rate when in reality the shoot content of Cu is comparable to the other samples, for which the average translocation rate of 7%.

6.3.2 Cellulose Hydrogel

Cellulose-based hydrogels offer several potential benefits for packaging nanoparticles, including improved stability, controlled release, and reduced toxicity. Valida is the brand name of a cellulose based microfibril gel agent used frequently as a base for many inks, coatings and adhesives.

Cellulose-based hydrogels are highly porous and water-absorbent, which can provide a stable and protective environment for nanoparticles. The hydrogel matrix can act as a barrier against external factors such as light, heat, and moisture, which can degrade or destabilize nanoparticles. This can improve the stability and shelf-life of the nanoparticles, which is important for their use in various applications. the hydrogel matrix can also control the release of nanoparticles, allowing for sustained and targeted delivery over time. This can be useful for drug delivery applications, where a controlled release of nanoparticles is needed to achieve optimal therapeutic effects. The hydrogel matrix can also modulate the release rate of nanoparticles, which can be tailored to match specific biological or environmental conditions. cellulose-based hydrogels are biocompatible and biodegradable, which can reduce their potential toxicity and environmental impact. Unlike synthetic polymers, which can persist in the environment and have negative impacts on ecosystem health, cellulose-based hydrogels can break down into harmless products, which can reduce their environmental impact.

Finally, cellulose-based hydrogels are abundant and renewable, as they can be sourced from plants such as wood, cotton, and hemp. This makes them a sustainable and cost-effective option for packaging nanoparticles, especially compared to synthetic materials that are derived from petrochemicals (Valida Fibrillated Cellulose for Coatings).

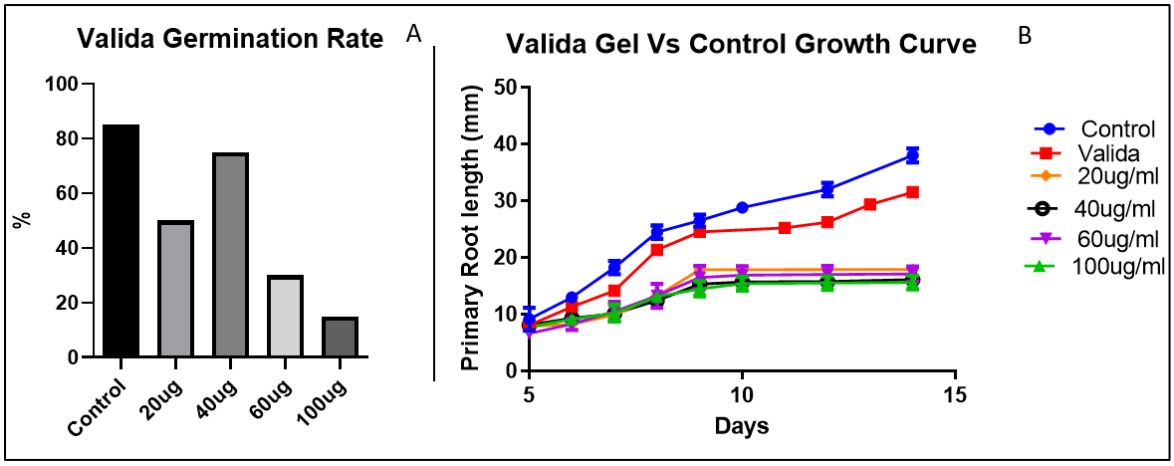

*Figure 6.13: (A) Valida germination rate, (B) Valida Gel vs control growth over 14 days, (n = 20 seedlings) one way ANOVA P = 0.008 ****

Valida gels without CuNPs closely followed the growth patterns of the control dataset over a 14-day growth period. Whereas the CuNP enriched media functionally halted the primary root growth. The Valida germination rate was 80% in the control non CuNP enriched product but the primary ingredient in the gel is cellulose, a plant based ingredient.

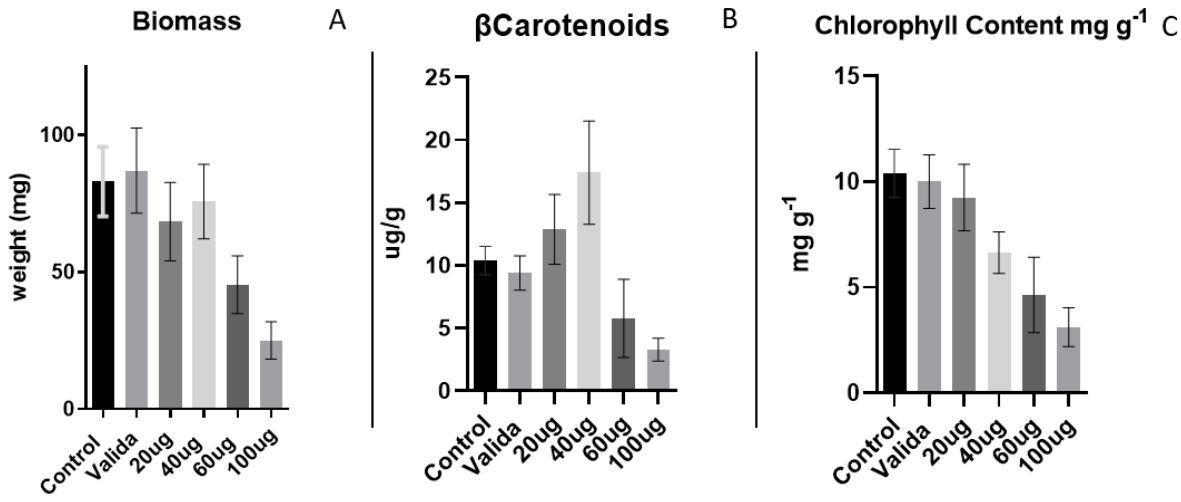

Figure 6.14: (A) Biomass measurements after 14 days following treatment and exposure to CuNPs. N = 20 seedlings. (B) β Carotenoid Content with the valida gel CuNPs, N = 15 seedlings (C) Chlorophyll Content measured in mg per gram of the same treated plants. N = 15 seedlings.

At lower concentrations of CuNPs we see the inhibitory effect of the nanoparticles while still maintaining an active systemic response to the stress, the 60 and 100 ug/ml treatments result

in the plant beginning a death spiral (evidenced by decreasing chlorophyll, β Carotenoid content and decreased biomass. Inhibition can be accomplished at 20 and 40 ug/ml without damaging the plants.

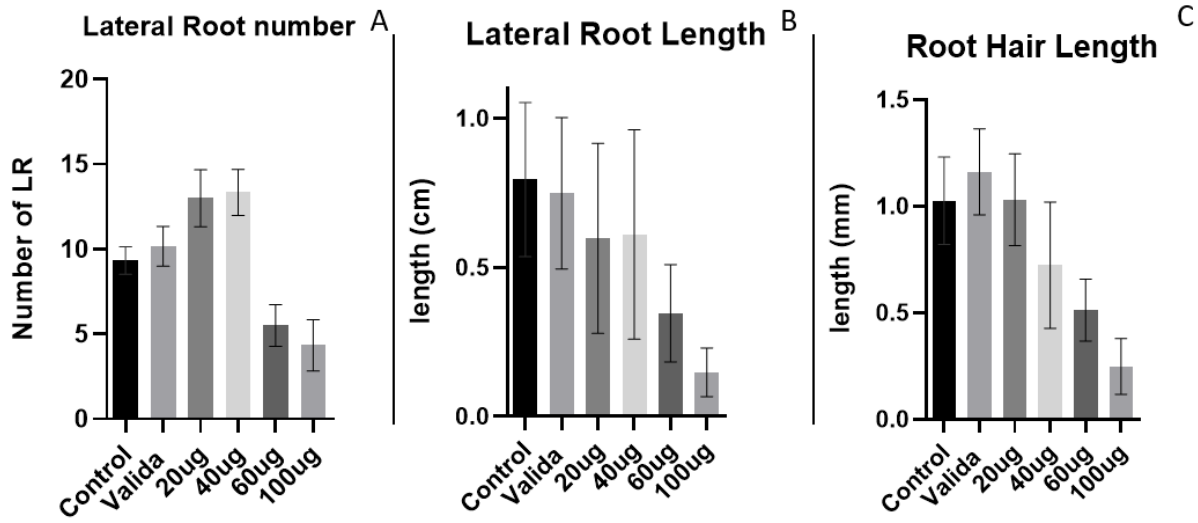

Figure 6.15: (A) lateral root numbers, (B) Lateral root length, (C) Root hair length

We see an increase in lateral roots with increased concentration until 60 and 100 when the plants growth is abruptly halted, while highly variable lateral root length is consistently similar length until 60 and 100ug treatment which results in halted growth. There is a general downward trend in root hair length with increased CuNP treatment concentration.

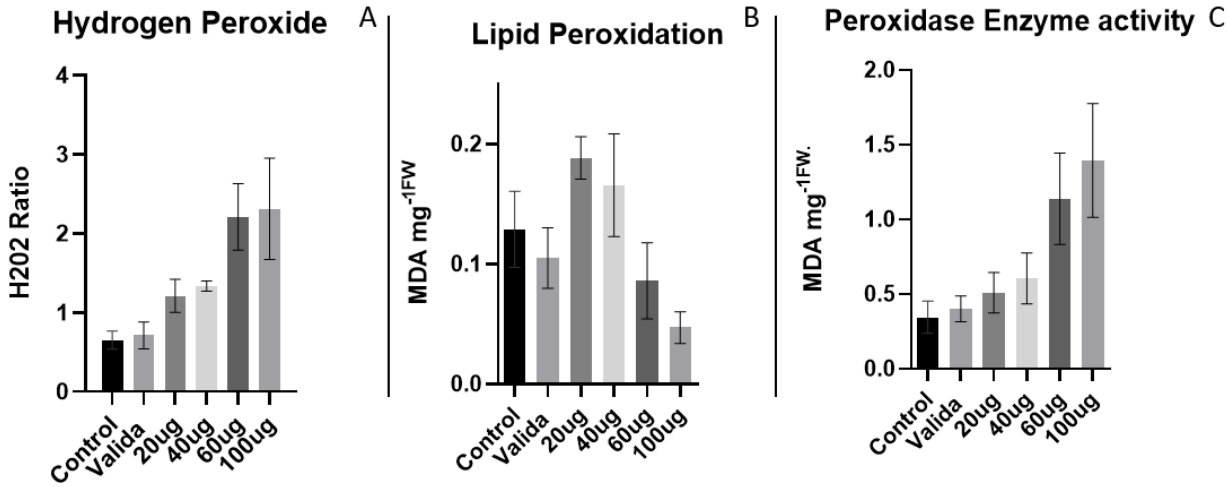

Figure 6.16: plants grown to day 14 and following assays performed (A) Hydrogen Peroxide ratio. (B) Lipid Peroxidation measuring the MDA concentration and indicator of stress

considerable increased in 20 and 40ug but 60 and 100ug having reduced detection. (C) Peroxidase enzyme activity again showing progressive increase with higher concentrations of copper nanoparticles.

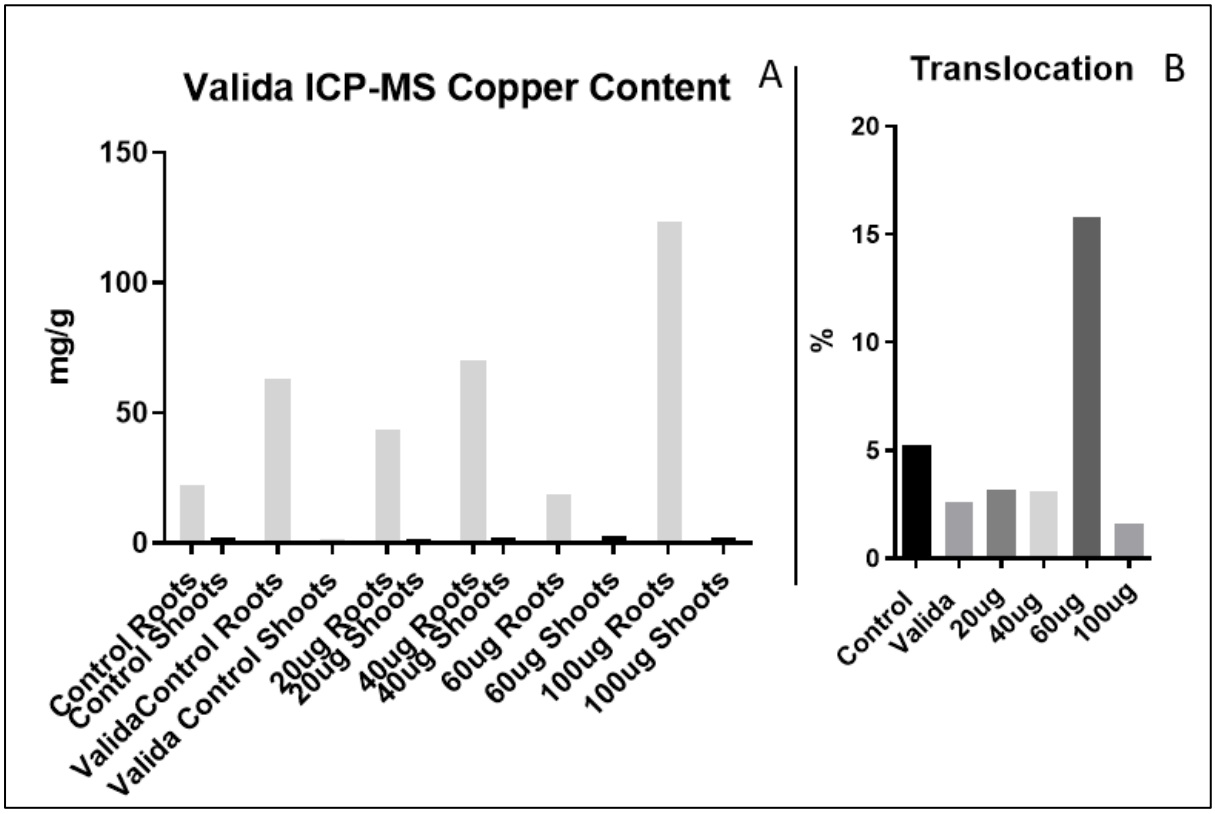

Figure 6.17 (A) ICP-MS analysis of Copper content in roots vs shoot tissue for the plants treated with the valida gel. (B) The translocation rate, the high translocation rate for 60 ug/ml was as a result of the lower root reading rather than an excessive amount of translocation occurring, avg translocation rate 9%.

Fig. 6.17 describes copper uptake and translocation in the same manner as Fig. 6.12. The average translocation rate was approximately 9%. There was a very high translocation rate for 60 ug/ml, but more as a result of the low root reading that was as detected than as an overall high root to shoot copper translocation.

Strengths	Weaknesses
Low cost (formulation & no robots). Fast. Ability to cope with different pipe sizes. Ability to cope with irregular pipe dimensions. Biodegradable.	Difficult to coat substrate uniformly. Poor adhesion to substrates. Pulls off substrate if it dries out. [Leaching of copper NPs?]

Table 6.2 : Summary of the strengths and weaknesses of the cellulose hydrogel Valida crosslinked gel as established by project stakeholders.

Table 6.2 summarises some useful benefits and advantages of the Valida gels but there are some potential drawbacks to the system.

6.4 Environmental Leakage – ICP-MS Diffusion

The addition of CuNPs to the soil can have several environmental implications, as copper is a toxic heavy metal that can accumulate in the soil and have negative impacts on soil health and ecosystem function.

The addition of CuNPs to the soil can lead to an increase in copper concentrations, which can have toxic effects on soil microorganisms and reduce soil fertility. the addition of copper nanoparticles to soil can also have negative impacts on soil biota, including earthworms, insects, and other soil organisms, which play important roles in nutrient cycling and ecosystem function. CuNPs can also leach into groundwater and surface water, contaminating and potentially harming aquatic organisms. Another potential environmental concern is the potential for the nanoparticles to accumulate in the food chain, as copper can be taken up by plants and consumed by herbivores and omnivores. This can lead to bioaccumulation and biomagnification of copper nanoparticles in higher trophic levels, which can have toxic effects on animals and potentially impact human health.

The addition of CuNPs to soil environments should be approached with caution, and their potential environmental impacts should be carefully assessed before any large-scale application. It is important to consider the potential risks and benefits of nanoparticle applications and to implement appropriate safety measures to minimize their environmental impacts, an example of such a safety to minimise environmental impact would be packaging

nanoparticles inside a gel matrix, this can have several effects on the behaviour and properties of the nanoparticles, as well as on their interactions with their environment. One major effect is that the gel matrix can act as a physical barrier that limits the diffusion and mobility of the nanoparticles, thus reducing their rate of release and potentially increasing their stability.

By entrapping nanoparticles within a gel matrix, their exposure to external factors such as light, heat, and moisture can be reduced, which may improve their stability and shelf life. The gel matrix can also protect the nanoparticles from degradation by enzymes and other biological agents, and from interactions with other molecules in the surrounding environment.

ICP-MS measurements have been taken to determine environmental diffusion rates in different gel types.

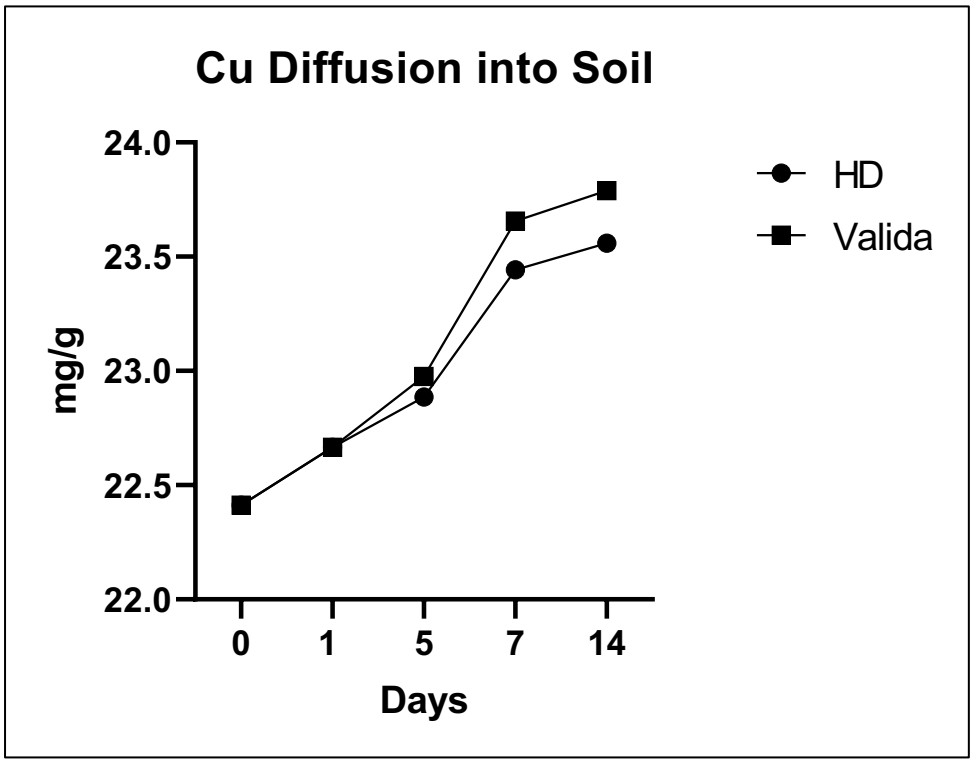

Figure 6.18: Diffusion rate of Cu into soil over the course of a 14 day period. 50mg soil samples in proximity to coated area was measured in order to determine an average leech rate of copper into soil environment.

In Fig. 6.18 there is analysis of copper content in soil within the plant pot during the willow plant experiment. How much CuNP is leaked from the gel into the soil within 15cm of the

coated region. Day zero was the control measurement as this was taken before the coating with gel. There is an increase in copper content which is to be expected as the plant has been taking up additional copper as evidenced by their phenotypic response. By day 14 there is an additional 1.5mg/g of copper in the soil.

6.5 Summary

In this chapter, several gel packaging agents were investigated for their suitability as packaging agents to be coated on pipe systems for further commercialisation. A list of ideal criteria was drawn up. The method of dispersing nanoparticles throughout a gel media was optimised. Growth tests of plants exposed to different gel agents, HD Seal, A17 and Valida gels were tested and measured growth metrics such as root architecture changes, biochemical assays and ICP-MS was carried out.

Further to this testing the potential leakage of CuNPs into the environment was also tested using ICP-MS. Additional work determining the existence of competing products in the marketplace was carried out via a patent search. It was found that while interest in gel-based and nanoparticles is a growing industry, they have not yet been applied to this problem before and the project retains its novelty.

Finally, some preliminary work into organogels has been carried out for a potential continuation of research.

Chapter 7 Discussion

7.1 Introduction

While copper is an essential micronutrient for plant growth and development, it plays a critical role in maintaining proper plant cell wall structure and function (Festa & Thiele, 2011). The literature demonstrates that CuNPs can enhance plant growth and development (Aruoja et al., 2009). They have been shown to increase seed germination, improve plant biomass, and enhance nutrient uptake by plants. However, the effects of CuNPs on plant growth and development are highly dependent on their concentration, size, and surface chemistry. Excessive amounts of copper can be toxic to plants. Copper toxicity can lead to oxidative stress, membrane damage, and cell death as previous results in this thesis and literature have demonstrated (Lee et al., 2008b). Copper can affect plant root architecture. (Services & Crawford, 2003). As copper is such a widely available metal in the environment (Festa & Thiele, 2011), it is not surprising that plants do have a biological system to tolerate metal stress and other abiotic stresses for resiliency in their environment. This system and how it can be both understood mechanistically and utilised to get advantageous and sustainable growth outcomes for both plant and for civil infrastructure lifespan is the main research question of this thesis.

The discussion objectives are to clarify and to discuss the wider implications of the work and to suggest ideas for further investigation. The hypotheses generated from work in this thesis and analysis of published literature resulted results in the presentation of a potential model of hypothesised response pathways resulting from exposure to CuNPs. This figure and its hypothesis will be discussed with reference to evidence collected from the results chapters. As will further research and experiments that may further elucidate the pathways and a discussion of interdisciplinary research that may further solve the problem of root ingress into built structures.

7.2 Pathway Hypothesis

When Arabidopsis plants were treated with CuNPs, there are several biological pathways that are clearly activated, some known to be associated with in specific response to metal stress and others that are known to be activated in response to abiotic stresses but also, including pathways involved in the immune response of the plant. The 3 primary response pathways referenced identified in Chapter 4 are plant-pathogen interaction, plant hormone signal

transduction and phenylpropanoid biosynthesis. These pathways are not necessarily exclusive of each other, and their co-activation suggests a broad-based defence response to CuNPs.

I will present a potential pathway of action by which these systems allow the plant to respond to immediate abiotic stress, and a systematic redistribution of auxin, as well as SAR development.

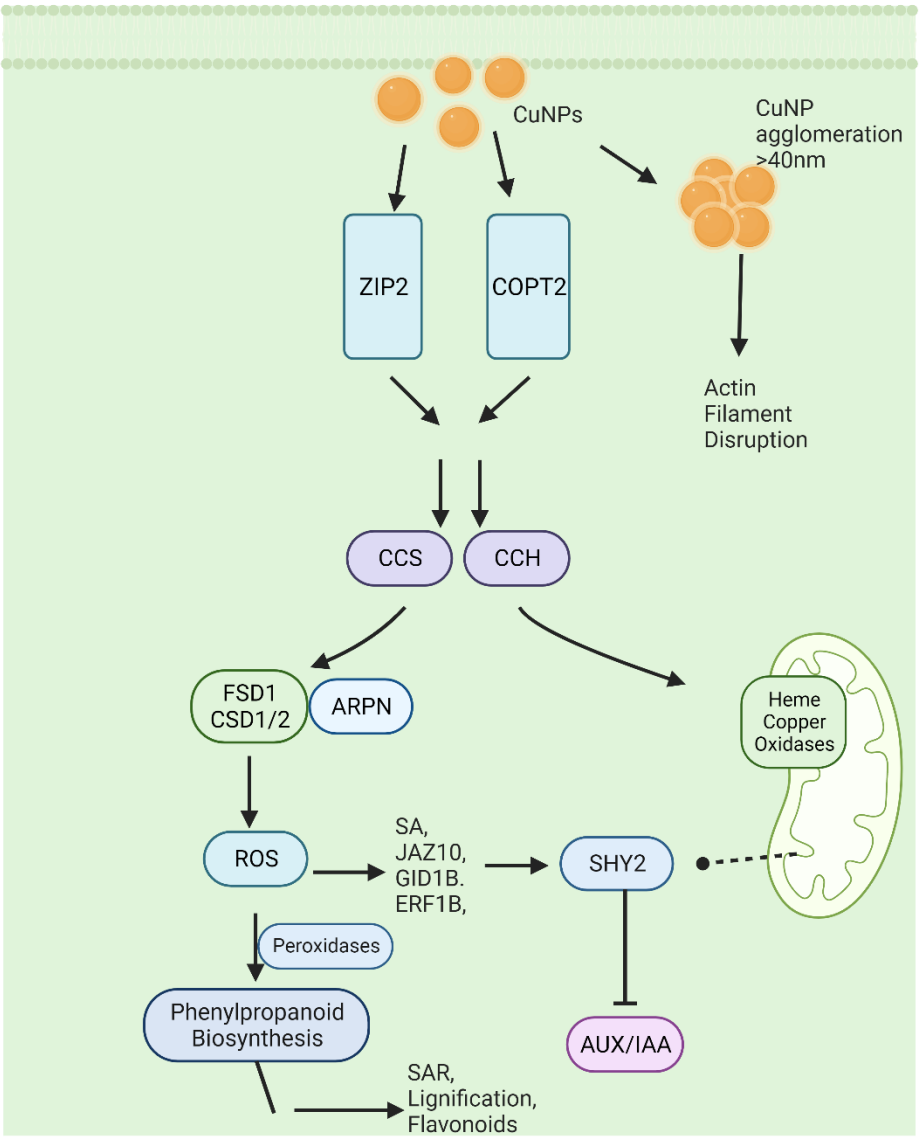

Figure 7.1 A putative pathway for the uptake and subsequent effects of CuNPs on the plant transcriptome. straight lines indicate evidence of a connection between pathways by transcriptomic or proteomic data, and dotted lines indicate a hypothesised interaction.

The model in Fig. 7.1 summarizes known and hypothesized pathways in response to CuNPs in plants. In this model, the plant is treated with copper nanoparticles, leading to an influx of copper ions into the plant system. Cu is uptaken up via the apoplastic pathway and transported across the plasma membrane. COPT2 and ZIP2 are upregulated, promoting the uptake and transport of Cu ions within the plant. CCS and CCH deliver and incorporate Cu (Markossian & Kurganov, 2003; Shin et al., 2012; Sturtz Field et al., 2002; Wintz & Vulpe, 2002). CCS delivers Cu ions to FSD1 and CSD1/2 while CCH is involved in delivering copper to heme-copper oxidases (Mira et al., 2001; Kolli et al., 2018; Llases et al., 2019).

Increased ROS production As FSD1 is a copper/zinc superoxide dismutase alongside CSD1/2 (just copper dismutase), it catalyses the dismutation of superoxide radicals into molecular oxygen and hydrogen peroxide (Olson, 1993). The upregulation of FSD1 indicates an increased ROS production in response to CuNP treatment (Fig. 4.19). It is hypothesized that the plant tries to combat the increased ROS levels by upregulating chelators like such as basic blue ARPN and heme copper oxidases, as well as ROS-scavenging enzymes like FSD1 and CSD1/2, which helps maintain a balance between ROS production and scavenging. The plant can only tolerate a certain quantity of treatment as evidenced by the death spiral of plants when subjected to high quantities of CuNPs.

The oxidative stress caused by the CuNPs treatment leads to a series of physiological changes in the plant which includes the upregulation of genes and proteins involved in ROS production, scavenging, and signalling and SAR such as phenylpropanoid synthesis, increased lignification and strengthening of the cell walls as well as the production of flavonoids which can act as metal chelators (Fig. 4.19).

7.2.1 Role of SHY2/IAA3 as an auxin regulator.

SHY2, also known as IAA3, is a member of the Aux/IAA family of transcriptional regulators in plants. These proteins play a significant role in the auxin signalling pathway. Aux/IAA proteins, including SHY2, act as repressors of auxin-responsive genes by interacting with ARF (Auxin Response Factor) transcription factors. Under low auxin conditions, Aux/IAA proteins form a complex with ARF transcription factors, inhibiting the transcription of auxin-responsive genes (see introduction).

Although SHY2 predominantly interacts with auxin, it is important to note that plant hormone signalling pathways are interconnected, and crosstalk between them is essential for proper growth and development (Moore et al., 2015). Consequently, the activity of SHY2 and other Aux/IAA proteins can be influenced by other plant hormones, such as cytokinins, abscisic acid, gibberellins, or ethylene, through complex regulatory networks. Through auxin SHY2 also negatively regulates *PIN* genes encoding auxin transport facilitators carriers which are important for establishing the polar auxin concentration gradients through which primary root growth is facilitated (Moubayidin et al., 2010).

This gene was downregulated in the 3hr timepoint in the transcriptomic data but significantly upregulated in the 24hr suggesting there was an important role in regulating the growth response to the presence of CuNPs in the cytosolic space.

7.2.2 Role of phenylpropanoids

The role of phenylpropanoid biosynthesis in metal stress response in plants is very important for the plant's resiliency. And has many useful benefits, some phenolic compounds such as flavonoids are involved in the chelation and sequestration of metals reducing their toxicity and facilitating their sequestration in plant tissue (Govender, 2017). This process helps plants to tolerate higher levels of metal stress by preventing the accumulation of toxic metal ions in sensitive cellular compartments. Phenolic compounds also possess antioxidant properties, allowing them to scavenge ROS and protect plant cells from oxidative damage. This antioxidant activity helps plants to maintain cellular homeostasis under metal stress conditions (Shen et al., 2022). They can act as signalling molecules that modulate the expression of stress-responsive genes. These compounds can help plants to fine-tune their response to metal stress by regulating the expression of genes involved in metal transport, chelation, and detoxification (Dias et al., 2021).

Lignin, a major product of the phenylpropanoid pathway, is a structural component of plant cell walls. Under metal stress, the biosynthesis of lignin can be upregulated, leading to the reinforcement of cell walls (Lin et al., 2005). This increased structural rigidity can help plants to withstand the mechanical stress imposed by metal ions and limit the uptake of toxic metals. Lignification involves the deposition of lignin in cell walls. Lignin is a complex polymer that provides structural support to the cell wall, making it more difficult for pathogens to penetrate the plant tissue. Lignin can act as a physical barrier, preventing the spread of

pathogens through the plant. Lignification is triggered by biotic and abiotic stresses, such as pathogen attack, mechanical damage, and environmental stress (Lin et al., 2005; Ralph et al., 2019). This is a highly regulated process, and its extent and timing can vary depending on what stress is present and the plant species involved. excessive lignification can lead to reduced growth and yield (Govender et al., 2017), so there is an important regulatory balance that is necessary. Phenylpropanoid biosynthesis is a crucial metabolic pathway in plants that generates a wide variety of secondary metabolites, including lignin, flavonoids, and phenolic acids. These compounds are involved in various aspects of plant growth, development, and response to biotic and abiotic stresses (Ralph et al., 2019).

The upregulation of phenylpropanoid pathway genes in response to CuNPs (Fig. 4.19) is therefore likely part of a general stress response to Cu ions, through likely activation of antioxidant activity.

7.2.3 Direct vs Indirect interaction with the cytoskeleton

There is evidence that larger agglomerates of nanoparticles have evidence of directly interacting with actin filaments and dysregulating dysregulate them, resulting in fewer F-actin filaments and thus potentially a delocalisation of PIN proteins (an actin-dependent process; Geldner et al., 2001) which therefore would be unable to perform their function appropriately.

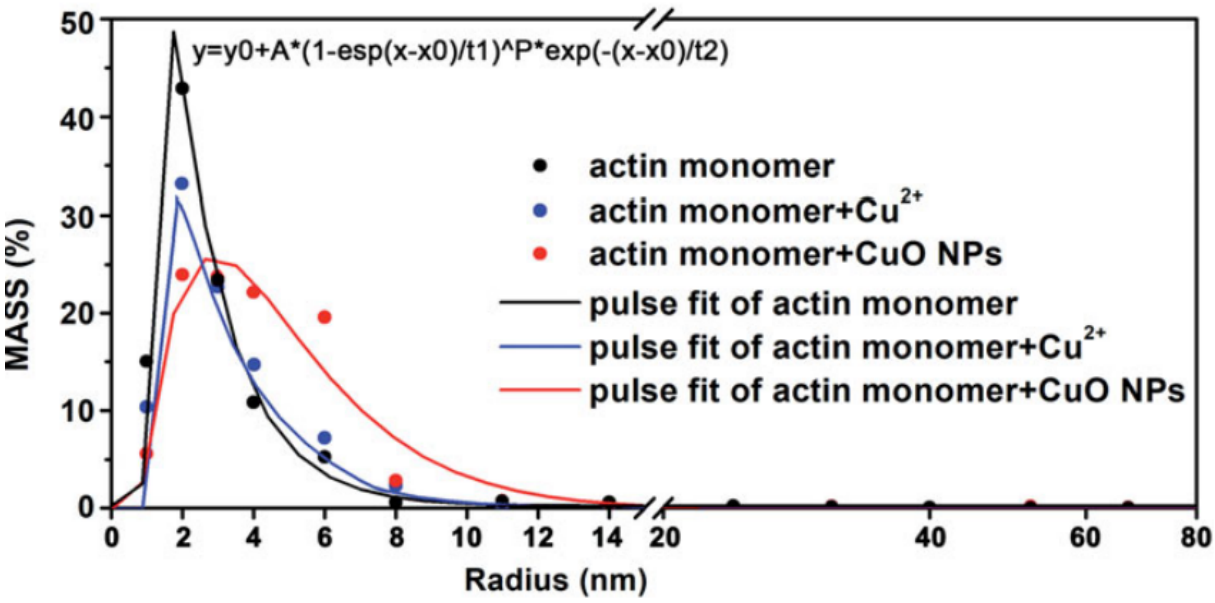

Figure 7.2 Dynamic light scattering (DLS) showing CuNPs attached to actin monomer. Actin monomers and CuNPs turbid liquid were mixed for 12 h at 4 C. The distribution of actin

monomer size was analysed by DLS. Data were shown by the Poisson Skewness Distribution. Taken from (Jia et al., 2020).

The longitudinal F-actin bundles in plant cells were found to undergo significant alterations in their arrangement upon exposure to increasing concentrations of CuNPs (Fig. 7.2; Jia et al., 2020). Specifically, the bundles shifted to a transverse arrangement, while the overall quantity of F-actin bundles in both epidermal cells and root hairs was reduced. Despite these changes, the total amount of actin remained consistent following treatment.

Notably, the G/F actin ratio increased in a dose-dependent manner, indicating a disruption in the actin's ability to polymerize. This suggests that while actin bundles were being reorganized, their overall expression was not downregulated. Under normal physiological conditions, F-actin bundles were stabilized within mature root epidermal cells. However, after treatment with 40 mg/L CuNPs for a 6-hour duration, the F-actin bundles experienced continuous breakage and reorganization.

Research presented in the study strongly implies that CuNPs directly interact with F-actin and actin monomers in vitro. In contrast, isolated copper ions (Cu^{2+}) did not demonstrate the same interaction. This highlights the importance of considering the potential impact of CuNPs as a very different material to just copper ions and its impact on the cellular architecture of plants and provides valuable insights into the mechanisms underlying these changes (Jia et al., 2020).

7.2.4 Plant systemic changes to treatment with excessive CuNPs

CuNPs can cause morphological abnormalities in plants, with effects on plant growth, particularly root development, and cause changes in plant tissues, such as the epidermis, cortex, and vascular bundles. Different heavy metals have varying diverse effects on plants, including dose-dependent decreases in shoot length, root length, fresh weight, and relative water content.

Physiologically, CuNPs can reduce leaf size, lamina thickness, and stomatal aperture size, which leads to decreased transpiration, water uptake, and translocation to the shoot. High concentrations of them can cause significant changes in plant height, shoot biomass, root

biomass, and damage to organelle structures. There also appears to be an effect on the concentration of essential elements in plants, such as potassium, iron, calcium, and magnesium which are required for various biological processes (Mishra et al., 2021).

Environmental signals control root hair development, with most studies on Arabidopsis focusing on phosphate and iron deficiency. The impact of salt stress on root hair growth and development remains largely unexplored. Wang et al. (2008) demonstrate that salt stress significantly influences root epidermal cell types and root hair development, decreasing root hair length and density in a dose-dependent manner. This response is sensitive to ion inhibition concentration but not osmotic stress.

High salinity alters root anatomical structure, reducing cell numbers and enlarging cells. The analysis of the *salt overly sensitive* (*sos*) mutant, which is defective in sodium homeostasis (Ji et al. 2013), reveals that this root hair response is an adaptive mechanism to reduce excessive ion uptake due to ion disequilibrium. Salt-induced root hair plasticity represents a coordinated strategy for early stress avoidance, tolerance, and adaptation. In this thesis, we see an increase in root hair length at low concentrations of CuNPs but a significant reduced increase at higher concentrations (Fig. 3.2). Root hairs can help plants tolerate heavy metal stress by limiting the uptake of toxic metals, such as cadmium, lead, or arsenic. Root hairs may also play a role in the secretion of compounds that bind and immobilize heavy metals, reducing their bioavailability in the soil (Mishra et al., 2021).

7.3 Nature and morphology of nanoparticles:

7.3.1 Particle Size

Physiological studies on higher plants have shown that NPs with a size of up to 40 nm can be taken up by roots and move through the vascular system, while larger NPs accumulate in the apoplastic space. Therefore, it is believed that some of the harmful effects of NPs may be due to mechanical damage or blockage of plant structures, such as plasmodesmata or stomata, which regulate water flow. In maize, the presence of TiO_2 and clay NPs has been found to decrease the size of cell-wall pores from 6.6 nm to 3.0 nm by pre-treatment of nanoparticles Click or tap here to enter text.(Ma et al., 2010b; Geisler-Lee et al., 2012), which causes a reduction in hydraulic conductivity and transpiration (Asli & Neumann, 2009). As a result,

plant molecular responses to mitigate the damage caused by NPs may involve mechanisms to control water stress. However, this hypothesis has never been tested. We know from chapter 5 Transcriptomics that there is a strong response to abiotic stress which would partially validate and is consistent with this theory, however, no specific experimental work was carried out on this question.

It is also important to note that the total particle surface area varies substantially depending on particle size (Table 7.1). This could potentially have dramatic effects on the bioavailability and reactivity of NPs depending on the size and morphology used in experiments.

Particle Diameter (μm)	**Particle no. (cm^3)**	**Particle surface area ($\mu m^2/cm^3$)**
5	153,000,000	12,000
20	2,400,000	3,016
250	1,200	240
5000	0.15	12

Table 7.1.: Particle number and particle surface area per 10 μg/m^3 airborne particles. A demonstration of how different particle sizes and number concentrations can dramatically impact biologically active surface area and thus have a large impact on how phytotoxic they can be. Adapted from (Oberdörster et al., 2005)

This small size and large surface area, as illustrated in table 7.1, confers properties to NPs such as making them useful as catalysts in the chemical reactions. Surface area is important to consider as surface atoms and molecules play a key role in determining bulk properties (News & 1989). The ratio of surface to total atoms or molecules increases exponentially with decreasing particle dimensions (Tungittiplakorn et al., 2004). The outcome of NPs interactions with plants or microbes is dependent on specific NP type, size, surface, charge, dose tested, species of plant or microbe examined, and test media. Test medium can be liquid, soil, agar or other solid media and has a significant effect on the outcome of NP plant-microbe interactions (Rao & Shekhawat, 2016). Metallic NPs have difficulty maintaining their stability (i.e. remaining in the nanosized range – there is a tendency to agglomerate; Walter, 2013).

The bioavailability of copper nanoparticles is influenced by their size, morphology, and oxidation state. Smaller nanoparticles exhibit higher bioavailability due to their increased surface area, which allows for better interactions with biological systems. The morphology

can affect the uptake and interaction of nanoparticles NPs with cells or biomolecules, either promoting or hindering their bioavailability. Oxidation of copper CuNPs can lead to the formation of copper oxide (CuO or Cu_2O) nanoparticles, which exhibit different bioavailability properties. The toxicity and uptake of copper oxide nanoparticles can vary depending on their size, morphology, and specific oxidation state (Prantner & Scholler, 2014)(W.-M. Lee et al., 2008a). This thesis investigated a uniform size and morphology of nanoparticle and oxidation states were not analysed and there is previously published evidence suggesting these variables do make a tangible impact on growth outcomes.

7.4 Soil Interactions vs gel interactions, implications for experimental design

7.4.1 Microbiome interactions with nanoparticles and potential issues caused by disruption of nitrogen fixation

Microbiome interactions with CuNPs copper nanoparticles can have both positive and negative effects on the environment and living organisms. One area of concern is the potential impact of copper nanoparticles on nitrogen-fixing microorganisms, which play a vital role in the nitrogen cycle and the maintenance of soil fertility. Nitrogen fixation is a process is essential for plant growth and the overall health of ecosystems. However, the increased presence of CuNPs copper nanoparticles in the environment may disrupt this critical process in several ways.:

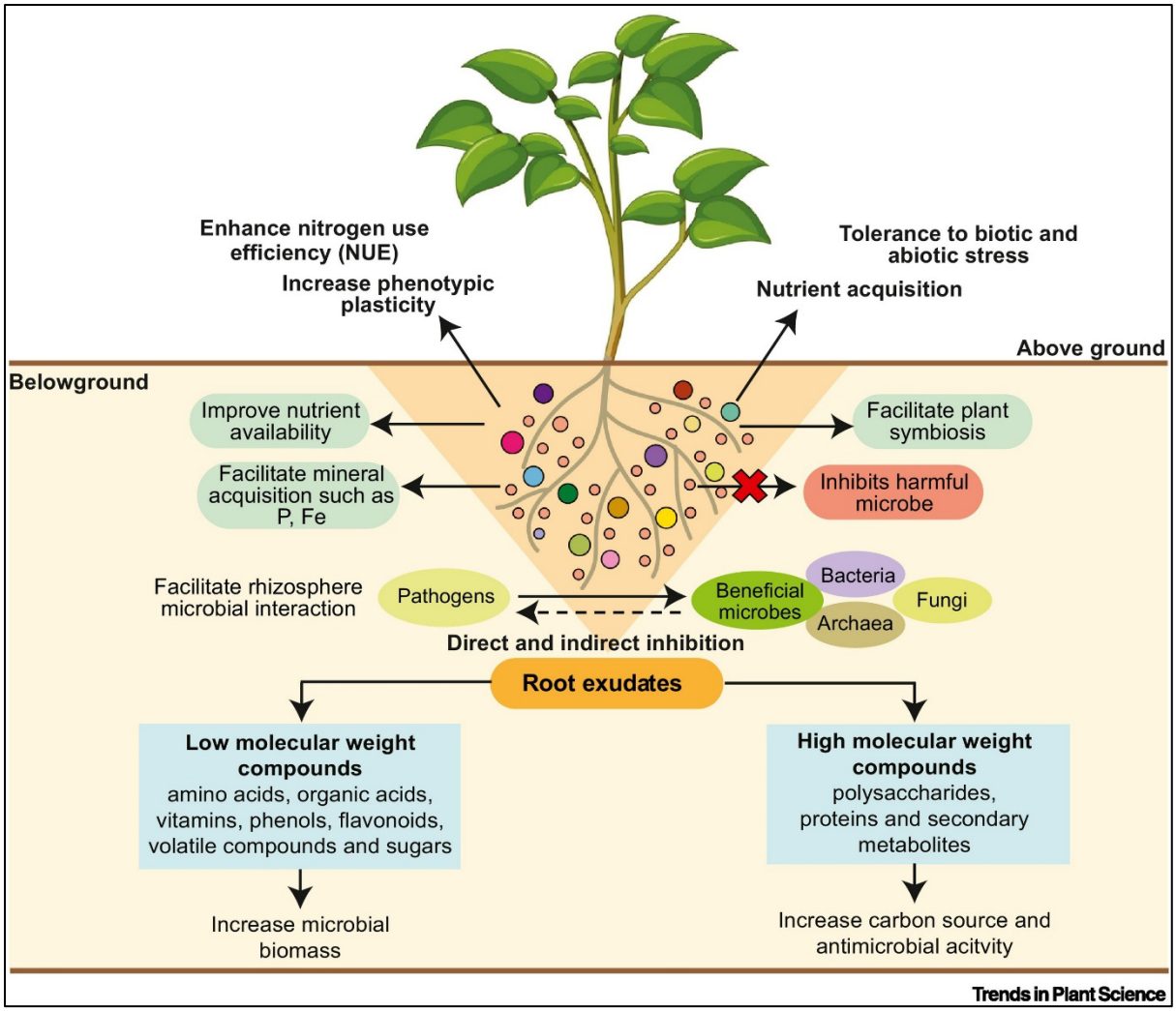

Figure 7.3 Schematic representation of the mutual relationship between roots and microbiome. The circles with different sizes and colours around the roots represent root exudate compounds. Abbreviations: P, phosphorus; Fe, iron. (Ghatak et al., 2023)

CuNPs can be toxic to nitrogen-fixing microorganisms, such as *Rhizobium* species, which form symbiotic relationships with legume plants. High concentrations of CuNPs nanoparticles can cause oxidative stress, DNA damage, and disruption of cell membranes, leading to the death or reduced activity of these important bacteria (Thomas, 2011). This disruption can negatively impact plant growth and, in turn, the overall health of ecosystems. CuNPs may not only affect nitrogen-fixing bacteria directly but also influence the overall microbial community structure. By altering the balance of microbial populations, CuNPs can disrupt the competitive relationships between different microorganisms. This disruption can lead to a decline in the

abundance or effectiveness of nitrogen-fixing bacteria, further affecting the nitrogen cycle and soil fertility (Ghatak et al., 2023; Khan et al., 2019).

Exposure to CuNPs can result in changes in gene expression in nitrogen-fixing bacteria (García-Sánchez, 2015). These changes can affect the bacteria's ability to fix nitrogen and form effective symbiotic relationships with plants. In some cases, this could lead to reduced nitrogen fixation rates and diminished plant growth. CuNPs can be transported through the soil and water, increasing their potential to interact with various microorganisms, including nitrogen-fixing bacteria.

It is important to consider the potential risks associated with the use of copper nanoparticles and their potential to disrupt nitrogen fixation. Further research is needed to understand the complex interactions between CuNPs and microbiomes, as well as to develop strategies for mitigating any negative consequences. This knowledge can help in the responsible development and application of copper nanoparticle-based technologies while minimizing their impact on essential ecological processes like nitrogen fixation (Ghatak et al., 2023).

7.5 Role of stress in governing plant responses:

It is clear from the literature and from the experimental work carried out in this thesis that stress or specifically ROS is a common denominator throughout many of a plants biochemical and homeostatic processes.

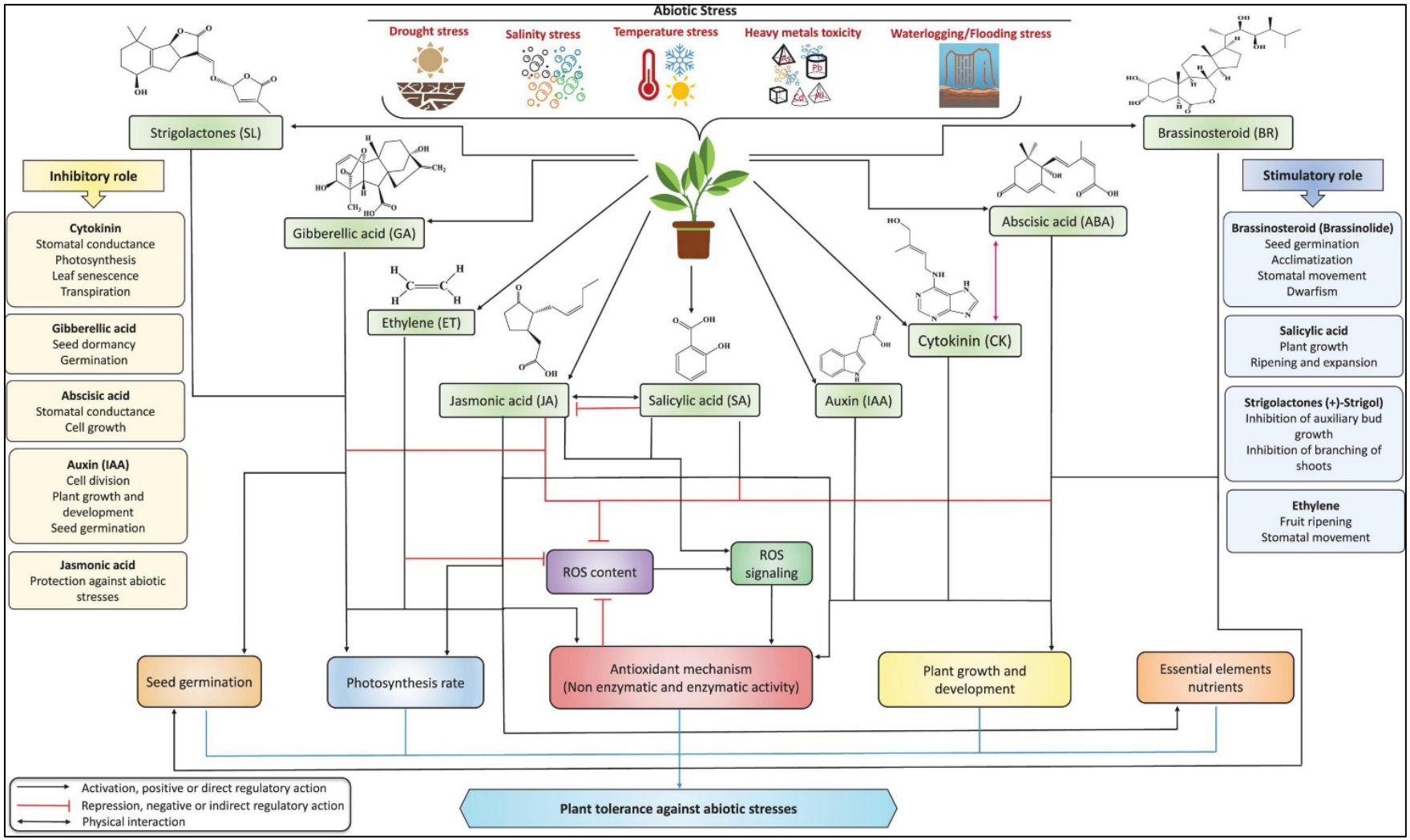
Abiotic Stress
Drought stress
Salinity stress
Temperature stress
Heavy metals toxicity
Waterlogging/Flooding stress
Strigolactones (SL)
Brassinosteroid (BR)
Inhibitory role
Stimulatory role
Cytokinin
Stomatal conductance
Photosynthesis
Leaf senescence
Transpiration
Gibberellic acid
Seed dormancy
Germination
Abscisic acid
Stomatal conductance
Cell growth
Auxin (IAA)
Cell division
Plant growth and development
Seed germination
Jasmonic acid
Protection against abiotic stresses
Gibberellic acid (GA)
Abscisic acid (ABA)
Ethylene (ET)
Cytokinin (CK)
Jasmonic acid (JA)
Salicylic acid (SA)
Auxin (IAA)
Brassinosteroid (Brassinolide)
Seed germination
Acclimatization
Stomatal movement
Dwarfism
Salicylic acid
Plant growth
Ripening and expansion
Strigolactones (+)-Strigol)
Inhibition of auxiliary bud growth
Inhibition of branching of shoots
Ethylene
Fruit ripening
Stomatal movement
ROS content
ROS signaling
Seed germination
Photosynthesis rate
Antioxidant mechanism
(Non enzymatic and enzymatic activity)
Plant growth and development
Essential elements nutrients
Activation, positive or direct regulatory action
Repression, negative or indirect regulatory action
Physical interaction
Plant tolerance against abiotic stresses

Figure 7.4.: The role of plant hormones in enhancing plant tolerance against multiple abiotic stresses is significant. Under stressful conditions, plant hormones can modulate stress intensity by activating defence mechanisms and regulating physiological and biochemical processes, thus increasing plant tolerance to environmental stress. Cytokinin's, gibberellins, abscisic acid, indole-3-acetic acid, and jasmonic acid primarily play inhibitory roles, while brassinosteroids, salicylic acid, strigolactones, and ethylene have stimulatory roles in improving various physiological and biochemical mechanisms under stress conditions. Abscisic acid, in particular, is a primary driving force, either acting alone or in combination with other hormones under stress. Additionally, cytokinins and auxin exhibit dual roles (both inhibitory and stimulatory) in regulating plant growth and development processes (Raza et al., 2022).

In plants under stress conditions, the management of ROS metabolism and signalling is crucial. Cellular ROS accumulation is regulated by three primary mechanisms: (1) ROS generation, (2) ROS scavenging, and (3) ROS transport. These mechanisms maintain ROS concentrations and create various ROS signatures and gradients, which act as signals in different abiotic stress-response signal transduction pathways. These redox regulations result in coordinated changes in the plant's physiology, metabolome, proteome, methylome, and transcriptome.

As can be seen from Fig. 7.4 there is a huge amount of hormonal cross talk and interaction between the systems that ROS govern. Plant hormones play a role in enhancing the activity of antioxidant defence systems, helping plants cope with stress. The interaction between ROS, antioxidants, and plant hormones, along with changes in metabolic networks, determine plant survival in stressful environments. Approaches using exogenous phytohormone supplementation can modulate gene expression and signalling pathways to improve stress tolerance in plants.

The roles of redox metabolism enzymes and metabolites are increasingly seen to extend beyond simple ROS-scavenging functions. They act as dedicated ROS signalling processors and are integral parts of a complex signalling system (Leister, 2019). The broader roles of ROS, particularly H_2O_2, under stress gained attention in the early 21st century. Researchers identified H_2O_2 as a signalling molecule that promotes acclimation progression and enhances tolerance to various environmental stresses (Khedia et al., 2019). Furthermore, ROS produced

in chloroplasts under stress may divert electrons from the photosynthetic apparatus, preventing related damage, and similarly protect mitochondria (Choudhury et al., 2017).

ROS can regulate plant metabolism under abiotic stress, activating redox responses that control the transcription and translation of stress acclimation proteins and enzymes, ultimately protecting plant cells from damage (Choudhury et al., 2017; Mittler, 2017; Mittler et al., 2022). H_2O_2 also modulates nitric oxide (NO) and Ca^{2+} signalling pathways, controlling plant growth, development, and other cellular and physiological responses (Niu and Liao, 2016; Singh et al., 2020). Importantly, when the balance between ROS production and ROS scavenging by the antioxidant defence system is disrupted, leading to ROS overproduction, it results in oxidative stress that causes molecular and cellular damage and ultimately cell death (Hasanuzzaman et al., 2020).

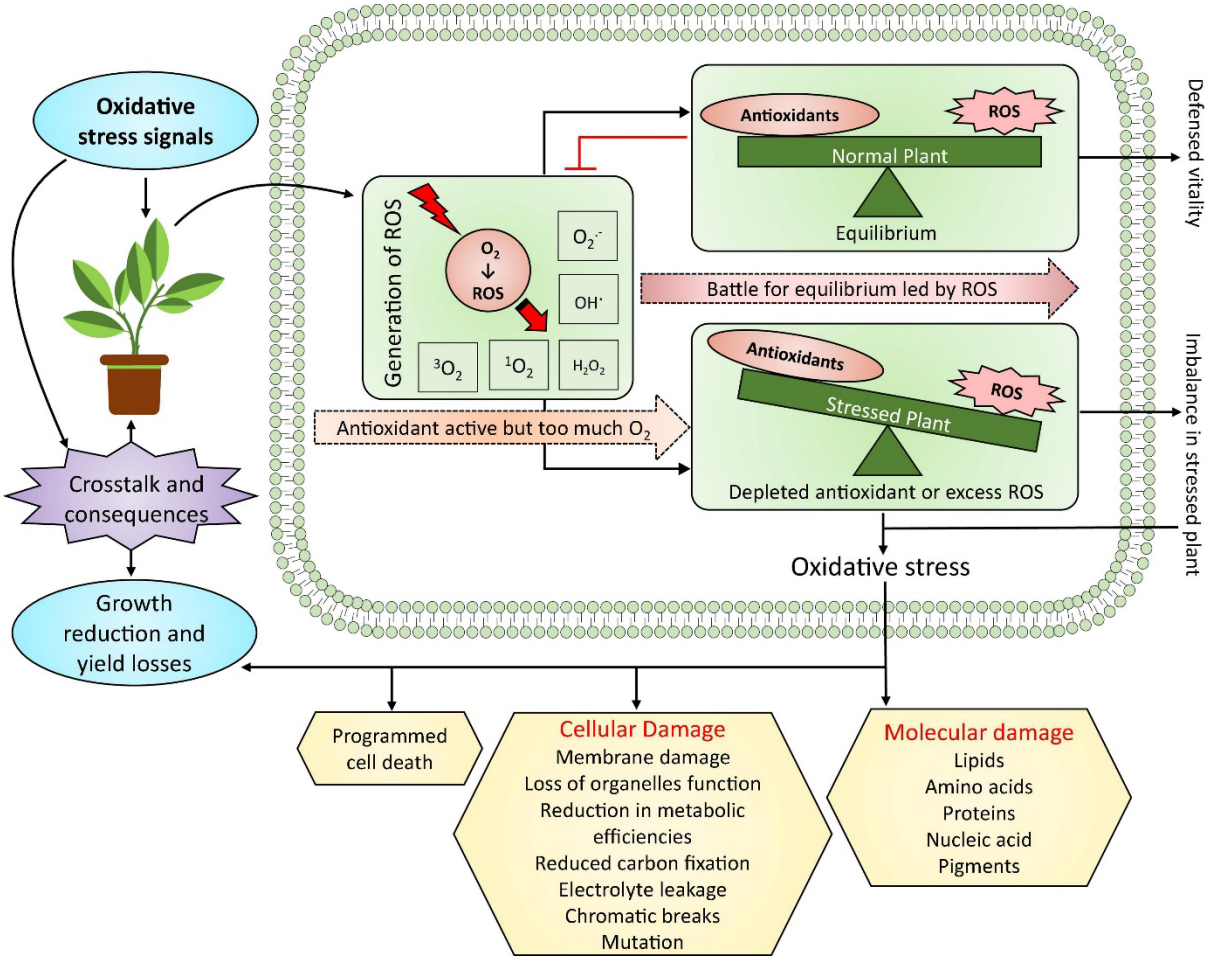

Figure 7.5. Diagrammatic representation of the ROS 'balancing act'. Oxidative stress in plants is a crucial aspect of their response to abiotic stress. It occurs when there is an imbalance between the generation of ROS and the plant's antioxidant defence system. This struggle for

equilibrium involves considerable crosstalk and consequences between stress signals and plant growth, ultimately impacting yield (Hasanuzzaman et al., 2020).

Under mild oxidative stress, ROS production can trigger adaptive responses that may improve growth and yield by activating defence mechanisms and promoting stress tolerance (Huang, 2019). However, when oxidative stress becomes severe, it can significantly reduce plant growth and yield. Excessive ROS accumulation can lead to molecular and cellular damage, disrupting various physiological processes, and potentially causing cell death.

This is the very balancing act the research in this thesis has observed under treatment of CuNPs. Where a resilient growth response can be observed up to as high as 40ul/ml, beyond this point the plant will struggle to handle the substantial dosage of CuNPs and enters the severe oxidative stress scenario depicted in Fig. 7.5. This will likely be dosage variable between different plant species and ages, but just like us every plant will have its tolerance limit.

7.6 Commercial Application and Phytoremediation Potential

While the work in this thesis has focused on the effect of CuNPs on the growth of plants there is potential to utilise their ability to uptake and sequester copper.

Copper consumption levels are projected to continue growing substantially this decade via the emerging market of electric vehicles and battery technology. The importance of its production and recycling in the creation of a sustainable economy is essential in order to meet this growing demand.

Contamination of land and waterways by heavy metals is a serious environmental problem (Dixit et al., 2015) particularly in areas of the UK where mineral mining was once widespread. This has had considerable long term consequences for the local landscape (Cooper et al., 2017) environment and ecology (Hyslop et al., 1997). However, if the polluting metal can be sequestered or collected via remediation techniques, the polluting metals can be reduced. Previous methods of doing this have focused on mechanical or chemical treatments, such as soil replacement, thermal desorption, membrane filtration, ion exchange, chemical precipitation, leaching, fixation or immobilisation (Dixit et al., 2015).

An emerging but potentially very valuable technique is bioremediation using either plants or bacteria to sequester metals. Many plants, bacteria and fungi have biological systems for the capture and detoxification of metals that are up taken into their cells. When plants sequester metals from soil, to reduce soil toxicity, the process is referred to as phytoremediation (Pivetz & Kovalick, 2001). Methods of phytoremediation include phytoextraction, phytostabilisation and Phytofiltration. Phytoextraction is a mechanism which results in metals being taken up and stored in the roots, and plants with rapid growth rates, substantial biomass and a complex root system are more commonly used in phytoextraction. Phytofiltration involves the roots and associated rhizosphere immobilising metals, leading to phytostabilisation, which effectively limits the possibility of metal mobility and bioavailability, so preventing migration into water systems and the local ecosystem (Karn et al., 2021).

The most popular plants used in previous studies include Indian mustard (*Brassica juncea*), the poplar tree (*Populus deltoides*) and willow tree (*Salix virminalis*). The research into phytoremediation is still in relatively nascent stages but could become one of the most sustainable tools in the creation of a circular economy and as a biological 'green' way of removing contaminating metals from polluted sites (Wuana & Okieimen, 2011). As evidenced in this thesis there is substantial uptake in willow tree, an organism used in growth experiments.

Collecting and retrieving bioactive metal nanoparticles (NPs) from up taken copper ions could have important commercial values e.g., copper NPs have diverse uses ranging from industrial catalysts to antimicrobials in food packaging (Llorens et al., 2012) or as part of the circular economy of a CuNP system to selectively inhibit the growth of plants.

7.7 Patent Search

A patent search was carried out to determine if any related products were already on the market - i.e. products related to nanoparticles and gelling agents as well as any products that exist on the market to clear roots from pipe systems and protect them from further ingress.

A search of currently used products and applications currently on the market:

1. RootX: RootX is a foaming root killer that is designed to kill roots in sewer lines and septic systems. It is a non-caustic, non-fumigating, and non-systemic product that is safe for use (its main activate ingredient is copper sulfate)

2. Copper sulfate: Copper sulfate is a chemical compound that is often used to control root growth in water pipes. It works by inhibiting cell division in plant roots, thereby preventing them from growing into the pipe.
3. Herbicidal foam: Herbicidal foam is a type of foam that is infused with herbicides designed to kill roots in water pipes. The foam is injected into the pipe and left to work for a period of time before being flushed out.
4. Pipe lining: Pipe lining is a process in which a new pipe is inserted into the existing water pipe, essentially creating a new pipe within the old one. This can help limit root growth by creating a smooth surface that is less hospitable to root growth.
5. Mechanical cutting: Mechanical cutting involves the use of tools such as root saws or augers to physically remove roots from the water pipe. This can be an effective method for removing large root masses, but may not be suitable for all types of pipes or root systems.

While all of these are products and techniques specifically related to removing or treating ingressing roots there is none that utilise nanoparticles or crosslinked gel agents, indicating that our technique is a novel one

A search of US Patents utilising keywords – 'water' 'nanoparticle' 'gel' revealed a significant number of nanogel based products but most focused on

1. US Patent 9,320,920 - Method for making a nanoparticle gel for use in water treatment: This patent describes a method for making a nanoparticle gel for use in water treatment. The gel is made by combining nanoparticles with a gelling agent and can be used to remove contaminants from water.
2. US Patent 9,050,126 - Nanoparticle hydrogel compositions for water treatment: This patent describes a nanoparticle hydrogel composition for use in water treatment. The hydrogel is made by combining nanoparticles with a hydrophilic polymer and can be used to remove heavy metals and other contaminants from water.
3. US Patent 10,180,324 - Antimicrobial nanoparticle gels for water treatment: This patent describes an antimicrobial nanoparticle gel for use in water treatment. The

gel is made by combining nanoparticles with a gelling agent and an antimicrobial agent and can be used to kill bacteria and other microorganisms in water.

4. US Patent 10,289,387 - Nanoparticle-enhanced gels for water treatment: This patent describes a nanoparticle-enhanced gel for use in water treatment. The gel is made by combining nanoparticles with a gelling agent and can be used to remove contaminants from water.
5. US Patent 10,785,441 - Nanoparticle-embedded hydrogels for water treatment: This patent describes a nanoparticle-embedded hydrogel for use in water treatment. The hydrogel is made by combining nanoparticles with a hydrophilic polymer and can be used to remove heavy metals and other contaminants from water.

The global nanotechnology market in water treatment is expected to grow at a compound annual growth rate (CAGR) of 17.1% from 2019 to 2025. So this does suggest a rapid growth in the industry and usage of crosslinked gels with nanoparticles, again though most of the patents found are related to water treatment in sewage plants and not as protective barriers to adhere to pipe systems (Khan et al., 2019).

7.8 Other Potential Gels

While there have been pros and cons to tested gels so far in this thesis and some have ticked boxes, they have not met all of the criteria required by the stakeholders of the project.

- Solvent free
- Adhere to wet surfaces
- Gel structure
- Ability to disperse and retain Copper NPs within them.
- 2-5 years effective life
- low cost
- Bio-based/sustainable
- Ability to crosslink

Epoxy/Amine based gelling or Organogels: Some of the benefits of utilising organogels include Stability: Organogels have high thermal and mechanical stability, which makes them useful for various applications where stability is important. Controlled release: Organogels can be designed to release active ingredients, such as drugs or nanoparticles at a controlled rate. Versatility: Organogels can be made from a wide range of organic liquids and gelling agents, which makes them a versatile material for various applications. Some of the potential drawbacks of using organogels include its Limited water solubility: Organogels are typically not soluble in water, which limits their use in certain applications (such as being utilised in water pipes). Limited biodegradability: Some organogels may not be biodegradable. Processing difficulties: Organogels can be difficult to process due to their high viscosity, which can require specialized equipment.

If such a gel were to be used it would need to itself be coated with a water soluble coating to package it further, as indicated in figure 6.20

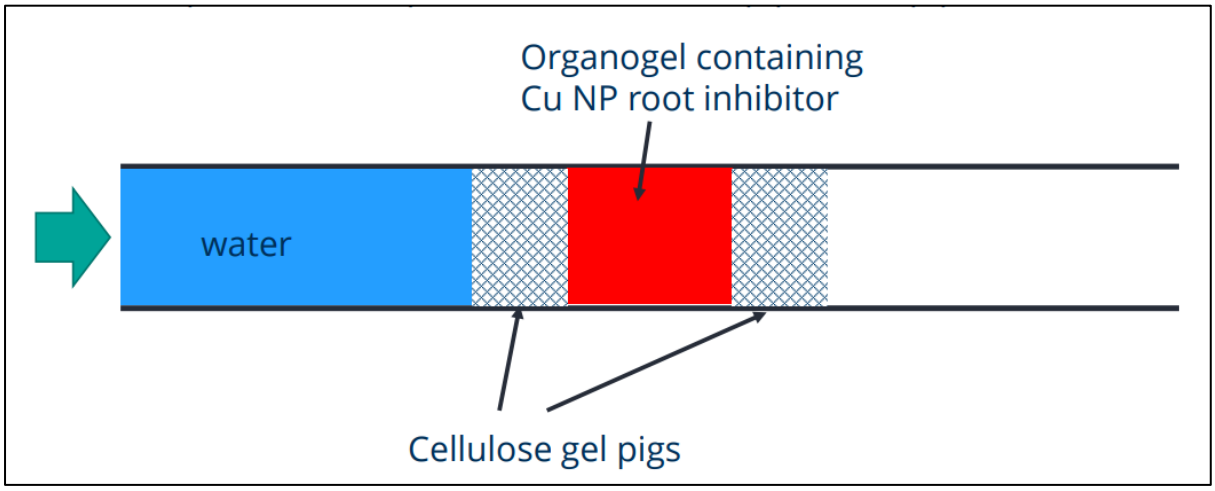

Figure 7.6 : figure of a potential organogel application indicating additional coating with cellulose gel pigs

The gel pig is designed to remove debris, wax, and other buildup from the inner walls of pipelines. It is propelled through the pipeline by the flow of the fluid inside the pipe, and as it moves, it scrubs the walls of the pipe, dislodging any buildup and carrying it along with it, they can be customized to fit different pipe diameters and configurations.

7.9 Future Work

7.9.1 Protein protein interactions (PPIs)

There were a lot of co- expressed or homologous expressed proteins and genes detected over the course of this research, and it would be interesting and provide much more insight into elucidating biological pathways, identifying the protein function. Understanding protein complex formation and exploring protein dynamics. can in the future be achieved using yeast two-hybrid, co-immunoprecipitation, pull-down assays, protein microarrays, fluorescence resonance energy transfer (FRET), and bioinformatics-based prediction methods. By leveraging these techniques to investigate PPIs, we could gain a deeper understanding of protein function, regulation, and their roles in these cellular processes.

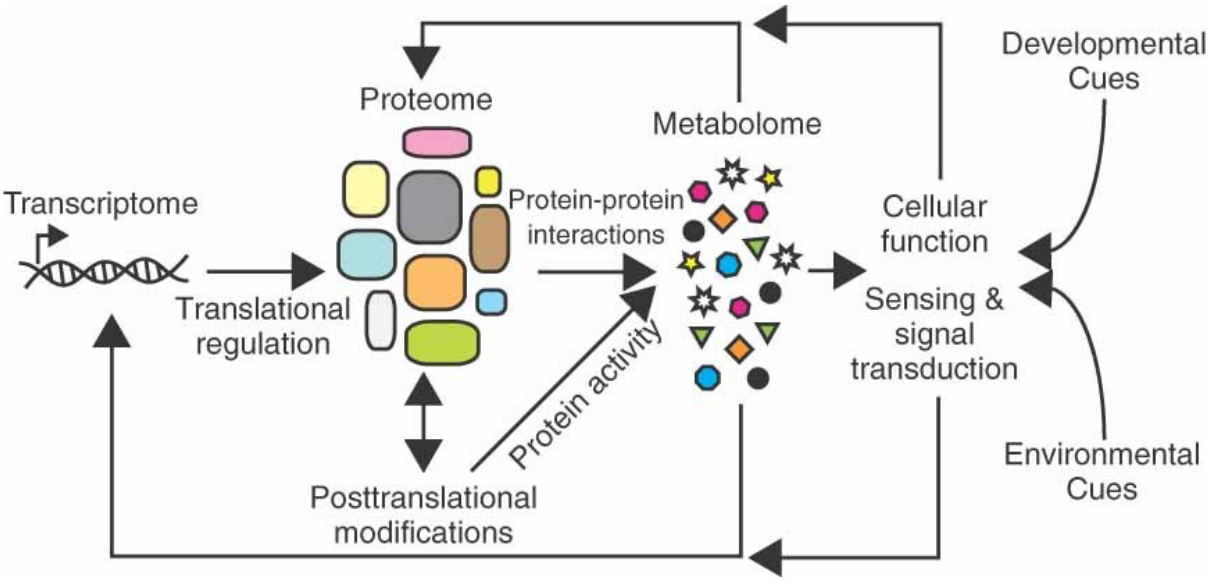

Figure 7.7: Diagram of systems biology interaction network – more work could be carried out on PPI, PTM and the metabolome for a more holistic approach.

7.9.2 Post translational modifications (PTMs)

While no major discrepancy in data between transcriptomic and proteomic data was found that does not mean they aren't there. It would be interesting to investigate the potential regulation occurring between the transcriptome and proteomic expression. Mass spectrometry (MS): MS is a powerful and widely used technique for identifying and characterizing PTMs. Protein samples are digested into peptides using specific proteases, and the resulting peptides are analysed by MS to determine their mass-to-charge ratios. Modified peptides can be identified based on the mass shift caused by the PTM. Some techniques that

could be utilised are Tandem mass spectrometry (MS/MS) which can provide further information on the modified peptides, including the specific site of modification.

Immunoprecipitation (IP) and co-immunoprecipitation (co-IP): IP and co-IP are techniques used to selectively isolate a specific protein or protein complex from a complex mixture. Using antibodies specific for a PTM, modified proteins can be enriched and subsequently analysed by western blotting or mass spectrometry to determine the presence and levels of the PTM.

Protein microarrays: Protein microarrays are high-throughput platforms that allow for the simultaneous analysis of multiple protein interactions, including PTMs. They can be used to study protein-protein, protein-nucleic acid, or protein-small molecule interactions, and can help identify substrates and binding partners of modified proteins.

Interesting candidate protein function could be further studied by the identification and characterization of mutants for the encoding genes, and their response to CuNPs and, potentially, other stresses, as was done for some genes/proteins in this thesis (Chapter 5).

7.9.3 Oxidation states of Cu

Not enough data was collected to establish the role and importance of oxidation states of Cu and CuNPs in this research., Copper predominantly exists in two oxidation states: Cu(I), or cuprous, and Cu (II), or cupric. The bioavailability of copper in these two oxidation states can vary, impacting its uptake and utilization by organisms.

Cuprous copper Cu(I) is a more soluble and bioavailable form of copper. It is the primary form of copper taken up by cells, as many transporters and binding proteins have a higher affinity for Cu(I) ions. Cupric copper Cu (II) is a less soluble form of copper and generally less bioavailable compared to Cu(I). However, it can still be taken up by cells and reduced to the Cu(I) state by specific cellular reductases before being utilized. In some cases, Cu (II) can form insoluble complexes with organic matter or other ions, further decreasing its bioavailability.

The bioavailability of copper in different oxidation states is influenced by other factors that weren't taken into account such as lower pH environments (higher Cu(II) solubility)(Sutton & Winterbourn, 1989). The presence of other ions such as zinc or iron can impact copper

bioavailability by competing for binding sites on transporters that uptake up proteins. There is significant redundancy in the heavy metal transport system (Prantner & Scholler, 2014).

7.9.4 Different kinds of nanoparticles

As evidenced earlier in the discussion and the introduction there is clearly a broad range of impacts that simply adjusting the parameters of the nanoparticles utilised can have on the end outcome for the plant response. This is something that could be further investigated, alongside further investigation of the microbiome and interactions here as this could have a long-term impact on any commercialisation attempt for these nanoparticles.

7.9.5 Scale up of gel experiments

Proving a system like this works on a small scale with Arabidopsis is useful but to truly test its commercial potential a viability trial would need to be carried out utilising waste water lines and commercial applicators of gels, samples to be taken and recorded via ICP-MS to determine leakage of CuNPs and uptake by surrounding plants.

7.10 Concluding Remarks

The use of CuNPs in enhancing plant growth and development is a promising area of research, but the effects of CuNPs on plants are highly dependent on their concentration, size, and surface chemistry. Excessive amounts of copper can be toxic to plants, leading to oxidative stress, membrane damage, and cell death. However, plants have developed a biological system to tolerate metal stress and other abiotic stresses for resiliency in their environment. This thesis has presented a potential model of hypothesized pathways resulting that are activated following from exposure to CuNPs, highlighting the importance of the plant's hormonal response to abiotic stress, phenylpropanoid biosynthesis, and direct and indirect interaction with the cytoskeleton. Further research and experiments are needed to elucidate these pathways fully. The size and morphology of nanoparticles have significant effects on their interactions with plants and microbes, and the bioavailability and reactivity of NPs depend on specific NP type, size, surface, charge, dose tested, and test media.

The proteomic and transcriptomic analysis revealed differential expression of proteins and genes involved in stress response and cellular signalling pathways. Additionally, the ability of willow tree to uptake up copper has also been demonstrated, suggesting its potential for use in phytoremediation.

The results of this study have important implications for understanding the environmental impacts of CuNPs and for developing strategies for their safe use. Further investigation of protein-protein interactions, post-translational modifications, oxidation states of Cu, and different kinds of nanoparticles (size and morphologies) as well as scaling up commercial gel crosslinking experiments, can provide valuable insights into the mechanisms underlying the impact of CuNPs on plant growth and development. Such insights can help in the development of sustainable methods for the remediation of polluted sites, as well as in the safe use of CuNPs in various industrial applications.

Bibliography

Adamowski, M., & Friml, J. (2015). PIN-dependent auxin transport: Action, regulation, and evolution. *Plant Cell*, *27*(1), 20–32. https://doi.org/10.1105/tpc.114.134874

Alexander, Ian. J., & Lee, S. S. (2005). Mycorrhizas and ecosystem processes in tropical rain forest: implications for diversity. In D. Burslem, M. Pinard, & S. Hartley (Eds.), *Biotic Interactions in the Tropics* (pp. 165–203). Cambridge University Press. https://doi.org/10.1017/CBO9780511541971.008

Alonso, J. M., Stepanova, A. N., Leisse, T. J., Kim, C. J., Chen, H., Shinn, P., Stevenson, D. K., Zimmerman, J., Barajas, P., Cheuk, R., Gadrinab, C., Heller, C., Jeske, A., Koesema, E., Meyers, C. C., Parker, H., Prednis, L., Ansari, Y., Choy, N., … Ecker, J. R. (2003). Genome-wide insertional mutagenesis of Arabidopsis thaliana. *Science*, *301*(5633), 653–657. https://doi.org/10.1126/science.1086391

Antisari, L. V., Carbone, S., Ferronato, C., Simoni, A., & Vianello, G. (2011). Characterization of heavy metals atmospheric deposition for assessment of urban environmental quality in the BOlogna CIty (ITALY). *EQA - International Journal of Environmental Quality*, *7*(7), 49–63. https://doi.org/10.6092/issn.2281-4485/3834

Arora, D., Jain, P., Singh, N., Kaur, H., & Bhatla, S. C. (2016). Mechanisms of nitric oxide crosstalk with reactive oxygen species scavenging enzymes during abiotic stress tolerance in plants. *Free Radical Research*, *50*(3), 291–303. https://doi.org/10.3109/10715762.2015.1118473

Aruoja, V., Dubourguier, H.-C., Kasemets, K., & Kahru, A. (2009). Toxicity of nanoparticles of CuO, ZnO and TiO2 to microalgae Pseudokirchneriella subcapitata. *Science of The Total Environment*, *407*(4), 1461–1468. https://doi.org/10.1016/j.scitotenv.2008.10.053

Asli, S., & Neumann, P. M. (2009). Colloidal suspensions of clay or titanium dioxide nanoparticles can inhibit leaf growth and transpiration via physical effects on root water transport. *Plant, Cell & Environment*, *32*(5), 577–584. https://doi.org/10.1111/J.1365-3040.2009.01952.X

Atha, D. H., Wang, H., Petersen, E. J., Cleveland, D., Holbrook, R. D., Jaruga, P., Dizdaroglu, M., Xing, B., & Nelson, B. C. (2012). Copper Oxide Nanoparticle Mediated DNA Damage in Terrestrial Plant Models. *Environmental Science & Technology*, *46*(3), 1819–1827. https://doi.org/10.1021/es202660k

Azmi, A. S., Uddin, M. H., & Mohammad, R. M. (2021). The nuclear export protein XPO1 - from biology to targeted therapy. *Nature Reviews. Clinical Oncology*, *18*(3), 152–169. https://doi.org/10.1038/S41571-020-00442-4

Barbez, E., Kubeš, M., Rolčík, J., Béziat, C., Pěnčík, A., Wang, B., Rosquete, M. R., Zhu, J., Dobrev, P. I., Lee, Y., Zažímalovà, E., Petrášek, J., Geisler, M., Friml, J., & Kleine-Vehn, J. (2012). A novel putative auxin carrier family regulates intracellular auxin homeostasis in plants. *Nature*, *485*(7396), 119–122. https://doi.org/10.1038/NATURE11001

Bartlett, R. E. (1979). *Public health engineering, sewerage*. Applied Science Publishers.

Baxter, S. S. (1958). Subsurface problems of trees and utility structures. *Trees Magazine*, *19*, 7–8.

Belousov, V. V., Fradkov, A. F., Lukyanov, K. A., Staroverov, D. B., Shakhbazov, K. S., Terskikh, A. V., & Lukyanov, S. (2006). Genetically encoded fluorescent indicator for intracellular hydrogen peroxide. *Nature Methods*, *3*(4), 281–286. https://doi.org/10.1038/nmeth866

Benková, E., Michniewicz, M., Sauer, M., Teichmann, T., Seifertová, D., Jürgens, G., & Friml, J. (2003). Local, Efflux-Dependent Auxin Gradients as a Common Module for Plant Organ Formation. *Cell*, *115*(5), 591–602. https://doi.org/10.1016/S0092-8674(03)00924-3

Bhawana, Basniwal, R. K., Buttar, H. S., Jain, V. K., & Jain, N. (2011). Curcumin nanoparticles: preparation, characterization, and antimicrobial study. *Journal of Agricultural and Food Chemistry*, *59*(5), 2056–2061. https://doi.org/10.1021/JF104402T

Birhanu Kitata, R., Yang, J.-C., Chen, Y.-J., & Yu-Ju Chen, C. (2022). *Advances in data-independent acquisition mass spectrometry towards comprehensive digital proteome landscape*. https://doi.org/10.1002/mas.21781

Brennan, G., Patch, D., Revised, S., Johnson, P., & Marshall, D. J. (1997). *Arboriculture Research Note Issued by the Arboricultural Advisory & Information Service Tree Roots and Underground Pipes*.

Brennan, G., Patch,D. Stevens, FR. W. (1997). Tree Roots and underground Pipes. *Arboriculture Research*, *Note No 36*.

Burda, C., Chen, X., Narayanan, R., & El-Sayed, M. A. (2005). Chemistry and Properties of Nanocrystals of Different Shapes. *Chemical Reviews*, *105*(4), 1025–1102. https://doi.org/10.1021/cr030063a

Burden, N., Aschberger, K., Chaudhry, Q., Clift, M. J. D., Fowler, P., Johnston, H., Landsiedel, R., Rowland, J., Stone, V., & Doak, S. H. (2017). Aligning nanotoxicology with the 3Rs: What is needed to realise the short, medium and long-term opportunities? *Regulatory Toxicology and Pharmacology : RTP*, *91*, 257–266. https://doi.org/10.1016/J.YRTPH.2017.10.021

Cataldo, D. A., & Wildung, R. E. (1978). Soil and plant factors influencing the accumulation of heavy metals by plants. *Environmental Health Perspectives*, *27*, 149–159. https://doi.org/10.1289/ehp.7827149

Celeghini, E. C. C., Alves, M. B. R., de Arruda, R. P., de Rezende, G. M., Florez-Rodriguez, S. A., & de Sá Filho, M. F. (2021). Efficiency of CellROX deep red® and CellROX orange® fluorescent probes in identifying reactive oxygen species in sperm samples from high and low fertility bulls. *Animal Biotechnology*, *32*(1), 77–83. https://doi.org/10.1080/10495398.2019.1654485

Chae, K., & Lord, E. M. (2011). Pollen tube growth and guidance: roles of small, secreted proteins. *Annals of Botany*, *108*(4), 627–636. https://doi.org/10.1093/aob/mcr015

Chandler, J. W. (2009). Local auxin production: a small contribution to a big field. *BioEssays*, *31*(1), 60–70. https://doi.org/10.1002/BIES.080146

Chivasa, S., Ndimba, B. K., Simon, W. J., Lindsey, K., & Slabas, A. R. (2005). Extracellular ATP functions as an endogenous external metabolite regulating plant cell viability. *Plant Cell*, *17*(11), 3019–3034. https://doi.org/10.1105/tpc.105.036806

Cloonan, N., Forrest, A. R. R., Kolle, G., Gardiner, B. B. A., Faulkner, G. J., Brown, M. K., Taylor, D. F., Steptoe, A. L., Wani, S., Bethel, G., Robertson, A. J., Perkins, A. C., Bruce, S. J., Lee, C. C., Ranade, S. S., Peckham, H. E., Manning, J. M., McKernan, K. J., & Grimmond, S. M. (2008). Stem cell

transcriptome profiling via massive-scale mRNA sequencing. *Nature Methods 2008 5:7*, *5*(7), 613–619. https://doi.org/10.1038/nmeth.1223

Conn, S. J., Hocking, B., Dayod, M., Xu, B., Athman, A., Henderson, S., Aukett, L., Conn, V., Shearer, M. K., Fuentes, S., Tyerman, S. D., & Gilliham, M. (2013). *Protocol: optimising hydroponic growth systems for nutritional and physiological analysis of Arabidopsis thaliana and other plants*. https://doi.org/10.1186/1746-4811-9-4

Cooper, N., Benson, N., McNeill, A., & Siddle, R. (2017). Changing coastlines in NE England: a legacy of colliery spoil tipping and the effects of its cessation. *Proceedings of the Yorkshire Geological Society*, *61*(3), 217–229. https://doi.org/10.1144/PYGS2016-369

Cox, A., Venkatachalam, P., Sahi, S., & Sharma, N. (2016). Silver and titanium dioxide nanoparticle toxicity in plants: A review of current research. *Plant Physiology and Biochemistry*, *107*, 147–163. https://doi.org/10.1016/J.PLAPHY.2016.05.022

Cutler, D. F. (David F., & Richardson, I. B. K. (1989). *Tree roots and buildings*. Longman Scientific & Technical.

DAB-Peroxidase Substrate Solution (Brown) | Protocols Online. (n.d.). Retrieved April 7, 2020, from https://www.protocolsonline.com/histology/immunohistochemistry-histology/dab-peroxidase-substrate-solution-brown/

Darwin, C. (1898). *The Power of Movement in Plants*.

Daudi, A., & O'Brien, J. (2012). Detection of Hydrogen Peroxide by DAB Staining in Arabidopsis Leaves. *Bio-Protocol*, *2*(18). https://doi.org/10.21769/bioprotoc.263

Davidson, P. (1999). WRC: Getting to the root of the problem. *Swindon UK*.

de Dorlodot, S., Forster, B., Pagès, L., Price, A., Tuberosa, R., & Draye, X. (2007). Root system architecture: opportunities and constraints for genetic improvement of crops. *Trends in Plant Science*, *12*(10), 474–481. https://doi.org/10.1016/j.tplants.2007.08.012

De Smet, I., Vassileva, V., De Rybel, B., Levesque, M. P., Grunewald, W., Van Damme, D., Van Noorden, G., Naudts, M., Van Isterdael, G., De Clercq, R., Wang, J. Y., Meuli, N., Vanneste, S., Friml, J., Hilson, P., Jurgens, G., Ingram, G. C., Inze, D., Benfey, P. N., & Beeckman, T. (2008). Receptor-Like Kinase ACR4 Restricts Formative Cell Divisions in the Arabidopsis Root. *Science*, *322*(5901), 594–597. https://doi.org/10.1126/science.1160158

De Smet, S., Cuypers, A., Vangronsveld, J., & Remans, T. (2015). Gene Networks Involved in Hormonal Control of Root Development in Arabidopsis thaliana: A Framework for Studying its Disturbance by Metal Stress. In *International Journal of Molecular Sciences* (Vol. 16, Issue 8, pp. 19195–19224). MDPI AG. https://doi.org/10.3390/ijms160819195

del Cueto, J., Møller, B. L., Dicenta, F., & Sánchez-Pérez, R. (2018). β-Glucosidase activity in almond seeds. *Plant Physiology and Biochemistry : PPB*, *126*, 163–172. https://doi.org/10.1016/J.PLAPHY.2017.12.028

Deutsche Forschungsgemeinschaft. Kommission zur Prüfung Gesundheitsschädlicher Arbeitsstoffe. (n.d.). *Nanomaterials*.

Dias, M. C., Pinto, D. C. G. A., & Silva, A. M. S. (2021). Plant Flavonoids: Chemical Characteristics and Biological Activity. *Molecules (Basel, Switzerland)*, *26*(17). https://doi.org/10.3390/molecules26175377

Dietz, K. J., Turkan, I., & Krieger-Liszkay, A. (2016). Redox- and reactive oxygen species-dependent signaling into and out of the photosynthesizing chloroplast. *Plant Physiology*, *171*(3), 1541–1550. https://doi.org/10.1104/pp.16.00375

Dimkpa, C. O. (2014). Can nanotechnology deliver the promised benefits without negatively impacting soil microbial life? *Journal of Basic Microbiology*, *54*(9), 889–904. https://doi.org/10.1002/jobm.201400298

Dimkpa, C. O., Latta, D. E., McLean, J. E., Britt, D. W., Boyanov, M. I., & Anderson, A. J. (2013). Fate of CuO and ZnO Nano- and Microparticles in the Plant Environment. *Environmental Science & Technology*, *47*(9), 4734–4742. https://doi.org/10.1021/es304736y

Dimkpa, C. O., Mclean, J. E., Britt, D. W., & Anderson, A. J. (2012). CuO and ZnO nanoparticles differently affect the secretion of fluorescent siderophores in the beneficial root colonizer, *Pseudomonas chlororaphis* O6. *Nanotoxicology*, *6*(6), 635–642. https://doi.org/10.3109/17435390.2011.598246

Dimkpa, C. O., Zeng, J., McLean, J. E., Britt, D. W., Zhan, J., & Anderson, A. J. (2012). Production of Indole-3-Acetic Acid via the Indole-3-Acetamide Pathway in the Plant-Beneficial Bacterium Pseudomonas chlororaphis O6 Is Inhibited by ZnO Nanoparticles but Enhanced by CuO Nanoparticles. *Applied and Environmental Microbiology*, *78*(5), 1404–1410. https://doi.org/10.1128/AEM.07424-11

Dixit, R., Wasiullah, Malaviya, D., Pandiyan, K., Singh, U. B., Sahu, A., Shukla, R., Singh, B. P., Rai, J. P., Sharma, P. K., Lade, H., & Paul, D. (2015). Bioremediation of Heavy Metals from Soil and Aquatic Environment: An Overview of Principles and Criteria of Fundamental Processes. *Sustainability 2015, Vol. 7, Pages 2189-2212*, *7*(2), 2189–2212. https://doi.org/10.3390/SU7022189

Dolan, L., Janmaat, K., Willemsen, V., Linstead, P., Poethig, S., Roberts, K., & Scheres, B. (1993). Cellular organisation of the Arabidopsis thaliana root. *Undefined*.

Dolan, L., & Roberts, K. (1995). The development of cell pattern in the root epidermis. In *Philosophical transactions of the Royal Society of London. Series B, Biological sciences* (Vol. 350, Issue 1331, pp. 95–99). https://doi.org/10.1098/rstb.1995.0143

Dong, J., Kim, S. T., & Lord, E. M. (2005). Plantacyanin plays a role in reproduction in Arabidopsis. *Plant Physiology*, *138*(2), 778–789. https://doi.org/10.1104/PP.105.063388

Douglas D. Drury and James M. Montgomery. (n.d.). *Operation and Maintenance of Wastewater Collection and Treatment Facilities on JSTOR*.

Du, M., Spalding, E. P., & Gray, W. M. (2020). Rapid Auxin-Mediated Cell Expansion. *Annual Review of Plant Biology*, *71*, 379–402. https://doi.org/10.1146/ANNUREV-ARPLANT-073019-025907

Duarte-Conde, J. A., Sans-Coll, G., & Merchante, C. (2022). RNA-binding proteins and their role in translational regulation in plants. *Essays in Biochemistry*, *66*(2), 87–97. https://doi.org/10.1042/EBC20210069

Dubois, M., Van den Broeck, L., & Inzé, D. (2018a). The Pivotal Role of Ethylene in Plant Growth. *Trends in Plant Science*, *23*(4), 311–323. https://doi.org/10.1016/j.tplants.2018.01.003

Dubois, M., Van den Broeck, L., & Inzé, D. (2018b). The Pivotal Role of Ethylene in Plant Growth. *Trends in Plant Science*, *23*(4), 311–323. https://doi.org/10.1016/j.tplants.2018.01.003

Dubrovsky, J. G., Doerner, P. W., Colón-Carmona, A., & Rost, T. L. (2000). Pericycle cell proliferation and lateral root initiation in Arabidopsis. *Plant Physiology*, *124*(4), 1648–1657. https://doi.org/10.1104/pp.124.4.1648

Duszyn, M., Świeżawska, B., Szmidt-Jaworska, A., & Jaworski, K. (2019). Cyclic nucleotide gated channels (CNGCs) in plant signalling—Current knowledge and perspectives. *Journal of Plant Physiology*, *241*, 153035. https://doi.org/10.1016/J.JPLPH.2019.153035

Edwards, K., Johnstone, C., & Thompson, C. (n.d.). A simple and rapid method for the preparation of plant genomic DNA for PCR analysis. In *Nucleic Acids Research* (Vol. 19, Issue 6).

Eichholz, S., Lerch, M., Heck, M., & Walter, D. (n.d.). *Various carbon dust particles Studies on thermal behaviour*. https://doi.org/10.1007/s10973-011-2188-z

El-Temsah, Y. S., & Joner, E. J. (2012). Impact of Fe and Ag nanoparticles on seed germination and differences in bioavailability during exposure in aqueous suspension and soil. *Environmental Toxicology*, *27*(1), 42–49. https://doi.org/10.1002/tox.20610

Eurasian Arabidopsis Stock Centre (uNASC). (n.d.). Retrieved September 19, 2019, from http://arabidopsis.info/

Exposito-Rodriguez, M., Laissue, P. P., Yvon-Durocher, G., Smirnoff, N., & Mullineaux, P. M. (2017). Photosynthesis-dependent H(2)O(2) transfer from chloroplasts to nuclei provides a high-light signalling mechanism. *Nature Communications*, *8*(1), 49. https://doi.org/10.1038/s41467-017-00074-w

Festa, R. A., & Thiele, D. J. (2011). Copper: an Essential Metal in Biology. *Current Biology : CB*, *21*(21), R877. https://doi.org/10.1016/J.CUB.2011.09.040

Fryer, M. J., Oxborough, K., Mullineaux, P. M., & Baker, N. R. (2002). Imaging of photo-oxidative stress responses in leaves. *Journal of Experimental Botany*, *53*(372), 1249–1254. https://doi.org/10.1093/jexbot/53.372.1249

Galvan-Ampudia, C. S., & Testerink, C. (2011). Salt stress signals shape the plant root. *Current Opinion in Plant Biology*, *14*(3), 296–302. https://doi.org/10.1016/J.PBI.2011.03.019

García-Sánchez, S., Bernales, I., & Cristobal, S. (2015). Early response to nanoparticles in the Arabidopsis transcriptome compromises plant defence and root-hair development through salicylic acid signalling. *BMC Genomics*, *16*(1), 341. https://doi.org/10.1186/S12864-015-1530-4

Gasson, P. E., & Cutler, D. F. (1998). CAN WE LIVE WITH TREES IN OUR TOWNS AND CITIES? *Arboricultural Journal*, *22*(1), 1–9. https://doi.org/10.1080/03071375.1998.9747188

Geisler-Lee, J., Wang, Q., Yao, Y., Zhang, W., Geisler, M., Li, K., Huang, Y., Chen, Y., Kolmakov, A., & Ma, X. (2012). Phytotoxicity, accumulation and transport of silver nanoparticles by *Arabidopsis thaliana*. *Nanotoxicology*, *7*(3), 323–337. https://doi.org/10.3109/17435390.2012.658094

Geisler-Lee, J., Wang, Q., Yao, Y., Zhang, W., Geisler, M., Li, K., Huang, Y., Chen, Y., Kolmakov, A., & Ma, X. (2013a). Phytotoxicity, accumulation and transport of silver nanoparticles by Arabidopsis thaliana. *Nanotoxicology*, *7*(3), 323–337. https://doi.org/10.3109/17435390.2012.658094

Geisler-Lee, J., Wang, Q., Yao, Y., Zhang, W., Geisler, M., Li, K., Huang, Y., Chen, Y., Kolmakov, A., & Ma, X. (2013b). Phytotoxicity, accumulation and transport of silver nanoparticles by Arabidopsis thaliana. *Nanotoxicology*, *7*(3), 323–337. https://doi.org/10.3109/17435390.2012.658094

Geyer, J. C., & Lentz, J. J. (1966). An evaluation of the problems of sanitary sewer system design. *Journal - Water Pollution Control Federation*, *38*(7), 1138–1147.

Ghatak, A., Chaturvedi, P., Waldherr, S., Subbarao, G. V., & Weckwerth, W. (2023). PANOMICS at the interface of root–soil microbiome and BNI. *Trends in Plant Science*, *28*(1), 106–122. https://doi.org/10.1016/J.TPLANTS.2022.08.016

Giehl, R. F. H., Gruber, B. D., & von Wirén, N. (2014). It's time to make changes: modulation of root system architecture by nutrient signals. *Journal of Experimental Botany*, *65*(3), 769–778. https://doi.org/10.1093/jxb/ert421

Govender, N. T., Mahmood, M., Seman, I. A., & Wong, M. Y. (2017). The Phenylpropanoid Pathway and Lignin in Defense against Ganoderma boninense Colonized Root Tissues in Oil Palm (Elaeis guineensis Jacq.). *Frontiers in Plant Science*, *8*. https://doi.org/10.3389/FPLS.2017.01395

Haber, Z., Lampl, N., Meyer, A. J., Zelinger, E., Hipsch, M., & Rosenwasser, S. (2021). Resolving diurnal dynamics of the chloroplastic glutathione redox state in Arabidopsis reveals its photosynthetically derived oxidation. *The Plant Cell*, *33*(5), 1828–1844. https://doi.org/10.1093/plcell/koab068

Halbeisen, R. E., Galgano, A., Scherrer, T., & Gerber, A. P. (2008). Post-transcriptional gene regulation: from genome-wide studies to principles. *Cellular and Molecular Life Sciences : CMLS*, *65*(5), 798–813. https://doi.org/10.1007/S00018-007-7447-6

Halliwell, B., & Gutteridge, J. M. C. (2015). *Free Radicals in Biology and Medicine*. Oxford University Press. https://doi.org/10.1093/acprof:oso/9780198717478.001.0001

Harris, R. W., Clark, J. R., Matheny, N. P., & Harris, V. M. (2004). *Arboriculture : integrated management of landscape trees, shrubs, and vines*. Prentice Hall.

Hasanuzzaman, M., Bhuyan, M. H. M. B., Raza, A., Hawrylak-Nowak, B., Matraszek-Gawron, R., Mahmud, J. Al, Nahar, K., & Fujita, M. (2020). Selenium in plants: Boon or bane? *Environmental and Experimental Botany*, *178*, 104170. https://doi.org/10.1016/J.ENVEXPBOT.2020.104170

Heale, E. L., & Ormrod, D. P. (1982). Effects of nickel and copper on *Acer rubrum, Cornus stolonifera, Lonicera tatarica* , and *Pinus resinosa*. *Canadian Journal of Botany*, *60*(12), 2674–2681. https://doi.org/10.1139/b82-325

Hernández-Barrera, A., Velarde-Buendía, A., Zepeda, I., Sanchez, F., Quinto, C., Sánchez-Lopez, R., Cheung, A., Wu, H.-M., & Cardenas, L. (2015). Hyper, a Hydrogen Peroxide Sensor, Indicates the Sensitivity of the Arabidopsis Root Elongation Zone to Aluminum Treatment. *Sensors*, *15*(1), 855–867. https://doi.org/10.3390/s150100855

Hipsch, M., Lampl, N., Zelinger, E., Barda, O., Waiger, D., & Rosenwasser, S. (2021). Sensing stress responses in potato with whole-plant redox imaging. *Plant Physiology*, *187*(2), 618–631. https://doi.org/10.1093/plphys/kiab159

Honys, D., Twell, D., Hennig, L., & Gruissem, W. (2003). Comparative analysis of the Arabidopsis pollen transcriptome. *Plant Physiology*, *132*(2), 640–652. https://doi.org/10.1104/pp.103.020925

Huang, H., Ullah, F., Zhou, D. X., Yi, M., & Zhao, Y. (2019). Mechanisms of ROS regulation of plant development and stress responses. In *Frontiers in Plant Science* (Vol. 10, p. 800). Frontiers Media S.A. https://doi.org/10.3389/fpls.2019.00800

Huang, S., Van Aken, O., Schwarzländer, M., Belt, K., & Millar, A. H. (2016). The roles of mitochondrial reactive oxygen species in cellular signaling and stress response in plants. *Plant Physiology*, *171*(3), 1551–1559. https://doi.org/10.1104/pp.16.00166

Hulsen, T., de Vlieg, J., & Alkema, W. (2008). BioVenn - a web application for the comparison and visualization of biological lists using area-proportional Venn diagrams. *BMC Genomics*, *9*, 488. https://doi.org/10.1186/1471-2164-9-488

Hunt, W. F., & Mineralogical Society of America. (1967). The American mineralogist. In *American Mineralogist* (Vol. 52, Issues 11–12). Mineralogical Society of America.

Huxley, J. S. (1935). Chemical regulation and the hormone concept. *Biological Reviews*, *10*(4), 427–441. https://doi.org/10.1111/j.1469-185X.1935.tb00491.x

Hyslop, B. T., Davies, M. S., Arthur, W., Gazey, N. J., & Holroyd, S. (1997). Effects of colliery waste on littoral communities in north-east England. *Environmental Pollution*, *96*(3), 383–400. https://doi.org/10.1016/S0269-7491(97)00039-0

Jafari-Raddani, F., Davoodi-Moghaddam, Z., Yousefi, A.-M., Ghaffari, S. H., & Bashash, D. (2022). An overview of long noncoding RNAs: Biology, functions, therapeutics, analysis methods, and bioinformatics tools. *Cell Biochemistry and Function*, *40*(8), 800–825. https://doi.org/10.1002/cbf.3748

Jefferson, R. A., Kavanagh, T. A., & Bevan, M. W. (1987). GUS fusions: beta-glucuronidase as a sensitive and versatile gene fusion marker in higher plants. *The EMBO Journal*, *6*(13), 3901–3907. http://www.ncbi.nlm.nih.gov/pubmed/3327686

Jia, H., Chen, S., Wang, X., Shi, C., Liu, K., Zhang, S., & Li, J. (2020). Copper oxide nanoparticles alter cellular morphology via disturbing the actin cytoskeleton dynamics in Arabidopsis roots. *Nanotoxicology*, *14*(1), 127–144. https://doi.org/10.1080/17435390.2019.1678693

John W. Groninger. (1997). *(PDF) Herbicides to control tree roots in sewer lines*. https://www.researchgate.net/publication/238752911_Herbicides_to_control_tree_roots_in_sewer_lines

Jungk, A. (1993). Kutschera, L., E. Lichtenegger, M. Sobotik: Wurzelatlas mitteleuropäischer Grünlandpflanzen. Band 2: Pteridophyta und Dicotyledoneae (Magnoliopsida). Teil 1: Von L. Kutschera und E. Lichtenegger: Morphologie, Anatomie, Ökologie, Verbreitung, Soziologie, Wirtschaft; mit 851 S., 364 Abb., 137 z. T. farb. Taf. Verlag Gustav Fischer 1992; Preis Ln. DM 390, 00. *Zeitschrift Für Pflanzenernährung Und Bodenkunde*, *156*(1), 97–97. https://doi.org/10.1002/jpln.19931560118

Kaksonen, M., & Roux, A. (2018). Mechanisms of clathrin-mediated endocytosis. *Nature Reviews. Molecular Cell Biology*, *19*(5), 313–326. https://doi.org/10.1038/NRM.2017.132

Karn, R., Ojha, N., Abbas, S., & Bhugra, S. (2021). A review on heavy metal contamination at mining sites and remedial techniques. *IOP Conference Series: Earth and Environmental Science*, *796*(1), 012013. https://doi.org/10.1088/1755-1315/796/1/012013

Kato, H., Suzuki, M., Fujita, K., Horie, M., Endoh, S., Yoshida, Y., Iwahashi, H., Takahashi, K., Nakamura, A., & Kinugasa, S. (2009a). Reliable size determination of nanoparticles using dynamic light scattering method for in vitro toxicology assessment. *Toxicology in Vitro*, *23*(5), 927–934. https://doi.org/10.1016/J.TIV.2009.04.006

Kato, H., Suzuki, M., Fujita, K., Horie, M., Endoh, S., Yoshida, Y., Iwahashi, H., Takahashi, K., Nakamura, A., & Kinugasa, S. (2009b). Reliable size determination of nanoparticles using dynamic light scattering method for in vitro toxicology assessment. *Toxicology in Vitro*, *23*(5), 927–934. https://doi.org/10.1016/J.TIV.2009.04.006

Kaul, S., Koo, H. L., Jenkins, J., Rizzo, M., Rooney, T., Tallon, L. J., Feldblyum, T., Nierman, W., Benito, M. I., Lin, X., Town, C. D., Venter, J. C., Fraser, C. M., Tabata, S., Nakamura, Y., Kaneko, T., Sato, S., Asamizu, E., Kato, T., … Somerville, C. (2000). Analysis of the genome sequence of the flowering plant Arabidopsis thaliana. *Nature*, *408*(6814), 796–815. https://doi.org/10.1038/35048692

Kaveh, R., Li, Y.-S., Ranjbar, S., Tehrani, R., Brueck, C. L., & Van Aken, B. (2013). Changes in *Arabidopsis thaliana* Gene Expression in Response to Silver Nanoparticles and Silver Ions. *Environmental Science & Technology*, *47*(18), 10637–10644. https://doi.org/10.1021/es402209w

KEGG PATHWAY Database. (n.d.). Retrieved January 27, 2023, from https://www.kegg.jp/kegg/pathway.html

Kelen, K. van der, Beyaert, R., Inzé, D., & Veylder, L. de. (2009). Translational control of eukaryotic gene expression. *Critical Reviews in Biochemistry and Molecular Biology*, *44*(4), 143–168. https://doi.org/10.1080/10409230902882090

Kellermeier, F., Armengaud, P., Seditas, T. J., Danku, J., Salt, D. E., & Amtmann, A. (2014). Analysis of the root system architecture of Arabidopsis provides a quantitative readout of crosstalk between nutritional signals. *Plant Cell*, *26*(4), 1480–1496. https://doi.org/10.1105/tpc.113.122101

Khan, I., Saeed, K., & Khan, I. (2019). Nanoparticles: Properties, applications and toxicities. *Arabian Journal of Chemistry*, *12*(7), 908–931. https://doi.org/10.1016/J.ARABJC.2017.05.011

Khan, J. M., Malik, A., Ahmed, M. Z., & Ahmed, A. (2022). SDS modulates amyloid fibril formation and conformational change in succinyl-ConA at low pH. *Spectrochimica Acta. Part A, Molecular and Biomolecular Spectroscopy*, *267*(Pt 1). https://doi.org/10.1016/J.SAA.2021.120494

Kiba, T., & Krapp, A. (2016). Plant Nitrogen Acquisition Under Low Availability: Regulation of Uptake and Root Architecture. *Plant & Cell Physiology*, *57*(4), 707–714. https://doi.org/10.1093/pcp/pcw052

Kim, D., Pertea, G., Trapnell, C., Pimentel, H., Kelley, R., & Salzberg, S. L. (2013). TopHat2: Accurate alignment of transcriptomes in the presence of insertions, deletions and gene fusions. *Genome Biology*, *14*(4), R36. https://doi.org/10.1186/gb-2013-14-4-r36

Kim, S., Lee, S., & Lee, I. (2012). Alteration of Phytotoxicity and Oxidant Stress Potential by Metal Oxide Nanoparticles in Cucumis sativus. *Water, Air, & Soil Pollution*, *223*(5), 2799–2806. https://doi.org/10.1007/s11270-011-1067-3

Kim, S., Mollet, J. C., Dong, J., Zhang, K., Park, S. Y., & Lord, E. M. (2003a). Chemocyanin, a small basic protein from the lily stigma, induces pollen tube chemotropism. *Proceedings of the National*

Academy of Sciences of the United States of America, *100*(26), 16125–16130. https://doi.org/10.1073/pnas.2533800100

Kim, S., Mollet, J.-C., Dong, J., Zhang, K., Park, S.-Y., & Lord, E. M. (2003b). Chemocyanin, a small basic protein from the lily stigma, induces pollen tube chemotropism. *Proceedings of the National Academy of Sciences*, *100*(26), 16125–16130. https://doi.org/10.1073/pnas.2533800100

Kochian, L. V. (2016). Root architecture. *Journal of Integrative Plant Biology*, *58*(3), 190–192. https://doi.org/10.1111/jipb.12471

Kolli, R., Soll, J., & Carrie, C. (2018). Plant mitochondrial inner membrane protein insertion. *International Journal of Molecular Sciences*, *19*(2). https://doi.org/10.3390/ijms19020641

Křeček, P., Skůpa, P., Libus, J., Naramoto, S., Tejos, R., Friml, J., & Zažímalová, E. (2009). The PIN-FORMED (PIN) protein family of auxin transporters. *Genome Biology*, *10*(12), 249. https://doi.org/10.1186/gb-2009-10-12-249

Kumari, M., Mukherjee, A., & Chandrasekaran, N. (2009). Genotoxicity of silver nanoparticles in Allium cepa. *The Science of the Total Environment*, *407*(19), 5243–5246. https://doi.org/10.1016/j.scitotenv.2009.06.024

Kwasniewski, M., Chwialkowska, K., Kwasniewska, J., Kusak, J., Siwinski, K., & Szarejko, I. (2013). Accumulation of peroxidase-related reactive oxygen species in trichoblasts correlates with root hair initiation in barley. *Journal of Plant Physiology*, *170*(2), 185–195. https://doi.org/10.1016/J.JPLPH.2012.09.017

Laskowski, M. J., Williams, M. E., Nusbaum, H. C., & Sussex, I. M. (1995). Formation of lateral root meristems is a two-stage process. *Development*, *121*(10), 3303–3310.

Leakage and Water Efficiency Office of Water Services. (n.d.).

Lee, S., Chung, H., Kim, S., & Lee, I. (2013). The Genotoxic Effect of ZnO and CuO Nanoparticles on Early Growth of Buckwheat, Fagopyrum Esculentum. *Water, Air, & Soil Pollution*, *224*(9), 1668. https://doi.org/10.1007/s11270-013-1668-0

Lee, W.-M., An, Y.-J., Yoon, H., & Kweon, H.-S. (2008a). Toxicity and bioavailability of copper nanoparticles to the terrestrial plants mung bean (Phaseolus radiatus) and wheat (Triticum aestivum): plant agar test for water-insoluble nanoparticles. *Environmental Toxicology and Chemistry*, *27*(9), 1915–1921.

Lee, W.-M., An, Y.-J., Yoon, H., & Kweon, H.-S. (2008b). Toxicity and bioavailability of copper nanoparticles to the terrestrial plants mung bean (Phaseolus radiatus) and wheat (Triticum aestivum): plant agar test for water-insoluble nanoparticles. *Environmental Toxicology and Chemistry*, *27*(9), 1915–1921.

Leigh RA, W. J. R. (1984). *A hypothesis relating critical potassium concentrations for growth to the distribution and functions of this ion in the plant cell*. New Phytologist.

Leyser, O. (2018). Auxin signaling. In *Plant Physiology* (Vol. 176, Issue 1, pp. 465–479). American Society of Plant Biologists. https://doi.org/10.1104/pp.17.00765

Li, T., Kang, X., Lei, W., Yao, X., Zou, L., Zhang, D., & Lin, H. (2020). SHY2 as a node in the regulation of root meristem development by auxin, brassinosteroids, and cytokinin. *Journal of Integrative Plant Biology*, *62*(10), 1500–1517. https://doi.org/10.1111/JIPB.12931

Lichtenthaler, H. K. (1987). [34] Chlorophylls and carotenoids: Pigments of photosynthetic biomembranes. *Methods in Enzymology*, *148*, 350–382. https://doi.org/10.1016/0076-6879(87)48036-1

Lin, C. C., Chen, L. M., & Liu, Z. H. (2005). Rapid effect of copper on lignin biosynthesis in soybean roots. *Plant Science*, *168*(3), 855–861. https://doi.org/10.1016/j.plantsci.2004.10.023

Lin, D., & Xing, B. (2007). Phytotoxicity of nanoparticles: Inhibition of seed germination and root growth. *Environmental Pollution*, *150*(2), 243–250. https://doi.org/10.1016/j.envpol.2007.01.016

Lister, R., O'Malley, R. C., Tonti-Filippini, J., Gregory, B. D., Berry, C. C., Millar, A. H., & Ecker, J. R. (2008). Highly Integrated Single-Base Resolution Maps of the Epigenome in Arabidopsis. *Cell*, *133*(3), 523–536. https://doi.org/10.1016/J.CELL.2008.03.029

Liu, L., Lu, S., Demissie, H., Yue, Y., Jiao, R., An, G., & Wang, D. (2021). Formation of Al30 aggregates and its correlation to the coagulation effect. *Chemosphere*, *278*. https://doi.org/10.1016/J.CHEMOSPHERE.2021.130493

Llases, M. E., Morgada, M. N., & Vila, A. J. (2019). Biochemistry of Copper Site Assembly in Heme-Copper Oxidases: A Theme with Variations. *International Journal of Molecular Sciences 2019, Vol. 20, Page 3830*, *20*(15), 3830. https://doi.org/10.3390/IJMS20153830

Llorens, A., Lloret, E., Picouet, P. A., Trbojevich, R., & Fernandez, A. (2012). Metallic-based micro and nanocomposites in food contact materials and active food packaging. *Trends in Food Science & Technology*, *24*(1), 19–29. https://doi.org/10.1016/J.TIFS.2011.10.001

Lüthje, S., Meisrimler, C. N., Hopff, D., & Möller, B. (2011). Phylogeny, topology, structure and functions of membrane-bound class III peroxidases in vascular plants. *Phytochemistry*, *72*(10), 1124–1135. https://doi.org/10.1016/J.PHYTOCHEM.2010.11.023

Lynch, J. (1995). Root Architecture and Plant Productivity. *Plant Physiology*, *109*(1), 7–13. https://doi.org/10.1104/PP.109.1.7

Lynch, J. P. (2022). Harnessing root architecture to address global challenges. *The Plant Journal*, *109*(2), 415–431. https://doi.org/10.1111/TPJ.15560

Ma, X., Geiser-Lee, J., Deng, Y., & Kolmakov, A. (2010a). Interactions between engineered nanoparticles (ENPs) and plants: phytotoxicity, uptake and accumulation. *The Science of the Total Environment*, *408*(16), 3053–3061. https://doi.org/10.1016/J.SCITOTENV.2010.03.031

Ma, X., Geiser-Lee, J., Deng, Y., & Kolmakov, A. (2010b). Interactions between engineered nanoparticles (ENPs) and plants: Phytotoxicity, uptake and accumulation. *Science of The Total Environment*, *408*(16), 3053–3061. https://doi.org/10.1016/j.scitotenv.2010.03.031

Macko, S., & H. E. Emmett, P. (1938). Brunauer, S., Emmett, P. H. & Teller, E. Adsorption of gases in multimolecular layers. J. Am. Chem. Soc. 60, 309-319. In *Journal of the American Chemical Society* (Vol. 60). https://doi.org/10.1021/ja01269a023

Maeshima, M. (2014). [Zinc homeostasis and zinc signaling thoughts from plant zinc transporters]. *Seikagaku. The Journal of Japanese Biochemical Society*, *86*(3), 407–410.

Malamy, J. E., & Benfey, P. N. (1997). Organization and cell differentiation in lateral roots of Arabidopsis thaliana. *Development*, *124*(1).

Malatesta, M. (2021). Transmission Electron Microscopy as a Powerful Tool to Investigate the Interaction of Nanoparticles with Subcellular Structures. *International Journal of Molecular Sciences*, *22*(23). https://doi.org/10.3390/IJMS222312789

Manos, D. P., & Xydis, G. (2019). Hydroponics: Are we moving towards that direction only because of the environment? a discussion on forecasting and a systems review. *Environmental Science and Pollution Research*, *26*(13), 12662–12672. https://doi.org/10.1007/S11356-019-04933-5/FIGURES/3

Markossian, K. A., & Kurganov, B. I. (2003). Copper Chaperones, Intracellular Copper Trafficking Proteins. Function, Structure, and Mechanism of Action. *Biochemistry (Moscow)*, *68*(8), 827–837. https://doi.org/10.1023/A:1025740228888

Marty, L., Bausewein, D., Müller, C., Bangash, S. A. K., Moseler, A., Schwarzländer, M., Müller-Schüssele, S. J., Zechmann, B., Riondet, C., Balk, J., Wirtz, M., Hell, R., Reichheld, J.-P., & Meyer, A. J. (2019). Arabidopsis glutathione reductase 2 is indispensable in plastids, while mitochondrial glutathione is safeguarded by additional reduction and transport systems. *The New Phytologist*, *224*(4), 1569–1584. https://doi.org/10.1111/nph.16086

Mascarenhas, J. P., Machlis, L., Sakamoto, S., Sasaki, N., Mori, T., Kuroiwa, H., Nakada, T., Nozaki, H., Kuroiwa, T., & Nakano, A. (1964). Chemotropic Response of the Pollen of Antirrhinum majus to Calcium. *Plant Physiology*, *39*(1), 70–77. https://doi.org/10.1104/pp.39.1.70

May, M. J., Hammond-Kosack, K. E., & Jones, JDG. (1996). Involvement of Reactive Oxygen Species, Glutathione Metabolism, and Lipid Peroxidation in the Cf-Gene-Dependent Defense Response of Tomato Cotyledons Induced by Race-Specific Elicitors of Cladosporium fulvum. *Plant Physiology*, *110*(4), 1367–1379. https://doi.org/10.1104/pp.110.4.1367

McDermaid, A., Monier, B., Zhao, J., Liu, B., & Ma, Q. (2019). Interpretation of differential gene expression results of RNA-seq data: review and integration. *Briefings in Bioinformatics*, *20*(6), 2044. https://doi.org/10.1093/BIB/BBY067

Meftahi, G. H., Bahari, Z., Zarei Mahmoudabadi, A., Iman, M., & Jangravi, Z. (2021). Applications of western blot technique: From bench to bedside. *Biochemistry and Molecular Biology Education : A Bimonthly Publication of the International Union of Biochemistry and Molecular Biology*, *49*(4), 509–517. https://doi.org/10.1002/BMB.21516

Meinke, D. W., Cherry, J. M., Dean, C., Rounsley, S. D., & Koornneef, M. (1998). Arabidopsis thaliana: a model plant for genome analysis. *Science (New York, N.Y.)*, *282*(5389). https://doi.org/10.1126/SCIENCE.282.5389.662

Meng, X., & Zhang, S. (2013). MAPK cascades in plant disease resistance signaling. *Annual Review of Phytopathology*, *51*, 245–266. https://doi.org/10.1146/ANNUREV-PHYTO-082712-102314

Miller, G., Suzuki, N., Ciftci-Yilmaz, S., & Mittler, R. (2010). Reactive oxygen species homeostasis and signalling during drought and salinity stresses. *Plant, Cell and Environment*, *33*(4), 453–467. https://doi.org/10.1111/j.1365-3040.2009.02041.x

Mino, T., & Takeuchi, O. (2018). Post-transcriptional regulation of immune responses by RNA binding proteins. *Proceedings of the Japan Academy Series B: Physical and Biological Sciences*, *94*(6), 248–258. https://doi.org/10.2183/pjab.94.017

Mira, H., Martínez-García, F., & Peñarrubia, L. (2001). Evidence for the plant-specific intercellular transport of the Arabidopsis copper chaperone CCH. *The Plant Journal : For Cell and Molecular Biology*, *25*(5), 521–528. https://doi.org/10.1046/J.1365-313X.2001.00985.X

Mironova, V. V, Omelyanchuk, N. A., Yosiphon, G., Fadeev, S. I., Kolchanov, N. A., Mjolsness, E., & Likhoshvai, V. A. (2010). A plausible mechanism for auxin patterning along the developing root. *BMC Systems Biology*, *4*, 98. https://doi.org/10.1186/1752-0509-4-98

Mirzajani, F., Askari, H., Hamzelou, S., Schober, Y., Römpp, A., Ghassempour, A., & Spengler, B. (2014). Proteomics study of silver nanoparticles toxicity on Oryza sativa L. *Ecotoxicology and Environmental Safety*, *108*, 335–339. https://doi.org/10.1016/j.ecoenv.2014.07.013

Mishra, D., Kumar, S., & Mishra, B. N. (2021). An Overview of Morpho-Physiological, Biochemical, and Molecular Responses of Sorghum Towards Heavy Metal Stress. *Reviews of Environmental Contamination and Toxicology*, *256*, 155–177. https://doi.org/10.1007/398_2020_61/COVER

Mitchell, P.J, Schnele, M. A. (1999). Controlling tree roots in sewer lines with copper sulfate. *Oklahoma Cooperative Extension Service*, CR-6428.

Mittal, M., Kumar, K., Anghore, D., & Rawal, R. K. (2017). ICP-MS: Analytical Method for Identification and Detection of Elemental Impurities. *Current Drug Discovery Technologies*, *14*(2), 106–120. https://doi.org/10.2174/1570163813666161221141402

Mittler, R. (2017). ROS Are Good. *Trends in Plant Science*, *22*(1), 11–19. https://doi.org/10.1016/j.tplants.2016.08.002

Mittler, R., Zandalinas, S. I., Fichman, Y., & Van Breusegem, F. (2022). Reactive oxygen species signalling in plant stress responses. *Nature Reviews Molecular Cell Biology*, *23*(10), 663–679. https://doi.org/10.1038/s41580-022-00499-2

Mizrachi, A., Graff van Creveld, S., Shapiro, O. H., Rosenwasser, S., & Vardi, A. (2019). Light-dependent single-cell heterogeneity in the chloroplast redox state regulates cell fate in a marine diatom. *ELife*, *8*. https://doi.org/10.7554/eLife.47732

Moore, S., Zhang, X., Mudge, A., Rowe, J. H., Topping, J. F., Liu, J., & Lindsey, K. (2015). Spatiotemporal modelling of hormonal crosstalk explains the level and patterning of hormones and gene expression in Arabidopsis thaliana wild-type and mutant roots. *The New Phytologist*, *207*(4), 1110–1122. https://doi.org/10.1111/NPH.13421

Mortazavi, A., Williams, B. A., McCue, K., Schaeffer, L., & Wold, B. (2008). Mapping and quantifying mammalian transcriptomes by RNA-Seq. *Nature Methods 2008 5:7*, *5*(7), 621–628. https://doi.org/10.1038/nmeth.1226

Morton, V., & Staub, T. (2008). A Short History of Fungicides. *APSnet Feature Articles*. https://doi.org/10.1094/APSnetFeature-2008-0308

Moubayidin, L., Perilli, S., Dello Ioio, R., Di Mambro, R., Costantino, P., & Sabatini, S. (2010). The rate of cell differentiation controls the Arabidopsis root meristem growth phase. *Current Biology : CB*, *20*(12), 1138–1143. https://doi.org/10.1016/J.CUB.2010.05.035

Multiple comparisons - Handbook of Biological Statistics. (n.d.). Retrieved March 17, 2023, from http://www.biostathandbook.com/multiplecomparisons.html

Murashige, T., & Skoog, F. (1962). A Revised Medium for Rapid Growth and Bio Assays with Tobacco Tissue Cultures. *Physiologia Plantarum*, *15*(3), 473–497. https://doi.org/10.1111/j.1399-3054.1962.tb08052.x

Nagalakshmi, U., Wang, Z., Waern K., Shou, C., Raha, D., Gerstein, M., Snyder, M. (2008). The transcriptional landscape of the yeast genome defined by RNA sequencing. *Science (New York, N.Y.)*, *320*(5881), 1344–1349. https://doi.org/10.1126/SCIENCE.1158441

Nair, P. M. G., & Chung, I. M. (2014). Impact of copper oxide nanoparticles exposure on Arabidopsis thaliana growth, root system development, root lignificaion, and molecular level changes. *Environmental Science and Pollution Research*, *21*(22), 12709–12722. https://doi.org/10.1007/s11356-014-3210-3

Nersissian, A. M., Immoos, C., Hill, M. G., Hart, P. J., Williams, G., Herrmann, R. G., & Valentine, J. S. (1998a). Uclacyanins, stellacyanins, and plantacyanins are distinct subfamilies of phytocyanins: plant-specific mononuclear blue copper proteins. *Protein Science : A Publication of the Protein Society*, *7*(9), 1915–1929. https://doi.org/10.1002/PRO.5560070907

Nersissian, A. M., Immoos, C., Hill, M. G., Hart, P. J., Williams, G., Herrmann, R. G., & Valentine, J. S. (1998b). Uclacyanins, stellacyanins, and plantacyanins are distinct subfamilies of phytocyanins: plant-specific mononuclear blue copper proteins. *Protein Science : A Publication of the Protein Society*, *7*(9), 1915–1929. https://doi.org/10.1002/PRO.5560070907

News, I. A.-S., & 1989, undefined. (n.d.). Making the right stuff. *JSTOR*.

Nietzel, T., Elsässer, M., Ruberti, C., Steinbeck, J., Ugalde, J. M., Fuchs, P., Wagner, S., Ostermann, L., Moseler, A., Lemke, P., Fricker, M. D., Müller-Schüssele, S. J., Moerschbacher, B. M., Costa, A., Meyer, A. J., & Schwarzländer, M. (2019). The fluorescent protein sensor roGFP2-Orp1 monitors in vivo H(2) O(2) and thiol redox integration and elucidates intracellular H(2) O(2) dynamics during elicitor-induced oxidative burst in Arabidopsis. *The New Phytologist*, *221*(3), 1649–1664. https://doi.org/10.1111/nph.15550

Nikhil R. Jana, *, Latha Gearheart, and, & Murphy*, C. J. (2001). *Wet Chemical Synthesis of High Aspect Ratio Cylindrical Gold Nanorods*. https://doi.org/10.1021/JP0107964

Oberdörster, G., Oberdörster, E., & Oberdörster, J. (2005). Nanotoxicology: an emerging discipline evolving from studies of ultrafine particles. *Environmental Health Perspectives*, *113*(7), 823–839. https://doi.org/10.1289/ehp.7339

Oka, H., Tomioka, T., Tomita, K., Nishino, A., & Ueda, S. (1994). Inactivation of enveloped viruses by a silver-thiosulfate complex. *Metal-Based Drugs*, *1*(5–6), 511. https://doi.org/10.1155/MBD.1994.511

Oloffs, A., Grosse-Siestrup, C., Bisson, S., Rinck, M., Rudolph, R., & Gross, U. (1994). Biocompatibility of silver-coated polyurethane catheters and silvercoated Dacron® material. *Biomaterials*, *15*(10), 753–758. https://doi.org/10.1016/0142-9612(94)90028-0

O'Malley, R. C., Barragan, C. C., & Ecker, J. R. (2015). A user's guide to the arabidopsis T-DNA insertion mutant collections. In *Plant Functional Genomics: Methods and Protocols: Second Edition* (Vol. 1284, pp. 323–342). Springer New York. https://doi.org/10.1007/978-1-4939-2444-8_16

Pal, S., Tak, Y. K., & Song, J. M. (2007a). Does the antibacterial activity of silver nanoparticles depend on the shape of the nanoparticle? A study of the Gram-negative bacterium Escherichia coli.

Applied and Environmental Microbiology, *73*(6), 1712–1720. https://doi.org/10.1128/AEM.02218-06

Pal, S., Tak, Y. K., & Song, J. M. (2007b). Does the antibacterial activity of silver nanoparticles depend on the shape of the nanoparticle? A study of the Gram-negative bacterium Escherichia coli. *Applied and Environmental Microbiology*, *73*(6), 1712–1720. https://doi.org/10.1128/AEM.02218-06

Paponov, I. A., Paponov, M., Teale, W., Menges, M., Chakrabortee, S., Murray, J. A. H., & Palme, K. (2008). Comprehensive transcriptome analysis of auxin responses in Arabidopsis. *Molecular Plant*, *1*(2), 321–337. https://doi.org/10.1093/mp/ssm021

Péret, B., De Rybel, B., Casimiro, I., Benková, E., Swarup, R., Laplaze, L., Beeckman, T., & Bennett, M. J. (2009). Arabidopsis lateral root development: an emerging story. In *Trends in Plant Science* (Vol. 14, Issue 7, pp. 399–408). Trends Plant Sci. https://doi.org/10.1016/j.tplants.2009.05.002

Petrášek, J., Mravec, J., Bouchard, R., Blakeslee, J. J., Abas, M., Seifertová, D., Wiśniewska, J., Tadele, Z., Kubeš, M., Čovanová, M., Dhonukshe, P., Skůpa, P., Benková, E., Perry, L., Křeček, P., Lee, O. R., Fink, G. R., Geisler, M., Murphy, A. S., … Friml, J. (2006). PIN proteins perform a rate-limiting function in cellular auxin efflux. *Science*, *312*(5775), 914–918. https://doi.org/10.1126/science.1123542

Petricka, J. J., Winter, C. M., & Benfey, P. N. (2012). Control of *Arabidopsis* Root Development. *Annual Review of Plant Biology*, *63*(1), 563–590. https://doi.org/10.1146/annurev-arplant-042811-105501

Peyrot, C., Wilkinson, K. J., Desrosiers, M., & Sauvé, S. (2014). Effects of silver nanoparticles on soil enzyme activities with and without added organic matter. *Environmental Toxicology and Chemistry*, *33*(1), 115–125. https://doi.org/10.1002/etc.2398

Piao, M. J., Kang, K. A., Lee, I. K., Kim, H. S., Kim, S., Choi, J. Y., Choi, J., & Hyun, J. W. (2011). Silver nanoparticles induce oxidative cell damage in human liver cells through inhibition of reduced glutathione and induction of mitochondria-involved apoptosis. *Toxicology Letters*, *201*(1), 92–100. https://doi.org/10.1016/j.toxlet.2010.12.010

Piepenbrock, M. O. M., Lloyd, G. O., Clarke, N., & Steed, J. W. (2010). Metal- and anion-binding supramolecular gels. *Chemical Reviews*, *110*(4), 1960–2004. https://doi.org/10.1021/CR9003067

Pivetz, B. E., & Kovalick, W. W. (2001). *Ground Water Issue Phytoremediation of Contaminated Soil and Ground Water at Hazardous Waste Sites*.

Postma, J. A., Dathe, A., & Lynch, J. P. (2014). The Optimal Lateral Root Branching Density for Maize Depends on Nitrogen and Phosphorus Availability. *PLANT PHYSIOLOGY*, *166*(2), 590–602. https://doi.org/10.1104/pp.113.233916

Prantner, A. M., & Scholler, N. (2014). Biological Barriers and Current Strategies for Modifying Nanoparticle Bioavailability. *Journal of Nanoscience and Nanotechnology*, *14*(1), 115–125. https://doi.org/10.1166/JNN.2014.8899

Priester, J. H., Ge, Y., Mielke, R. E., Horst, A. M., Moritz, S. C., Espinosa, K., Gelb, J., Walker, S. L., Nisbet, R. M., An, Y.-J., Schimel, J. P., Palmer, R. G., Hernandez-Viezcas, J. A., Zhao, L., Gardea-Torresdey, J. L., & Holden, P. A. (2012). Soybean susceptibility to manufactured nanomaterials with evidence

for food quality and soil fertility interruption. *Proceedings of the National Academy of Sciences of the United States of America*, *109*(37), E2451-6. https://doi.org/10.1073/pnas.1205431109

Q700 Sonicator | Ultrasonic Homogenizer & Emulsifier | Qsonica. (n.d.). Retrieved February 24, 2023, from https://www.sonicator.com/products/q700-sonicator

Qian, H., Peng, X., Han, X., Ren, J., Sun, L., & Fu, Z. (2013). Comparison of the toxicity of silver nanoparticles and silver ions on the growth of terrestrial plant model Arabidopsis thaliana. *Journal of Environmental Sciences*, *25*(9), 1947–1956. https://doi.org/10.1016/S1001-0742(12)60301-5

Rakusová, H., Gallego-Bartolomé, J., Vanstraelen, M., Robert, H. S., Alabadí, D., Blázquez, M. A., Benková, E., & Friml, J. (2011). Polarization of PIN3-dependent auxin transport for hypocotyl gravitropic response in Arabidopsis thaliana. *The Plant Journal*, *67*(5), 817–826. https://doi.org/10.1111/j.1365-313X.2011.04636.x

Ralph, J., Lapierre, C., & Boerjan, W. (2019). Lignin structure and its engineering. *Current Opinion in Biotechnology*, *56*, 240–249. https://doi.org/10.1016/J.COPBIO.2019.02.019

Randrup, T. B., McPherson, E. G., & Costello, L. R. (2001). Tree Root Intrusion in Sewer Systems: Review of Extent and Costs. *Journal of Infrastructure Systems*, *7*(1), 26–31. https://doi.org/10.1061/(ASCE)1076-0342(2001)7:1(26)

Rao, S., & Shekhawat, G. S. (2016). Phytotoxicity and oxidative stress perspective of two selected nanoparticles in Brassica juncea. *3 Biotech*, *6*(2), 244. https://doi.org/10.1007/s13205-016-0550-3

Raza, A., Salehi, H., Rahman, M. A., Zahid, Z., Madadkar Haghjou, M., Najafi-Kakavand, S., Charagh, S., Osman, H. S., Albaqami, M., Zhuang, Y., Siddique, K. H. M., & Zhuang, W. (2022). Plant hormones and neurotransmitter interactions mediate antioxidant defenses under induced oxidative stress in plants. *Frontiers in Plant Science*, *13*, 3061. https://doi.org/10.3389/FPLS.2022.961872/BIBTEX

Rhee, S. Y., & Mutwil, M. (2014). Towards revealing the functions of all genes in plants. In *Trends in Plant Science* (Vol. 19, Issue 4, pp. 212–221). Elsevier Ltd. https://doi.org/10.1016/j.tplants.2013.10.006

Ringnér, M. (2008). What is principal component analysis? *Nature Biotechnology 2008 26:3*, *26*(3), 303–304. https://doi.org/10.1038/nbt0308-303

Roberts, J., Jackson, N., & Smith, M. (2006). *Tree roots in the built environment*.

Rodrigues, O., Reshetnyak, G., Grondin, A., Saijo, Y., Leonhardt, N., Maurel, C., & Verdoucq, L. (2017). Aquaporins facilitate hydrogen peroxide entry into guard cells to mediate ABA- and pathogen-triggered stomatal closure. *Proceedings of the National Academy of Sciences of the United States of America*, *114*(34), 9200–9205. https://doi.org/10.1073/pnas.1704754114

Rolf, K., & Stål, Ö. (1994). Tree Roots in Sewer Systems in Malmo, Sweden. *Arboriculture & Urban Forestry*, *20*(6), 329–335. https://doi.org/10.48044/JAUF.1994.058

Rong, D., Zhao, S., Tang, W., Luo, N., He, H., Wang, Z., Ma, H., Huang, Y., Yao, X., Pan, X., Lv, L., Xiao, J., Liu, R., Nagawa, S., & Yamamuro, C. (2022). ROP signaling regulates spatial pattern of cell division and specification of meristem notch. *Proceedings of the National Academy of Sciences of the United States of America*, *119*(47). https://doi.org/10.1073/PNAS.2117803119

Rousk, J., Ackermann, K., Curling, S. F., & Jones, D. L. (2012). Comparative Toxicity of Nanoparticulate CuO and ZnO to Soil Bacterial Communities. *PLoS ONE*, *7*(3), e34197. https://doi.org/10.1371/journal.pone.0034197

Ruiter, JM, Ramakers, C, Hoogaars, WM, Karlen, Y, Bakker O, van den Hoff MJB, & Moorman,AFM. (2009). Amplification efficiency: linking baseline and bias in the analysis of quantitative PCR data. *Nucleic Acids Research*, *37*(6). https://doi.org/10.1093/NAR/GKP045

Ruiz Rosquete, M., Barbez, E., & Rgen Kleine-Vehn, J. (2012). Cellular Auxin Homeostasis: Gatekeeping Is Housekeeping. *Molecular Plant*, *5*, 772–786. https://doi.org/10.1093/mp/ssr109

Sabatini, S., Beis, D., Wolkenfelt, H., Murfett, J., Guilfoyle, T., Malamy, J., Benfey, P., Leyser, O., Bechtold, N., Weisbeek, P., & Scheres, B. (1999). An auxin-dependent distal organizer of pattern and polarity in the Arabidopsis root. *Cell*, *99*(5), 463–472. https://doi.org/10.1016/s0092-8674(00)81535-4

Sandalio, L. M., & Romero-Puertas, M. C. (2015). Peroxisomes sense and respond to environmental cues by regulating ROS and RNS signalling networks. In *Annals of Botany* (Vol. 116, Issue 4, pp. 475–485). Oxford University Press. https://doi.org/10.1093/aob/mcv074

Scheres, B. (2013). Rooting plant development. *Development (Cambridge)*, *140*(5), 939–941. https://doi.org/10.1242/dev.093559

Scheres B Benfey P Dolan L . (2002). Root development. In: Somerville CR Meyerowitz EM,. *America Society of Plant Biologists.*

Scheres, B., Wolkenfelt, H., Willemsen, V., Terlouw, M., Lawson, E., Dean, C., & Weisbeek, P. (1994). Embryonic origin of the Arabidopsis primary root and root meristem initials. *Development*, *120*(9).

Schiefelbein, J. W., Somerville, C., Ashworth, S. L., Sherman, D. M., Yuan, M., & Staiger, C. J. (1990). Genetic Control of Root Hair Development in Arabidopsis thaliana. *THE PLANT CELL ONLINE*, *2*(3), 235–243. https://doi.org/10.1105/tpc.2.3.235

Schmalzried, Hermann., & Navrotsky, Alexandra. (1975). *Festkörperthermodynamik*. Verlag Chemie.

Schneider, C. A., Rasband, W. S., & Eliceiri, K. W. (2012). NIH Image to ImageJ: 25 years of image analysis. *Nature Methods*, *9*(7), 671–675. http://www.ncbi.nlm.nih.gov/pubmed/22930834

Serre, N. B. C., Kralík, D., Yun, P., Slouka, Z., Shabala, S., & Fendrych, M. (2021). AFB1 controls rapid auxin signalling through membrane depolarization in Arabidopsis thaliana root. *Nature Plants*, *7*(9), 1229–1238. https://doi.org/10.1038/S41477-021-00969-Z

Services, B., & Crawford, M. (2003). *Copper Coated Containers and their impacton the Environment*. 76–78.

Shahzad, Z., Kellermeier, F., Armstrong, E. M., Rogers, S., Lobet, G., Amtmann, A., & Hills, A. (2018). EZ-Root-VIS: A Software Pipeline for the Rapid Analysis and Visual Reconstruction of Root System Architecture. *Plant Physiology*, *177*(4), 1368–1381. https://doi.org/10.1104/PP.18.00217

Shaw, A. K., & Hossain, Z. (2013). Impact of nano-CuO stress on rice (Oryza sativa L.) seedlings. *Chemosphere*, *93*(6), 906–915. https://doi.org/10.1016/j.chemosphere.2013.05.044

Shen, N., Wang, T., Gan, Q., Liu, S., Wang, L., & Jin, B. (2022). Plant flavonoids: Classification, distribution, biosynthesis, and antioxidant activity. *Food Chemistry*, *383*, 132531. https://doi.org/10.1016/j.foodchem.2022.132531

Shin, L.-J., Lo, J.-C., & Yeh, K.-C. (2012). Copper chaperone antioxidant protein1 is essential for copper homeostasis. *Plant Physiology*, *159*(3), 1099–1110. https://doi.org/10.1104/pp.112.195974

Shin, R. (2014). Strategies for Improving Potassium Use Efficiency in Plants. *Molecules and Cells*, *37*(8), 575. https://doi.org/10.14348/MOLCELLS.2014.0141

Smith, S., & de Smet, I. (2012). Root system architecture: Insights from Arabidopsis and cereal crops. *Philosophical Transactions of the Royal Society B: Biological Sciences*, *367*(1595), 1441–1452. https://doi.org/10.1098/rstb.2011.0234

Soumya, R. S., Vineetha, V. P., Reshma, P. L., & Raghu, K. G. (2013). Preparation and characterization of selenium incorporated guar gum nanoparticle and its interaction with H9c2 cells. *PloS One*, *8*(9). https://doi.org/10.1371/JOURNAL.PONE.0074411

Sprague, N., & Edwards, M. (2001). *Copper in the Urban Water Cycle*.

Stampoulis, D., Sinha, S. K., & White, J. C. (2009). Assay-dependent phytotoxicity of nanoparticles to plants. *Environmental Science & Technology*, *43*(24), 9473–9479. https://doi.org/10.1021/es901695c

Stewart, J. L., & Nemhauser, J. L. (2010). Do trees grow on money? Auxin as the currency of the cellular economy. In *Cold Spring Harbor perspectives in biology* (Vol. 2, Issue 2). Cold Spring Harb Perspect Biol. https://doi.org/10.1101/cshperspect.a001420

Sturtz Field, L., Luk, E., & Culotta, V. C. (2002). Copper chaperones: Personal escorts for metal ions. *Journal of Bioenergetics and Biomembranes*, *34*(5), 373–379. https://doi.org/10.1023/A:1021202119942

Supek, F., Bošnjak, M., Škunca, N., & Šmuc, T. (2011). REVIGO summarizes and visualizes long lists of gene ontology terms. *PloS One*, *6*(7). https://doi.org/10.1371/JOURNAL.PONE.0021800

Sutton, H. C., & Winterbourn, C. C. (1989). On the participation of higher oxidation states of iron and copper in Fenton reactions. *Free Radical Biology & Medicine*, *6*(1), 53–60. https://doi.org/10.1016/0891-5849(89)90160-3

Swarup, R., Perry, P., Hagenbeek, D., Van Der Straeten, D., Beemster, G. T. S., Sandberg, G., Bhalerao, R., Ljung, K., & Bennett, M. J. (2007). Ethylene upregulates auxin biosynthesis in Arabidopsis seedlings to enhance inhibition of root cell elongation. *The Plant Cell*, *19*(7), 2186–2196. https://doi.org/10.1105/tpc.107.052100

Szklarczyk, D., Gable, A. L., Lyon, D., Junge, A., Wyder, S., Huerta-Cepas, J., Simonovic, M., Doncheva, N. T., Morris, J. H., Bork, P., Jensen, L. J., & Von Mering, C. (2019). STRING v11: Protein-protein association networks with increased coverage, supporting functional discovery in genome-wide experimental datasets. *Nucleic Acids Research*, *47*(D1), D607–D613. https://doi.org/10.1093/NAR/GKY1131

Thao, N. P., Khan, M. I. R., Thu, N. B. A., Hoang, X. L. T., Asgher, M., Khan, N. A., & Tran, L.-S. P. (2015). Role of Ethylene and Its Cross Talk with Other Signaling Molecules in Plant Responses to Heavy Metal Stress. *Plant Physiology*, *169*(1), 73–84. https://doi.org/10.1104/pp.15.00663

Thomas Berleth and Gerd Jürgens. (1993). The role of the monopteros gene in organising the basal body region of the Arabidopsis embryo. *Development*, *118*, 575–587. http://citeseerx.ist.psu.edu/viewdoc/download?doi=10.1.1.96.9227&rep=rep1&type=pdf

Thomas, P. D., Campbell, M. J., Kejariwal, A., Mi, H., Karlak, B., Daverman, R., Diemer, K., Muruganujan, A., & Narechania, A. (2003). PANTHER: A library of protein families and subfamilies indexed by function. *Genome Research*, *13*(9), 2129–2141. https://doi.org/10.1101/gr.772403

Thomson, G. (n.d.). *"2007 Kwatye Prize Report" INVESTIGATION OF SEWER BLOCKAGES DUE TO TREE ROOTS*.

Tizro, P., Choi, C., & Khanlou, N. (2019). Sample Preparation for Transmission Electron Microscopy. *Methods in Molecular Biology (Clifton, N.J.)*, *1897*, 417–424. https://doi.org/10.1007/978-1-4939-8935-5_33

Tokumaru, T., Shimizu, Y., & Fox, C. L. (1974). Antiviral activities of silver sulfadiazine in ocular infection. *Research Communications in Chemical Pathology and Pharmacology*, *8*(1), 151–158.

Torres, M. A., Dangl, J. L., & Jones, J. D. G. (2002). Arabidopsis gp91phox homologues AtrbohD and AtrbohF are required for accumulation of reactive oxygen intermediates in the plant defense response. *Proceedings of the National Academy of Sciences of the United States of America*, *99*(1), 517–522. https://doi.org/10.1073/pnas.012452499

Tsikas, D. (2017). Assessment of lipid peroxidation by measuring malondialdehyde (MDA) and relatives in biological samples: Analytical and biological challenges. *Analytical Biochemistry*, *524*, 13–30. https://doi.org/10.1016/J.AB.2016.10.021

Tungittiplakorn, W., Lion, L. W., Cohen, C., & Kim, J.-Y. (2004). Engineered polymeric nanoparticles for soil remediation. *Environmental Science & Technology*, *38*(5), 1605–1610.

Uchida, Y., Chiba, T., Kurimoto, R., & Asahara, H. (2019). Post-transcriptional regulation of inflammation by RNA-binding proteins via cis-elements of mRNAs. *Journal of Biochemistry*, *166*(5), 375–382. https://doi.org/10.1093/JB/MVZ067

Valida fibrillated cellulose for coatings. (n.d.). Retrieved March 30, 2023, from https://www.l-i.co.uk/blog/blog-archive/video-valida-fibrillated-cellulose-for-coatings

Van Norman, J. M., & Benfey, P. N. (2009). Arabidopsis thaliana as a model organism in systems biology. *Wiley Interdisciplinary Reviews: Systems Biology and Medicine*, *1*(3), 372–379. https://doi.org/10.1002/WSBM.25

Verma, C., Hussain, C. M., Quraishi, M. A., & Alfantazi, A. (2023). Green surfactants for corrosion control: Design, performance and applications. *Advances in Colloid and Interface Science*, *311*. https://doi.org/10.1016/J.CIS.2022.102822

Vissenberg, K., Claeijs, N., Balcerowicz, D., & Schoenaers, S. (2020). Hormonal regulation of root hair growth and responses to the environment in Arabidopsis. *Journal of Experimental Botany*, *71*(8), 2412–2427. https://doi.org/10.1093/jxb/eraa048

Vittori Antisari, L., Carbone, S., Gatti, A., Vianello, G., & Nannipieri, P. (2015). Uptake and translocation of metals and nutrients in tomato grown in soil polluted with metal oxide (CeO_2, Fe_3O_4, SnO_2, TiO_2) or metallic (Ag, Co, Ni) engineered nanoparticles. *Environmental Science and Pollution Research International*, *22*(3), 1841–1853. https://doi.org/10.1007/s11356-014-3509-0

Vogt, T. (2010). Phenylpropanoid biosynthesis. *Molecular Plant*, *3*(1), 2–20. https://doi.org/10.1093/MP/SSP106

Vollath, D. (2020). Agglomerates of nanoparticles. *Beilstein Journal of Nanotechnology*, *11*, 854–857. https://doi.org/10.3762/BJNANO.11.70

Waadt, R., Seller, C. A., Hsu, P.-K., Takahashi, Y., Munemasa, S., & Schroeder, J. I. (2022a). Plant hormone regulation of abiotic stress responses. *Nature Reviews Molecular Cell Biology*, *23*(10), 680–694. https://doi.org/10.1038/s41580-022-00479-6

Waadt, R., Seller, C. A., Hsu, P.-K., Takahashi, Y., Munemasa, S., & Schroeder, J. I. (2022b). Plant hormone regulation of abiotic stress responses. *Nature Reviews Molecular Cell Biology*, *23*(10), 680–694. https://doi.org/10.1038/s41580-022-00479-6

Walter, D. (2013). Primary Particles - Agglomerates - Aggregates. In *Nanomaterials* (pp. 9–24). Wiley-VCH Verlag GmbH & Co. KGaA. https://doi.org/10.1002/9783527673919.ch1

Wang, L., Leister, D., Guan, L., Zheng, Y., Schneider, K., Lehmann, M., Apel, K., & Kleine, T. (2020). The Arabidopsis SAFEGUARD1 suppresses singlet oxygen-induced stress responses by protecting grana margins. *Proceedings of the National Academy of Sciences of the United States of America*, *117*(12), 6918–6927. https://doi.org/10.1073/pnas.1918640117

Wang, Y., Zhang, W., Li, K., Sun, F., Han, C., Wang, Y., & Li, X. (2008). Salt-induced plasticity of root hair development is caused by ion disequilibrium in Arabidopsis thaliana. *Journal of Plant Research*, *121*(1), 87–96. https://doi.org/10.1007/S10265-007-0123-Y

Wang, Z., Gerstein, M., & Snyder, M. (2009). RNA-Seq: a revolutionary tool for transcriptomics. *Nature Reviews Genetics 2008 10:1*, *10*(1), 57–63. https://doi.org/10.1038/nrg2484

Ward, W. H. (1948). "The Effect of Vegetation on the Settlement of Structures."*. *Biology and Civil Engineering. Conference*, *Sept 1948*. https://doi.org/10.1680/BACE.45132.0011

Waszczak, C., Carmody, M., & Kangasjärvi, J. (2018). Reactive Oxygen Species in Plant Signaling. *Https://Doi.Org/10.1146/Annurev-Arplant-042817-040322*, *69*, 209–236. https://doi.org/10.1146/ANNUREV-ARPLANT-042817-040322

Western Blot Protocol | Immunoblotting Protocol | Sigma-Aldrich. (n.d.). Retrieved April 6, 2020, from https://www.sigmaaldrich.com/technical-documents/protocols/biology/western-blotting.html

Wiesollek, D., Müller-Arnecke, H. W., Hold, U., Rödelsperger, K., Brückel, B., Podhorsky, S., & Schneider, J. (n.d.). *Charakterisierung von ultrafeinen Partikeln für den Arbeitsschutz-Teil 2*. Retrieved June 5, 2019, from www.baua.de

Wintz, H., & Vulpe, C. (2002). Plant copper chaperones. *Biochemical Society Transactions*, *30*(4), 732–735. https://doi.org/10.1042/BST0300732

Wrc. (2013). *Manual of Sewer Condition Classification 5th Edition (MSCC)*. Wrc.

Wuana, R. A., & Okieimen, F. E. (2011). Heavy Metals in Contaminated Soils: A Review of Sources, Chemistry, Risks and Best Available Strategies for Remediation. *ISRN Ecology*, *2011*, 1–20. https://doi.org/10.5402/2011/402647

Xie, C., Guo, Z., Zhang, P., Yang, J., Zhang, J., Ma, Y., He, X., Lynch, I., & Zhang, Z. (2022). Effect of CeO2 nanoparticles on plant growth and soil microcosm in a soil-plant interactive system.

Environmental Pollution (Barking, Essex : 1987), *300*. https://doi.org/10.1016/J.ENVPOL.2022.118938

Y. Zhou, †,‡, S. H. Yu, †,‡, X. P. Cui, †, C. Y. Wang, † and, & Z. Y. Chen*, †,‡. (1999). *Formation of Silver Nanowires by a Novel Solid−Liquid Phase Arc Discharge Method*. https://doi.org/10.1021/CM981122H

Yang, Y. N., Kim, Y., Kim, H., Kim, S. J., Cho, K. M., Kim, Y., Lee, D. S., Lee, M. H., Kim, S. Y., Hong, J. C., Kwon, S. J., Choi, J., & Park, O. K. (2021). The transcription factor ORA59 exhibits dual DNA binding specificity that differentially regulates ethylene- and jasmonic acid-induced genes in plant immunity. *Plant Physiology*, *187*(4), 2763–2784. https://doi.org/10.1093/PLPHYS/KIAB437

Yugang Sun, Brian Mayers, Thurston Herricks, and, & Xia*, Y. (2003). *Polyol Synthesis of Uniform Silver Nanowires: A Plausible Growth Mechanism and the Supporting Evidence*. https://doi.org/10.1021/NL034312M

Zhang, R., Yang, D., Zhou, C., Cheng, K., Liu, Z., Chen, L., Fang, L., & Xie, P. (2012). β-actin as a loading control for plasma-based Western blot analysis of major depressive disorder patients. *Analytical Biochemistry*, *427*(2), 116–120. https://doi.org/10.1016/J.AB.2012.05.008

Zhu, H., Han, J., Xiao, J. Q., & Jin, Y. (2008). Uptake, translocation, and accumulation of manufactured iron oxide nanoparticles by pumpkin plants. *Journal of Environmental Monitoring*, *10*(6), 713. https://doi.org/10.1039/b805998e

Zuo, H., Gu, Z., Cooper, H., & Xu, Z. P. (2015). Crosslinking to enhance colloidal stability and redispersity of layered double hydroxide nanoparticles. *Journal of Colloid and Interface Science*, *459*, 10–16. https://doi.org/10.1016/J.JCIS.2015.07.063

Appendices:

A Digital version of the RNA sequencing data, proteomic sequencing data and raw data formats for the graphpad figures and metadata for the confocal microscopy can be found at : https://drive.google.com/drive/folders/1zh1js-RD2gbn0GJgcwm60-22lHY5oPdP?usp=sharing